Second Series *August 15, 1930* *Vol. 36, No. 4*

THE

PHYSICAL REVIEW

REPORT ON NOTATION FOR SPECTRA OF DIATOMIC MOLECULES

By Robert S. Mulliken

Ryerson Physical Laboratory, University of Chicago

(Received March 18, 1930)

I. Introduction

FOR some time there has been much confusion and little agreement between different investigators in the field of band spectra, in respect to the symbols used for quantum numbers, spectroscopic terms, spectrum lines, and molecular constants as obtained from spectrum analysis. In the hope of remedying this situation, a number of those interested in the subject discussed the matter at Washington in April, 1929, and reached a tentative agreement on certain main points. The writer then undertook to obtain further discussion by correspondence, and for this purpose sent out on August 10 a circular letter embodying the results of the above discussion, somewhat modified and amplified as a result of subsequent experience. Copies of this letter were sent to about eighty spectroscopists. Many replies were received, and the matter was also discussed at the Faraday Society symposium on band spectra at Bristol in September.[1] On the basis of the foregoing, and of the replies to a second circular letter, sent out November 1, and of considerable additional correspondence with various individuals, the following report was prepared in tentative form, and copies were sent out with a third circular letter on March 15, 1930. After some changes based on replies to this third letter, the report is now presented.

In this report, the expression "it is recommended" is used in some cases, "it is suggested" in others. The *recommendations* represent the opinion, either active or acquiescent, of nearly everyone whose opinion has become known to the writer. They deal for the most part with important points about which definite conclusions have been reached. The *suggestions* are of a more tentative character. They deal in part with less important points and with matters where the need of general agreement is less imperative than in the case of the

[1] "Molecular Spectra and Molecular Structure. A General Discussion held by the Faraday Society." Published in book form (Gurney and Jackson, 1930), also in Trans. Faraday Soc., pp. 611–950 (1929). In regard to nomenclature, cf. pp. 628–633 and pp. 768–772 and the Errata.

recommendations. In part they refer to topics which have not yet been sufficiently discussed to make definite recommendations.—In all the proposals given, the attempt has been made to take properly into account the varied needs of experimentalists and theorists.

The recommendations and suggestions given here have been made in such a way as to supplement and to be in harmony with those in the recent Report on Notation for Atomic Spectra.[2] In particular, the principle of using capital letters for quantum numbers representing angular momenta belonging to the molecule as a whole, and small letters for angular momenta of individual electrons, has been adopted. The recommendations apply for the most part only to diatomic molecules, but the manner of their extension to polyatomic molecules is in some cases obvious. Although a standard notation for polyatomic molecules would be very desirable, our knowledge of their spectra is as yet so undeveloped that it is perhaps best not to attempt this now. The only recommendation made here is that any notation chosen for polyatomic molecules be such as to harmonize with and supplement those used for atoms and diatomic molecules.

In addition to making recommendations and suggestions, opportunity has been taken to discuss a few matters of definition and nomenclature in regard to which misunderstandings have arisen or are likely to arise (Λ-type doubling, ρ-type multiplicity, band-origins, system-origins, "electronic," "vibrational," and "rotational" energy, etc.).

II. Quantum Numbers for Molecule as a Whole

General. For the *vibrational quantum number, v is recommended* to replace the hitherto usual symbol n.[3] The quantum number v has integral values (0, 1, 2, $\cdots$), the vibrational energy being given by $E_v=(v+\frac{1}{2})hc\omega_e+\cdots$ (in regard to ω_e, cf. Section V).

For the resultant angular momentum of any molecule, and its projection on an external field, the quantum number *designations* J and M *are respectively recommended* ($M=J, J-1, \cdots -J$). These designations are identical with corresponding designations for atoms.[4] The possible J values are 0, 1, 2, $\cdots$ for molecules with an even number of electrons, $\frac{1}{2}$, $1\frac{1}{2}$, $\cdots$ for those with an odd number. In certain coupling cases, J loses its meaning, and another quantum number K becomes prominent; in singlet states, J and K are identical, and may be used interchangeably: cf. p. 615 below.

Normal coupling: Hund's cases a and b. Before speaking in more detail about various quantum numbers associated with the angular momenta of

[2] H. N. Russell, A. G. Shenstone, and L. A. Turner, Phys. Rev. **33**, 900 (1929).

[3] This change has been urged by a number of people, because of the increasing need of referring to v in the same paper, or even in the same sentence, in which n is used to designate the principal quantum number of an electron. The symbol v has already been used by J. H. Van Vleck (Phys. Rev. **33**, 477, 1929) and subsequently also by others.

[4] The use of J both for resultant *atomic* and for resultant *molecular* angular momentum is likely to cause some confusion. If its use were less well established for molecules (in the form j), J ought perhaps to be replaced by some other symbol, such as P (Hund proposed the symbol p). If this were done, M for molecules should also be replaced by another symbol.

electrons and nuclei in various coupling cases, it is desirable to review briefly the underlying theory.[5] We have always as angular momentum elements (1) the orbital angular momentum of the electrons, (2) their spin angular momentum, and (3) the angular momentum of the nuclear rotation. There are two coupling cases which may be regarded as normal,—cases *a* and *b* of Hund.

In both cases *a* and *b* we have for the resultant angular momentum of *spin* of the electrons a *quantum number S, exactly as in an atom.* Further, we have a quantum number [formerly called i_l, or σ_k or σ_l] for which *the designation* Λ *is here recommended*; $\Lambda h/2\pi$ represents (the numerical value of) the projection, on the electric axis of the molecule,[6] of the resultant orbital angular momentum of the electron system. The resultant orbital momentum itself is not at all rigorously quantized in molecules; nevertheless in comparing a molecule with the atom which would be obtained if its nuclei could be united, a resultant orbital *quantum number L may sometimes be assigned* as in the case of the atom; then Λ is the projection of L.[7] The possible values of Λ are $0, 1, 2, \cdots$.

In case *a* (possible only if $\Lambda > 0$) we have strong coupling of S to the electric axis, as a result of the magnetic field associated with Λ. Here the projection of S on the axis is a quantum number [formerly called i_s or σ_s] for which *the designation* Σ *is now recommended.*[7,8] Σ *has values* $S, S-1, \cdots -S$; it is considered to be a positive or negative quantity according as it is parallel or antiparallel to Λ. The numerical value of the algebraic sum of Λ and Σ is a quantum number [formerly called i, or σ] for which *the symbol* Ω *is recommended.* For given values of Λ and S, Ω has values $\Lambda+S, \Lambda+S-1, \cdots |\Lambda-S|$.[9] $\Omega h/2\pi$ is the total angular momentum parallel to the electric axis. This may be considered as combining vectorially with the angular momentum of the nuclei (a vector perpendicular to the electric axis)[10] to give the resultant angular momentum of the molecule (quantum number J, cf. Fig. 1). The possible values of J are $\Omega, \Omega+1, \Omega+2, \cdots$. The quantum num-

[5] F. Hund, Zeits. f. Physik, **36**, 657 (1926). For further details, cf. R. S. Mulliken, Reviews of Modern Physics **2**, 60 (1930).

[6] *I. e.*, on the line joining the nuclei.

[7] More accurately, according to the new quantum mechanics, the resultant orbital angular momentum is $L^*h/2\pi$, where $L^* \equiv [L(L+1)]^{\frac{1}{2}}$; then Λ is the projection of L^* (each in units $h/2\pi$). Similarly the angular momenta associated with S, K, J, J^a, R, l, are, in units $h/2\pi$, really S^*, K^*, etc., and Σ is really the projection of S^*, etc. [A *recommendation* of the symbols L^*, S^*, etc. is not intended here.]

[8] Σ (Greek S) has been chosen,—after much discussion (the use of Greek X was at first proposed),—for the projection of S, in spite of the other common uses of this symbol, because its use here is analogous to that of Λ (Greek L) for the projection of L, and to the use of the symbols Σ, Π, Δ, $\cdots$, (Greek S, P, D, $\cdots$,) for states with $\Lambda = 0, 1, 2, \cdots$, as compared with S, P, D, for $L = 0, 1, 2, \cdots$.

[9] Usually, for a given Λ, a given value of Ω occurs only once, but if $S > \Lambda$, one or more values of Ω occur twice. For example, if we have $\Lambda = 1$, $S = 1\frac{1}{2}$, we have $\Omega = 2\frac{1}{2}, 1\frac{1}{2}, \frac{1}{2}, \frac{1}{2}$ corresponding to $\Sigma = 1\frac{1}{2}, \frac{1}{2}, -\frac{1}{2}, -1\frac{1}{2}$.

[10] The component of angular momentum perpendicular to the electric axis, which in the text is for brevity called "the nuclear angular momentum," *is* really *mainly* angular momentum of the nuclei, but *also* includes small contributions from orbital (and spin, in cases *a* and *c*) angular momenta of the electrons. Cf. R. S. Mulliken, reference 5.

bers associated with the molecule as a whole in case a are thus v; L (sometimes, but never very rigorously quantized), Λ; S, Σ; Ω, J, M.

In case b we have Λ and S just as in case a, but S is not coupled to the electric axis, and there is no quantum number Σ. Case b exists whenever the magnetic field associated with Λ is too weak to couple S to the axis, a condition which is possible for any value of Λ, but which is automatically fulfilled when $\Lambda=0$. In case b, $\Lambda h/2\pi$ and the nuclear angular momentum[10] combine to give a quantized resultant (cf. Fig. 1). For the corresponding

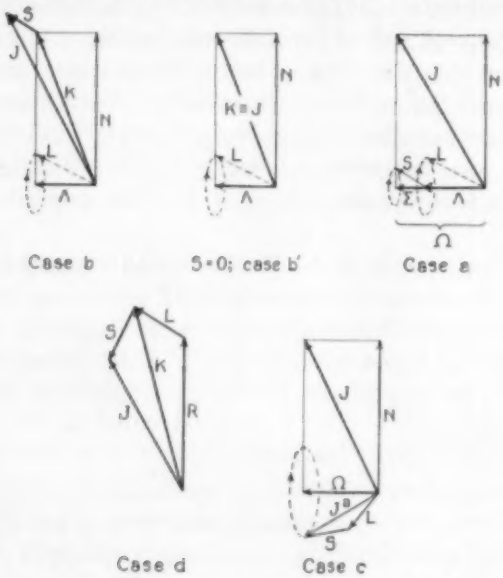

Fig. 1. Angular momentum vectors in Hund's cases a, b, c, d, expressed in units $h/2\pi$. In cases a, b, c, the angular momentum of the nuclear rotation[10] is represented by N, which is *not a quantum number*; in case d it is represented by the quantum number R. In all the figures, the horizontal base line perpendicular to N represents the direction of the electric axis (line joining the two nuclei). In cases a and b, Λ is shown as the projection of L, which is represented as precessing around the direction of Λ, i.e. around the electric axis; L is given by a dotted line to indicate that it is not rigorously quantized. In case a, Σ is shown as the projection of S, which is represented as precessing around the electric axis. In case c, Ω is shown as the projection of J^a (resultant of L and S), which is represented as precessing around the electric axis.[12a] In all cases, each pair of vectors which form a *resultant* must be thought of as precessing around the latter with a frequency which differs for each such pair. In each case, the only vector whose direction remains fixed is J. Precessing pairs are: Λ and N around J in the case $S=0$; Ω and N around J in cases a and c; Λ and N about K, and K and S about J, in case b; L and S about J^a in case c[12a]; R and L about K, K and S about J, in case d. [The use of N in Fig. 1 is not intended as a notation suggestion to be followed. In Ref. 5 the writer has used O where N appears here, and has used N with a somewhat different meaning than here.]

quantum number [formerly called p_l or j_k] *the designation K is now recommended.*[7] The possible values of K are $\Lambda, \Lambda+1, \Lambda+2, \cdots$. There is usually a small magnetic field in the molecule parallel to K, so that K and S form a resultant J (cf. Fig. 1).[7,11] The quantity $J-K$ is often called ρ; ρ is approxi-

[11] The combination of K and S to give J in a molecule is closely analogous to that of L and S to give J in an atom, and the designation K has been chosen with this in mind.

mately equal to the component of S parallel to J or K; ρ has sometimes been thought of as a quantum number, but this is incorrect. The splitting of a rotational level with given K into two or more levels differing in J might be referred to as ρ-type multiplicity (the expression "ρ-type doubling" has been in common use for the case $S=\frac{1}{2}$). This is, however, not recommended. Such an expression as "case b spin multiplicity" would be better.

In the presence of a "weak" external field J gives M. If the field is strong enough, however, the coupling of K and S is broken down (molecular Paschen-Back effect) so that J loses its significance, while K and S separately give projections for which *the designations* M_K and M_S (magnetic quantum numbers) *are recommended.* (M_K has as possible values, $K, K-1, \cdots -K$; M_S has values $S, S-1, \cdots -S$). Here $M = M_K + M_S$.

Sometimes the coupling of K and S in case b is practically zero; this situation can conveniently be distinguished as case b'. In case b', J is without significance. When $S=0$, cases a and b' become identical, as do K and J (cf. Fig. 1); here either K or J may be used to designate the resultant angular momentum; the designation K is the better in comparisons with case b' or b states with $S>0$, the designation J in comparisons with case a states.

Other coupling cases. In addition to cases a and b there are other less common cases which are nevertheless of sufficient importance to deserve consideration here. Hund's "case c" is an ideal limiting case in which L is assumed to be as rigorously quantized as in an atom, and, also, to be so strongly coupled to S as to give a quantized resultant as in an atom. *It is recommended that this resultant,* which in an atom would be called J, *be called* J^a in the case of a molecule.[12,12a] Λ and Σ here have no (quantum) meaning, but Ω is rigorously quantized, and is (the numerical value of) the projection of J^a on the electric axis. Ω has as possible values, $J^a, J^a-1 \cdots$ down to 0 or $\frac{1}{2}$ according as J^a is an integer or a half integer. Ω combines vectorially with the nuclear angular momentum to give J as in case a (cf. Fig. 1). In an external field J gives M.

In Hund's "case d," examples of which are found in the higher electron levels of H_2 and He_2, L is as rigorously quantized as in an atom,[13] but is unusually little influenced by the electric axis; so that it does not give a projection Λ on the axis. S also exists as usual, but it does not give a projection Σ. In case d the angular momentum of the *nuclei* by themselves is quantized; for this *the quantum number* R [same as Hund's p_r] *is recommended.* ($R=0, 1, 2, \cdots$). L is weakly coupled to R to give a resultant for which *the designa-*

[12] The superscript a serves to indicate the relation to the *atomic* J.

[12a] There is also another, probably more important, form of case c in which L, J^a, and even S are not at all rigorously quantized, and in which Ω is the only rigorous electronic quantum number of the molecule. This case is found in loosely-bound molecular states formed by the union of two atoms one or both of which when alone has its own L and S strongly coupled to each other.

[13] Actually in He_2 the relations are more complicated: we have essentially case b for the inner electron or electrons, but case d for the excited electron, whose l is coupled in accordance with case d to an R which is really the K of the He_2^+ ion.

tion K is recommended; K has the values $R+L$, $R+L-1$, $\cdots|R-L|$.[14] K and S may now combine vectorially to give J, exactly as in case b (cf. Fig. 1.). In external fields we have, (1) in "weak" fields, a quantum number M as in previous cases; (2) in "strong" fields, M_K and M_S as in case b; (3) in stronger fields, M_R, M_L, M_S. If, as is true in H_2 and He_2, the coupling of K and S is very small, J is lacking in significance, just as in case b'. When $S=0$, we have $K \equiv J$. In such cases, we may speak of case d'. The quantity $K-R$ in case d', like $J-K$ in case b (cf. above) is frequently called ρ; ρ is here approximately equal to the component of L parallel to K or R; it is not a quantum number.

As a variation on case d, we might have "case e," in which L and S are coupled to give a J^a as in case c, while J^a and R give a resultant J.

III. Term Symbols

For coupling cases approximating Hund's a or b, or intermediate between them, the use of the *symbols* Σ, Π, Δ, Φ, Γ, H, $\cdots$ *to indicate* $\Lambda=0, 1, 2, 3, 4, 5, \cdots$ *is recommended*. [Until recently the symbols $S, P, D, \cdots$ have been used for $\Lambda=0, 1, 2, \cdots$ as well as for $L=0, 1, 2, \cdots$.] In coupling cases resembling or tending toward case d, or also in theoretical discussions where a molecule is to be compared with the atom obtainable by uniting its nuclei, L values can be indicated by using the symbols $S, P, D, \cdots$ for $L=0, 1, 2 \cdots$. To indicate both L and Λ, symbols such as $P\Sigma$, $D\Pi$, etc., may be used.

The multiplicity (equal to $2S+1$) should be indicated, as in the case of atoms, by a superscript at the left, as $^1\Sigma$, $^2\Pi$, etc. In coupling cases approximating case a, *it is recommended that the value of* $\Lambda+\Sigma$ be indicated by a *subscript at the right.*[15] (For singlet states, however, no subscript is needed, since $\Sigma=0$ always, so that $\Lambda+\Sigma=\Lambda$; while for case b states no subscript is possible, since a quantum number Σ does not exist). Examples, $^1\Sigma$, $^1\Pi$, $^2\Sigma$, $^3\Delta_2$, $^4\Pi_{2\frac{1}{2}}$, $^4\Pi_{1\frac{1}{2}}$, $^4\Pi_{\frac{1}{2}}$, $^4\Pi_{-\frac{1}{2}}$.[16]

There are two kinds of Σ states, which differ in respect to the symmetry of their wave-functions with respect to a plane through the line joining the nuclei. In the one kind the *electronic factor* of the wave-function ψ (corresponding to the motion of the electrons with reference to the nuclei) is unchanged on reflection in such a plane, in the other kind it changes sign.

[14] K in case d has a somewhat different physical meaning than K in case b, but is exactly like the latter in that it combines with S to give J. Further, there is a one to one correspondence between the K values in case d and those in case b, and K is quantized throughout the whole range of intermediate cases.

[15] The recommendation that the value of $\Lambda+\Sigma$, rather than that of Ω, be used for the subscript in molecular multiplets is based on the fact that when $S>\Lambda$, $\Lambda+\Sigma$ takes on negative as well as positive values. In such cases [none of which, however, have yet been observed] it would not suffice to specify Ω, since $\Omega=|\Lambda+\Sigma|$. In $^4\Pi$ states, for example, we should have $\Omega=\frac{1}{2}$ for both $^4\Pi_{\frac{1}{2}}$ and $^4\Pi_{-\frac{1}{2}}$.[9] In this connection it may be well to remind the reader that in molecular multiplets, in contrast to many cases of atomic multiplets with $L>0$, the full multiplicity is always developed whenever $\Lambda>0$. For example, the molecular level $^4\Pi$ is quadruple (cf. reference 9) while the atomic ^4P is only triple.

[16] For subscripts which are multiples of $\frac{1}{2}$, either of the two forms such as $\frac{3}{2}$ or $1\frac{1}{2}$ may be used, but the second form ($1\frac{1}{2}$) is preferable for typographical reasons (cf. reference 2, p. 900).

It is recommended that these be distinguished, when one wishes, by calling them respectively Σ^+ and Σ^- states.[16a] [The designations Σ^+ and Σ^- respectively correspond to Σ and Σ' of Wigner and Witmer.[17,18]].

In the case of homonuclear molecules (molecules composed of atoms whose nuclei are identical in charge and mass), any electron state may be either "odd" or "even."[19] An electron state of a homonuclear molecule is said to be *odd* if the *electronic factor* of ψ changes sign on reflection in the midpoint of the line joining the nuclei, *even*, if it does not change sign.[19,19a] *It is recommended* that the odd or even character of an electron state, *when known*, and *if desired*, be indicated by a subscript at the right of the electronic term symbol. The subscripts *g* (German *gerade*) for even terms and *u* (German *ungerade*) for odd terms are recommended.[20] Examples, ${}^1\Sigma_g$, or ${}^1\Sigma_g^+$, or ${}^1\Sigma_g^-$, ${}^2\Sigma_u$;

[16a] Corresponding to the frequently used empirical designations such as Π_b and Π_a (cf. Section VI, Fig. 2, etc.), theoretical designations such as Π^+ (even terms[19a] when K is even) and Π^- (odd terms when K is even) might be introduced, in analogy to Σ^+ and Σ^-.

[17] E. Wigner and E. E. Witmer, Zeits. f. Physik, **51**, 859, 1928. In Σ^+ states the rotational levels with even values of K are "even" or "positive," those with odd K are "odd" or "negative," while in Σ^- states these relations are reversed.[19a]

[18] Wigner and Witmer's use of Σ where Σ^+ is proposed here is obviously undesirable, since the symbol Σ is needed to imply *merely* $\Lambda = 0$ in cases where one cannot, or does not wish to, decide between Σ^+ and Σ^-, as well as in general discussions. Wigner and Witmer's use of Σ' where Σ^- is proposed here is undesirable because of the frequent use of the prime ($'$), in the analysis of spectra, to denote the upper of two energy levels.

[19] The use of "odd" and "even" in this sense was introduced by Hund. Cf. the useful summary by W. Weizel, Zeits. f. Physik, **54**, 324–6 (1929).

[19a] The words even and odd are applied by Kronig, in a sense different from that used by Hund,[19] to the *complete* ψ function of any molecule, homonuclear or heteronuclear; a molecular term is odd or even in this sense according as its ψ function does or does not change sign on reflection in the origin of coordinates; this definition is the same as that which holds for odd and even atomic terms. Instead of "even" and "odd" Wigner uses "positive" and "negative" for atomic terms, and Wigner and Witmer (l.c., Ref. 17) for molecular terms.

In speaking of molecular terms, the designations "even" and "odd" (which may be abbreviated *g* and *u*, as in Fig. 2) may be preferred to "positive" and "negative" on two grounds: (1) they were introduced earlier (R. de L. Kronig, Zeits. f. Physik, **50**, 351, 1928), and (2) they refer to the same properties which in atoms are generally described by "even" and "odd." But "positive" and "negative" (which may be abbreviated + and −) may be preferred on other grounds: (1) they avoid possible confusion with the earlier-introduced and equally well-founded use of "even" and "odd" in another sense for electronic terms;[19a] (2) they avoid the confusing situation that molecular levels with even, or with odd, K values may be either "even" or "odd." In Fig. 2 and elsewhere in this report, "even" and "odd" are used, but the writer now intends personally to use "positive" and "negative."

[20] In the report on line spectra (reference 2), it was suggested that a superscript° (degree mark) always be used for odd terms, and *no* superscript for even terms. It may be that this precedent should be followed, although "odd" and "even" do not have just the same meaning here as in atoms. But this would hardly be feasible anyway in molecular spectra, since in some cases we do not yet *know* whether a term is even or odd. Further, there are many purposes for which the odd or even character is a matter of indifference, and it is desirable in such cases to be able to drop the superscript, without thereby implying that the term is even. The choice of *g* and *u* in preference to the English *e* (even) and *o* (odd) is based mainly on the fact that *e* is often used as a subscript for other purposes, as in E_e and r_e, while *o* is easily confused with zero.

The choice of the subscript position is governed by the fact that *g* and *u* are sometimes

$^2\Pi_{\frac{1}{2}g}$; $^3\Pi_u$. [The designations Σ_g^+, Σ_u^+, Σ_g^-, Σ_u^-, Π_u, Π_g, Δ_g, Δ_u, etc. as here proposed, respectively correspond to Σ_+, Σ_-, Σ'_+, Σ'_-, Π_+, Π_-, Δ_+, Δ_-, etc. of Wigner and Witmer.]

The term symbols just recommended are of course not sufficient to identify completely the electronic state of a molecule. This purpose can be accomplished by the use of an identifying symbol of an empirical character, as for example A, B, X, a, etc.; or by the use of a symbol describing the electron configuration (cf. section IV, below.) *It is recommended* that such symbols be placed before the symbol giving S, Λ and Σ, as in the following examples: $A\ ^3\Pi_2$; $X\ ^1\Sigma$; $1s\sigma^2 2p\sigma 2s\sigma\ ^3\Sigma$ (if the meaning is clear from the context, this last may be abbreviated to $2s\sigma\ ^3\Sigma$ or $2s\ ^3\Sigma$). These and similar designations can be adapted to the individual case, and varied to suit the need of experimentalist and theorist.

If one desires to express the relation of a molecular electronic state to the states of its atomic dissociation products, it is suggested that designations such as the following be used: $X\ ^1\Sigma(^2S+^2P)$. Here ^2S and ^2P represent the states of the two atoms. If desired, the electron configurations of atoms and molecule can also be given.

Some writers have used a superscript number, appended to the electronic term symbol, to indicate v. Example, $^3\Sigma^2$, for $v=2$. It is suggested that this practice be avoided if possible, and that simpler, although longer, expressions such as "the level $v=2$ of $^3\Sigma$" be used. In case, however, a necessity is felt for including v in the term symbol, it is suggested that this be given as a superscript *in parentheses to indicate* that it represents an element foreign to the rest of the symbol. Examples, $^3\Sigma^{(2)}$; $^3\Sigma_g^{-(2)}$.

If one needs to give the rotational quantum number (K or J) as well as v, it may be given in parentheses as in the following example: $^3\Sigma^{+(1)}$ (10), for $v=1$, $K=10$.

IV. Quantum Numbers for Individual Electrons; Electron Configurations

The designation Λ was recommended above as the quantum number for the component, parallel to the electric axis, of the resultant orbital angular momentum of the entire electron system. The *designation* λ *is now recommended* [to replace the former designation i_{l_τ} or σ_{l_τ} or σ_{k_τ}] for the corresponding quantum number for an *individual electron*.[21] It is *recommended* further

needed for *individual electrons* (cf. Section IV below), as in σ_g, σ_u, π_g, etc., where the superscript position would lead to awkwardness in the symbols for electron configurations. For example, $\sigma_g^2\sigma_u^2\pi_u^4$ is much less awkward than $\sigma^{g2}\sigma^{u2}\pi^{u4}$. It is also preferable in such symbols as $^2\Sigma_g^+$, $^2\Sigma_u^{+(1)}$, etc. In cases such as $^2\Pi_{\frac{1}{2}g}$ it is not so good, but also not very bad, and furthermore, one is usually not interested in the $\frac{1}{2}$ and the g at the same time, so that one will usually write just $^2\Pi_{\frac{1}{2}}$ or else $^2\Pi g$, depending on the nature of the discussion.

[21] The quantization leading to the assignment of λ values for individual electrons is rigorous only to the extent that the interactions of the electrons with one another can be replaced by an axially symmetrical electric field. Ordinarily, however, the assignment of individual λ *values in molecules* should be about as justifiable as the assignment of individual l *values in atoms.*

that electrons having $\lambda = 0, 1, 2, 3, 4, 5, \cdots$ be respectively *designated* σ, π, δ, ϕ, γ, η, $\cdots$ electrons. [These were formerly named $s, p, d, \cdots$ electrons by the present writer, although not with the same meaning as $s, p, d, \cdots$ in atoms.]

Under some circumstances quantum numbers n, l, and s can also be assigned to the individual electrons in a molecule, just as to those in an atom. In Hund's case d these quantum numbers have practically the same meaning as in an atom (examples, excited orbits of series electron in H_2, He_2).[22] Ordinarily, however, n and l are not at all rigorous quantum numbers and have a definite meaning only in terms of some ideal limiting case, such as that of the atom which would be obtained ("united-atom") if one could unite the two nuclei of the molecule.[22,23] To designate the values of l in a molecule the symbols $s, p, d, \cdots$ *are recommended* for $l = 0, 1, 2$, just as in the case of an atom. When n, l, and λ are all to be indicated for an electron, *symbols such as* $2p\sigma$, $3s\sigma$, $3p\pi$, $4d\sigma$, $\cdots$ *are recommended*; the number represents n. [In the notation formerly used by the present writer, the equivalents of these symbols are $2s^p$, $3s^s$, $3p^p$, $4s^d$, $\cdots$ respectively.][24] When several electrons (1, 2, 3, $\cdots$) are present, their several values of n, l, λ can be indicated, if desired, by numerical subscripts, as $l_1, l_2, \cdots \lambda_1, \lambda_2$, etc.

The quantum number λ represents the projection of l on the electric axis of the molecule.[7] Ordinarily any λ is considered a positive quantity, but in a molecule with several electrons some of the λ's must be considered as having a negative sign. Λ is then the algebraic sum of the individual λ's. Those individual λ's whose direction is opposite to Λ are regarded as having a negative sign.

Even when the assignment of an l value to an electron has little meaning there is still, *in symmetrical molecules*, a definite distinction between *odd* and *even* states of an electron. Thus one may speak of σ_g, σ_u, $\pi_u, \pi_g, \cdots$ etc. electrons. Insofar as an l can be assigned, an even value of l always gives an even type of electron (σ_g, π_g etc.), and an odd value of l an odd type.—In a similar way, the even or odd character of the resultant electron state of a symmetrical molecule is determined, like that of an atom, by the (*arithmetic*) sum of the individual l values. If this sum is even, the term is even (Σ_g, Π_g, $\cdots$ etc.), and conversely.

Often one may wish to indicate not the "united-atom" values of l and n for an electron, but the values of l and n which the electron would have if the molecule were separated into its atoms. For this purpose, symbols such as $\sigma(1s)$, $\sigma_g(2p)$, $\pi(2p)$, etc., are suggested. Here the symbol σ or π gives the

[22] For the series electron in H_2 and He_2, most of the orbits are large compared with the distance between the nuclei, so that "united-atom" conditions are closely approximated.

[23] In terms of spherical coordinates (r, θ, φ) as in the ideal limiting case of the "united-atom," l is defined as $n_\theta + n_\phi$, where n_θ and n_ϕ are quantum numbers associated with θ and φ. In terms of elliptical coordinates (ξ, η, φ), as in another ideal limiting case where the electrons move under the influence of two point charges (as in H_2^+), l is defined as $n_\eta + n_\theta$ ($\eta =$ const. is a hyperboloid of revolution).

[24] The symbols $2s^p$ etc. were introduced by the present writer (Phy. Rev. **32**, 186, 1928); $2p\sigma$, etc. by F. Hund. (Zeits. f. Physik, **51**, 759, 1928).

value of λ for the electron in the molecule, while the symbol in parentheses describes the state of the electron as it would exist in one of the atoms on dissociation of the molecule.

Electron configurations. A rather complete description of the state of a molecule is possible if the term symbol, which gives the quantum numbers associated with the molecule as a whole, is preceded by a set of symbols giving the electron configuration. Examples: $1s\sigma^2 2p\sigma^2 2s\sigma^2 2p\pi^3\ ^2\Pi$; or more briefly, $\sigma^2\sigma^2\sigma^2\pi^3\ ^2\Pi$; or, if the molecule is symmetrical, $\sigma_g^2\sigma_u^2\sigma_g^2\pi_u^3\ ^2\Pi_u$. The electron configuration designations used here are similar to those used in line spectra. Such a symbol as $1s\sigma^2$ really means $(1s\sigma)^2$, i.e., it indicates the presence of two $1s\sigma$ electrons; while σ^2 indicates any two σ electrons of identical type (equivalent σ electrons). The order in which successive symbols are written is that of decreasing firmness of binding.—Such a symbol as $\sigma^2\sigma^2\sigma^2\pi^3$ rather than $1s\sigma^2 2p\sigma^2 2s\sigma^2 2p\pi^3$ is often to be preferred, since the assignment of definite n and l values is usually rather lacking in meaning. The symbol $\sigma^2\sigma^2\sigma^2\pi^3$ signifies the existence of three different kinds of σ electrons without attempting to describe them in detail.

V. Symbols for Molecular Constants

The energy E of a diatomic molecule is commonly written as a sum of three parts (for exact definitions, cf. Section VI):

$$E = E_e + E_v + E_r \tag{1}$$

Here E_e is the "electronic energy," E_v is the "vibrational energy," and E_r is the "rotational energy."

For the energy of a molecule in a singlet state[25] we had according to the old quantum theory (using, however, the new symbols v and J in place of n and j)[26]

$$E = E_e + hc[\omega_0 v - x\omega_0 v^2 + y\omega_0 v^3 + \cdots] + hc[B_v(J^2 + \text{const.}) + D_v J^4 + F_v J^6 + H_v J^8 + \cdots] \tag{2}$$

Here the first expression following E_e represented E_v, the second E_r. In Eq. (2), we had

$$B_v = B_0 - \alpha v + \gamma v^2 + \cdots, \text{ where } B_0 = h/8\pi^2 c\mu r_0^2 = h/8\pi^2 c I_0. \tag{3}$$

Also,

$$D_v = D_0 + \beta v + \cdots, \text{ where } D_0 = -4B_0^3/\omega_0^2. \tag{4}$$

In Eqs. (2)–(4), the subscript zero attached to a coefficient implied that this coefficient corresponded to $v=0$. *At the same time*, since the energy of vibra-

[25] The "*const.*" in (J^2+*const.*) depends on the electronic motions (cf. R. S. Mulliken, ref. 5, Eq. (29)). Small constants should also be added to the terms in J^4, etc.; and other small terms should be added.

[26] The notation used for the coefficients in Eqs. (2)–(4) etc. is mainly that which is now most usual. Instead of ω_0 one often finds ν_0 or ω^0; instead of D_v, $-\beta$. The designation $y\omega_0$ in Eq. (2) and γ in Eq. (3) are not in common use, but have been introduced here to supply an existing lack. No *recommendation* of this use of y and γ is intended here.

tion was supposed to be zero when $v=0$, it implied a molecule with stationary nuclei in a state of *equilibrium*. Thus $c\omega_0$ was supposed to represent the frequency of vibration for $v=0$, and so the limiting frequency for infinitesimal amplitudes. Similarly B_0 referred to $v=0$, and so supposedly to a molecule in equilibrium; and the quantities r_0 and I_0 calculated by means of Eqs. (3) likewise were supposed to correspond to a molecule in equilibrium.

According to the new quantum theory, however, Eqs. (2)–(4) must be replaced by equations of the following form:[26a]

$$E = E_e + hc\{\omega_0(v+\tfrac{1}{2}) - x\omega_0(v+\tfrac{1}{2})^2 + y\omega_0(v+\tfrac{1}{2})^3 + \cdots\} + hc\{B_v[(J+\tfrac{1}{2})^2 + \text{const.}] + D_v(J+\tfrac{1}{2})^4 + \cdots\} \quad (2a)$$

$$B_v = B_0 - \alpha(v+\tfrac{1}{2}) + \gamma(v+\tfrac{1}{2})^2 + \cdots, \text{ where } B_0 = h/8\pi^2 c\mu r_0^2 = h/8\pi^2 c I_0 \quad (3a)$$

$$D_v = D_0 + \beta(v+\tfrac{1}{2}) + \cdots, \text{ where } D_0 = -4B_0^3/\omega_0^2. \quad (4a)$$

If one assumes the validity of Eqs. (2a)–(4a) one gets somewhat *different numerical values* for E_e, ω_0, x, B_0, r_0, I_0, etc. than if one assumes Eqs. (2)–(4). In the literature most of the recorded values are based on Eqs. (2)–(4), although in some recent articles Eqs. (2a)–(4a) have been used as a basis of calculation. Thus the same symbols are now being used in different articles in two different ways, with resulting confusion on the part of the reader.

To remedy this situation a *revision of nomenclature is suggested*, at least for discussions dealing with the analysis of band spectra, such that Eqs. (2a)–(4a) are replaced by the following Eqs. (2c)–(4c).[26,26a,27,28] At the same time, equations of the form of Eqs. (2)–(4), except for the substitution of $(J+\frac{1}{2})^2$ for J^2, may usefully be retained (Eqs. 2b–4b).[29] Eqs. (2b)–(4b) represent the more useful form for the empirical description of spectra, Eqs. (2c)–(4c) for the analysis of the isotope effect and for the theoretical application of band spectrum data as in the construction of $U(r)$ curves (cf. second paragraph following).

$$E = E_0 + hc[\omega_0 v - x\omega_0 v^2 + y\omega_0 v^3 + \cdots] + hc\{B_v[(J+\tfrac{1}{2})^2 + \text{const.}] + D_v(J+\tfrac{1}{2})^4 + \cdots\} \quad (2b)$$

$$B_v = B_0 - \alpha v + \gamma v^2 + \cdots \quad (3b)$$

$$D_v = D_0 + \beta v^2 + \cdots \quad (4b)$$

$$E = E_e + hc\{\omega_e(v+\tfrac{1}{2}) - x_e\omega_e(v+\tfrac{1}{2})^2 + y_e\omega_e(v+\tfrac{1}{2})^3 + \cdots\} + hc\{B_v[(J+\tfrac{1}{2})^2 + \text{const.}] + D_v(J+\tfrac{1}{2})^4 + F_v(J+\tfrac{1}{2})^6 + \cdots\} \quad (2c)$$

[26a] Although the form $(J+\frac{1}{2})^2$ is used here, it is immaterial to the present discussion whether this or the rival form $J(J+1)$ is used.

[27] The use of the symbol E for energy, as in E and E_0, although it seems desirable, is not definitely included in the recommendations made here.

[28] The coefficients of Eqs. (2b)–(4b) are related to those of Eqs. (2c)–(4c) as follows: E_0 (Eq. 2b) $= E_e$ (Eq. 2c) $+ hc\,[\frac{1}{2}\omega_e - (1/4)\,x_e\omega_e + (1/8)\,y_e\omega_e + \cdots]$; $\omega_0 = \omega_e\,[1 - x_e + (3/4)\,y_e + \cdots]$; $x\omega_0 = \omega_e[x_e - (3/2)\,y_e + \cdots]$; $y\omega_0 = \omega_e\,(y_e + \cdots)$; etc.

[29] The quantities r_0 and I_0 calculated as in Eq. (3) are no longer of much interest, since they are not empirical coefficients, nor have they the theoretical importance of r_e and I_e.

$B_v = B_e - \alpha_e(v+\frac{1}{2}) + \gamma_e(v+\frac{1}{2})^2 + \cdots$, where

$B_e = h/8\pi^2 c\mu r_e^2 = h/8\pi^2 cI_e$ (3c)

$D_v = D_e + \beta_e(v+\frac{1}{2}) + \cdots$, where $D_e = -4B_e^3/\omega_e^2$. (4c)

The coefficients ω_e, B_e, etc. and the quantities I_e and r_e (and E_e) refer to a molecule with stationary nuclei in equilibrium; such a molecule, however, in contrast to the state of affairs in the old quantum theory, would *not* at the same time have $v=0$. B_0, D_0, E_0, etc., refer to a molecule with $v=0$.[29]

For the *energy of dissociation* of a molecule, the symbol D has been widely adopted. To be accurate, one must distinguish D_e, the energy of dissociation for the imaginary case of a molecule with nuclei stationary at the distance r_e; and D_0 or D, the energy of dissociation from the actual lowest energy level of the molecule ($v=0$). The values of D for various states of a molecule may be conveniently distinguished by putting identifying designations in parentheses, as $D(X)$ or $D(X\,^1\Sigma)$; $D(A\,^3\Pi)$; etc. In all cases the symbol D should stand for the energy of dissociation alone, and should not include, in the case of an excited electron state, the energy of excitation.

If the energy of a molecule in a definite electron state, with nuclei held stationary, is expressed as a function $U(r)$ of the distance between the nuclei, then $E_e \equiv U(r_e)$, while the dissociation energy $D_e \equiv U(\infty) - U(r_e)$. Also, $4\pi^2\mu c^2\omega_e^2 = (d^2U/dr^2)_{r=re}$

It may eventually be worth while to discard the heterogeneous and cumbersome set of symbols B_v, D_v, α, β, ω_e, $x_e\omega_e$, etc.[26] in favor of a simpler set. If, or when, this is done, the double use of D for heat of dissociation and for the coefficient of $(J+\frac{1}{2})^4$ might well be done away with. One might perhaps use d_v instead of D_v in the E_r expression (also, for consistency, f_v instead of F_v and possibly also b_v instead of B_v). This would, however, interfere with the possible future use of a, b, c, $\cdots$ in place of ω_e, $x_e\omega_e$, $y_e\omega_e \cdots$ in Eq. (2c), or perhaps better in place of ω_0, $x\omega_0$, $y\omega_0$, $\cdots$ in Eq. (2b); a, b, $\cdots$ have already often been used in this way.

VI. Description and Analysis of Spectra

Term designations. In the analysis of spectra, one is usually concerned with the determination of energy values (E) or term-values (E/hc) through the use of the relation $\nu = (E'-E'')/hc$. The prime ($'$) and double prime ($''$) are used merely to indicate that $E'>E''$.[27] *It is recommended that the prime and double prime* be always used in a similar manner when one wishes to distinguish the *upper* and *lower* of two energy levels involved in the production of the lines of a band spectrum, and that this method be applied to all quantum numbers and coefficients pertaining to these energy levels. In discussing spectra, it is best to avoid where possible the expressions "initial" and "final" levels, since in terms of E' and E'' these have opposite meanings in absorption and emission spectra.

In the analysis of spectra, it is convenient to have a symbol to denote term-values. *It is suggested* that T be used for this purpose ($T \equiv E/hc$).[30] For

[30] The symbol F has sometimes been used for E/hc. (The present writer has in fact used this, and also F^{el} for E_e/hc, F^v for E_v/hc, and F^r for E_r/hc). But F has *usually* been used

the upper and lower levels involved in the production of a spectrum line, T' and T'' would be used.

In dealing with the analysis of a particular spectrum, the symbol T, followed by the rotational quantum number designation in parentheses, also the vibrational quantum number, if desired, as a superscript in parentheses, is suggested as a convenient symbol. Examples: $T(8)$, $T^{(2)}(8)$; also, $T_1(8\frac{1}{2})$, $T_{2a}(7\frac{1}{2})$, $T_a(9)$, etc., using numerical and literal subscripts in a manner to be discussed below in connection with the symbol F(cf. paragraphs following Eq. (7)).

For some purposes it is extremely convenient to have separate symbols for "electronic terms" (E_e/hc), "vibrational terms" (E_v/hc), and "rotational terms" (E_r/hc). *It is suggested* that the symbols G and F be used for vibrational and rotational terms respectively.[30] For electronic terms the symbol T_e *is suggested*. Thus we have, paralleling Eq. (1),

$$T = T_e + G + F. \tag{5}$$

Definitions of electronic, vibrational, and rotational energies and terms. It is important to define with some care the quantities F, G, and T_e, or the corresponding quantities E_r, E_v, and E_e. The following definitions appear to be unambiguous.

(1) The energy E_r is the difference between the energy of the actual molecule and that of an idealized molecule obtained by the following imaginary process: the rotation of the nuclei is gradually stopped without placing any new constraint on the vibration of the nuclei or on the electron motions, in such a way as might be realized by gradually (i.e. adiabatically) coupling an infinite moment of inertia to the axis of rotation of the molecule. In Eqs. (2c)–(4c), B_v and all the coefficients of powers of $(J+\frac{1}{2})^2$ then go to zero.

(2) The energy E_v is the difference between the energy of a molecule idealized just to the extent of making $E_r=0$ and the energy of a further idealized molecule obtained by the following imaginary process: the vibration of the nuclei is gradually stopped without placing any new constraint on the electron motions, in a way such as might be realized by leaving the charges of the nuclei unchanged but gradually increasing the masses until they are infinite. In Eqs. (2b)–(4b), ω_e and all the coefficients of powers of $(v+\frac{1}{2})$ then go to zero.

(3) The energy E_e is the total internal energy of a molecule in a definite electronic state with the nuclei stationary (this condition may be realized in imagination by making the masses infinite) at their equilibrium distance (r_e) apart. E_e consists of (a) kinetic energy of the electrons, plus (b) their potential energy with respect to the nuclei and to one another, plus (c) the mutual potential energy of repulsion of the two nuclei. As was mentioned above, $E_e \equiv U(r_e)$.

---

with the meaning E_r/hc, and this usage is therefore recommended here (cf. Eq. (5)). The use of T for E/hc (or for $-E/hc$, measured from an arbitrary zero of energy at ionization) has been frequent in the field of line spectra. The use of G for E_v/hc (cf. Eq. (5) and ref. 38) was suggested by Birge and recommended in the National Research Council Report on Molecular Spectra, but this recommendation has not been widely followed.

Rotational term differences. In the analysis of band spectra, it is customary to use such designations as $\Delta F(J)$, $\Delta_1 F(J)$, $\Delta_2 F(J)$ for the difference between two rotational terms differing only in the value of J. [Formerly Δf and ΔF were often used to distinguish these term intervals respectively for the upper and lower of the two electron levels involved, but it is recommended that this distinction be made only by the use of ($'$) and ($''$), as in $\Delta F'$, $\Delta F''$].

It is recommended that in designating rotational term intervals, the forms which are defined in the following equations be used:[31,32]

$$\Delta_1 F(J + \tfrac{1}{2}) = F(J + 1) - F(J) \tag{6}$$

$$\Delta_2 F(J) = F(J + 1) - F(J - 1). \tag{7}$$

Examples,

$$\Delta_1 F(3\tfrac{1}{2}) = F(4) - F(3); \quad \Delta_2 F(4) = F(5) - F(3).$$

In all states with $\Lambda > 0$ there are, for a given value of Σ and of J in case a, or of K and of J in case b, two rotational levels (cf. Fig. 2). (These are usually

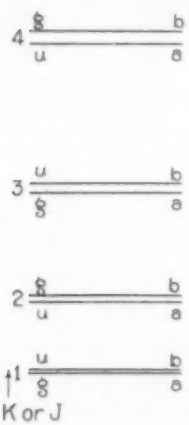

Fig. 2. Λ-type doublets for the case $S = 0$, $\Lambda = 1$. The order shown for the g and u levels represents only one of two possibilities; the case in which $1(g)$ lies above $1(u)$, $2(u)$ above $2(g)$, and so on, is the other (g and u respectively stand for even and odd[19a]). There is also no fixed rule as to the relative position of a and b levels; nor is there any fixed rule for correlating the a, b, and the g, u descriptions (cf. references 35, 36, 19a).

very close together, but separate widely on approach to case d). This doubling may be called Λ-*type doubling* because it occurs if, and only if, $\Lambda > 0$. [It was formerly, but less correctly, called "σ-type doubling," where "σ" is a former designation for our present Ω.[33]] It is suggested that, in each

[31] $\Delta_1 F(J+\frac{1}{2})$ and $\Delta_2 F(J)$ may be read as "delta one $F\ J+\frac{1}{2}$" and "delta two $F\ J$."

[32] $\Delta_1 F(J+\frac{1}{2})$ is commonly denoted by $\Delta_1 F(J)$, but the use of the symbol $\Delta_1 F(J+\frac{1}{2})$ as in Eq. (6) seems preferable. In practise, $\Delta_1 F(J+\frac{1}{2})$ is much less important then $\Delta_2 F(J)$, since $\Delta_1 F(J+\frac{1}{2})$ cannot be directly and exactly evaluated from the analysis of a spectrum; instead one usually obtains $F_a(J+1) - F_b(J)$, or $F_b(J+1) - F_a(J)$.

[33] The name "σ-type-doubling" was given by the writer before Hund's development of the theory of molecular electronic states, and was based on the idea that this type of doubling occurs whenever $\sigma > 0$ [in the present symbols, whenever $\Omega > 0$]. Later Hund showed that this doubling is to be expected, not whenever $\Omega > 0$ but whenever $\Lambda > 0$. *Usually* $\Lambda > 0$ and $\Omega > 0$

rotational doublet of this kind, the component levels be distinguished as a and b sublevels,[34] and that the term values be distinguished by corresponding subscripts, as, $T_a^{(v)}(J)$, $T_b^{(v)}(J)$, $F_a(J)$, $F_b(J)$.[16a,35,31] For rotational term differences, we have then $\Delta_2 F_a(J)$, $\Delta_2 F_b(J)$, $\cdots$ etc.

In case b, it is necessary to provide a means of indicating both K and J. The writer[35a] suggested the use of the symbols F_1, F_2; $\Delta_1 F_1$, $\Delta_1 F_2$; $\Delta_2 F_1$, $\Delta_2 F_2$ for case b with $S=\frac{1}{2}$, where F_1 refers to the terms with $J-K=+\frac{1}{2}$ and F_2 to $J-K=-\frac{1}{2}$. For $S=1$, the suggested symbols were F_1, F_2, F_3, for $J-K=+1$, 0, -1 respectively. These suggestions are now renewed,[35b] with the added suggestion that this use of numerical subscripts be applied both to the rotational terms F and to the complete terms T; when $\Lambda>0$, a and b subscripts are needed in addition to the numerical subscripts. Examples, $T_1^{(v)}(J)$; $T_{2a}^{(v)}(J)$; $F_{2b}(J)$; $\Delta_2 F_1(J)$; $\Delta_2 F_{1a}(J)$; $\Delta_2 F_{2b}(J)$; $\Delta_2 F_{2a}(J)$, etc.; specifically, $\Delta_2 F_{1a}(5\frac{1}{2})$ would mean $F_{1a}(6\frac{1}{2}) - F_{1a}(4\frac{1}{2})$, with the K values 6 and 4. Sometimes when K is the important rotational quantum number, J is lacking in significance (case b', cf. Section II above). In such a case, one naturally will use such forms as $\Delta_2 F(K)$, $\Delta_2 F_a(K)$. Also when $S=0$, so that $J \equiv K$, one *may* use K instead of J as the argument of a ΔF expression.

Vibrational term differences. It is suggested that in designating vibrational term differences, the forms which are defined in the following equations be used:[37]

$$\Delta G(v+\tfrac{1}{2}) = G(v+1) - G(v) \tag{6}$$

$$\Delta^2 G(v) \left[\equiv \Delta G(v+\tfrac{1}{2}) - \Delta G(v-\tfrac{1}{2}) \right] = G(v+1) - 2G(v) + G(v-1). \tag{7}$$

---

go hand in hand. A familiar exception is $^3\Pi_0(\Lambda=1, \Omega=0)$. Experimentally this shows Λ-type doubling as predicted by Hund.

[34] The use of the designations A and B was suggested by the present writer (Phys. Rev., **30**, 791, 1928). Some people have followed this suggestion, others have substituted a and b. The difference is not essential, but a and b seem to be preferred by the majority. (These designations have nothing to do with Hund's cases a and b).

[35] The designations a and b are essentially temporary empirical labels, and have no *definite* relation to any designations of theoretical significance (but cf. ref. 36). For two formal schemes for choosing which levels to call a and which to call b, cf. (1) R. S. Mulliken, Phys. Rev. **28**, 1205 (1926) and (2) R. S. Mulliken, Phys. Rev. **30**, 791 (1927). Some writers follow the first scheme, more the second. Both schemes lead to the same use of the labels a and b in the case of Π states, but give opposite labellings in the cases of Σ and of Δ states.

[36] The division into a and b levels is related to the theoretical division (cf. Ref. 19a and Wigner and Witmer, l.c. Ref. 17) of all molecular terms into even or positive and odd or negative terms. In the case of Π states, if *either* of the methods of labelling mentioned in ref. 36 is followed, the result is *usually* that in the b set of sub-levels, the even-numbered levels are even and the odd-numbered are odd; in the a set of sub-levels, the relations are always the reverse of those in the b set. The nature of the correlation between a and b and even and odd levels is illustrated in Fig. 2. For the case of Σ levels, cf. reference 18. In the case of Δ, Φ, $\cdots$ levels, the relations are of the same type as in Π levels.

[35a] Cf. R. S. Mulliken, Phys. Rev. **30**, 788 (1927).

[35b] A more logical method would be to use the values of $J-K$ as subscripts, as in $F_{+\frac{1}{2}}(J)$, $F_{-\frac{1}{2}a}(J)$, $\Delta_2 F_{+\frac{1}{2}}(J)$, $Q_{-\frac{1}{2}-\frac{1}{2}}(J)$, instead of $F_1(J)$, $F_{2a}(J)$, $\Delta_2 F_1(J)$, $Q_{12}(J)$. But since the present notation is simple and reasonably satisfactory, it does not seem wise in this report definitely to suggest a change.

[37] $\Delta G(v+\frac{1}{2})$ and $\Delta^2 G(v)$ may be respectively read as "delta $Gv+\frac{1}{2}$" and "delta second Gv."

Examples, $\Delta G(3\frac{1}{2}) = G(4) - G(3)$; $\Delta^2 G(4) = \Delta G(4\frac{1}{2}) - \Delta G(3\frac{1}{2}) = G(5) - 2G(4) + G(3)$. It will be seen that the argument of ΔG is always a half-integer midway between the v values (always integers) of two energy levels, while the argument of $\Delta^2 G$ is always an integer. [$\Delta G(v+\frac{1}{2})$ as here used is synonymous with Birge's $\Delta G_{v+\frac{1}{2}}$ and with $\omega_{v+\frac{1}{2}}$ as introduced by Birge and Sponer.[38]]

Band and system origins. In describing a band spectrum, it is convenient to consider the frequency of each line as a sum of three parts, just as it is convenient to consider the energy and the term-value each as a sum of three parts (cf. Eqs. (1), (5)). Thus for the wave number ν we may write[39]

$$\nu = T' - T'' = (T_e' - T_e'') + (G' - G'') + (F' - F'') = \nu_e + \nu_v + \nu_r. \quad (8)$$

The concepts of the "origin" of a band and of a band system are frequently used in theoretical discussions. These can be unambiguously defined as follows:[39]

$$\text{System-origin: } \nu = \nu_e$$

$$\text{Band-origin: } \nu = \nu_e + \nu_v.$$

These definitions do not in general correspond to wave-number positions which are of importance in the analysis of band spectra, except in the study of the isotope effect. Band and system origins are discussed here only in order to remove possible misconceptions as to their meaning.

In *simple types* of bands, an equation for the band lines can often be given in the form

$$\nu = \nu_0 + aM + bM^2 + \cdots, \quad (9)$$

where M is a parameter which takes on positive and negative integral or half-integral values, related to values of K'' or J''. The line given by $\nu = \nu_0$, and often other lines, are ordinarily missing. In the simplest cases, ν_0 is approximately the same as $\nu_e + \nu_v$, but the agreement is never exact if we use accurate expressions for E_e, E_v, and E_r; and the difference between ν_0 and $\nu_e + \nu_v$ varies from one type of band to another. The term "band-origin" is often loosely applied to ν_0, but it is evident that this usage is inaccurate and tends to produce confusion.

In a system of bands, the band origins can be expressed by the equation

$$\nu_e + \nu_v = \nu_e + \omega_e'(v' + \tfrac{1}{2}) - \omega_e''(v'' + \tfrac{1}{2}) - x_e'\omega_e'(v' + \tfrac{1}{2})^2 + x_e''\omega_e''(v'' + \tfrac{1}{2})^2 + \cdots. \quad (10)$$

The origin of the 0, 0 band (obtained by putting $v' = 0$, $v'' = 0$ in Eq. 10) obviously does not coincide with the origin of the band system ($\nu = \nu_e$). If

[38] For the original proposal to use ΔG, cf. the National Research Council Report on Molecular Spectra, p. 123, Eq. (76). (In Eq. (76) the old symbol n appears instead of v.) In regard to $\omega_{v+\frac{1}{2}}$ cf. R. T. Birge and H. Sponer, Phys. Rev. **28**, 259, (1926).

[39] Where ν_v, ν_r are used here, other designations such as ν_n, ν_m are frequently used. No definite recommendation of ν_e, ν_v, and ν_r is intended here, although they are preferred by the present writer. It is pretty obvious, however, that ν_n and ν_m should be dropped, since their subscripts are the now discarded symbols n and m formerly used for the vibrational and rotational quantum numbers.

the old quantum theory formula for E_v (cf. Eq. (2)) were correct, the system-origin *would* coincide with the origin of the 0, 0 band. In existing tables of band spectrum data, based on the old quantum theory formulation, the origin, or even the ν_0 position, of the 0, 0 band is in fact commonly referred to as the system-origin.[39]

Designations for band systems and bands. For designating a transition between two electronic states, it is suggested that the following forms be used: $^2\Pi \rightarrow {}^2\Sigma$ for emission bands (to be read "$^2\Pi$ to $^2\Sigma$"); $^2\Pi \leftarrow {}^2\Sigma$ for absorption bands (this might be read "$^2\Pi$ from $^2\Sigma$"); and simply $^2\Pi$, $^2\Sigma$ in general discussions. It is recommended that the equivalent form $^2\Sigma - {}^2\Pi$, which is analogous to atomic symbolism such as $1s-2p$, be abandoned.[40] In the suggested symbols, the *first mentioned* (here $^2\Pi$) always refers to the state of higher energy.

In indicating the two vibrational levels concerned in the production of a particular band, one speaks of the (0, 3) band, the (5, 2) band, and so on, where the first number refers to v', the second to v''. Usually the parentheses can safely be dropped, so that one can write "the 0, 3 band," and so on.

Designations for band-lines. The lines of a band can always be divided into one or more series ("branches"). For all the lines in one branch, $J'-J''$ (also $K'-K''$ in case b) has a constant value. *It is recommended* that the symbols O, P, Q, R, S be used, in a way now to be described, to denote various types of branches. In *case a*, we define

$$\begin{aligned}
O(J) &= T'(J-2) - T''(J) = \nu_e + \nu_v + F'(J-2) - F''(J) \\
P(J) &= T'(J-1) - T''(J) = \nu_e + \nu_v + F'(J-1) - F''(J) \\
Q(J) &= T'(J) \quad - T''(J) = \nu_e + \nu_v + F'(J) \quad - F''(J) \\
R(J) &= T'(J+1) - T''(J) = \nu_e + \nu_v + F'(J+1) - F''(J) \\
S(J) &= T'(J+2) - T''(J) = \nu_e + \nu_v + F'(J+2) - F''(J)
\end{aligned}$$

In these symbols, the usual arbitrary convention has been adopted of *using the value of* J'', rather than that of J' or of $\frac{1}{2}(J'+J'')$, *as the argument*, but at the same time *substituting the symbol* J for the symbol J'' for the sake of brevity. *It is recommended* that, to avoid confusion, the convention of using the value of J'' as argument be uniformly followed.

Branches $O(J)$ and $S(J)$ ordinarily exist only in Raman spectra, and there only in the form

$$\nu = \nu_{exc} \mp [O(J) \text{ or } S(J)].$$

Here ν_{exc} is the wave number of the exciting line; in $O(J)$ or $S(J)$, ν_e is zero in the cases usually investigated (vibration-rotation Raman bands), or ν_e and ν_v are both zero and at the same time we have only $S(J)$, not $O(J)$ (pure rotation Raman bands).

When, in *case b*, the fine structure corresponding to different values of $J-K$ is unresolved (case b', cf. Section III), or narrow, one will naturally

[40] The form $^2\Sigma - {}^2\Pi$ is really sensible only in case each term is a member of a series converging to a known limit from which the term can be *measured downwards*. Except in H_2 and He_2 such series are not known for molecular terms, and the use of the corresponding notation has no point. Even in atomic spectra, its usefulness is limited to the simplest types of series spectra.

define and use $O(K), P(K), \cdots$, in analogy to $O(J)$, $P(J)$, $\cdots$, of case *a*. For example, in a $^2\Sigma$, $^2\Sigma$ transition, one has a branch $P(K)$ and a branch $R(K)$, each line of each branch being a usually narrow, often unresolved, doublet.[41] Also when $S=0$, so that $J=K$, one may use K instead of J as argument.

In cases where both ΔK and ΔJ are important, it is necessary to designate both. For this purpose symbols such as $Q_{21}(J)$, $R_{12}(J)$, etc. are suggested, in which J'' (*written as* J) is used as argument in the usual manner, and in which the numerical subscripts indicate values of $J-K$. It was suggested above that the rotational term designations F_1, F_2, F_3, $\cdots$, be used in case *b* for $J=K+S,\ K+S-1, \cdots, |K-S|$. Similarly,[39b] one may speak of branches $Q_{21}(J)$, $R_{11}(J)$, $Q_{22}(J)$, $Q_{12}(J)$, etc., where the first numerical subscript refers to the upper energy level, the second to the lower. (Symbols such as $R_{11}(J)$ and $Q_{22}(J)$ can ordinarily be abbreviated to $R_1(J)$ and $Q_2(J)$.) For example, $Q_{21}(5\frac{1}{2})$ means $\nu_e+\nu_v+F_2'(5\frac{1}{2})-F_1''(5\frac{1}{2})$, or, more briefly expressed, $T_2'(5\frac{1}{2})-T_1''(5\frac{1}{2})$; here $K'=6$, $J'=5\frac{1}{2}$, $K''=5$, $J''=5\frac{1}{2}$, so that $K'-K''=+1$, while $J'-J''=0$. This notation is incomplete, however, until designations are added to indicate the *a* or *b* character of the rotational levels involved. When this is included, we have symbols such as $Q_{2a1a}(5\frac{1}{2})$, $Q_{2b1b}(5\frac{1}{2})$, $R_{1a1b}(J)$, $R_{1b1a}(J)$, $Q_{2b1b}(J)$, and $Q_{2a2a}(4\frac{1}{2})$ or more briefly $Q_{2\,1}(4\frac{1}{2})$. If Λ' or Λ'' is zero, the *a* or *b* subscripts can be omitted.[36] The notation just suggested can be made more explicit by the addition of a superscript symbol to indicate $K'-K''$; examples, ${}^RQ_{2a1a}(5\frac{1}{2})$, ${}^RR_{1a1b}(J)$. The added superscript is, however, not necessary, since the value of $K'-K''$ is already implied in the remainder of the symbol. For a more detailed discussion of this notation, references 35 and 36 may be consulted.

In the analysis of band spectra, temporary designations for band lines are sometimes needed before the true J or K values involved are known. *It is recommended* that in such cases the lines and branches be designated and numbered in some way that will not be confused with approved theoretically significant designations. For example, one might use $X(m)$, $Y(m)$, $Z(m)$, etc.; or if ΔJ or ΔK is known, but the correct numbering is uncertain, $P(m)$, $R(m)$, etc.; or $P_\alpha(m)$, $P_\beta(m)$, $R_\gamma(m)$, $R_\delta(m)$, etc. The parameter m could be given values 1, 2, 3, $\cdots$.

Conclusion

In Table I some of the most important changes recommended or suggested here are summarized.

Table I. *Some new designations and some of their older equivalents.*

New	Old	New	Old
v	n	λ	$i_{1r}, \sigma_{1r}, \sigma_{k_r}$
J	j, m, etc.	$\sigma, \pi, \delta, \cdots$	$s, p, d, \cdots$
M	(magnetic quantum number)	$2p\sigma, 3s\sigma,$ $3p\pi, 3d\sigma$, etc.	$2s^p, 3s^s$ $3p^p, 4s^d$, etc.
Λ	i_l, σ_k, σ_l	$T; T_e; G$	$E/hc; E_e/hc; E_v/hc$
Σ	i_s, σ_s, X	Λ-type doubling	σ-type doubling
Ω	i, σ	$^3\Pi\rightarrow{}^3\Sigma$, or $^2\Pi$, $^2\Sigma$; etc.	$^1\Sigma-{}^2\Pi$, etc.
K	p_l, j_k	Σ^+, Σ^-	Σ, Σ'
$\Sigma, \Pi, \Delta, \cdots,$	$S, P, D, \cdots$	$\Sigma_g, \Sigma_u, \Pi_u, \Pi_g$, etc.	

[41] Strictly, each line except the first is a triplet (cf. R. S. Mulliken, Phys. Rev. **30**, 138, 1927).

Among those who have expressed approval of the recommendations and suggestions made in this report (except for possible minor reservations) are the following: H. S. Allen, G. M. Almy, E. Bengttson, R. T. Birge, A. Christy, E. U. Condon, F. H. Crawford, W. E. Curtis, D. M. Dennison, G. H. Dieke, R. Fortrat, A. Harvey, W. Heitler, G. Herzberg, E. L. Hill, E. Hulthén, F. Hund, F. A. Jenkins, W. Jevons, R. C. Johnson, J. Kaplan, E. C. Kemble, R. de L. Kronig, J. E. Lennard-Jones, F. London, F. W. Loomis, J. C. McLennan, R. Mecke, P. M. Morse, O. Oldenberg, R. W. B. Pearse, F. Rasetti, Lord Rayleigh, O. W. Richardson, B. Rosen, E. C. G. Stueckelberg, T. Takamine, H. C. Urey, J. H. Van Vleck, W. W. Watson, W. Weizel, E. Wigner, E. E. Witmer. The writer wishes to express his sincere thanks to these and others for their contributions in the way of criticisms, suggestions, and expressions of opinion. These form the basis of the present report. He is particularly indebted to Professors R. T. Birge and F. Hund for their very active cooperation and support.

THE APPLICATION OF THE FERMI-THOMAS STATISTICAL MODEL TO THE CALCULATION OF POTENTIAL DISTRIBUTION IN POSITIVE IONS

By Edward B. Baker
Department of Physics, University of Michigan

(Received June 26, 1930)

Abstract

The statistical method of Fermi and Thomas of calculating atomic potential distributions has been extended to include positive ions. A table of potentials for any positive ion is given. The results have been applied to the calculation of (a) ionic radii, (b) successive ionization potentials, (c) deviations from the Mosely law in optical spectra.

I. The Theory

FERMI[1] and Thomas[2] have considered the electrons in a neutral atom as a completely degenerate electron gas under the influence of the Coulomb field of the nucleus. Assuming radial symmetry, and using Poisson's equation, the Fermi-Dirac statistics permitted a calculation of the distribution of potential for neutral atoms. The present work provides a generalization of the method to include all positive ions also.

Fermi and Thomas obtained the differential equation

$$\frac{1}{r}\frac{d}{dr}\left(\frac{1}{r}\frac{dv}{dr}\right) = -4\pi\rho = \frac{2^{13/2}\pi^2 m^{3/2}e^{5/2}}{3h^3}v^{3/2} \tag{1}$$

with the boundary conditions

$$v \sim Ze/r \text{ near } r = 0, \text{ or } \lim_{r\to 0} vr = Ze \tag{2.0}$$

$$v(\infty) = 0 \tag{2.1}$$

which determine the solution for the neutral atom uniquely. The additional condition

$$\int \rho d\tau = -Ze \tag{3}$$

is simultaneously satisfied.

Introducing dimensionless variables

$$\psi = v/\gamma; \quad \gamma = \frac{2^{13/3}\pi^{4/3}me^2Z^{4/3}}{3^{2/3}h^2} \tag{4}$$

[1] E. Fermi, Zeits. f. Physik **48**, 73 (1928).
[2] L. H. Thomas, Proc. Camb. Phil. Soc. **23**, 542 (1927).

and

$$x = r/\mu; \qquad \mu = \frac{3^{2/3}\hbar^2}{2^{13/3}\pi^{4/3}me^2Z^{1/3}}$$

then Eq. (1) becomes

$$\frac{d^2\psi}{dx^2} + \frac{2}{x}\frac{d\psi}{dx} = \psi^{3/2} \tag{5}$$

Substituting $\phi = \psi x$, we have

$$\phi'' = \frac{\phi^{3/2}}{x^{1/2}} \tag{6}$$

and Eqs. (2) and (3) become

$$\phi(0) = 1 \tag{7}$$

$$\phi(\infty) = 0 \tag{7.1}$$

and

$$\int_0^\infty \phi^{3/2}(x)^{1/2}dx = 1. \tag{8}$$

For the positive ion having z electrons and the atomic number Z, which we shall call an ion of order σ ($\sigma = z/Z$), we have, in place of Eq. (3),

$$\int \rho d\tau = -ze \tag{9}$$

and, in place of Eq. (8),

$$\int_0^{x_m} \phi^{3/2}x^{1/2}dx = z/Z = \sigma. \tag{10}$$

Since Eq. (9) is not fulfilled by the former solution, it follows that the boundary condition, Eq. (2.1), must be modified, since Eq. (2.0) must remain the same. A suggestion of how this is to be done may be obtained by a comparison of Eq. (5) with the equations

$$\frac{d^2\psi}{dx^2} + \frac{2}{x}\frac{d\psi}{dx} = -\psi^n \tag{11}$$

which have been extensively studied by Emden[3] in connection with the distribution of matter in polytropic gas spheres. Emden found that for certain values of n, and certain boundary conditions, there are solutions of Eqs. (11) describing gas spheres of *finite* radius. This suggests that Eq. (3) may also have such solutions if the boundary conditions are modified.

Fermi[4] and Razetti[5] have used the approximate potential

$$v = -\frac{e}{r}\left[1 + (Z-1)\phi\left(\frac{r}{\mu}\right)\right] \tag{12}$$

[3] Emden, "Gaskugeln," Leipzig, 1907.
[4] E. Fermi, Zeits. f. Physik **49**, 550 (1928).
[5] F. Razetti, Zeits. f. Physik **49**, 546 (1928).

(where μ is evaluated for $Z-1$), for a singly ionized atom. This is obtained by considering the ion of nuclear charge Z as a neutral atom of nuclear charge $Z-1$ plus an extra proton in the nucleus. This approximation neglects the "packing effect" that the added proton will have upon the electron cloud. It is not possible to generalize this result for much higher ionizations, for then the neglect of the packing effect becomes serious. The present method is designed to remove this difficulty.[6]

We propose a model of the positive ion having a finite radius x_m, beyond which the charge density is zero. The solution ϕ_σ of Eq. (6), representing a positive ion of order σ, must obey the boundary condition

$$\phi_\sigma(x_m) = \phi_{\sigma m} = 1 - \sigma = 1 - z/Z \tag{13}$$

instead of Eq. (7.1). We find that ϕ_σ then fulfills the extra condition of Eq. (10). For the neutral atom $x_m = \infty$, Eq. (13) reduces to Eq. (7.1), and Eq. (10) reduces to Eq. (8), as required.

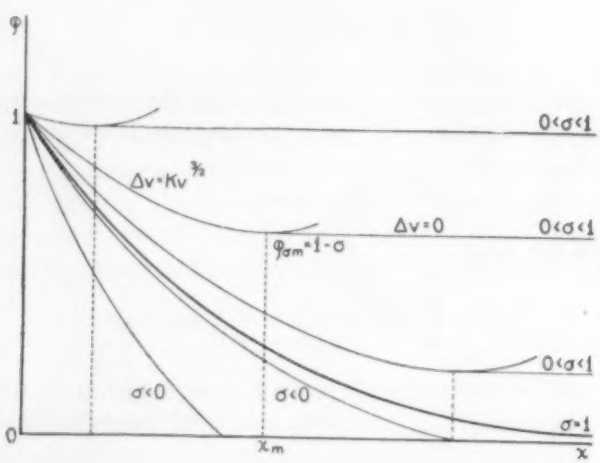

Fig. 1.

In Fig. 1 are displayed the possible forms the solution of Eq. (6) may take if the boundary condition of Eq. (7.0) is satisfied. The curve ϕ_1 is the only solution for which $\phi(\infty)=0$, and is that already obtained for the neutral

[6] The two dimensional analogue of Eq. (5) is

$$\frac{d^2\psi}{dx^2} + \frac{1}{x}\frac{d\psi}{dx} = \psi$$

the solution of which is any cylinder function $Z_0(ix)$. The only cylinder function which has the required logarithmic behavior for $x=0$, and which vanishes for $x=\infty$, is the Hankel function of the first kind $H_0^1(ix)$. As this function becomes asymptotically equal to $e^{-x}/x^{\frac{1}{2}}$, it can only represent a neutral two dimensional atom. The corresponding fact is true for Eq. (5); there is no solution of Eq. (5) which satisfies the conditions of Eqs. (2.0) and (2.1) other than the one obtained by Thomas and Fermi for neutral atoms. This can also be shown by a direct method of inequalities. This remarkable property of Eq. (5) made necessary the linking up of two solutions as described above.

atom by Fermi and Thomas. For this solution we have found the starting slope $\phi_1'(0) = -B_1 = -1.588558$.

Since the differential equation is of the second order, a particular value of the initial slope $-B_\sigma$ at $x=0$ uniquely determines a single solution passing

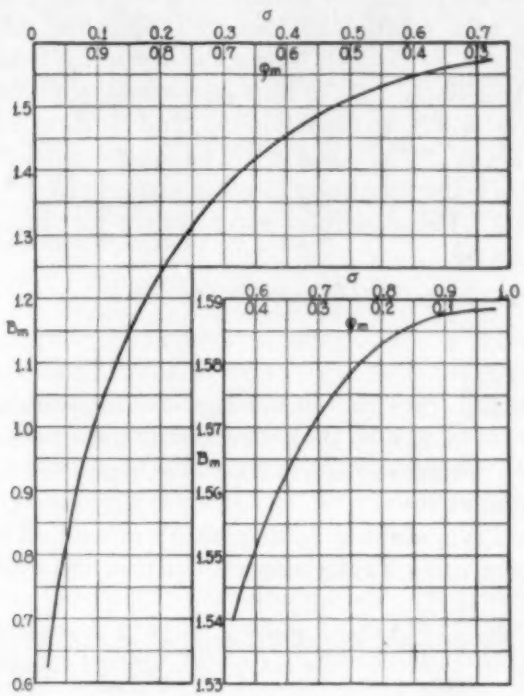

Fig. 2.

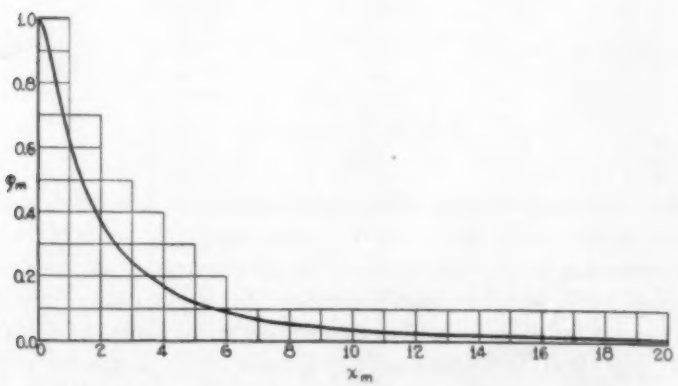

Fig. 3.

through $\phi=1$, $x=0$. All solutions with $0 > -B_\sigma > -\infty$ are single valued in ϕ, and no two cross each other.

All solutions with $0 > -B_\sigma > -B_1$ have each a single minimum, the coordinates of which $(\phi_{\sigma m}, x_m)$ are monotonous functions of B_σ (see Fig. 2), so that

the locus of minima (see Fig. 3) is monotonous in both x and ϕ. The ordinates at the minimum range from $\phi_{1m}=0$ to $\phi_{\sigma m}=1$, for values of B_σ from B_1 to B_0 respectively. These solutions describe any positive ion ($0\leqq\sigma\leqq 1$) as far as the minimum, which is the boundary of the ion; beyond that point the Coulomb field requires a straight line parallel to $\phi=0$, and a distance $1-\sigma$ above it, corresponding to a solution of Laplace's equation, which joins at the minimum a solution ϕ_σ of Eq. (8). The value of σ which belongs to a solution ϕ_σ, having a starting slope $-B_\sigma$, is thus *determined* by numerical integration from $\phi=1$, $x=0$, $\phi'=-B_\sigma$ to the minimum, and by there *assigning* the value $1-\sigma$ to the ordinate $\phi_{\sigma m}$. The value of σ is known to characterize the straight line $1-\sigma=\phi$, which is the solution of Laplace's equation for the region outside of an ion of order σ. This condition expresses the fact that the potential of a positive ion must be

$$v\sim\frac{(Z-z)e}{r}=\frac{Ze}{r}(1-\sigma)$$

for large values or r.

All solutions of Eq. (8) with $-B_1>-B_\sigma>-\infty$ lie below ϕ_1 and terminate abruptly at $\phi=0$, so that they do *not* represent negative ion distributions. Negative ions, as a matter of fact, will not find a place in any theory which assumes radial symmetry.

Since $x=0$, $\phi=1$ is a winding point with ϕ'' infinite, it is not possible to integrate from there using Taylor's series. Instead the expansions

$$\phi=1-Bx+\frac{4}{3}x^{3/2}-\frac{2}{5}Bx^{5/2}+\frac{1}{3}x^3+\frac{3}{70}B^2x^{7/2}-\frac{2}{15}Bx^4+\frac{4}{63}\left(\frac{2}{3}+\frac{1}{16}B^3\right)x^{9/2}+\cdots \tag{14}$$

and

$$\phi'=-B+2x^{1/2}-Bx^{3/2}+x^2+\frac{3}{20}B^2x^{5/2}-\frac{8}{15}Bx^3+\frac{2}{7}\left(\frac{2}{3}+\frac{1}{16}B^3\right)x^{7/2}+\cdots \tag{15}$$

obtained by a method of successive approximations, are used, since they are rapidly convergent near $\phi=1$, $x=0$. Starting with an arbitrary value of B_σ, the integration is carried out to the minimum by an extension of the method given by Whittaker and Robinson[7] for equations of the first order. The results must be given in a bivariate table, with values of ϕ for each value of x and B_σ or σ. This would be very extensive, were it not for the fact that, for each particular value of x, the values of both ϕ_σ and ϕ_σ', from one curve to another, depend linearly upon B_σ. By means of the formulae:

$$\phi_\sigma=k(B_\sigma-B_p)+\phi_p \tag{16}$$

$$\phi_\sigma'=k'(B_\sigma-B_p)+\phi_p' \tag{17}$$

[7] Whittaker and Robinson, "The Calculus of Observations."

and Table I, we may easily find the values of ϕ_σ and ϕ_σ' for each value of σ, at the values of x given in the table. For intermediate values linear interpolation is sufficiently accurate. The constants k and k', being functions of x, are also tabulated, as well as the values B_p, ϕ_p and ϕ_p' of the reference solutions. The values of $B_{\sigma m}$ and $\phi_{\sigma m}$ are also listed; they are the initial slopes and minimal ordinates, respectively, of the solutions having their minima at the given value of x. Since $\phi_{\sigma m}= 1-\sigma$, this part of the table is used to find the initial slope B_σ, needed in Eqs. (16) and (17), corresponding to the given order σ of the ion. This may also be done using Fig. 2. In Fig. 3 values of $\phi_{\sigma m}$ are plotted against x_m, and from this, since $\phi_{\sigma m}=1-\sigma$, we may find the radius x_m of an ion of order σ.

Values are listed from $x=0.10$ to $X=14.88$. For values of $x<0.10$ the series in Eqs. (14) and (15) may be used.

II. Ionic Radii

Herzfeld[8] has given a summary of some fourteen different methods of determining ionic radii, most of which are experimental, or semi-experimental. It may be seen from his collection of data, that the radius of any particular ion has a wide range of values, according to the method of determination. This uncertainty is not experimental, but lies in the variation of meaning of the radius with the method. It is consequently quite useless to

Table I.
$B_p=1.60$.

x	ϕ_p	$-(\partial\phi/\partial x)_p$	$-k$	$-k'$	B_m	ϕ_m
0.10	0.880448	1.0077	0.10126	1.0306	0.62221	0.97950
0.11	0.870539	0.9826	0.11159	1.0362	0.65170	0.97636
0.12	0.860832	0.9587	0.12197	1.0410	0.67901	0.97316
0.13	0.851358	0.9362	0.13240	1.0449	0.70399	0.96999
0.14	0.842103	0.9151	0.14287	1.0511	0.72935	0.96650
0.15	0.833053	0.8948	0.15342	1.0548	0.75166	0.96320
0.16	0.824201	0.8758	0.16401	1.0610	0.77453	0.95958
0.17	0.815535	0.8576	0.17464	1.0665	0.79592	0.95597
0.18	0.807046	0.8402	0.18418	1.0728	0.81678	0.95130
0.20	0.790574	0.80745	0.20576	1.0861	0.85655	0.94355
0.22	0.774731	0.7772	0.22761	1.0985	0.89248	0.93577
0.24	0.759471	0.7492	0.24971	1.1115	0.92596	0.92779
0.26	0.744751	0.72315	0.27208	1.1255	0.95746	0.91957
0.28	0.730535	0.69875	0.29473	1.1391	0.98658	0.91133
0.30	0.716792	0.67585	0.31765	1.1540	1.01434	0.90283
0.32	0.703492	0.6544	0.34089	1.1698	1.04059	0.89419
0.34	0.690609	0.63415	0.36447	1.1856	1.06513	0.88556
0.38	0.666003	0.5968	0.41251	1.2184	1.11013	0.86808
0.42	0.642812	0.5633	0.46193	1.2523	1.15018	0.85060
0.46	0.620895	0.5330	0.51275	1.2887	1.18639	0.83298
0.50	0.600134	0.50545	0.56505	1.3264	1.21892	0.81546
0.54	0.580427	0.4803	0.61888	1.3659	1.24839	0.79804
0.58	0.561684	0.4572	0.67434	1.4069	1.27500	0.78084
0.62	0.543825	0.4360	0.73146	1.4492	1.29916	0.76388
0.66	0.526781	0.41645	0.79031	1.4935	1.32216	0.74715
0.74	0.49490	0.3816	0.91345	1.5882	1.35972	0.71444
0.82	0.46561	0.35125	1.0443	1.6851	1.39155	0.68329
0.90	0.43858	0.3250	1.1833	1.7913	1.41856	0.65326
0.98	0.41352	0.30225	1.3310	1.9052	1.44136	0.62467

[8] K. F. Herzfeld, Jahrb. der Radioakt. und Electronik **19**, 259 (1922).

TABLE I. (*continued*)

x	ϕ_p	$-(\partial\phi/\partial x)_p$	$-k$	$-k'$	B_m	ϕ_m
1.06	0.39017	0.2819	1.4882	2.0239	1.46072	0.59744
1.14	0.36836	0.2639	1.6551	2.1502	1.47728	0.57148
1.22	0.34789	0.24825	1.8325	2.2866	1.49143	0.54684
1.30	0.32859	0.2341	2.0212	2.4293	1.50362	0.52339
1.38	0.31037	0.22175	2.2216	2.5827	1.51414	0.50112
1.46	0.29308	0.21075	2.4347	2.7470	1.52328	0.47987
1.54	0.27662	0.2006	2.6612	2.9547	1.53210	0.45732
			$B_p=1.589$			
1.649	0.28827	0.1546	2.9889	3.1213	1.53939	0.43653
1.822	0.26312	0.1361	3.5600	3.4885	1.55001	0.40192
2.014	0.23878	0.1186	4.2678	3.906	1.55863	0.36839
2.226	0.21538	0.1027	5.149	4.408	1.56569	0.33540
2.460	0.19305	0.08866	6.250	5.027	1.57136	0.30327
2.718	0.17180	0.07616	7.649	5.764	1.57579	0.27286
3.004	0.15167	0.06515	9.367	6.572	1.579133	0.24410
3.320	0.13266	0.05560	11.62	7.701	1.581780	0.21656
3.669	0.11472	0.04748	14.38	9.085	1.583774	0.18986
4.055	0.09776	0.04069	18.21	10.79	1.585230	0.16640
4.482	0.08165	0.03512	23.26	12.74	1.586243	0.14577
4.953	0.06619	0.03081	30.11	15.32	1.586989	0.12673
5.474	0.05105	0.02758	38.90	18.56	1.587515	0.10883
6.050	0.03587	0.02537	50.63	22.61	1.587878	0.09268
			$B_p=1.5886$			
6.686	0.04672	0.01340	66.60	28.12	1.5881234	0.07846
7.389	0.03817	0.01108	88.40	34.24	1.5882763	0.06679
8.166	0.03029	0.00932	118.2	42.37	1.5883801	0.05629
9.025	0.02286	0.00806	159.3	53.19	1.5884485	0.04699
9.974	0.01565	0.00723	216.3	66.97	1.5884921	0.03900
			$B_p=1.58857$			
11.02	0.01716	0.00434	296.0	85.30	1.5885191	0.03218
12.18	0.01252	0.00373	408.0	107.6	1.5885353	0.02666
13.46	0.00802	0.00335	563.0	136.7	1.5885454	0.02182
14.88	0.00341	0.00319	782.0	171.4	1.5885514	0.01798

expect quantitative agreement of the radii determined by this theory, which themselves have little real meaning, with his values. Never-the-less, they do correspond in order of magnitude, and show the same general variation with atomic number. The class of ions considered by Herzfeld is a restricted class, having values of z equal to $Z-q$, where q is the valence of the element Z. When their radii are plotted against Z, a Lothar Meyer curve is obtained. We have made a similar curve, Fig. 4, of the values found from Fig. 3, but only for elements having positive ions.

III. Successive Ionization Potentials

Milne[9] has applied the Fermi-Thomas theory of the neutral atom to the calculation of the total potential necessary to remove all of the electrons from

[9] E. A. Milne, Proc. Camb. Phil. Soc. **23**, 794 (1927).

a neutral atom. Since our theory also gives a description of positive ions, the natural extension of the work of Milne is the calculation of the *successive* ionization potentials of atoms, or the successive potentials necessary to remove the electrons from an atom one at a time, further "stripping" the atom at each step.

The method of calculation consists in finding the total potential $X = X(\sigma, Z)$, necessary to remove all of the electrons from each kind of a positive ion that an element of atomic number Z may have, including the neutral atom.

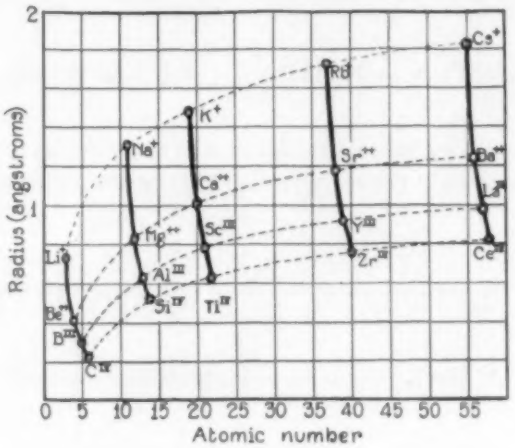

Fig. 4.

Successive differences of these quantities give the desired successive ionization potentials.

Milne considered the total electrostatic potential V to consist of two parts, Ze/r due to the nucleus, and $v(r)$ due to the charge cloud. At the nucleus $v(r)$ takes the constant value v_0, the "back potential" of the charge cloud, and this he showed proportional to the starting slope of ϕ_1, which is $-B_1$. There is a charge Ze at the nucleus, and at any other point a charge ρv. The total electrostatic potential is then

$$W = \Sigma \tfrac{1}{2} ev = \tfrac{1}{2} \int \rho v d\tau + \tfrac{1}{2} Z e v_0, \tag{18}$$

and the total energy is half of this.

The integral in the first term of Eq. (18) he showed to be proportional to B_1, which becomes B_σ for the ion. His result may be written:

$$X(1, Z) = -13.11 B_1 Z^{7/3} \text{ volts}. \tag{19}$$

He obtained his value of B_1 from Thomas' calculations of ϕ_1 near $x = 0$, which, however, are slightly in error. Using our value of $B_1 = -1.588558$, we obtain

$$X(1, Z) = 20.824 Z^{7/3} \text{ volts} \tag{20}$$

which does not agree as well with experiment as Milne's

$$X(1, Z) = 17Z^{7/3} \text{ volts}. \tag{21}$$

This agreement must be regarded as accidental.

For the positive ion of order σ we obtain

$$X(\sigma, Z) = -13.11B_\sigma Z^{7/3} \text{ volts}. \tag{22}$$

If the approximation of Fermi and Razetti is generalized for ions of any order we obtain

$$X_F(\sigma, Z) = -13.11B_1\frac{7}{13}\left(\frac{6}{7}\sigma + 1\right)Z^{7/3} \text{ volts}, \tag{23}$$

since z must be used for the evaluation of v in the first term of Eq. (18). In successive differences only the term in Eq. (23) containing σ gives a contribution.

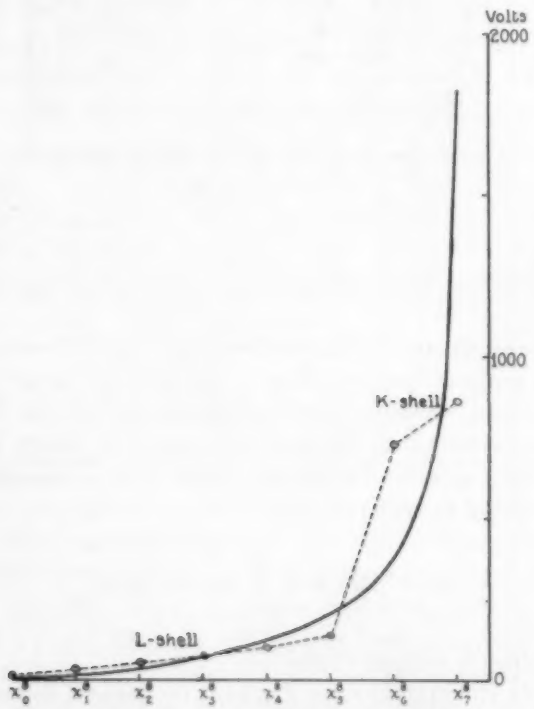

Fig. 5. Successive ionization potentials of oxygen. $Z=8$. Circles represent Hartree's Values.

In Figs. 5 and 6 we have plotted such differences of $X(\partial, Z)$ for the elements oxygen and iron. The broken curves are the semi-experimental values of Hartree.[10] As with most results of this statistical theory, a smooth curve

[10] D. R. Hartree, Proc. Camb. Phil. Soc. **22**, 473 (1924).

running through the jagged experimental one is obtained. Differences of X according to (23) give a curve of successive ionization potentials having a negative slope and going from the upper left hand corner to the lower right hand corner of the diagrams 5 and 6.

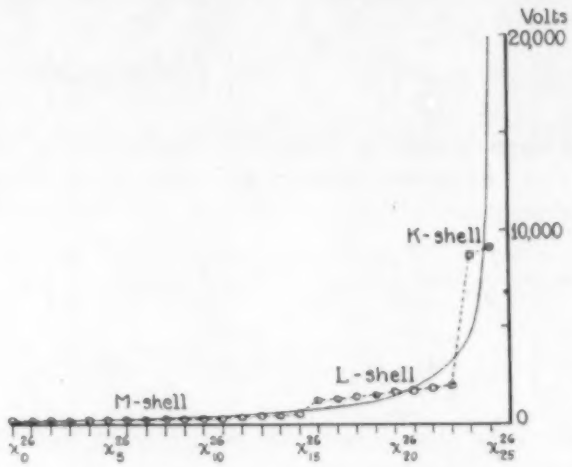

Fig. 6. Successive ionization potentials of iron. $Z=26$. Circles represent Hartree's values.

IV. Application to the Behavior of Optical Term Values in the Limit of Very High Frequencies

Sommerfeld has shown that x-ray terms may be represented by the semi-empirical term formula

$$-\frac{T}{R} = [Z/n - a(Z, n) - b(n, l)]^2 + \alpha^2\left[\frac{Z - d(n, l, j)}{n}\right]^4\left(\frac{n}{j+\frac{1}{2}} - \frac{3}{4}\right) + \cdots \tag{24}$$

Laporte[11] has shown that this same formula may be used to represent optical terms, though the number $a(Z, n)$, which represents the screening of the outer electrons, is zero for optical terms, and $b(n, l)$ is a function of Z, except for very high ionizations ($\partial << 1$). For low ionizations its dependence upon Z may be expressed as the series

$$b(n, l, Z) = A(n, l) + \frac{B(n, l)}{Z} + \frac{C(n, l)}{Z^2} + \cdots \tag{25}$$

so that

$$\lim_{Z\to\infty} b(n, l, Z) = A(n, l). \tag{26}$$

It is possible to calculate the quantity $A(n, l)$, by means of the present theory, for hydrogenic ion series like Na I, Mg II, Al III, etc. It is also

[11] O. Laporte, "Sommerfeld Festschrift," Leipzig, 1928, p. 128.

possible to derive this from the experimental values of the line frequencies for such isoelectronic series. We shall be interested first in the latter problem.

Combining Eqs. (24) and (25) we have:

$$-\frac{T}{R}=\left\{\frac{Z}{n}-\left[A(n,l)+\frac{B(n,l)}{Z}+\frac{C(n,l)}{Z^2}+\cdots\right]\right\}^2 + \alpha^2\left\{\frac{Z-d(n,l,j)}{n}\right\}^4\left(\frac{n}{j+\frac{1}{2}}-\frac{3}{4}\right)+\cdots \tag{27}$$

Terms in α^2 and higher powers of α^2 represent the "relativity" correction, and if we subtract them from both sides of Eq. (27), we obtain the "reduced" term values t, thus

$$-\frac{t}{R}=-\frac{T}{R}-\alpha^2\left\{\frac{Z-d(n,l,j)}{n}\right\}^4\left(\frac{n}{j+\frac{1}{2}}-\frac{3}{4}\right)+\cdots = \left\{\frac{Z}{n}-\left[A(n,l)+\frac{B(n,l)}{Z}+\frac{C(n,l)}{Z^2}+\cdots\right]\right\}^2. \tag{28}$$

We wish now to be able to calculate $A(n, l)$ from observed values of t. This may be done in at least two ways.

The first is to take the square root of the absolute values of both sides of Eq. (28), obtaining:

$$\left(\frac{t}{R}\right)^{1/2}=\frac{Z}{n}-A(n,l)-\frac{B(n,l)}{Z}-\frac{C(n,l)}{Z^2}+\cdots \tag{29}$$

which shows that the Moseley law holds for large values of Z. If we form the difference

$$\left(\frac{t(l_2)}{R}\right)^{1/2}-\left(\frac{t(l_1)}{R}\right)^{1/2}=[A(n,l_1)-A(n,l_2)]+\frac{1}{Z}[B(n,l_1)-B(n,l_2)] \tag{30}$$

and go to the limit for very large Z, we obtain the quantity

$$\lim_{Z\to\infty}\left\{\left(\frac{t(l_2)}{R}\right)^{1/2}-\left(\frac{t(l_1)}{R}\right)^{1/2}\right\}=[A(n,l_1)-A(n,l_2)]. \tag{31}$$

This quantity may be directly calculated from the experimental term values of an isoelectronic sequence, it being the asymptotic value that the quantities in Eq. (30) seem to approach for the heavier elements in the sequence. Such quantities have been calculated by Wentzel[12] and Unsöld,[13] on the basis of a model of the atomic core composed of concentric spherical surface charges. This quantity has the disadvantage that the absolute term values must be known in order to calculate it.

The second quantity which may be used as a medium of comparison of theory and experiment is the asymptotic value of the first differences, for

[12] G. Wentzel, Ann. d. Physik **76**, 803 (1925).
[13] A. Unsöld, Zeits. f. Physik **33**, 843 (1925).

neighboring elements in the isoelectronic sequence, of the line frequencies themselves. We may form this quantity from Eq. (28). It is

$$\lim_{Z\to\infty}\left\{\frac{\nu(l_2,l_1,Z+1)}{R}-\frac{\nu(l_2,l_1,Z)}{R}\right\}$$
$$=\lim_{Z\to\infty}\left\{\left[\frac{t(n,l_2,Z+1)}{R}-\frac{t(n,l_1,Z+1)}{R}\right]-\left[\frac{t(n,l_2,Z)}{R}-\frac{t(n,l_1,Z)}{R}\right]\right\} \tag{32}$$
$$=\frac{2}{n}[A(n,l_1)-A(n,l_2)],$$

which is just $2/n$ times the quantity in Eq. (31).

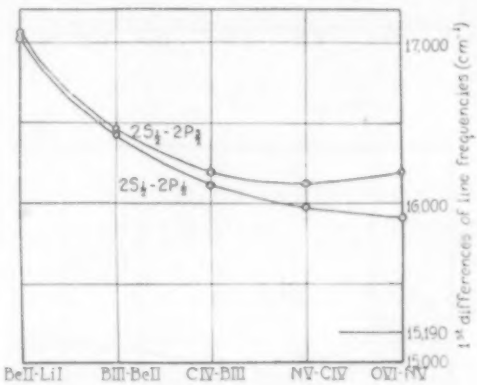

Fig. 7.

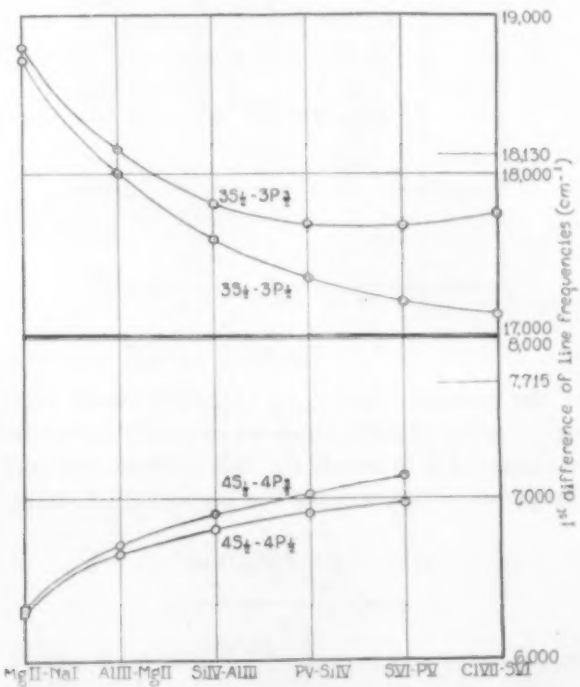

Fig. 8.

These two quantitites, in Eqs. (31) and (32), have been calculated by means of this theory, and have been compared with the experimental values of Bowen and Millikan[14] for the series Na I, Mg II, etc., and Li I, Be II, etc. in Figs. 7, 8, 9, and 10.

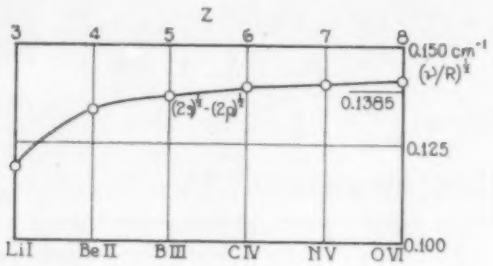

Fig. 9.

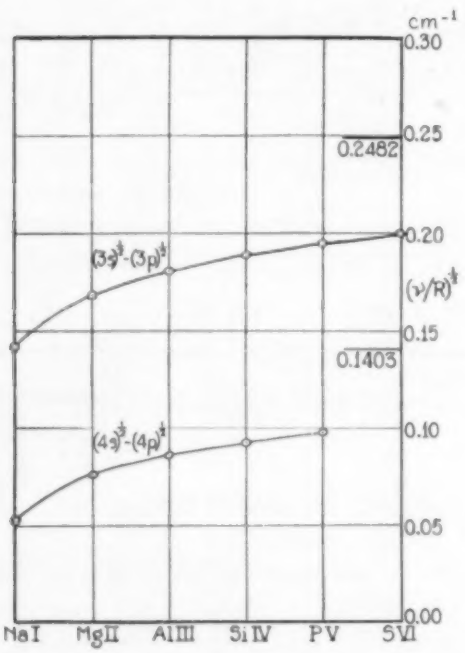

Fig. 10.

The use of the present theory to calculate these values involves the Schrödinger perturbation theory, since we are only interested in the energy values for large values of Z (σ nearly 0). We consider the core as a perturbation of an "hydrogenic" atom, writing the perturbation energy as

$$\epsilon = \frac{\int_0^\infty P(r)\psi^2 r^2 dr}{\int_0^\infty \psi^2 r^2 dr} \tag{33}$$

[14] I. S. Bowen and R. A. Millikan, Phys. Rev. **25**, 299 (1925), **27**, 145 (1926).

where ψ is the wave function of the unperturbed hydrogenic atom, and $P(r)$ is the perturbation function of the core. We proceed to construct $P(r)$.

Consider an ion of nuclear charge Z, with z electrons in the core, and one valence electron in addition. The potential energy of the valence electron in the field of the nucleus plus core is

$$-\frac{Ze^2}{r}\phi_\sigma\left(\frac{r}{\mu}\right) \tag{34}$$

where ϕ_σ is the generalized Fermi function for an ion of order σ. The net charge of the ion is $(Z-z-1)$.

The potential energy of the valence electron in the field of the nucleus alone (of charge Ze) is

$$-\frac{Ze^2}{r}. \tag{35}$$

If we add and subtract Eq. (35) to Eq. (34), we still have the potential energy of the valence electron in the field of the nucleus plus core as

$$-\frac{Ze^2}{r}+\frac{Ze^2}{r}\left[1-\phi_\sigma\left(\frac{r}{\mu}\right)\right]=-\frac{Ze^2}{r}+\Phi. \tag{36}$$

The quantity $\Phi=Ze^2/r[1-\phi_\sigma]$ may be split into two parts Φ_1 and Φ_2, such that

$$\Phi = \Phi_1 \text{ for } r \leqq r_m$$

$$\Phi = \Phi_2 \text{ for } r \geqq r_m,$$

where r_m is the radius of the core. If $r>r_m$, then

$$\phi_\sigma = \phi_{\sigma m} = 1 - \sigma = 1 - z/Z,$$

so that

$$\Phi_2 = \frac{Ze^2}{r}(1 - 1 + z/Z) = \frac{ze^2}{r}. \tag{37}$$

We may rewrite Eq. (36) in the form

$$-\frac{(Z-z)e^2}{r}+P(r) \tag{38}$$

where P is a function defined by

$$\begin{aligned} P &= \Phi_1 - Ze^2r \quad \text{for } r < r_m \\ P &= 0 \qquad\qquad \text{for } r > r_m. \end{aligned} \tag{39}$$

Now, if Z is very large, we may think of the valence electron as being primarily in the field of a point charge $(Z-z)e$, and then being perturbed by

another system, with the perturbation energy $P(r)$. So, without the perturbation we have an hydrogenic atom with nuclear charge $(Z-z)e$ (i.e. the quantity z is the first approximation to the screening number $b(n, l, Z)$).

If $Z>>z$ (σ nearly 0), we may use the series approximation of ϕ_s given in Eq. (14), since x_m is also nearly zero. By means of the analytical expressions of Eqs. (14) and (15) we are able to find an analytical expression for B_s as a function of σ. To do this we notice that at the minimum

$$\phi' = 0 = -B + 2x_m^{1/2} - Bx_m^{3/2} + x_m^2 + \cdots . \tag{40}$$

Since both B and x_m are small, all terms after the first two are of lower order, so that, approximately,

$$B = 2x_m^{1/2};\ x_m^{1/2} = B/2;\ x_m = B^2/4. \tag{41}$$

Then, substituting in Eq. (14), we have

$$\begin{aligned} \phi_m = 1 - \sigma &= 1 - B(B^2/4) + \frac{4}{3}(B/2)^3 - \frac{2}{5}(B/2)^5 + \cdots \\ &= 1 - B^3/12 - B^6/80 + \cdots \end{aligned} \tag{42}$$

or, to the same approximation as in Eq. (41),

$$B^3/12 = \sigma;\ B = (12\sigma)^{1/3} \tag{43}$$

which is the required function. If we eliminate B from Eqs. (14) and (43), we obtain ϕ_s in terms of x and σ explicitly. Thus

$$\phi_s = 1 - (12\sigma)^{1/3}x + \frac{4}{3}x^{3/2} - \frac{2}{5}(12\sigma)^{1/3}x^{5/2} + \cdots \tag{44}$$

and therefore

$$\begin{aligned} \Phi_1 &= \frac{Ze^2}{r}\left[(12\sigma)^{1/3}x - \frac{4}{3}x^{3/2} + \frac{2}{5}(12\sigma)^{1/3}x^{5/2} + \cdots\right] \\ &= Ze^2\left[\frac{(12\sigma)^{1/3}}{\mu} - \frac{4}{3}\frac{r^{1/2}}{\mu^{3/2}} + \frac{2}{5}(12\sigma)^{1/3}\frac{r^{3/2}}{\mu^{5/2}} + \cdots\right]. \end{aligned} \tag{45}$$

Finally, we may write our perturbation function as

$$P(r) = Ze^2\left[\frac{(12\sigma)^{1/3}}{\mu} - \frac{4}{3}\frac{r^{1/2}}{\mu^{3/2}}\right] - \frac{ze^2}{r};\ r \leqq r_m \tag{46.0}$$

$$P(r) = 0;\ r \geqq r_m. \tag{46.1}$$

If we introduce the dimensionless variable

$$\rho = 2\frac{r}{r_0};\quad r_0 = \frac{r(Z-z)}{na_0}, \tag{47}$$

where Ze = the real nuclear charge

$(Z-z)e$ = the nuclear charge of our hypothetical hydrogenic atom

a_0 = the normal radius of the hydrogen atom

n = the principal quantum number,

we have the perturbation function

$$Q(\rho) = P(r) = a + b\rho^{1/2} + c/\rho, \tag{48}$$

with

$$a = \frac{Ze^2(12\sigma)^{1/3}}{\mu} = \left(\frac{Ze^2}{a_0}\right)\frac{8Z^{1/3}}{3^{1/3}\pi^{2/3}} \tag{49.0}$$

$$b = -\frac{4Ze^2}{3\mu^{3/2}}\left(\frac{a_0 n}{2(Z-z)}\right)^{1/2} = -\left(\frac{Ze^2}{a_0}\right)\frac{32n^{1/2}}{9\pi(1-\sigma)^{1/2}} \tag{49.1}$$

$$c = -\frac{2ze^2(Z-z)}{a_0 n} = -2\left(\frac{Ze^2}{a_0}\right)\left(\frac{1-\sigma}{n}\right) \tag{49.2}$$

$$\rho_m = 2\frac{r_m}{r_0} = \frac{2r_m(Z-z)}{na_0} = (1-\sigma)\frac{\pi^{2/3}3^{4/3}z^{2/3}}{4n} \tag{49.3}$$

and ϵ takes the form

$$\epsilon = \frac{\int_0^{\rho_m} Q(\rho)\psi^2(\rho)\rho^2 d\rho}{\int_0^{\infty} \psi^2(\rho)\rho^2 d\rho} \tag{50.0}$$

since $Q(\rho) = 0$ for $\rho \geqq \rho_m$.

The limiting forms of Eqs. (49) for $\sigma = 0$ are

$$b]_{\sigma=0} = -\left(\frac{Ze^2}{a_0}\right)\frac{32n^{1/2}}{9\pi} \tag{50.1}$$

$$c]_{\sigma=0} = -\frac{2}{n}\left(\frac{Ze^2}{a_0}\right) \tag{50.2}$$

$$\rho_m]_{\sigma=0} = \frac{\pi^{2/3}3^{4/3}z^{2/3}}{4n}. \tag{50.3}$$

We have passed to the limit several times during the process in order to simplify the calculations. The asymptotic form of the perturbation energy is

$$\epsilon_\infty = -L(n, l, z)\frac{Ze^2}{a_0} \tag{51}$$

If we were to extend the calculation for ϵ near the limit, we would find[15]

$$\epsilon = [-LZ + M + N/Z + \cdots]\frac{e^2}{a_0}. \tag{52}$$

The energy of the unperturbed hydrogenic ion, of nuclear charge $(Z-z)\,e$, is

$$E = -\frac{e^2(Z-z)^2}{2a_0 n} = -\frac{e^2}{2a_0 n}(Z^2 - 2zZ + z^2) \tag{53}$$

and therefore the sum

$$E_p = E + \epsilon = -\frac{e^2}{2a_0 n}[Z^2 - 2(Z - n^2L)Z + (z^2 - M) - N/Z + \cdots] \tag{54}$$

is the energy of the perturbed ion. From this the reduced term value is seen to be

$$-\frac{t}{R} = \frac{1}{n^2}[Z^2 - 2(z - n^2L)Z + (z^2 - M) - N/Z + \cdots] \tag{55}$$

In order to compare this with Eq. (28) we must place the square root of the right hand side under an indicated square. Thus

$$-\frac{t}{R} = \left\{\frac{Z}{n} - \frac{1}{n}(z - n^2L) - \frac{M - 2zn^2L - n^4L^2}{2Zn} + \cdots\right\}^2. \tag{56}$$

Comparing Eqs. (56) and (28) we may make the following identifications:

$$A(n, l) = \frac{1}{n}(z - n^2L) \tag{57.0}$$

$$B(n, l) = \frac{M - 2zn^2L - n^4L^2}{2n}, \text{ etc.} \tag{57.1}$$

From Eqs. (57.0) and (51) we may calculate quantitites such as those of Eqs. (30) and (31).

The quantitites of Eq. (30), which Wentzel introduced, must be calculated from "reduced" absolute term values. They are practically insensitive

[15] Since the perturbation function has the form of Eq. (48), the perturbation integrals reduce to sums of integrals of the type

$$I(\mu, \nu) = \int_0^\nu x^{\mu-1}e^{-x}dx$$

which are known as "incomplete Γ-functions." They are special cases of the "confluent hypergeometric functions." Tables of these functions have been prepared by K. Pearson ("The Incomplete Γ-function"), but interpolation is very laborious. However, since we encounter only whole or half integral values of μ, it is much simpler to reduce the integrals to polynomials (integral values), or to polynomials plus Gauss error functions, by partial integration.

to relativity corrections, but the absolute term values are only known by somewhat approximate calculations from line frequencies. The unreduced values of Bowen and Millikan are plotted in Figs. 9 and 10.

The quantitites calculated according to Eq. (31), though found directly from line frequencies, are very sensitive to relativity corrections, which are difficult to estimate accurately for *s* terms. Instead, in Figs. 7 and 8, the actual "unreduced" values are plotted for each of the doublet lines, to give an idea of the error involved in not reducing them. The lines on the right hand margin indicate the theoretical asymptotes.

In conclusion I wish to express my appreciation to Professor H. M. Randall, Director of the Physics department, for courtesies shown me during my graduate study at the University of Michigan. I am indebted to Professor O. Laporte for suggesting this problem to me, and for his constant advice. I also wish to thank Professors D. M. Dennison and E. A. Milne for valuable advice and criticism.

FINE STRUCTURE IN THE X-RAY ABSORPTION SPECTRA OF THE K SERIES OF THE ELEMENTS CALCIUM TO GALLIUM

By Ben Kievit and George A. Lindsay
University of Michigan
(Received July 10, 1930)

Abstract

The K x-ray absorption spectra of the free elements Ca, Cr, Mn, Co, Ni, Cu and Zn have been photographed and for each of these elements an extended fine structure has been obtained. The fine structure, consisting of six or seven secondary edges, extends over an energy range of more than 200 volts. In every instance the element was used as the absorbing screen except Mn where it was present in the alloy manganin. No detectable difference was found in the absorption spectrum of copper between that obtained with a brass screen and that with the element alone. An attempt was made to show more definitely the relation of the $K\beta_2$ emission line to the principal K absorption limit for Fe, Co, Ni and Cu. Indications are that the main edge is produced by the ejection of a K electron to an optical level rather than to infinity. It is shown that the Kossel theory alone is quite inadequate to explain all the secondary edges. On the basis of multiple ionization the probable electron transitions have been determined and tabulated to account for the observed separations of the various secondary edges from the principal K edge. The methods employed herein to account for probable electron transitions, when applied to the transitions proposed by Ray, in his treatment of the fine structure in K and Ca, give very different energy values from those which he has computed.

Introduction

THE more or less complicated appearance of absorption spectra which is often found on the short wave-length side of the edge is known as absorption fine-structure. Stenstrom,[1] Fricke,[2] Hertz[3] and Lindh[4] were among those who made the earlier investigations. The latter made an extensive study of the K absorption spectra of the elements P(15) to Fe(26) and found as many as three white lines on the plates i.e., in addition to the ordinary absorption discontinuity there appeared lighter and darker regions on the short wave-length side. Coster and van der Tuuk[5] found a very limited fine structure associated with the K edge of argon. An extended fine structure of the edge was found by Lindsay and Van Dyke[6] in the K absorption of calcium, where the element was present in the crystals used as reflectors and served also in the capacity of absorbing material. Nuttall's[7] investiga-

[1] W. Stenstrom, Diss. Lund, 1919.
[2] H. Fricke, Phys. Rev. **16**, 202 (1920).
[3] G. Hertz, Zeits. f. Physik **3**, 19 (1920).
[4] A. E. Lindh, Diss. Lund, 1923.
[5] D. Coster, and J. H. van der Tuuk, Zeits. f. Physik **37**, 367 (1926).
[6] G. A. Lindsay and G. Van Dyke, Phys. Rev. **27**, 508 (1926).
[7] J. M. Nuttall, Phys. Rev. **31**, 742 (1928).

tion of the *K* edges of potassium and chlorine in compounds showed as many as five secondary edges. Voorhees and one of the authors[8] have shown that the multiple structure for iron, both as a metal and in compounds, extends over a range considerably greater than that of any fine structure previously reported. They found that the outstanding features for the element alone were in the structure which was apparent in the main edge itself, the absence of the intense white-line absorption, the increase in extent or range of the secondary edges, and verified the fact that the free element has the principal absorption edge of longest wave-length[9] which should therefore be more characteristic of the substance.

Since metallic iron afforded such an excellent fine-structure it was felt that other neighboring elements in the free state might also under suitable conditions, give an extended structure of the *K* absorption edge. Besides it was hoped that with information regarding the secondary edges of a considerable number of adjacent elements, it might be possible to arrive more readily at a satisfactory explanation for the observed phenomena. It was with such aims in view that the present work was undertaken. The general method employed was that of placing films of the absorbing metal in the path of the x-ray beam and obtaining photographic records of the absorption spectrum by reflection of the radiation from a sylvite or a calcite crystal.

Apparatus and Experimental Procedure

A Siegbahn precision vacuum spectrograph was used for obtaining photographs of the absorption edges. For absorption spectra of all the elements investigated a natural potassium chloride crystal served as the reflector. The dispersion with this crystal varied from about 15 X.U. per mm for Ca to about 17 X.U. per mm in the case of zinc. Since the secondary edges become more crowded together with increasing atomic number it was necessary to increase the dispersion for Cu and Zn in order to obtain plates showing the fine structure which could be measured with a fair degree of accuracy. Accordingly, a calcite crystal was ground parallel to the (111) planes and mounted in the usual manner. This provided a dispersion of about 7 X.U. per mm.

Proper screens are one of the most essential requirements necessary to insure success in obtaining fine structure in the absorption edges. One must have uniformity as well as optimum thickness and both of these are troublesome factors in many cases. An excellent principal edge can be produced with screens which are either too thick or too thin to show the secondary edges. The surest method of determining the proper thickness is by trial.

Using such a trial method it was found that a nickel film about 0.007 mm thick gave excellent fine structure. This nickel had been prepared electrolytically and annealed in hydrogen. The copper, brass and zinc screens were prepared simply by carefully rolling out the metals to suitable thicknesses. It may be pointed out here that the results obtained for copper in

[8] G. A. Lindsay and H. R. Voorhees, Phil. Mag. **6**, 910 (1928).
[9] Kath. Chamberlain, Nature **114**, 500 (1924), Phys. Rev. **26**, 525 (1925).

brass showed no measurable deviations from that obtained when copper screens were used.

Considering the results obtained with brass screens for copper fine structure it was thought permissible to use an alloy of manganese as an absorber. Manganin, a copper-manganese alloy containing 15% manganese, was used since it could be easily rolled to the proper thickness and also because the manganese content is high in this alloy.

The preparation of cobalt screens presented no difficulties. The metal was deposited electrolytically on chromium plated electrodes from which it was then easily removed. The chromium screens required a different procedure. Due to its extreme hardness and brittleness rolling was out of the question. A layer of Cr about 0.003 mm thick was plated on a thin steel electrode. Then a thin coating of paraffin was applied over the Cr to strengthen the film, this added support being necessary during the following chemical process. HCl was used to etch away the iron from a small area leaving the Cr film which was supported by the remainder of the steel.

Calcium screens required extra precautions due to the rapid oxidation. Pure Ca was rolled out to the desired thickness and immediately given a thin coating of paraffin. In this manner Ca films could be used for a hundred or more hours.

Although no very definite results were obtained for gallium (31) and selenium (34), as far as fine structure is concerned, the preparation of these screens is described. Ga melts at 30.1°C. Like Hg in the liquid state its surface tension is great. Fortunately one is able to spread it out into a thin layer when applied on aluminum. If the Al is used in the form of thin foil there will be only a very slight amount of absorption due to this element since the wave-length of the K edge of Ga is below 1.2A. Selenium screens were made by heating the element somewhat above its melting point and then when temperature conditions were just right it was possible to spread out the substance on thin pieces of paper. Here again the amount of absorption by the supporting material was negligible.

Measurements on all plates were made on a comparator having a least count of 0.005 mm. In making settings on the various edges the cross-hair of the instrument was brought across the blackening to such a position that it was possible just to see no falling off in the intensity on the long wave-length side of the cross-hair. Settings were also made on any good emission lines, if they were present on the plate, since they served as convenient reference lines to determine the wave-length of the principal edge and also permitted a check on the dispersion for the adjacent regions. The photometric curves incorporated in this paper were made on a Moll microphotometer. Duplicate runs over different portions of the plate gave curves which were essentially the same.

To aid in the interpretation of the fine structure data additional plates were made to show more definitely the location of the KB_2 line of an element with respect to the principal K absorption limit of the same substance. Copper, nickel, iron and cobalt were studied. The method employed was

to photograph on a plate the main K edge and any suitable reference line so that the distance between these two could be measured on the comparator. On another plate the emission spectrum of the element was obtained in which the $K\beta_2$ line was sufficiently prominent to be measured. The same reference line was photographed with the $K\beta_2$ line and therefore the distance between the lines could be determined. In each case of absorption the screens were of the free element, no attempt being made to obtain fine structure. For copper absorption the continuous spectrum came from a molybdenum target while in the other three cases a copper anode was employed. This procedure prevented the appearance of the $K\beta_2$ line in the absorption spectrum and therefore aided in making more reliable settings on the main edge. For the emission spectra targets of these various metals were used. At least two plates of each type for each element were obtained and measured.

In every case the value used in the computation of the wave-length of edge or line was the mean value of ten settings on the comparator. The general method used was that of reference measurements. Since the wave-length of the principal absorption edge depends upon the chemical combination of the absorber it was desirable to determine the wave-length of the absorption limits for each of the free elements studied. Having determined the wave-lengths of the main K edge for each element the wave-lengths of the secondary edges were computed by multiplying each linear separation, from the principal edge to the secondary edge, by the proper dispersion factor and subtracting each product from the known absorption limit. The reciprocal of the wave-length gives the frequency ν in cm^{-1} and division by the Rydberg constant 109737 gives ν/R for each edge. The separation $\Delta\nu/R$ of any secondary edge from the main edge may then be expressed in equivalent volts by multiplying the by the factor 13.56.

Data and Results

I. Wave-Length determinations of principal K absorption limits.

In Table I have been recorded the mean values, expressed to the nearest 0.1 X.U., of the principal K absorption limits. The value of iron is included, this result having been taken from the work of Voorhees and one of the authors.[8]

Table I. *Wave-lengths of the K absorption limits.* λ *in X.U.*

Element	λ	Element	λ
20 Ca	3063.9	28 Ni	1484.6
24 Cr	2066.1	29 Cu	1377.8
25 Mn	1891.3	30 Zn	1280.8
26 Fe	1739.3*	31 Ga	1192.9
27 Co	1604.3	34 Se	977.8

* Lindsay and Voorhees.[8]

II. Absorption fine structure.

The general appearance of the plates showing absorption spectra in which the principal edges are accompanied by several secondary edges

may be seen in Fig. 1. The micro-photograms are reproduced in Fig. 2. The discontinuity designated by "K" marks the location of the main edge

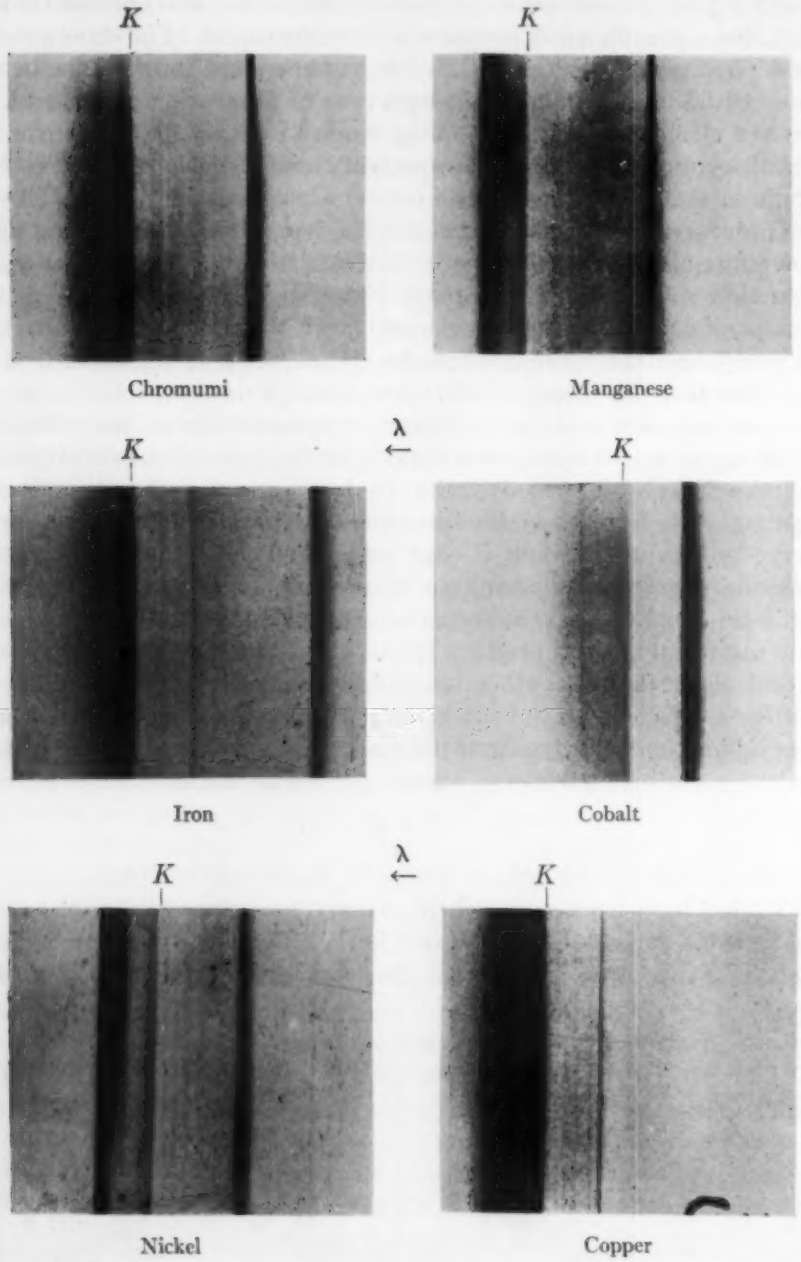

Fig. 1. Fine structure in the absorption spectra of the K series of several elements.

and it is in the lighter region to the short wave-length side of this edge that one observes the fine structure, whose general appearence is that of a series

of alternately light and dark regions. The "white lines" are not of the same width, nor of the same intensity, neither are they equally spaced on the plate but appear farther and farther apart as one proceeds to shorter wave-lengths. In the discussion below an attempt is made to trace the most

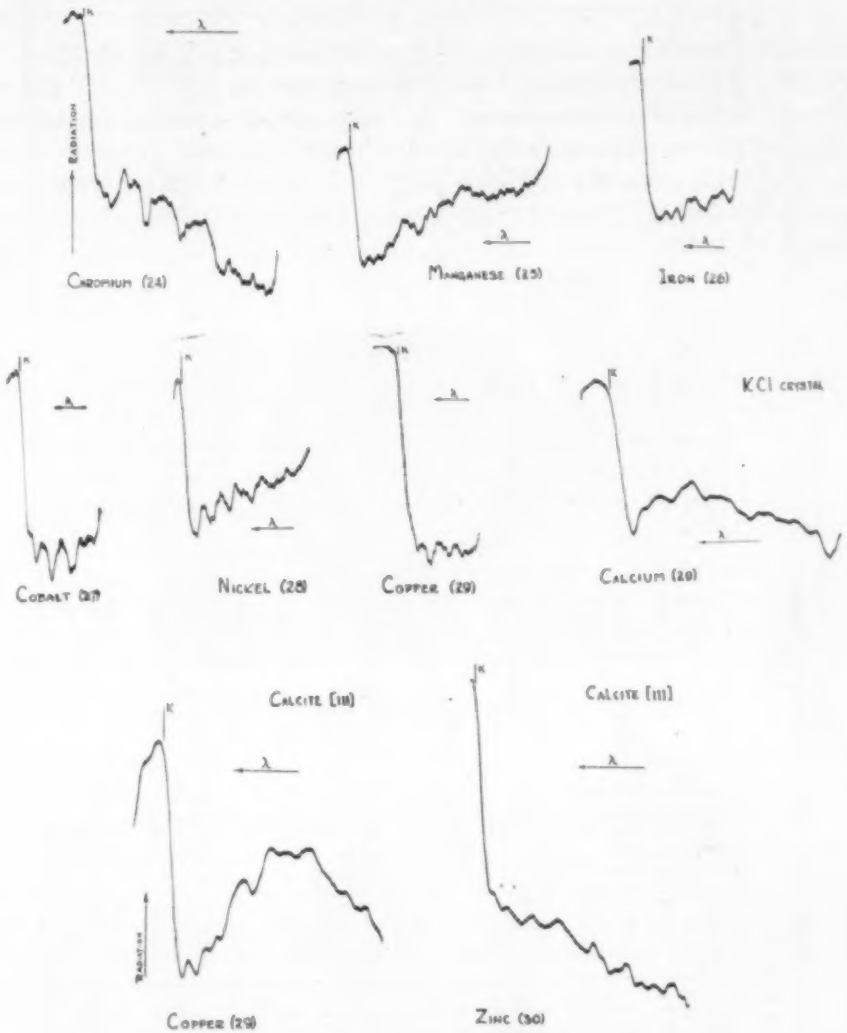

Fig. 2. Photometric records of K x-ray absorption spectra.

intense white line, or better, the adjacent secondary edge, through the various elements.

The results obtained from data on each element for which fine structure was observed and measured have been collected in Table II. In this table are given the mean values of the wave-lengths of the secondary edges, expressed to 0.1 X.U. together with the separations of these edges from the

TABLE II. *Secondary absorption edges.*

	λ—Wave-length in X. U. K								ΔV $\Delta(\nu/R)$ (volts)	Separation from Principal Edge		
Ca λ	3063.9	3059.0	3048.5	3041.8	3034.7	3014.2	2987.3	2959.9				
Ca $\Delta(\nu/R)$		.48	1.50	2.16	2.87	4.90	6.93	10.45				
Ca ΔV		6.5	20.2	29.3	38.9	66.4	94.0	142.				
Cr λ	2066.1	2060.5	2049.1	2040.0	2030.5	2019.9	2009.3	1984.9	1958.6			
Cr $\Delta(\nu/R)$		1.19	3.67	5.66	7.73	10.1	12.48	18.08	24.23			
Cr ΔV		16.2	49.8	76.7	105.	137.	169.	245.	329			
Mn λ	1891.3	1886.8	1880.6	1876.6	1870.4	1867.6	1857.6	1850.7	1842.3	1838.1	1827.4	1811.2	1787.0
Mn $\Delta(\nu/R)$		1.13	2.73	3.77	5.38	6.10	8.74	10.23	12.81	13.95	16.85	21.3	28.1
Mn ΔV		15.4	37.1	51.	73.	83.	118.	139.	174.	189.	228.	289.	381.
Fe λ	1739.3	1737.1	1731.4	1726.7	1721.1	1715.2	1706.9	1701.3	1690.9	1683.4	1663.0		
Fe $\Delta(\nu/R)$		.67	2.39	3.82	5.54	7.36	9.90	11.7	14.9	17.4	24.0		
Fe ΔV		9.1	32.4	51.8	75.	100.	134.	159.	202.	236.	325.		
Co λ	1604.3	1601.9	1595.4	1586.6	1573.3	1557.0							
Co $\Delta(\nu/R)$		.86	3.17	6.32	11.2	17.25							
Co ΔV		11.6	43.	86.	152.	234.							
Ni λ	1484.6	1483.0	1478.3	1471.0	1458.2	1449.4	1442.7	1431.3	1413.0				
Ni $\Delta(\nu/R)$		.69	2.61	5.65	11.14	14.97	17.86	22.95	31.2				
Ni ΔV		9.3	35.3	77.	151.	203.	242.	311.	423.				
Cu λ	1377.8	1375.8	1374.2	1372.4	1365.3	1363.2	1357.0	1354.1	1349.5	1348.0	1342.2	1337.0	1329.1
Cu $\Delta(\nu/R)$		.96	1.74	2.64	6.06	7.09	10.11	11.56	13.9	14.6	17.5	20.2	24.3
Cu ΔV		13.0	23.6	36.	82.	96.	137.	157.	188.	191.	238.	273.	330.
Zn λ	1280.8	1278.7	1277.2	1275.6	1273.7	1270.6	1265.6	1261.5	1258.4	1253.5	1249.5	1238.9	
Zn $\Delta(\nu/R)$		1.15	2.0	2.88	3.95	5.71	8.46	10.85	12.63	15.48	17.75	24.0	
Zn ΔV		15.6	27.	39.	54.	77.	115.	147.	171.	209.	241.	326.	

* Lindsay & Voorhees.[6]

principal edge. The separations are tabulated in ν/R units as well as in equivalent volts. The values for iron were taken from the results of Lindsay and Voorhees[8] and were incorporated in order to have a complete sequence from Cr to Zn.

III. Relation between the $K\beta_2$ line and the principal K edge for the elements Fe, Co, Ni and Cu.

In the discussion of possible electron transitions corresponding to secondary edges it is evidently necessary to know as much as possible of the transition related to the principal edge. It has been rather assumed that the K electron goes to infinity. Now the $K\beta_2$ line represents a transition from the $N_{II,III}$ level to the K level, and if the K electron in absorption goes to infinity we should have for the elements here considered a difference between the K edge and the KB_2 line about equal to the first ionization potential.

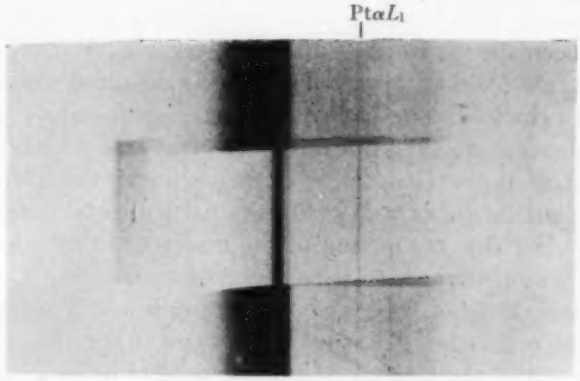

Fig. 3. K absorption and emission spectrum of copper.

Measurements from a number of plates of the relative positions of the K edge and the $K\beta_2$ line with respect to a chosen reference line show a separation smaller than that of the ionizing potential. The difference also varies with different elements. In fact, for nickel, what we have been accustomed to take as the position of the K edge is slightly longer in wave-length than the $K\beta_2$ line, while for Cu the two are sensibly the same. Fig. 3 shows the K absorption spectrum and the $K\beta_1$ and $K\beta_2$ emission lines for Cu photographed on the same plate. The reference lines is Pt$L\alpha_1$.

Theoretical Aspects of the Problem

Several hypotheses have been set forth to account for the observed structure of x-ray absorption edges. Since in this investigation free elements were used as absorbers there was no possibility of observing the white line absorption on the long wave-length side of the principal edge, similar to that found by Coster[10] and by Lindh,[11] resulting from reduction of the com-

[10] D. Coster, Zeits. f. Physik **25**, 83 (1924).
[11] A. E. Lindh, Zeits. f. Physik **31**, 210 (1925).

pounds in the screen by the x-ray beam thus producing some of the free element. It has been demonstrated that the free element has its principal absorption limit at a longer wave-length than any of the ionized forms.

According to Kossel's[12] viewpoint, published in 1920, the principal K absorption limit corresponds to the absorption of a quantum of energy sufficient to eject a K electron to the first permissible, unoccupied orbit. For the elements studied in this investigation this would mean a transition from the K level to the N_{II} level, or what is the same, from a $1s$ to a $4p$ state. That many atoms are excited to this state by the absorption of energy, is evidenced by the fact that the $K\beta_2$ line is emitted with considerable intensity by these elements. Thus one may conclude, as did Kossel, that the probability of a K electron stopping in the first unoccupied orbit is large. However, it is very likely that in many atoms the K electron would be ejected to the $5p$ or $6p$ level if the atom absorbed a quantum sufficient for such a jump. One would therefore expect absorption limits corresponding to these various transitions. The limiting position for these secondary edges would be that which corresponds to absorption of energy sufficient to remove a K electron completely from an atom. The energy required would be in excess of that for the principal edge by an amount corresponding approximately to the first ionization potential of an atom of atomic number one greater. The first ionization potentials for the elements under consideration are 6 to 9 volts. Edges within this small range are hardly to be detected although results indicate that the separation of the first secondary edge corresponds to the limiting value, that is, to the energy of ionization. Coster and Van der Tuuk in their study of the K edge of argon found a secondary edge at 1.7 volts from the main edge. They attributed this to the absorption of energy sufficient to eject a K electron to one of the optical levels of the atom.

There is rather convincing evidence that the main edge results from absorption of energy which will remove a K electron to an outer orbit rather than from that which would completely remove the K electron from the atom. As stated under Part III, the principal edge, at least for iron, cobalt, nickel and copper, has a separation from the $K\beta_2$ line which is never more than about half the ionizing potential. The $K\beta_2$ line is ascribed to the transition of an electron from the N_{II} level to the K level. To exactly what orbit the K electron goes in the absorption process is difficult to say, although the results would indicate an excitation to a higher optical level in the cases of cobalt, iron and copper than in nickel. Allowance for this condition was made in the determination to account for the secondary edges.

The extent of absorption fine structure such as that observed by Lindsay and VanDyke for calcium in calcium compounds, by Nuttall for potassium and for chlorine in compounds of those elements, by Lindsay and Voorhees for iron (free and in combinations), by Coster[13] for copper and that by the authors has all been such that Kossel's theory, which he himself

[12] W. Kossel, Zeits. f. Physik **1**, 119 (1920).
[13] D. Coster, Nature **124**, 652 (1929).

pointed out would explain only a small range of fine structure, would alone be quite inadequate to account for it. Secondary edges occur whose separations from the main edge are much greater than that which one could ascribe to an amount of energy of the order of the first ionization potentials. Thus one is led immediately to the supposition that a multiple ionization may result from the absorption of a single quantum of energy. It was this idea of multiple ionization that Wentzel[14] proposed to account for the so-called "spark lines" or non-diagram lines which were found in x-ray emission spectra.

If Wentzel's hypothesis is a valid one to account for the emission of the "spark" lines then the atoms must absorb energy sufficient to excite them to the states which would give rise to such lines and one ought to be able to obtain absorption edges for the corresponding states. Lindsay and Voorhees, in their work on the K absorption in iron and iron compounds sought to locate an edge which would result when the incident quantum of energy ejected an L electron with a K electron. This edge would have a separation of about 750 volts from the principal edge. The indications of such an edge were too feeble to furnish any conclusive evidence for this double ionization. Likewise, no one has reported absorption edges to confirm a double ionization of the K state. However, this does not lead to the conclusion that simultaneous multiple ionization is improbable. Ionizations involving K and M or N electrons may occur and edges corresponding to these have been found by several investigators.

To calculate the energy difference in states represented by the separation of any secondary edge from the main edge one must know, or determine, or possibly assume, the electron transition which resulted from absorption of energy to produce the main edge. It was by means of measurements on the K edge and $K\beta_2$ line for several elements that one could say with some degree of assurance to which orbit the K electron went in the case of the main edge.

Consider first the zinc absorption spectrum. Zinc, atomic number 30, has the normal configuration of electrons $3d^{10}\ 4s^2$, and all the inner orbits are filled. To excite the atom to the K state means that a K electron must be ejected at least to an N_{II} level, i.e., to a $4p$ orbit. This will be designated by $(K \rightarrow N_{II})$. The ejected electron cannot stop in an inner orbit since there are no vacant ones in the neutral zinc atom. If this be the case then the wave-length for the main edge would correspond exactly to the wave-length of the $K\beta_2$ line. Although this was not verified for zinc in a manner similar to that for iron, nickel, cobalt and copper, there are other reasons to believe that one should attribute the main K edge to the transition $K \rightarrow N_{II}$ as recorded in Table III under zinc. In the first place it seems reasonable to assume that when one K electron is missing, then to an outer electron the nucleus and remaining K shell together, or the core of the atom, is very much like the central portion of the element with atomic number one

[14] G. Wentzel, Ann. d. Physik **66**, 437 (1921)

greater. Thus the nucleus and K shell of neutral zinc taken as a unit acts like a charge of 30–2 or 28 to an outer electron. This assumes that the K electrons have a complete screening effect. But with one K electron gone the effective charge would be 29. This is just the value of the charge of the

TABLE III. *Probable multiple ionizations for secondary absorption edges.*

Edge	Electron transitions	Separation from K edge in ν/R units	
	Calcium	Calculated	Observed
K	$(K\rightarrow M_{IV})$	0.00	0.00
1	$(K\rightarrow M_{IV})+(N_I\rightarrow\infty)$	0.48	0.48
2	$(K\rightarrow M_{IV})+(N_I\rightarrow\infty)+(N_I\rightarrow\infty)$	1.43	1.50
3	$(K\rightarrow M_{IV})+(M_{III}\rightarrow\infty)$	2.70	2.87
4	$(K\rightarrow M_{IV})+(M_I\rightarrow\infty)$	4.70	4.90
5	$(K\rightarrow M_{IV})+(M_I\rightarrow N_{II})+(M_{II\,III}\rightarrow N_{IV})$	6.90	6.93
6	$(K\rightarrow M_{IV})+(M_I\rightarrow\infty)+(M_I\rightarrow\infty)$	10.20	10.45
	Chromium		
K	$(K\rightarrow N_{II})$	0.00	0.00
1	$(K\rightarrow\infty)+(N_I\rightarrow O_{II})$	1.0	1.19
2	$(K\rightarrow N_{II})+(M_{II}\rightarrow N_I)$	3.5	3.67
3	$(K\rightarrow\infty)+(M_{II}\rightarrow\infty)+(M_{IV}\rightarrow N_{II})$	5.3	5.66
4	$(K\rightarrow\infty)+(M_I\rightarrow\infty)$	7.55	7.73
5	$(K\rightarrow N_{II})+(M_I\rightarrow M_{IV})+(M_{II}\rightarrow N_I)$	10.1	10.1
6	$(K\rightarrow N_{II})+(M_I\rightarrow N_{II})+(M_I\rightarrow M_{IV})$	12.7	12.48
7	$(K\rightarrow N_{II})+(M_I\rightarrow\infty)+(M_I\rightarrow\infty)+(M_{II}\rightarrow N_{IV})$	18.2	18.08
8	$(K\rightarrow\infty)+(M_I\rightarrow\infty)+(M_I\rightarrow\infty)+(M_{II}\rightarrow N_{IV})+(M_{II}\rightarrow N_{IV})$	24.1	24.23
	Manganese		
K	$(K\rightarrow N_{II})+(N_I\rightarrow M_{IV})$	0.00	0.00
1	$(K\rightarrow N_{II})+(M_{IV}\rightarrow N_{II}+(M_{IV}\rightarrow N_{II})$	1.2	1.13
2	$(K\rightarrow\infty)+(N_I\rightarrow\infty)+(M_{IV}\rightarrow N_{II})$	2.8	2.73
3	$(K\rightarrow\infty)+(N_I\rightarrow\infty)+(M_{IV}\rightarrow\infty)$	3.71	3.77
4	$(K\rightarrow\infty)+(M_{II}\rightarrow\infty)$	5.3	5.38
5	$(K\rightarrow\infty)+(M_{II}\rightarrow\infty)+(M_{IV}\rightarrow N_{II})$	5.9	6.10
6	$(K\rightarrow N_{II})+(M_{II}\rightarrow\infty)+(M_{II}\rightarrow N_I)$	8.9	8.74
7	$(K\rightarrow\infty)+(M_{II}\rightarrow\infty)+(M_{II}\rightarrow N_{IV})$	10.1	10.23
8	$(K\rightarrow N_{II})+(M_I\rightarrow\infty)+(M_{II}\rightarrow\infty)$	12.6	12.80
9	$(K\rightarrow N_{II})+(M_{II}\rightarrow\infty)+(M_{II}\rightarrow\infty)+(M_{III}\rightarrow N_I)$	13.9	13.95
10	$(K\rightarrow\infty)+(M_I\rightarrow\infty)+(M_{II}\rightarrow N_I)+(M_{II}\rightarrow N_{IV})$	17.1	16.85
11	$(K\rightarrow N_{II})+(M_I\rightarrow\infty)+(M_I\rightarrow\infty)+(M_{II}\rightarrow\infty)$	21.6	21.30
12	$(K\rightarrow\infty)+(M_I\rightarrow\infty)+(M_I\rightarrow\infty)+(M_{II}\rightarrow\infty)+(M_{II}\rightarrow N_I)$	27.9	28.10
	Iron		
K	$(K\rightarrow N_{II})+(N_I\rightarrow M_{IV})$	0.00	0.00
1	$(K\rightarrow\infty)+(N_I\rightarrow N_{II})$	0.72	0.67
2	$(K\rightarrow\infty)+(N_I\rightarrow\infty)+(M_{IV}\rightarrow N_{II})$	2.4	2.39
3	$(K\rightarrow\infty)+(N_I\rightarrow\infty)+(M_{IV}\rightarrow\infty)$	3.73	3.82
4	$(K\rightarrow\infty)+(M_{II}\rightarrow\infty)$	5.8	5.54
5	$(K\rightarrow\infty)+(M_I\rightarrow M_{IV})$	7.4	7.36
7	$(K\rightarrow\infty)+(M_{II}\rightarrow N_I)+(M_{II}\rightarrow N_{IV})$	9.9	9.90
7	$(K\rightarrow N_{II})+(M_I\rightarrow N_{II})+(M_{II}\rightarrow M_{IV})$	11.9	11.70
8	$(K\rightarrow N_{II})+(M_I\rightarrow M_{IV})+(M_I\rightarrow N_{III})$	15.0	14.90
9	$(K\rightarrow\infty)+(M_I\rightarrow\infty)+(M_I\rightarrow N_{II})+(M_{IV}\rightarrow N_{II})$	17.4	17.40
10	$(K\rightarrow\infty)+(M_I\rightarrow\infty)+(M_{II}\rightarrow N_I)+(M_{II}\rightarrow N_{IV})+(M_{II}\rightarrow N_{IV})$	24.2	24.00
	Cobalt		
K	$(K\rightarrow\infty)+(N_I\rightarrow M_{IV})$	0.00	0.00
1	$(K\rightarrow\infty)+(N_I\rightarrow O_{II})$	0.86	0.86
2	$(K\rightarrow\infty)+(N_I\rightarrow\infty)+(M_{IV}\rightarrow O_{II})$	3.1	3.17
3	$(K\rightarrow\infty)+(M_{II}\rightarrow\infty)$	6.33	6.32
4	$(K\rightarrow\infty)+(M_{II}\rightarrow\infty)+(M_{II}\rightarrow M_{IV})$	11.23	11.14
5	$(K\rightarrow\infty)+(M_I\rightarrow\infty)+(M_I\rightarrow M_{IV})$	17.0	17.25

TABLE III. (*Continued*)

Edge	Electron transitions	Separation from K edge in ν/R units	
	Nickel	Calculated	Observed
K	$(K\rightarrow M_{IV})+(N_I\rightarrow M_{IV})$	0.00	0.00
1	$(K\rightarrow M_{IV})+(N_I\rightarrow\infty)$	0.57	0.69
	$(K\rightarrow\infty\ )$	0.79	0.69
2	$(K\rightarrow\infty\ )+(N_I\rightarrow\infty)+(M_{IV}\rightarrow N_I)$	2.6	2.61
3	$(K\rightarrow M_{IV})+(M_{II}\rightarrow N_{IV})$	5.7	5.65
4	$(K\rightarrow M_{IV})+(M_{II}\rightarrow N_{IV})+(M_{II}\rightarrow N_I)$	11.3	11.14
5	$(K\rightarrow M_{IV})+(M_I\rightarrow N_{II})+(M_{II}\rightarrow\infty)$	15.0	14.97
6	$(K\rightarrow M_{IV})+(M_I\rightarrow N_{II})+(M_I\rightarrow N_{III})$	18.0	17.86
7	$(K\rightarrow\infty\ )+(M_I\rightarrow\infty)+(M_I\rightarrow\infty)+(M_{IV}\rightarrow N_{II})$	22.7	22.95
8	$(K\rightarrow\infty\ )+(M_I\rightarrow\infty)+(M_I\rightarrow\infty)+(M_{II}\rightarrow\infty)$	31.2	31.20
	Copper		
K	$(K\rightarrow N_{II})$	0.00	0.00
1	$(K\rightarrow\infty\ )+(N_I\rightarrow N_{II})$	.86	.96
2	$(K\rightarrow\infty\ )+(N_I\rightarrow\infty)$	1.72	1.74
3	$(K\rightarrow\infty\ )+(M_{IV}\rightarrow\infty)$	2.45	2.64
4	$(K\rightarrow N_{II})+(M_{II}\rightarrow N_I)$	6.50	6.06
5	$(K\rightarrow N_{II})+(M_{II}\rightarrow\infty)$	7.20	7.09
6	$(K\rightarrow N_{II})+(M_I\rightarrow N_{II})$	10.10	10.11
7	$(K\rightarrow N_{II})+(M_I\rightarrow N_{II})+(M_{IV}\rightarrow\infty)$	11.7	11.56
8	$(K\rightarrow N_{II})+(M_{II}\rightarrow\infty)+(M_{II}\rightarrow N_I)$	13.9	13.89
9	$(K\rightarrow N_{II})+(M_{II}\rightarrow\infty)+(M_{II}\rightarrow N_{IV})$	14.5	14.60
10	$(K\rightarrow N_{II})+(M_I\rightarrow\infty)+(M_{II}\rightarrow N_{IV})$	17.8	17.50
11	$(K\rightarrow N_{II})+(M_I\rightarrow N_{II})+(M_I\rightarrow N_{III})$	20.7	20.20
12	$(K\rightarrow N_{II})+(M_I\rightarrow N_{II})+(M_{II}\rightarrow N_{IV})+(M_{II}\rightarrow N_I)$	24.3	24.30
	Zinc		
K	$(K\rightarrow N_{II})$	0.00	0.00
1	$(K\rightarrow\infty\ )+(N_I\rightarrow N_{II})$	1.11	1.15
2	$(K\rightarrow\infty\ )+(N_I\rightarrow\infty)$	1.95	2.00
3	$(K\rightarrow\infty\ )+(M_{IV}\rightarrow\infty)$	2.88	2.88
4	$(K\rightarrow N_{II})+(M_{IV}\rightarrow\infty)+(N_{IV}\rightarrow N_{II})$	3.95	3.95
5	$(K\rightarrow\infty\ )+(N_I\rightarrow\infty)+(M_{IV}\rightarrow\infty)$	5.75	5.71
6	$(K\rightarrow N_{II})+(M_{II}\rightarrow\infty)$	8.24	8.46
7	$(K\rightarrow N_{II})+(M_{II}\rightarrow\infty)+(M_{IV}\rightarrow\infty)$	11.0	10.85
8	$(K\rightarrow\infty\ )+(M_I\rightarrow\infty)$	12.88	12.63
9	$(K\rightarrow\infty\ )+(N_I\rightarrow\infty)+(M_I\rightarrow\infty)$	15.35	15.48
10	$(K\rightarrow N_{II})+(M_{II}\rightarrow\infty)+(M_{II}\rightarrow\infty)$	17.3	17.75
11	$(K\rightarrow N_{II})+(M_I\rightarrow\infty)+(M_I\rightarrow N_{II})$	24.14	24.00

core of neutral gallium. The electron configuration for gallium is $3d^{10}4s^24p$. Hence the K electron of zinc in being ejected by the absorption of energy sufficient to excite the K state would probably stop in the $4p$ orbit so as to give an outer configuration like gallium, and there would now be 29 electrons outside the K shell just as there are in neutral gallium.

Further evidence that this assumption is valid comes from the results expressed in Table III for the energy separations of the secondary edges in the zinc absorption spectrum. By taking the K electron to an N_{II} level for the main edge remarkably good agreement has been obtained between calculated and observed values for the energy separations of secondary edges from the K edge. The method employed in calculating these energy separations follows.

Column one in Table III lists the edges in order of decreasing wave-length beginning with the main edge (which has the longest wave-length) marked

"K". In the second column appear the probable electron transitions which involve absorptions of energy of sufficient amounts to account for the observed edges. Calculated and observed values (expressed in the customary ν/R units) of the energy differences which correspond to the separations of the main and secondary edges are given in the last two columns.

Confining attention to the tabulation on zinc, one notes that the K edge has been recorded as resulting from the transition $K \rightarrow N_{II}$ as mentioned above. The first secondary edge, might arise from the transitions:

$$(K \rightarrow \infty) + (N_I \rightarrow N_{II})$$

which may also be written as: $(K \rightarrow N_{II}) + (N_I \rightarrow \infty)$ although the former is easier to compute. The additional energy involved here, above that for $(K \rightarrow N_{II})$, may be determined since it amounts to:

$$(N_{II} \rightarrow \infty) + (N_I \rightarrow N_{II}).$$

Keeping in mind that the configuration after $(K \rightarrow N_{II})$ is $3d^{10}4s^24p$, it is evident that the term $(N_{II} \rightarrow \infty)$ requires energy measured by the first ionization potential for gallium which is 5.97 volts or 0.44 in ν/R units. One must then add to this the energy to excite a gallium ion from a $4s^2$ state to a $4s$ $4p$ state. From Ga II, as given by Sawyer and Lang[15], the separation of these states is about 0.67 in ν/R. Hence the total separation of the first secondary edge from the K edge is $0.44 + 0.67 = 1.11$ whereas the observed value is 1.15.

For edge #2 we have written:

$$(K \rightarrow \infty) + (N_I \rightarrow \infty)$$

and since we are interested in the separation from the K edge we may write:

$$(N_{II} \rightarrow \infty) + (N_I \rightarrow \infty).$$

The first term as before is the energy to ionize the gallium atom once leaving the configuration $4s^2$, and the second term is the energy to remove the second ion after the first one is gone or, in other words, the second ionization potential which one obtains from the Ga II spectrum. Its value is 20.45 volts or 1.51 in ν/R. Thus the energy difference is computed to be: $0.44 + 1.51 = 1.95$. This corresponds favorably with the observed value of 2.0.

The next edge involves changes in the atom whereby two electrons, a K electron and an M_{IV} electron, are ejected from the atom. The transitions are given by:

$$(K \rightarrow \infty) + (M_{IV} \rightarrow \infty)$$

Similar to the preceding case the first term requires 0.44 in ν/R units to ionize the atom once. With the values of the energy levels as given in the thesis of F.P. Mulder,[16] the energy to remove an M_{IV} electron to an N_{II} level is found to be 1.6. But to remove the M_{IV} electron completely from

[15] R. A. Sawyer and R. J. Lang, Phys. Rev. **34**, 712 (1929).
[16] F. P. Mulder, Diss. Groningen, 1927.

the atom will take more than that amount. In the computation for the first secondary edge it was seen that ($N_{\text{I}} \rightarrow N_{\text{II}}$) required 0.67 providing the K electron was ejected to infinity, while in #2 the energy was the second ionization potential if ($N_{\text{I}} \rightarrow \infty$). Hence to take the M_{IV} electron out completely would require $1.51-0.67$ or 0.84 in addition to that necessary to eject it from an M_{IV} level to the N_{II} level. This gives as the total energy of separation of the third edge from the main edge:

$$0.44 + (1.6 + 0.84) = 2.88.$$

The observed value for this edge is also equal to 2.88.

Edge #4 may be accounted for by the transitions:

$$(K \rightarrow N_{\text{II}}) + (M_{\text{IV}} \rightarrow \infty) + (M_{\text{IV}} \rightarrow N_{\text{II}})$$

and for the separation value we need consider just the last two terms. With the K electron stopping in the N_{II} orbit the atom is much like neutral gallium. We need therefore 1.6 in ν/R to take an M_{IV} electron to the N_{II} orbit but this time only 0.44 more to remove it entirely from the atom since this amounts to the first ionization. Hence the term ($M_{\text{IV}} \rightarrow \infty$) requires $1.6+0.44=2.04$. The next step necessitates the excitation of a second M_{IV} electron to the N_{II} level. Since one electron has already been taken from this group it should require more than 1.6 for the second M_{IV} electron. In order to estimate what increase ought to be made one needs to consider the value of the screening constant for the $M_{\text{IV,V}}$ levels, which Sommerfeld[17] gives as 13.0. This means that the average screening effect for each electron is not more than about one half so that it seems reasonable to assume the value of the M_{IV} level to be increased by approximately one third the amount that the germanium M_{IV} level exceeds the gallium M_{IV} level. Thus the term ($M_{\text{IV}} \rightarrow N_{\text{II}}$) requires 1.9 and the total amount of energy that corresponds to the separation of edge #4 from the K edge is:

$$1.6 + 0.44 + 1.9 = 3.94.$$

Experimentally the separation was found to be 3.95.

The fifth secondary edge is associated with the following changes in electron configuration:

$$(K \rightarrow \infty) + (N_{\text{I}} \rightarrow \infty) + (M_{\text{IV}} \rightarrow \infty)$$

which may be written:

$$(K \rightarrow \infty) + (N_{\text{I}} \rightarrow \infty) + (N_{\text{I}} \rightarrow \infty) + (M_{\text{IV}} \rightarrow N_{\text{I}})$$

since in both the resulting configuration is the same, and the latter form lends itself more readily to computation. Considering again only the energy corresponding to the separation of the secondary edge and the K edge we may write:

$$(N_{\text{II}} \rightarrow \infty) + (N_{\text{I}} \rightarrow \infty) + (N_{\text{I}} \rightarrow \infty) + (M_{\text{IV}} \rightarrow N_{\text{I}})$$

[17] A. Sommerfeld, "Atomic Structure and Spectral Lines," Methuen, London.

and recalling that the configuration after ($K \rightarrow N_{II}$) is $3d^{10}4s^2\ 4p$ we see that the first, second and third terms require energy equal to the first, second and third ionization potentials of gallium respectively. The last term amounts to the excitation of a Ga^{+++} ion from a $3d^{10}$ state to a $3d^9 4s$ state. From the Ga IV spectrum as reported by Mack, LaPorte and Lang,[18] the separation of the terms $3d^{10}$ and $3d^9\ 4s$ is approximately 1.3. The four terms above give then:

$$0.44 + 1.51 + 2.5 + 1.3 = 5.75$$

compared with 5.71 which is the observed value for the separation in energy of the fifth secondary edge from the K edge.

In quite an analogous manner one can account for the other observed secondary edges. For each case one must choose those transitions such that the energy involved will correspond as nearly as possible to the observed values. This has been done for six more edges in zinc as well as for those found for the other elements studied. In most cases the agreement is good.

The question naturally arises as to the uniqueness of the transitions involved. Are there other possible combinations of transitions that will serve equally well to account for any given edge? In most instances the answer would probably be in the negative. One exception has been recorded in Table III for edge #1 in nickel. For the first few edges in each spectrum one must restrict the choice of electron transitions to those involving only the outer or valence electrons, since levels inside $M_{IV,V}$ are already too deep. In contrast with this one has difficulty (especially with the lighter elements studied) in finding transitions which involve enough energy to account for the shortest wave-length secondary edges. As mentioned above, changes calling for transitions from the L levels do not aid in this situation since one change such as ($L \rightarrow M$) would involve too much energy to account for any observed secondary edge.

The predominating factors which governed the choice of transitions to account for a given separation (other than that the total energy be correct) were:

(1) the electron configuration corresponding to the K edge
(2) minimum number of electron transitions.

The first of these had been discussed at length under the calculations of the various secondary edges. Some verification of the second is shown by the fact that the most prominent secondary edges seem to be associated with those changes in which the K electron and only one other (usually an M_I or an M_{II}) electron are excited. Thus two electron jumps seem more probable than those involving three or more, which is to be expected.

In connection with this characteristic feature concerning the excitation of M electrons with K electron it has been mentioned above that Coster has observed a fine structure in copper that is in good agreement with the results herein reported for that element. However, he obtained no secondary

[18] J. E. Mack, Otto Laporte and R. J. Lang, Phys. Rev. **31**, 748 (1928).

edges in zinc and attributed this negative result to the fact that in zinc (normal configuration $3d^{10}4s^2$) the $3d$ group of electrons is completely filled, so that it would be much more difficult to break into this configuration than it would be in the case of let us say—iron, nickel or even copper. A glance at Table III will indicate, however, that transitions of M electrons enter into practically every computation for zinc secondary edges.

When one compares the general method of computing the energy separations of the secondary edges from the K edge as outlined and applied in this investigation with the method used by Ray[19] for potassium, calcium and chlorine, it is very evident that there will be wide deviations in the results. One or two specific calculations will be given to confirm this statement.

Ray has used the experimental data of Nuttall[7] for potassium in various compounds, and also the data of Lindsay and Van Dyke[6] for calcium in calcium compounds. The normal configuration of potassium is $2p^6 4s$. The K edge, according to Ray, is associated with the transition $(K \rightarrow \infty)$. The first secondary edge is related to the change:

$$(K \rightarrow \infty) + (N_{\mathrm{I}} \rightarrow \infty)$$

so that the separation of this edge from the main edge is due to the term $(N_{\mathrm{I}} \rightarrow \infty)$ which Ray gives as the first inoization potential of potassium or 4.1 volts. The observed value for the separation varies from 2.8 to 4.9 volts in different compounds. Several objections to this treatment may be noted.

In the first place, when the K electron is ejected either to an outer orbit or to infinity it seems more reasonable to assume that to an outer electron, such as an N_{I} electron, the core of the atom should be more like calcium than potassium. If the K electron remained in the outer portion of the atom then the transition $(N_{\mathrm{I}} \rightarrow \infty)$ ought to correspond to the first ionization potential of calcium (6.09 volts), instead of to that for potassium (4.3 volts). But with the assumption that the K electron is ejected to infinity one ought therefore to regard $(N_{\mathrm{I}} \rightarrow \infty)$ as requiring energy equal to the second ionization potential of calcium which is 11.8 volts rather than 4.1 volts. A further objection arises since the potassium is present as an ion and not as an atom in the free state. In the ionic state there might not even be an N electron which could be ejected. The calculations on subsequent edges for potassium are also open to quite similar objections.

Ray's treatment of the calcium edges seems equally unsatisfactory. The normal configuration is $2p^6 4s^2$ and for the K edge he has assigned the transition $(K \rightarrow \infty)$. For the first edge he gives as the electron jumps:

$$(K \rightarrow \infty) + 2(N_{\mathrm{I}} \rightarrow \infty)$$

so that the latter term involves the energy which corresponds to the separation of this edge from the main edge. This he gives as twice the first ioniza-

[19] B. B. Ray, Zeits. f. Physik **55**, 119 (1929).

tion potential for calcium (6.1 volts) or 12.2 volts, as compared with the observed value of 13.3 to 16.0 volts.

Neglecting the fact that the calcium is in a compound, the following interpretation of the transitions:

$$(K \rightarrow \infty) + 2(N_{\mathrm{I}} \rightarrow \infty)$$

seems more preferable:

Since the K electron is completely ejected the atom is now much like ionized scandium (Sc^{+}). Removing one of the N_{I} electrons would require energy equal to the second ionization potential of scandium which is 12.8 volts. To remove the second N_{I} electron ought to take an amount of energy equal to the third ionization potential which is about 25 volts. Thus the total energy separation would be approximately 38 volts instead of 12.2. volts as given by Ray. The value for the next secondary edge in calcium is about 31 volts. Thus the transitions:

$$(K \rightarrow \infty\ ) + 2(N_{\mathrm{I}} \rightarrow \infty\ )$$

as chosen by Ray, which under our interpretation given above corresponds to an energy separation from the K edge of 38 volts, represent not only a great deal in excess of the 15 volts demanded for the first edge, but even too much to account for the separation of the second secondary edge from the main edge.

FALSE LINES IN X-RAY GRATING SPECTRA

By J. M. Cork

Department of Physics, University of Michigan

(Received July 5, 1930)

Abstract

Because of the arrangement of slits, x-ray source and diffraction grating generally employed in x-ray spectroscopy, certain false lines may be obtained on the photographic plate in addition to those due to defects in the grating. Spectrograms of such spurious lines having their origin in a non-uniform focal spot or reflection from slit faces, as well as those due to certain grating imperfections are shown. One type of companion line is present at wave-lengths about 13 percent greater than the parent line, whose origin is not explained.

THE existence and explanation of false lines in grating spectra in the optical region has been dealt with by many writers. Meggers and Kiess, Anderson and Runge[1] have treated the lines known as Rowland ghosts and Lyman ghosts in spectra obtained with several particular gratings. Since such false lines or 'ghosts' may occur in any spectral region and be of intensity comparable with that of fainter true lines, they may lead to confusion in interpretation of the spectra. In x-ray spectra, beside false lines of this type there may occur others due to the nature of the source. Fig. 1 shows spectrograms illustrating false lines c f four different types. While with sufficient care most of these false lines may be avoided, the possibility of their existence makes them worthy of description.

The arrangement of x-ray source, slits and grating usually employed is shown in Fig. 2. Slit widths are generally less than 0.1 mm and the distance between slits A and B not less than 15 cm. The minimum width of spectral line to be expected for a given set of conditions may be readily computed by means of the diffraction formula $\lambda = d(\cos\theta - \cos\phi)$ where λ, d, θ and ϕ denote respectively wave-length, grating constant, grazing angle of incidence, and grazing angle of diffraction. For a slit width at A of 0.1 mm and distance between slits of 15 cm, assuming the grating very close to the second slit, a variation is obtained in the grazing angle θ at the grating of 2.27 minutes of arc which combined with an assumed width of 0.1 mm at B would give a maximum variation of 4.54 minutes of arc. It is perhaps remarkable that this apparently unfavorable slit arrangement when used with a grating having 30,000 lines per inch and an incident angle θ of 20 minutes of arc for the first order molybdenum L series lines as shown in A Fig. 1 should yield a variation in ϕ of only 40 seconds of arc. This divergence in the diffracted beam would cause an increment in width of line on a photographic plate at a distance of 50 cm of only 0.097 mm. For higher orders the width is cor-

[1] Meggers and Kiess, Anderson and Runge, Jour. Opt. Soc. and Rev. Sci. Ins. **6**, 417 (1922).

respondingly reduced so that for the fourth order spectrum under the same conditions the maximum width increment is 0.0531 mm. Now while slits 0.1 mm wide when used with the 30,000 line grating as shown yield lines of satisfactory sharpness, with coarser gratings and larger values of the incident angle θ, much wider lines are produced. Thus for an incident angle of 40 minutes and a grating of 14,400 lines per inch a divergence in ϕ of 2.0 minutes of arc is obtained, giving a width increment of 0.29 mm for the first order L series lines of molybdenum.

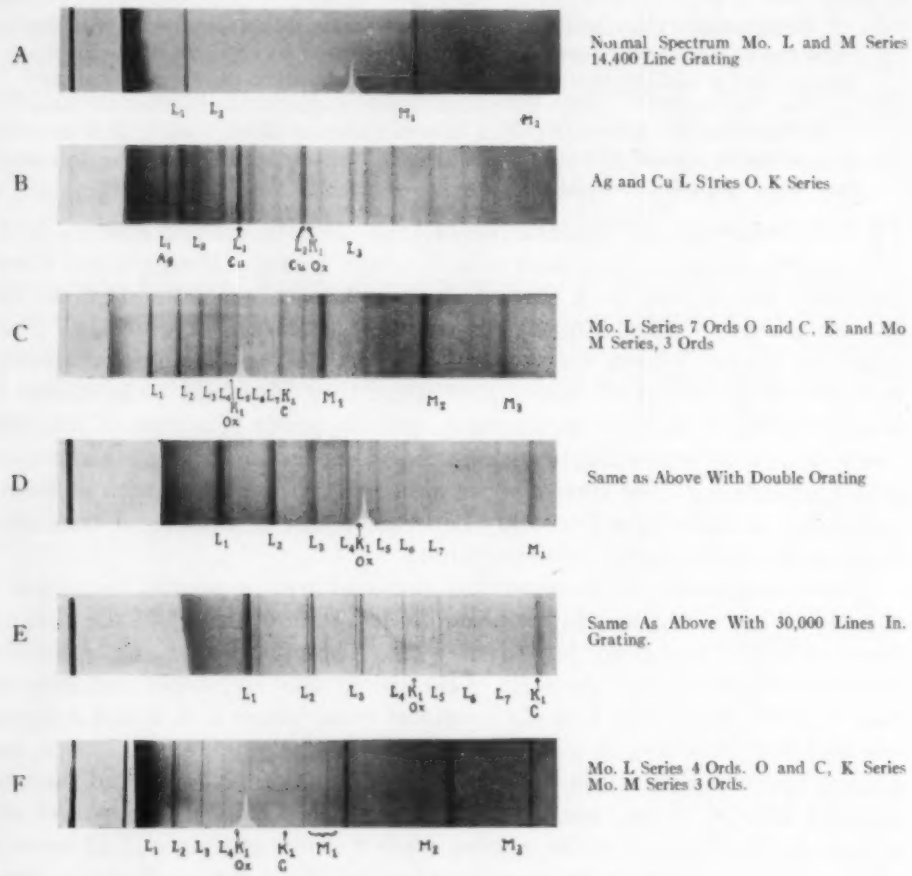
A
Normal Spectrum Mo. L and M Series 14,400 Line Grating
B
Ag and Cu L Stries O. K Series
C
Mo. L Series 7 Ords O and C, K and Mo M Series, 3 Ords
D
Same as Above With Double Orating
E
Same As Above With 30,000 Lines In. Grating.
F
Mo. L Series 4 Ords. O and C, K Series Mo. M Series 3 Ords.

Fig. 1. Spectrogram showing false x-ray lines.

In this case the line very often appears to consist of a group of very fine lines. This fine structure may be due to either of two causes, namely (a) a multi-point focal spot on x-ray target, (b) reflection or scattering of ex-radiation from the faces of slit A. Spectrogram C in Fig. 1 illustrates this multiple structure. The $L\alpha_1$ line on the original photographic plate shows clearly as five fine lines. This is undoubtedly due to the existence of several radiating spots in the main focal spot. These fine spots originating perhaps by surface irregularities become heated to incandescence and are plainly

visible. A multiplicity of this sort might account for the fine structure reported for the $K\alpha$ line of carbon[2] as it would be in agreement with the statement that the relative intensity of the observed components varied with voltage. The second type of defect may be produced if the main part of the focal spot is not included between limiting lines drawn through slits *A* and *B* as shown in Fig. 2, but lies outside as at *C*. This may result in a line of the usual width with more intense blacking at either border, the type of line depending upon relative position of focal spot and slits as well as shape of slit faces. In spectrogram *D*, Fig. 1 each main line has a blacking of this type on the long wave length side disappearing at high orders. Similarly if the total focal spot is very small and located as at *m* in Fig. 2, then a strong-fine line with a faint companion on each side might be obtained. These defects may be largely reduced by using sharp slit faces arranged as shown in Fig. 2 with a narrow opening.

Another peculiar type of defect in spectra is shown in spectrogram *D*, Fig. 1. In this case each line is doubled and the distance between components

Fig. 2. Arrangement of target, slits and grating in x-ray spectrograph. (Relative slit width enlarged.)

is the same regardless of the distance between grating and photographic plate and varies only slightly with the spectral order. An examination of the grating showed that in the part of the surface being used there were two surface levels due perhaps to some abrupt change in condition during the ruling process, this being a portion of a test grating. Two such parallel gratings when used at grazing incidence would produce doubled lines having a minimum separation of $\sin\phi/\sin\theta$ times the difference in level. A proper selection of grating surface would of course avoid defects of this sort.

Rowland ghosts as observed in optical spectra would be difficult to observe in the x-ray region. They consist of spurious lines close to and on each side of the real line with apparent wave-lengths

$$\lambda_g = \lambda(1 \pm n/Nm)$$

where n and m denote the order of spurious line and order of real line respectively, and N stands for the number of lines ruled for one revolution of the ruling machine screw. These lines are due to the superposition of a coarser period upon the nominal period of the grating caused by imperfections connected with the pitch of the screw in the ruling machine. Such false lines may have intensities less than 1/1000 that of the parent line for gratings

[2] Bazzoni, Faust and Weatherby, Nature **123**, 717 (1929).

ruled on the excellent machines now existant. This low intensity, combined with the minute separation that would be obtained for say a 30,000 line per inch grating in high orders, make ghosts of this type of no moment in x-ray spectroscopy.

False lines of the Lyman type having wave-lengths such as 3/5, 4/5, 6/5, 7/5 etc. the wave-length of a real line but with intensities less than 1/1000 that of the parent line might be observed in the x-ray region. These lines have been explained by Runge as due to the superposition of two periods on the grating, one large and one small but neither necessarily a simple multiple of the fundamental period, caused by some mechanical irregularity in the ruling machine. In spectrogram *F*, Fig. 1 the principal Mo *M* line whose wave-length is 64.52 A is shown over-exposed in three orders. Situated almost symmetrically with each of these are two pairs of fainter lines. The inner pair is separated from the parent line by fractional wave-length differences of 0.067 less and 0.073 more than the central line. The wave-length (of that one) of the outer pair on the short wave-length side is 55.17A which agrees with a wave-length value already attributed to a molybdenum *M* line.[3] The component on the long wave-length side may be a satellite of the type to be described in the following paragraph. Although the arrangement of these lines looks supiciously like a parent line with satellites on either side, there is no definite assurance so far, that they are not all real lines.

It will be observed in Fig. 1 in every spectrogram that on the long wave length side of every strong line there appears a companion line of perhaps 1/10 the intensity whose wave-length is approximately 1.133 times that of the strong line. The principal lines in most of these spectra are the Mo *L*, α_1 and β_1 lines. Wave-lengths greater than the α_1 and β_1, by the factor 1.133 would come very close to the fainter Mo *L* series, 1 and η lines. However, the relative intensity of these lines is not similar to that found for the 1 and η lines in crystal spectrometry. Further, similar lines are found on the long wave-length side of the copper $L\alpha_1$ and oxygen $K\alpha$ lines in the same relative position as shown in spectrogram 3, Fig. 1. Accompanying lines of this sort were obtained in the same relative position, both with gratings ruled 14,400 lines per inch on the University of Michigan ruling machine and those with 30,000 lines per inch from Johns Hopkins University. At present a satisfactory explanation of these lines is not available.

[3] Thibaud, Jour. Opt. Soc. & Rev. Sci. Inst. **17**, 145.

THE ARC SPECTRUM OF PALLADIUM

By A. G. Shenstone

Palmer Physical Laboratory, Princeton University

(Received June 30, 1930)

Abstract

A practically complete analysis of Pd I is given, based on previous analyses. The electron structures are d^{10}, $d^9 5s$, $6s$, $7s$, $8s$ (part of) $d^8 s^2$ (incomplete) $d^9 5p$, $d^8 sp$ and $d^9 6p$ (parts of), $d^9 5d$, $d^9 6d$ (almost complete).

The presence of an unidentified level k_1 is discussed and it is shown that the only explanation within the Hund theory is that k_1 is a hyperfine structure component of $5d^3P_1$. Such an assignment presents very great difficulties.

THE ARC spectrum of palladium has played a considerable part in the development and correction of the Hund theory of atomic spectra. It was partially analyzed by Beals[1] and, later, more completely by McLennan and Smith[2] and by Bechert and Catalan.[3] About the time when McLennan was engaged on the analysis, there appeared Hund's[4] paper, on the correlation between components of terms and the components of the limit terms on which they are built. This circumstance was unfortunate because the accuracy of the theory was quite naturally accepted by McLennan and the naming of the levels of the spectrum was carried out to agree with that theory instead of with the usual criteria, intensities and Zeeman effects. A little later Hund's book[5] was published; and, in it, McLennan's analysis of Pd I appeared as the most conclusive evidence for the theory of limits. That theory has since been proved to be correct in only a few trivial cases.[6] The analysis of Pd I has been only partially corrected in a paper on Ag II by McLennan and McLay[7] and by Shenstone.[8] The present designation of terms was communicated to Gibbs and White and was used by them in their paper[9] on Cd III.

The following analysis is based on the numerical analyses of McLennan and Smith, and Bechert and Catalan. A considerable number of new terms has been found, some of which can be identified as second series members of the d-electron series. The spectrum in the ultraviolet has been measured, and new lines have been found by long exposures throughout the whole visible and ultraviolet.

As much information as possible has been collected in the term table.

[1] Beals, Proc. Roy. Soc. **109A**, 369 (1925).
[2] McLennan and Smith, Proc. Roy. Soc. **112A**, 110 (1926).
[3] Bechert and Catalan, Zeits. f. Physik **35**, 449 (1926).
[4] Hund, Zeits. f. Physik **34**, 296 (1925).
[5] Hund, Linien Spektren und Periodisches System.
[6] Hund, Zeits. f. Physik **52**, 601 (1929).
[7] McLennan and McLay, Trans. Roy. Soc. Can. **22**, 10 (1928).
[8] Shenstone, Nature **121**, 619 (1928).
[9] Gibbs and White, Phys. Rev. **31**, 776 (1928).

Electron configurations, the notation used by Bechert and Catalan, and by McLennan and Smith, the present notation, the level, the level connections, the g-values where known, the Landé g-values, and the Rydberg denominators are given in successive columns. The intervals and g-sums are tabulated separately at the end of the term table.

TABLE I. *Term Table, Pd I.*

Origin.	B. & C.	McL.	S.	Level	Obs. "g"	Landé "g"	Ryd. Den.
$4d^{10}$	$^1S_0$	1^1S_0	a^1S_0	0.0			
$4d^9(^2D_{2\frac{1}{2}})5s$	$^3D_3$	1^3D_3	$5s^3D_3$	6564.0*	1.33	1.33	1.3446
"	$^3D_2$	1^3D_2	$5s^3D_2$	7755.0*	1.17	1.17	1.3579
$4d^9(^2D_{1\frac{1}{2}})5s$	$^3D_1$	1^3D_1	$5s^3D_1$	10093.9*	.50	.50	1.3445
"	$^1D_2$	1^1D_2	$5s^1D_2$	11721.7	1.00	1.00	1.3629
$4d^85s^2$	$^1G_4$	b^3F_4	a^3F_4	25101.1 *			1.2775
"		b^3F_3	a^3F_3	28213.5 *			
"			a^3F_2	29711.0 *			
$4d^9(^2D_{2\frac{1}{2}})5p$	$^3P_2$	1^3P_2	$5p^3P_2$	34068.8*	1.50	1.50	1.8185
"	$^3F_3$	1^1F_3	$5p^3F_3$	35451.3· *	1.08	1.08	1.8576
"	$^3F_4$	1^3F_4	$5p^3F_4$	35927.8· *	1.25	1.25	1.8717
"	$^3P_1$	1^3P_1	$5p^3P_1$	36180.5*·	1.42	1.50	1.8793
"	$^3D_3'$	$1^1D_2'$	$5p^3D_2$	36975.8· · *	1.03	1.17	1.9038
"	$^3D_3'$	1^3F_3·	$5p^3D_3$	37393.5· · *	1.33	1.33	1.9171
$4d^85s^2$			a^3P_2	37952.0· · ·			1.2935
$4d^9(^2D_{1\frac{1}{2}})5p$	$^3P_0$	1^3P_0	$5p^3P_0{}^0$	38088.0*· ·			1.8318
"	$^3F_2$	1^3F_2	$5p^3F_2{}^0$	38811.7 *·	.72	.67	1.8524
"	$^1F_3$	$1^3D_3'$	$5p^1F_3{}^0$	39858.1 ·	1.08	1.00	1.8835
"	$^3D_1'$	1^1P_1	$5p^3D_1{}^0$	40368.6 *	.82	.50	1.8993
"	$^1D_2'$	$1^3D_2'$	$5p^1D_2{}^0$	40771.3	1.14	1.00	1.9120
"	$^1P_1$	$1^3D_1'$	$5p^1P_1{}^0$	40838.7	.76	1.00	1.9141
$4d^9(^2D_{2\frac{1}{2}})6s$	a_3	2^3D_3	$6s^3D_3$	48804.2*			2.4394
"	b_2	2^1D_2	$6s^3D_2$	49019.5*			2.4537
$4d^85s5p$?			$z^5D^{7\,0}$?	50910.4·	1.47?	1.50	
$4d^9(^2D_{1\frac{1}{2}})6s$	d_1	2^3D_1	$6s^3D_1$	52336.3*			2.4389
			$1_3{}^0$	52457.0	1.26?		
$4d^9(^2D_{1\frac{1}{2}})6s$	e_2	2^3D_2	$6s^1D_2$	52487.7			2.4490
			$z^3F_3{}^0$?	53761.6			
			$2_2{}^0$	54335.9			
$4d^9(^2D_{2\frac{1}{2}})5d$	f_1	a^3S_1	$5d^3S_1$	54574.1			2.9431
			$3_4{}^0$	54600.2?			
			$4_3{}^0$	54673.2	1.29?		
$4d^9(^2D_{2\frac{1}{2}})5d$	$^3G_5$	a^3G_5	$5d^3G_5$	54806.1 *			2.9705
"	$^3G_4$	a^1G_4	$5d^3G_4$	54811.3 *			2.9711
"	h_2	a^3P_2	$5d^3P_2$	54820.6 · *			2.9722
"	i_1	a^1P_1	$5d^3P_1$	54822.7 · *			2.9724
?	k_1		k_1	54825.9 · ·			
$4d^9(^2D_{2\frac{1}{2}})5d$	l_3	a^3D_3	$5d^3D_3$	54947.7 · · *			2.9875
"	m_2	a^1D_2	$5d^3D_2$	54998.5 · · *			2.9937
"	n_3	a^1F_3	$5d^3F_3$	55012.2 · · · *			2.9954
"	o_4	a^3F_4	$5d^3F_4$	55025.2 · · · *			2.9970
"	p_0	a^1S_0	$5d^3P_0$	55373.0 · *· ·			3.0279
			$6_2{}^0$	55634.1 · · ·	.92?		
			$7_2{}^0$	56335.9 · · ·			
			$8_4{}^0$	56544.6 · · ·	1.06		
$4d^85s5p$?			$y^5D_3{}^0$	56910.9 · · ·	1.33	1.33	
			$9_3{}^0$	57255.0 · · ·			
			$10_2{}^0$	57565.2 · · ·			
			$11_3{}^0$	57926.2?· · ·			
$4d^9(^2D_{2\frac{1}{2}})7s$		a^3G_4	$7s^3D_3$	58064.1 · *· ·			3.4581
			$12_3{}^0$	58103.7 · · · ·			
$4d^9(^2D_{2\frac{1}{2}})7s$	q_2	3^1D_2	$7s^3D_2$	58138.3 · *· ·			3.4721
$4d^9(^2D_{1\frac{1}{2}})5d$	r_1	a^3P_1	$5d^1P_1$	58195.3 · · · ·			2.9527

TABLE I. (*Continued*).

Origin.	B. & C.	McL.	S.	Level	Obs. "g"	Landé "g"	Ryd. Den.
$4d^95s5p$?			$y^3F_4^0$	58316.8	1.25	1.25	
$4d^9(^2D_{1\frac{1}{2}})5d$	$^3G_3$	a^3G_3	$5d^3G_3$	58348.9			2.9710
"	I_4		$5d^1G_4$	58387.8			2.9757
			13_3^0	58389.8			
"	u_1	a^3D_1	$5d^3D_1$	58408.1			2.9781
			14_2^0	58415.1	.91?		
"	v_2	a^3D_2	$5d^1D_2$	58448.5			2.9830
"	w_2	a^3F_2	$5d^3F_2$	58555.8			2.9961
"	x_3	a^3F_3	$5d^1F_3$	58561.7			2.9968
"	y_0	a^3P_0	$5d^1S_0$	58681.3			3.0108
			15_3^0	59143.1	1.04?		
			16_1^0	59588.4			
			17_2^0	59731.2			
$4d^9(^2D_{2\frac{1}{2}})6d$			$6d^3S_1$	60225.8?			3.9556
"			$6d^3G_5$?	60315.5			3.9809
"			$6d^3G_4$	60318.2			3.9817
"			$6d^3P_2$	60322.0			3.9829
"			$6d^3P_1$	60323.4			3.9832
"			$6d^3D_3$	60370.4			3.9968
"			$6d^3F_3$	60397.9			4.0050
"			$6d^3D_2$	60397.9			4.0050
"			$6d^3F_4$	60404.0			4.0068
$4d^85s5p$?			$y^3F_3^0$	60722.6	1.20?	1.08	
			18_1^0	60729.8			
$4d^9(^2D_{1\frac{1}{2}})7s$	z_1	3^3D_1	$7s^3D_1$	61602.8			4.4581
"	a_3'	3^3D_3	$7s^1D_2$	61638.6			4.4649
$4d^9(^2D_{2\frac{1}{2}})8s$			$8s^3D_3$	61736.2			4.4656
			19_3^0	62316.3	1.08		
$4d^9(^2D_{2\frac{1}{2}})9s$			$9s^3D_3$	63571.7?			5.4715
$4d^9(^2D_{1\frac{1}{2}})6d$			$6d^3G_3$	63853.0			3.9806
"			$6d^1G_4$	63872.7			3.9863
"			$6d^3D_1$	63896.3			3.9929
"			$6d^3F_2$	63937.4			4.0050
"			$6d^1F_3$	63939.8			4.0059
$4d^9$			$4d^2D_{2\frac{1}{2}}$	67236.0			
"			$4d^2D_{1\frac{1}{2}}$	70775.0			
$4d^85s^2$			$5s^4F_{4\frac{1}{2}}$	92307.0			
"			$5s^4P_{2\frac{1}{2}}$	103507.5			

Column 1 Electron Configuration.
" 2 Notation of Bechert and Catalan.
" 3 Notation of McLennan and Smith.
" 4 Notation of Shenstone.
Column 5 Numerical Value of Level.
" 6 "g" Value, observed.
" 7 "g" Value, Landé.
" 8 Rydberg Denominator.

Term separations.

d^95s	^3D	1191; 2339.
$6s$		215; 3317.
$7s$		74; 3465.
$5p$	$^3P^0$	2112; 1908.
	D	−418; 3393.
	F	−477; 3360.
$5d$	^3P	2; 550.
$6d$		1; ?
$5d$	D	51; 3410.
$6d$		17; 3498.
$5d$	F	−13; 3544.
$6d$		−6; 3540.
$5d$	G	5; 3538.
$6d$		3; 3535.
d^8s^2	a^3F	3112; 1497.

"g-sums"

Structure	J	Obs.	Lande.
d^95s	3	1.33	1.33
	2	2.17	2.17
	1	.50	.50
d^95p	4	1.25	1.25
	3	3.49	3.41
	2	4.39	4.34
	1	3.00	3.00

Certain levels given by other authors have not been included. They are given in Table II.

TABLE II. *Rejected terms.*

Author	Level	Explanation
McL. & S.	45489.3	Unidentified line
	56519.6	Unidentified line and spark line
	56695.	Unidentified line
	57650.	Unidentified line and spark line
	58028.	Unidentified line
	64701.	Insufficient evidence
B. and C.	49533.6	2 of 3 lines used elsewhere
	51285.0	2 or 3 lines are spark lines
	56168.4	2 or 3 lines used elsewhere

The 6 levels rejected from McLennan and Smith's list are all founded on lines observed by them in the underwater spark or in absorption in palladium vapor. These lines are all either spark lines or lines which have not been identified as palladium lines in any other source.

Of the 3 levels rejected from Bechert and Catalan's list, one is founded on spark lines, and the other two give only three combinations and of those, two in each case are lines otherwise used in the analysis. Those two levels are therefore possible but extremely improbable.

1. *Determination of the term types.* The information from which the term types may be determined consists of intensities of lines and Zeeman effects. For the low multiplets, the intensities[10] give sufficient evidence that Bechert and Catalan's selection of terms was correct. The intensity diagram (Figure 1) demonstrates this result. Beals' Zeeman effect measurements must also be considered. These measurements are not altogether satisfactory since they are in some cases inconsistent. I have remeasured some of the ultra-

	$5s^3D_3$	$^3D_2$	$^3D_1$	$^1D_2$
$5p^3P_2^0$	700R	75	20	50
$^3P_1$		500*r*	75	50
$^3P_0$			200	
$^3D_3$	1000R	300		200
$^3D_2$	50	500R	100	200
$^3D_1$		100	400	200
$^3F_4$	1000R			
$^3F_3$	300r	600R		200
$^3F_2$		20	400r	200
$^1P_1$		10	200	250
$^1D_2$	40	100	300	300
$^1F_3$	50	200		500*r*

Fig. 1. Intensity diagram of low multiplets.

[10] The intensities are Meggers' estimates and are somewhat different from those used in Table III of the paper, Phil. Mag. **8**, 765 (1929).

violet lines, and from all the evidence available have calculated the probable values of the g-factors for a considerable number of terms. They are not to be considered as having an accuracy of better than about 3%. It is worth notice that the g-values would hardly permit of a choice between $5p^3D_1^0$ and $5p^1P_1^0$ although the evidence of the intensity diagram is reasonably certain.

The terms of prefix $5d$ are all from old levels. Intensities again suffice to determine the types unambiguously except perhaps for the two levels of $J=0$. The lower of the two levels has been chosen as $^3P_0$ because its combinations with triplet terms are considerably stronger than those of the higher level. In Ag II the equivalent levels in my analysis have both been found by Blair (to be published shortly) to be false and a new $^3P_0$ has been found which agrees in position and characteristics with the level chosen in Pd I. No very probable $^1S_0$ has been found in Ag II. The terms of prefix $6d$ were identified partly from intensities and partly from series extrapolation. In some cases they are doubtful levels and are followed by a question sign. In addition there are the terms of prefix $6s$, $7s$, $8s$, $9s$ which will be discussed below; and a large number of unidentified or doubtfully identified high odd levels. The designation of one level as k is carried over from Bechert and Catalan and the level is discussed below.

2. *Structures.* From the atomic number (46) of Pd it can be predicted that the spectrum should have low terms from the structures $4d^{10}$, $4d^9 5s$, $4d^8 5s^2$; and, from the general relations amongst similar structures in other spectra, their relative energies can be roughly predicted. Such a prediction is in agreement with the discovery of $^1S_0$ as the lowest term, ^3D, ^1D as the next and ^3F as the next. The relatively high position of the ^3F and, therefore, of all other terms based on $4d^8 5s$ makes the spectrum very much less complicated than Ni I in which $3d^9 4s$ and $3d^8 4s^2$ are of practically equal energy and importance. Except for a^3F and a^3P_2 no terms founded on $4d^8 5s$ can be definitely identified although a few high odd terms probably do belong to that structure.

3. *Limits.* All terms based on the ion $4d^9$ are prefixed by the symbols which indicate the quantum numbers of the one electron whose change of condition is responsible for the emission of spectral lines. Amongst the even terms it is possible to pick out directly three members of the series ns^3D^1D. A calculation of a Ritz formula then allows the prediction of the position of higher terms. The $8s^3D_3$ and the doubtful $9s^3D_3$ were found in this way. The series was then recalculated using the $6s$, $7s$, $8s$ terms. The limit of this series is $4d^9\ ^2D_{2\frac{1}{2}}$ of Pd II and the addition of 3529, known from Pd II, yields $4d^9\ ^2D_{1\frac{1}{2}}$. Those terms are given at the end of the table, together with $4d^8 5s\ ^4F_{4\frac{1}{2}}$ and $^4P_{2\frac{1}{2}}$ which were used to calculate the Rydberg denominators of a^3F_4 and a^3P_2. The separation of the ^2D limit is so great (3529) that even the $5p$ terms break up naturally into two groups corresponding to the components of ^2D. This effect is very much more in evidence in the higher terms where we find the groups much closer together and separated by about 3500 wave numbers. In spite of such evidence of practically complete jj coupling, the intensities of the lines indicate at least as close an approach to

LS coupling as occurs amongst the lower levels. The $6d$ group of terms is new and almost complete. Its combinations with the $5p$ group give the diffuse lines in the visible and near ultraviolet previously unassigned. In particular, the two lines λ4020 and λ4098 which are given in the tables as reversed are in reality double lines and belong to this group. Part of one of these lines is unassigned though it would fit well as the prohibited combination $5p^3F_3^0 - 6d^3G_5$. There is therefore some doubt of the naming of $^3G_5$.

The Rydberg denominator of every level whose limit is known is given in the term table. The values of these numbers for the $5d$ and $6d$ terms form confirmation of the accuracy of the calculation of the series limit.

The Ritz formula calculated from the terms $6s$, $7s$ and $8s^3D_3$ is

$$T = 67236 - T^1 = 67236.0 - \frac{R}{(n + 0.47681 - 2.037 \times 10^{-6}T^1)^2}.$$

4. *High odd terms.* The wave-length list was extended as far into the ultraviolet as possible in the hope that the terms from the structure $4d^96p$ could be found and give some evidence concerning the still rather unsatisfactory theory of limits. A large number of levels was found in the proper energy range but in most cases there is insufficient evidence on which to classify them. There are undoubtedly numbers of odd levels of the structure $4d^85s5p$ in that same region and they naturally add to the difficulty. An attempt has been made to classify by means of Zeeman effects, but this also was not very successful. Some possible levels of the latter structure are indicated in the term table, the evidence being mainly Zeeman effect and intensity of combination with the term a^3F. A number of rather strong sharp lines in the region around λ 3000–3200 have been used to form these terms and there remain a few such lines unidentified.

5. *The level k_1.* The designation k_1 for the level 54825.9 found by Bechert and Catalan has been retained as a distinguishing mark because of the very peculiar nature of that level. It is an even level of $J=1$ or 2 (but almost certainly 1) and it makes 5 exact combinations, all of which are diffuse.[11] It is distant from $5d\ ^3P_1$ only 3.2 wave numbers and all of its combinations occur with those terms with which $5d^3P_1$ combines strongly. There are no other diffuse lines in Meggers' list except λ4631.37, which is triply assigned.

There are three possible origins for the level k_1: (1) A term of the system $4d^9nx$; (2) A term of the system $4d^85s\ nx$; (3) A hyperfine structure component of $5d^3P_1$. The first possibility may be eliminated by the observation that all terms of that structure which could have such an energy have been discovered. The second possibility reduces to a consideration of $4d^85s^2$ only, since all other even configurations yield terms much too high. The configuration d^8s^2 contains only one level of $J=1$. It is a $^3P_1$ level, but an examination of the analogous spectra Ni I, and Pt I and the spectrum Pd II demonstrates that k_1 is about 10,000 wave numbers too far above $^3F_4$ and $^3P_2$. There is

[11] The line λ4816.27 is of the same character as the other k_1 lines on Meggers' plates and has been so labelled in the wave-length list.

a remote possibility that the level is $^1D_2$ but it is at least 5000 wave numbers too high and it does not combine with either $^1F_3$ or $^1D_2$. The third possibility, that k_1 is a hyperfine structure component of $5d^3P_1$, appears to be extremely improbable. There is certainly no expectation that a single level in a whole spectrum should show a structure of 3.2 units and that level one not involving an s-electron at all. If it is hyperfine structure, then the hyperfine structure is wider than the fine structure since $^3P_2-{}^3P_1$ is only 2.2 units.

I believe that the level k_1 is the only level yet found in any spectrum which cannot be logically explained on the Hund theory; but a single exception is sufficient to indicate that there is a factor which is yet to be considered. It would be of great interest to examine the Zeeman effect of a group of lines involving the levels $5d^3P_2$, $^3P_1$ and k_1. The fields produced by an ordinary magnet are sufficient to produce the beginnings of a Paschen-Back effect of the three levels if they have the necessary structural affiliation.

I would like to point out in this connection that the type of analysis which has been carried out since the development of the Hund theory is unlikely to give anything but confirmation since the theory is assumed correct to start with. But that theory has been shown to be incorrect in one part, the prediction of limits, and it is possible that it is either incomplete or incorrect in other details. There is, of course, no doubt of the essential correctness of the theory.

The wave-length table (Table III) contains all the identified lines of Pd I and, in addition, the few remaining unidentified lines of any strength. The intensities are the estimates of Dr. Meggers except for a short range from λ3700 to λ4500 and a number of newly observed lines for which I have made estimates on about the same scale. As usual, Dr. Meggers has been extremely kind in placing at my disposal considerable unpublished data.

TABLE III

λ	I	A	ν	Combination	λ	I	A	ν	Combination
9234.02	1	M	10826.6	$a^3F_4-5p^3F_4^0$	7026.91	1	M	14227.1	$5p^3D_3^0-5d^3D_3$
8761.34	2	M	11410.7	$5p^3D_3^0-6s^3D_3$	7016.44	8	M	14248.3	$5p^3P_2^0-6s^3D_1$
8695.03	1	M	11497.7	$5p^3P_1^0-6s^3D_1$	6917.56	2	M	14452.0	$5p^3D_2^0-5d^3P_2$
8644.38	1	M	11565.0	$5p^3D_2^0-6s^3D_1$	16.56	9	M	14454.1	$5p^3D_1^0-5d^3P_1$
8599.06	2	M	11626.0	$5p^3D_3^0-6s^3D_3$	6914.98	2h	M	14457.4	$5p^3D_1^0-k_1$
8585.28	1	M	11644.6	$a^3F_3-5p^1F_3^0$	6892.52	0	M	14504.5	$a^3P_2-1_4^0$
8581.99	2	M	11649.1	$5p^1P_1^0-6s^1D_2$	78.35	2	M	14534.4	$5p^1P_1^0-5d^3P_0$
8532.67	2	M	11716.5	$5p^1D_2^0-6s^1D_2$	56.89	0	M	14579.9	
8451.93	0	M	11828.4	$5p^3D_1^0-6s^3D_1$	6833.42	8	M	14629.9	$5p^3D_1^0-5d^3D_2$
8353.54	2	M	11967.7	$5p^3D_2^0-6s^3D_2$	6784.52	10	M	14735.4	$5p^3P_2^0-6s^3D_2$
8300.81	5	M	12043.7	$5p^3D_3^0-6s^3D_3$	6774.54	12	M	14757.1	$a^3F_4-5p^1F_3^0$
8132.85	6	M	12292.4	$a^3F_4-5p^3D_3^0$	6739.16	0	M	14834.6	
7961.04	4	M	12557.7	$a^3F_3-5p^1D_2^0$	6712.10	0	M	14894.4	
7915.84	7	M	12629.4	$5p^1F_3^0-5d^1D_2$	6686.79	3	M	14950.7	$5p^3P_2^0-6s^3D_1$
7786.66	7	M	12839.0	$5p^3P_1^0-6s^3D_2$	85.71	2	M	14953.2	$5p^1F_3^0-5d^3G_4$
7763.99	12	M	12876.4	$5p^3F_3^0-6s^3D_3$	81.56	3	M	14962.4	$5p^3F_2^0-5d^3P_2$
7486.93	7	M	13352.9	$5p^3F_4^0-6s^3D_3$	62.86	4	M	15004.6	$5p^3D_1^0-5d^3P_0$
7391.91	8	M	13524.6	$5p^3F_3^0-6s^3D_2$	25.28	4	M	15089.5	$5p^1F_3^0-5d^3D_2$
68.14	15	M	13568.2	$5p^3F_2^0-6s^3D_2$	23.26	4	M	15094.1	$5p^3D_2^0-6s^1D_2$
7310.06	5	M	13676.0	$5p^3F_2^0-6s^1D_2$	6603.03	1	M	15140.4	$5p^1F_3^0-5d^3D_2$
7278.44	2	M	13735.4	$5p^1P_1^0-5d^3S_1$	6599.32	0	M	15148.9	
42.90	2	M	13802.8	$5p^1D_2^0-5d^3S_1$	97.08	1	M	15154.0	$5p^1F_3^0-5d^3F_3$
7228.99	1	M	13829.4	Pb?	6591.44	3	M	15167.0	$5p^1F_3^0-5d^3F_4$
7149.11	6	M	13983.9	$5p^1P_1^0-5d^3P_1$	6508.41	6	M	15360.5	$5p^3D_3^0-6s^3D_1$
*7147.45	1h	M	13987.2	$5p^1P_1^0-k_1$	6465.90	0	M	15461.5	
7115.84	3	M	14049.1	$5p^1D_2^0-5d^3P_2$	6464.68	0	M	15464.4	
7060.29	5	M	14159.8	$5p^1P_1^0-5d^3D_2$	6444.89	2	M	15511.9	$5p^3D_2^0-6s^1D_2$
52.04	2	M	14176.4	$5p^1D_2^0-5d^3D_3$	6342.46	1	M	15762.4	$5p^3F_2^0-5d^3S_1$
37.58	3	M	14205.5	$5p^3D_1^0-5d^3S_1$	6268.23	0	M	15949.1	Cu?

* Previously unpublished line observed by Dr. Meggers of the Bureau of Standards.

TABLE III (*continued*)

λ	I	A	ν	Combination
6244.78	1	M	16009.0	$5p^3F_3^0-5d^3P_2$
43.97	2	M	16011.0	$5p^3F_4^0-5d^3P_1$
03.73	0	M	16114.9	
03.13	0	M	16116.4	
6195.61	2	M	16136.0	$5p^3F_2^0-5d^3D_3$
88.02	6	M	16155.8	$5p^3P_2^0-6s^3D_1$
76.15	5	M	16186.8	$5p^3F_3^0-5d^3D_2$
70.94	5	M	16200.5	$5p^3F_2^0-5d^3F_3$
36.99	1	M	16290.1	
30.59	8	M	16307.2	$5p^3P_1^0-6s^1D_2$
29.45	0	M	16310.2	
01.65	0	M	16384.5	$a^3P_2-2_0^0$
6064.08	1	M	16486.0	$5p^3P_0^0-5d^3S_1$
5995.94	0?	M	16673.3	
78.96	0	M	16720.7	$a^3P_2-4_0^0$
74.03	0	M	16734.5	$5p^3P_0-5d^3P_1$
5868.14	2	M	17036.4	$5p^3F_3^0-6s^1D_2$
5782.14	3	M	17289.9	Cu
5778.85	1	M	17299.7	$5p^1P_1^0-7s^3D_2$
59.92	4	M	17356.6	$5p^1P_1^0-5d^1P_1$
39.68	7	M	17417.8	$5p^3D_3^0-5d^3G_4$
37.65	4	M	17423.9	$5p^1D_2^0-5d^1P_1$
36.52	12	M	17427.0	$5p^3D_2^0-5d^3P_2$
30.52	0	M	17445.6	
5698.10	0	S	17544.9	
95.08	20	M	17554.1	$5p^3D_3^0-5d^3D_3$
90.14	8	M	17569.4	$5p^1P_1^0-5d^3D_2$
87.49	3	M	17577.6	$5p^1D_2^0-5d^3G_3$
80.80	2	M	17598.3	$5p^3D_2^0-5d^3S_1$
77.07	1	M	17609.9	$5p^1P_1^0-5d^1D_2$
74.25	3	M	17618.6	$5p^3D_2^0-5d^3F_3$
70.90	0	S	17629.0	V?
70.06	30	M	17631.6	$5p^3D_3^0-5d^3F_4$
68.42	3	M	17636.7	$5p^1D_2^0-5d^3D_2$
55.42	10	M	17677.3	$5p^1D_2^0-5d^1D_2$
42.71	8	M	17717.1	$5p^1P_1^0-5d^3F_2$
21.33	3	M	17784.4	$5p^1D_2^0-5d^3F_2$
19.46	12	M	17790.4	$5p^3D_3^0-5d^1F_3$
08.02	7	M	17826.7	$5p^3D_3^0-5d^1P_1$
03.00	4	M	17842.6	$5p^1P_1^0-5d^1S_0$
02.29	2	M	17844.9	$5p^3D_2^0-5d^3P_2$
01.65	8	M	17846.9	$5p^3D_3^0-5d^3P_1$
5600.62	2h	M	17850.2	$5p^3D_1-k_1$
5562.70	3	M	17971.9	$5p^3D_3^0-5d^3D_3$
47.02	20	M	18022.7	$5p^3D_3^0-5d^3D_2$
42.80	30	M	18036.4	$5p^3D_2^0-5d^3F_3$
41.88	1	M	18039.4	$5p^3D_3^0-5d^3D_1$
29.45	9	M	18080.0	$5p^3D_1^0-5d^1D_2$
5496.85	6	M	18187.2	$5p^3D_1^0-5d^3F_2$
72.67	1	M	18267.5	$5p^3P_2^0-6s^3D_1$
59.16	2	M	18312.8	$5p^3D_1^0-5d^3S_1$
35.16	7	M	18393.6	$5p^3P_2^0-5d^3S_1$
27.69	4	M	18419.0	$5p^3P_2^0-6s^1D_2$
06.59	5	M	18490.9	$5p^1F_3^0-5d^3G_3$
5395.26	25	M	18529.6	$5p^3F_4^0-5d^3G_4$
94.76	6	M	18531.4	
85.44	2	M	18563.4	
77.62	3	M	18590.4	$5p^1F_3^0-5d^1D_2$
63.26	4	M	18640.2	$5p^3P_1^0-5d^3P_2$
62.69	15	M	18642.2	$5p^3P_1^0-5d^3P_1$
61.72	2hv	M	18645.5	$5p^3P_1^0-k_1$
46.79	2	M	18697.6	$5p^1F_3^0-5d^3F_2$
45.10	10	M	18703.5	$5p^1F_3^0-5d^1F_3$
12.57	12	M	18818.1	$5p^3P_1^0-5d^3D_2$
11.50	1	M	18821.9	
5295.61	50	M	18878.5	$5p^3F_4^0-5d^3G_5$
94.15	7	M	18883.5	$5p^3F_3^0-5d^3G_4$
5256.17	10	M	19020.0	$5p^3F_4^0-5d^3D_3$
38.41	2	M	19084.5	$5p^3F_4^0-5d^3F_4$
34.85	20	M	19097.5	$5p^3F_4^0-5d^3F_4$
20.93	0	M	19151.6	Cu
08.93	10	M	19192.5	$5p^3P_1^0-5d^3P_0$
5179.31	0	M	19302.7	$a^3P_2-9_0^0$
63.83	40	M	19360.1	$5p^3F_3^0-5d^3G_4$
61.36	5	M	19369.4	$5p^3F_3^0-5d^3P_2$
57.56	0	M	19383.6	$5p^3F_3^0-5d^3P_1$
27.71	7	M	19496.5	$5p^3F_3^0-5d^3D_2$
17.01	20	M	19537.3	$5p^3F_3^0-5d^3G_3$
14.38	8	M	19547.3	$5p^3F_3^0-5d^3D_3$
10.81	15	M	19560.9	$5p^3F_3^0-5d^3F_3$
07.43	1	M	19573.9	$5p^3F_3^0-5d^3F_4$
01.51	3	M	19596.4	$5p^3F_3^0-5d^3D_1$
5092.53	0	M	19631.1	
63.40	10	M	19744.1	$5p^3F_2^0-5d^3F_2$
09.95	1	S	19954.7	$5p^3D_1^0-6d^3P_{2,1}$
04.99	0h	S	19974.5	$a^3P_2-11_0^0$
4991.62	2	S	20028.0	$5p^3D_1^0-6d^3D_2$
71.95	9	M	20107.3	$5p^3P_2^0-5d^3P_1$
62.05	0h	S	20151.4	$a^3P_2-12_0^0$
29.99	3	M	20278.4	
24.20	2	M	20302.2	
4919.87	8	M	20320.1	$5p^3P_0^0-5d^3D_1$
4875.43	20	M	20505.3	$5p^3P_1-5d^3S_1$
36.44	4	M	20670.6	$5p^3D_3^0-7s^3D_3$
19.15	2	M	20744.8	$5p^3D_2^0-7s^3D_2$
17.51	30	M	20751.8	$5p^3P_2^0-5d^3P_2$
17.02	9	M	20754.0	$5p^3P_2^0-5d^3P_1$
16.27	1h	M	20757.2	$5p^3P_2^0-k_1$
14.65	1	M	20764.2	$5p^1P_1^0-7s^3D_1$
06.37	1	M	20799.9	$5p^1P_1^0-7s^1D_2$
4799.02	1	M	20831.8	$5p^1D_2^0-7s^3D_1$
90.85	2	M	20867.3	$5p^1D_2-7s^1D_2$
88.18	20	M	20879.0	$5p^3P_1^0-5d^3D_2$
76.56	4	M	20929.7	$5p^3P_1^0-5d^3D_1$
73.37	0	S	20943.7	$5p^3P_2^0-5d^3F_3$
71.37	0	M	20952.5	
93.52	0	S	20955.7	$5p^3D_3^0-5d^3G_3$
61.88	3	M	20994.3	$5p^3D_2^0-5d^3G_4$
24.01	6	M	21162.5	$5p^3D_3^0-5d^3F_3$ $5p^3D_2^0-7s^3D_1$
22.75	1	M	21168.2	$5p^3D_3^0-5d^1F_3$
08.06	2	M	21234.3	$5p^3D_1^0-7s^3D_1$
4700.12	1	M	21270.1	$5p^3D_1^0-7s^1D_2$
4677.46	8	M	21373.2	$5p^3D_2^0-5d^3G_3$
4664.54	0	M	21432.4	$5p^3D_2^0-5d^3D_3$
32.63	3	M	21580.0	$5p^3D_2^0-5d^3F_2$
31.37	2h	M	21585.9	$5p^3D_2^0-5d^1F_2$ $5p^3F_2^0-6d^3F_3(^3D_3)$
4589.99	4	M	21780.5	$5p^1F_3^0-7s^1D_2$
59.83	1	M	21924.5	
52.91	4	M	21957.8	$5p^3P_1^0-7s^3D_2$
41.13	10	M	22014.8	$5p^3P_1^0-5d^1P_1$
23.33	1	M	22106.3	
16.20	10	M	22136.3	$5p^3F_3^0-7s^3D_3$
4497.66	3	M	22227.6	$5p^3P_1^0-5d^3D_1$
89.46	15	E	22268.2	$5p\ P_1^0-5d^1D_2$
73.59	50	E	22347.2	$5s^1D_2-5p^3P_2^0$
58.62	1h	K	22422.2	$5p^3F_3^0-5d^3G_3$
43.04	5	E	22500.8	$5p^3P_2^0-5d^1S_0$
21.03	3	E	22612.8	$5p^3F_3^0-7s^3D_3$
06.55	8	E	22687.1	$5p^3F_3^0-7s^3D_2$
4388.62	5	E	22779.8	$a^3P_2-18_1^0?$
86.48	3	E	22790.9	$5p^3F_2^0-7s^3D_1$
79.58	2	E	22826.8	$5p^3F_3^0-7s^1D_2$
60.23	8h	E	22928.1	$5p^3D_3^0-6d^3P_2$
58.58	8	E	22936.8	$5p^3F_3^0-5d^1G_4$
51.00	10h	E	22976.8	$5p^3D_3^0-6d^3D_3$
4344.66	20h	E	23010.3	$5p^3D_3^0-6d^3F_4$
28.04	2h	E	23038.7	$5p^1P_1^0-6d^3F_2$
26.97	1h	S	23104.4	$5p^3F_3^0-5d^3F_2$
23.04	2h	E	23125.4	$5p^3D_3^0-6d^3D_1$
14.96	6h	E	23168.7	$5p^1D_2^0-6d^1G_3$
4281.89	3h	E	23347.6	$5p^3D_2^0-6d^1P_{2,1}$
68.26	30hd	E	23422.2	$5p^3D_3^1-6d^{1\,2}_{3}(^1D_2)$
51.49	1	E	23514.6	$5p^3P_2^0-7s^3D_1$
49.0	1h	E	23528.3	$5p^3D_1^0-6d^1D_2$
41.7	1h	E	23568.8	$5p^3D_1^0-6d^{1\,2}_{3}$
12.95	200	E	23729.7	$5s^1D_2-5p^3F_3^0$
4169.86	20	E	23974.8	$5s^1D_2-5p^3P_2^0$
66.31	10d	S	23995.3	$5p^3P_2^0-7\,^3D_2$ $5p^1F_3^0-6p^3G_3$
62.84	3h	S	24015.3	$5p^1F_3^0-6p^3G_4$
56.98	3	S	24049.2	$a^3F_2-2^3F_3^0$
52.12	3h	S	24077.3	
51.36	3h	S	24081.7	$5p^1F_3^0-6d^1F_3$
40.83	5h	S	24142.9	$5p^3P_1^0-6p^3P_{2,1}$
28.37	3h	S	24215.8	$5p^3P_2^0-6p^3D_3$
23.64	5	S	24243.6	$a^{3\,2}_{3}-1_0^0$
4106.85	1h	S	24342.7	$5p^3D_3^0-8s^3D_2$
4099.27	20h	S	24387.7	$5p^3F_4^0-6f^3G_5$
98.87	10h	S	24390.1	$5p^3F_4^0-6p^3G_4$
4090.05	2h	S	24442.7	$5p^3F_4^0-6p^3D_3$
87.37	50	E	24458.7	$5^1D_2-5p\ P_1^0$
84.35	5h	S	24476.8	$5p^3F_3^0-6p^3F_4$
82.72	1h	S	24486.6	$5p^3P_2^0-5p^3F_2$
81.68	3h	S	24492.8	$5p^3F_2^0-5d^1F_2$
20.66	5h	S	24854.5	
20.20	15h	S	24857.4	$5p^3F_4^0-6p^3G_5$
11.74	0h	S	24919.8	$5p^3F_3^0-6p^3D_3$
4007.5	3h	E	24946.2	$5p^3F_3^0-6p^3F_3(^3D_3)$
4004.93	1h	S	24962.2	$a^3F_2-4_0^0$
3992.3	3h	E	25041.2	$5p^3F_3^0-6d^3G_4$

TABLE III (*continued*)

λ	*I*	*A*	ν	Combination
3985.48	0h	S	25084.0	$5p^3F^0-6s^3D_1$
78.88	1h	S	25125.6	$5p^3F^0-6s^3F_2$
58.64	200	E	25254.1	$5s^3D_2-5p^3D^0$
26.93	0	S	25458.0	$5p^3P^0-7s^3D_1$
13.07	1	S	25548.2	$a^3F_2-z^3F^0$
3894.18	200	E	25672.1	$5s^3D_3-5p^3D^0$
73.57	1h	S	25808.7	$5p^3P^0-6s^3D_1$ $a^3F_4-z^3D^0$ $5p^3F^0-8s^3D_1$
3832.30	75	E	26086.6	$5s^3D_1-5p^3P^0$
27.15	3	S	26121.9	$a^3F_3-2_4^0$
21.99	5h	S	26157.0	$5p^3P^0-6p^3S_1$?
18.89	1	S	26178.2	$5p^3F^0-9s^3D_3$?
3807.87	3h	S	26254.0	$5p^3P^0-6p^3P_{2,1}$
3800.96	1	S	26301.7	$5p^3P^0-6p^3D_3$
3799.16	75	E	26314.2	$5s^3D_3-5p^3P^0$
78.28	1	S	26459.6	$a^3F_4-4_5^0$
54.85	1	S	26624.7	$a^3F_2-7_3^0$
18.91	100	E	26882.0	$5s^3D_1-5p^3D^0$
3690.34	200	E	27090.1	$5s^3D_2-5p^3F^0$
54.41	2	E	27356.4	$a^3F_4-1_4^0$
45.97	2	E	27419.8	$a^3F_3-6_4^0$
34.70	700R	E	27504.8	$5s^3D_3-5p^3P^0$
13.39	0	S	27667.0	$5p^3P^0-8s^3D_3$
3609.56	600R	M	27696.3	$5s^3D_2-5p^3F^0$
3596.66	4	S	27795.7	
89.16	2	S	27853.7	$a^3F_2-10_3^0$
84.11	2	S	27893.0	
81.06	1	S	27916.8	
77.56	1	S	27944.1	$5p^3F^0-6d^3G_3$
71.16	200	M	27994.1	$5s^3D_1-5p^3P^0$
66.63	5	M	28029.7	
53.10	500r	M	28136.4	$5s^1D_2-5p^1F^0$
43.25	1	S	28214.6?	$a^3F_2-11_3^0$
28.72	5	M	28330.8	$a^3F_3-8_4^0$
21.14	2	S	28391.8	$a^3F_2-12_3^0$
16.95	500r	M	28425.6	$5s^3D_2-5p^3P_1^0$
3489.79	200r	M	28646.9	$5s^3D_3-5p^3D_3^0$
3488.15	1	M	28660.3	$a^3F_4-z^3F_4^0$
81.17	400r	M	28717.8	$5s^3D_1-5p^3F_2^0$
60.76	300r	M	28887.2	$5s^3D_3-5p^3F_3^0$
42.40	3	M	29041.2	$a^3F_3-9_4^0$
41.40	300	M	29049.6	$5s^1D_2-5p^1D_2^0$
33.44	250	M	29117.0	$5s^1D_2-5p^1P_1^0$
21.24	500	M	29220.8	$5s^3D_2-5p^3D_2^0$
19.66	6	M	29234.3	$a^3F_4-2_4^0$
3406.04	3	M	29351.2	$a^3F_3-10_4^0$
3404.60	1000R	M	29363.6	$5s^3D_1-5p^3F_4^0$
3396.79	4	M	29431.1	$a^3F_2-15_3^0$
89.05	3	M	29498.4	$a^3F_4-3_4^0$
80.69	20	M	29571.3	$a^3F_4-4_5^0$
73.02	300	M	29638.5	$5s^3D_1-5p^3D_2^0$
46.12	0	K	29876.8	$a^3F_3-16_4^0$
21.00	5	M	30102.8	$a^3F_3-y^3F_4^0$
12.99	5	M	30175.6	$a^3F_2-13_3^0$
11.04	3	M	30193.3	
10.14	2	K	30201.5	$a^3F_3-14_3^0$
3307.08	2	S	30229.5	
3302.15	400	M	30274.6	$5s^3D_1-5p^3D_1^0$
3287.26	50	M	30411.7	$5s^3D_3-5\ ^3D_3^0$
58.80	300	M	30677.3	$5s^3D_1-5p^3D_2^0$
3251.66	200	M	30744.7	$5s^3D_1-5p^3P_1^0$
42.72	1000R	M	30829.4	$5s^3D_3-5p^3D_3^0$
32.33	5	S	30928.5	$a^3F_3-15_3^0$
18.98	20	M	31056.8	$5s^3D_3-5p^3F_2^0$
3179.41	8	S	31443.3	$a^3F_4-8_4^0$
3171.93	1	S	31517.5	$a^3F_3-17_4^0$
3142.82	50	M	31809.4	$a^3F_4-y^3D_3^0$
3114.05	200	M	32103.2	$5s^3D_2-5p^1F_3^0$
3109.19	5	M	32153.4	$a^3F_4-9_4^0$
3075.17	10	M	32509.1	$a^3F_3-y^3F_2^0$
3066.09	3	M	32605.4	$a^3F_3-19_4^0$
3065.30	100	M	32613.8	$5s^3D_3-5p^3D_1^0$
3028.76	3	M	33007.2	
3027.92	100	M	33016.4	$5s^3D_1-5p^1D_2^0$
3021.74	10	M	33083.9	$5s^3D_3-5p^1P_1^0$
3009.77	20	M	33215.5	$a^3F_4-y^3F_3^0$
3002.66	50	M	33294.1	$5s^3D_1-5p^1F_3^0$
2936.77	2	S	34041.1	$a^3F_4-15_4^0$
2931.47	4	M	34102.6	$a^3F_3-19_3^0$
2922.50	40	M	34207.3	$5s^3D_1-5p^1D_2^0$
2875.75	2	M	34763.4	
2806.45	1	M	35621.7	$a^3F_4-y^3F_3^0$
2763.08	100R	M	36180.8	$a^1S_0-5p^3P_1^0$
2686.29	3	M	37215.0	$a^3F_4-19_4^0$
2605.08	4	M	38375.1	
2476.43	50R	M	40368.5	$a^1S_0-5p^3D_1^0$
2447.95	10R	M	40838.1	$a^1S_0-5p^1P_1^0$
2360.51	5	M	42350.8	
2327.49	5	S	42951.5	$5s^1D_1-4_4^0$
2216.48	6	S	43155.5	$5s^3D_1-z^3D_2^0$
2276.54	2	M	43912.7	$5s^1D_2-6_3^0$
2254.28	15	M	44346.3	$5s^3D_1-z^3D_2^0$
1240.76	4	M	44613.8	$5s^1D_2-7_3^0$
2236.38	8	M	44701.2	$5s^3D_3-1_4^0$
2225.28	10	M	44924.1	
2195.49	6	M	45533.5	$5s^1D_2-9_3^0$
2178.26	10	M	45893.7	$5s^3D_3-1_4^0$
2174.67	4	M	45969.6	
2172.92	10	M	46006.6	$5s^3D_3-z^3F_4^0$
2151.00	5	S	46475.3	
2142.11	10	S	46668.1	$5s^1D_2-13_3^0$
2130.69	3d	S	46918.2	$5s^3D_3-4_3^0$
2123.76	2	S	47071.4	
2118.09	6	S	47197.4	$5s^3D_3-z^3F_3^0$
2108.09	4	S	47421.1	$5s^1D_2-15_3^0$
2105.87	10	S	47471.3	$5s^3D_1-10_3^0$
2092.61	7	S	47771.9	$5s^3D_3-2_3$
2089.97	2	S	47832.3	$5s^3D_1-11_3^0$
2088.47	8	S	47866.7	$5s^3D_1-16_3^0$
2087.93	10	S	47879.3	$5s^3D_3-6_3^0$
2082.24	10	S	48009.7	$^{\text{a}}5s^3D_1-12_3^0$ $5s^1D_2-17_3^0$
2081.10	10	S	48036.2	$5s^3D_3-3_4^0$
2079.35	0	S	48076.5	
2077.93	4	S	48109.4	$5s^3D_3-4_3^0$
2076.47	3	S	48143.2	
2068.78	8	S	48322.2	$5s^3D_1-14_4^0$
2061.98	2	S	48481.5	
2057.76	2	S	48580.9	$5s^3D_3-7_4^0$
2057.42	2	S	48588.9	
2042.98	3	S	48932.3	
2040.19	0	S	48992.2	
2039.81	1	S	49008.3	$5s^1D_2-18_3^0$
2019.75	4	S	49495.0	$5s^3D_1-16_3^0$
2019.53	4	S	49500.4	$5s^3D_3-9_4^0$
2013.96	3	S	49637.4	$5s^3D_1-17_4^0$
2006.96	10	S	49810.5	$5s^3D_2-10_3^0$
λ (vac)				
2000.72	2	S	49982.0	$5s^3D_3-8_4^0$
1993.18	3	S	50171.2	$5s^3D_1-11_3^0$
1986.14	2	S	50348.7	$5s^3D_3-12_3^0$ $5s^3D_3-y^3D_3^0$
1976.48	5	S	50594.9	$5s^1D_2-19_3^0$
1974.88	3	S	50635.9	$5s^3D_2-13_3^0$
1973.94	3	S	50660.1	$5s^3D_3-14_4^0$
1972.74	8	S	50690.8	$5s^3D_3-9_3^0$
1968.33	5	S	50804.4	
1963.71	2	S	50924.0	
1945.98	2	S	51388.1	$5s^3D_2-15_3^0$

For convenience in visualizing the energy relations in the spectrum, a diagram of electron configurations is given in Fig. 2.

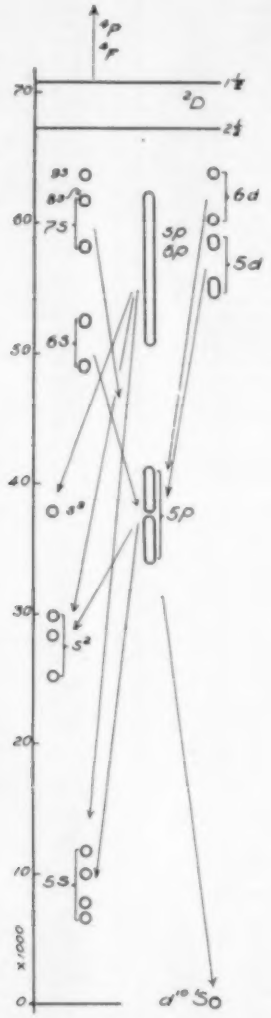

Fig. 2. Diagram of the energies of the electron configurations of Pd I. The last electron only is given except for structures based on 8 *d* electrons for which the characteristics of two electrons are given.

INTENSITY MEASUREMENTS IN THE SPECTRUM OF NICKEL AND COBALT

By L. S. Ornstein and T. Bouma
Physical Laboratory of the University of Utrecht
(Received June 2, 1930)

Abstract

Quantitative intensity measurements have been carried out in the Ni I and Ni II, and the Co I spectrum. The spectrographic outfit for the intensity measurements consisted of a stigmatic concave grating mounting used with step weakeners, and a Hilger E 1 used with the method of slit width variation. The *summation rules* have been tested both for *multiplets* and *supermultiplets*, also the intensity ratio for singlets and triplets, doublets and quartets. Serious divergencies have been found everywhere. In the Ni II spectrum an extension of the summation rules to supermultiplets gives better results in several cases. Intensity tables are given of the lines measured.

QUANTITATIVE intensity measurements have been carried out in the nickel I and II and the cobalt I spectrum. In the Ni I spectrum the analysis of Becher and Sommer[1] has been utilized; later on also the very extensive analysis by Russell, obtained through the courtesy of Professor Harrison.[2] For Ni II the analysis has been given by Shenstone;[3] for Co I by Catalan and Bechert.[4]

In the Co II spectrum no intensity measurements have been carried out, the classified multiplets[5] being situated in the far ultraviolet where intensity measurements meet with special difficulties.

Although the material used was the purest Ni and Co that could be obtained, the Ni contained some Fe, and the Co some Fe and Ni as impurities.

The Experimental Methods

In the first measurements for the Ni I spectrum an image of the light source through step-reducers was formed on the slit of a stigmatic concave grating-mounting; the line intensities was determined by the usual method.[6] For the subsequent investigation a Hilger E 1 quartz-spectrograph was used. The density curves were obtained by the method of variable slit width.[7]

Frequently the photometer curves of two or more lines lying close together coalesced. In such cases it is necessary to change the photometer curve accurately point for point into the intensity curve of the complex of

[1] K. Bechert and L. A. Sommer, Ann. d. Physik **77**, 351 (1925) and **77**, 537 (1925).
[2] Afterwards published, Phys. Rev. **34**, 821 (1929).
[3] A. G. Shenstone, Phys. Rev. **30**, 255 (1927).
[4] Catalan and Bechert, Zeits. f. Physik **32**, 336 (1925).
[5] Meggers and Walters. Scientific Papers of the Bureau of Standards No. 551.
[6] L. S. Ornstein, Intensity of Multiple Spectrallines, Proc. Phys. Soc. **37**, 334 (1925).
[7] L. S. Ornstein, Proc. Phys. Soc. **37**, 337 (1925).

lines. The same thing is done for a neighbouring isolated line. It may be assumed that the shape of the intensity curve for all these lines is the same[8] and that therefore the intensity curve of the complex can be analysed into a few separate curves of this shape.

The First Measurements

The Ni I quintet $z^5G^0 - e^5F$ was photographed with the above mentioned concave grating in second order. The results will be found in Table I, and for 0.95 amp. also in an intensity scheme (Table II).

Table I. *Intensities of the lines of the $z^5G^\circ - e^5F$ multiplet of Ni I.*

Line λ	Intensity 1.4 amp.	0.95 amp.	Line λ	Intensity 1.4 amp.	0.95 amp.
4900.97	1	~1	4714.416	100	100
4874.803	1.1	~1	4686.209	11	11
4814.59	0.95	~1	4648.656	40	44
4786.541	38	41	4604.990	27	25
4756.529	26	29	4600.364	10	9.5
4715.757	22	24.5	4592.532	17	16

Table II. *Intensity scheme for the $z^5G^\circ - e^5F$ multiplet of Ni I.*

Statistical Weight		z^5G^0 5	7	9	11	13	Sum	Quotient
3		9.5					9.5	3.2
5		11	16				27	5.4
e^5F 7		~1	24.5	25			50.5	7.2
9			~1	29	44		74	8.2
11				~1	41	100	142	12.9
Sum		21.5	41.5	55	85	100		
Quotient		4.3	5.9	6.1	7.7	7.7		

According to the summation rule the quotients in Table II ought to be equal. The divergencies are serious, as will be seen. Self-reversal cannot be the cause of this divergency for it would diminish the contrasts, whereas the divergencies lie in the opposite direction.

Although in the case under consideration the summation rule does not determine the intensity of each line separately, it gives the ratio of the extreme diagonal terms; this ought to be 27:91 i.e. 29.7:100. As this is a sensitive test, the intensity ratio between these two lines has been measured several times. (Table III).

Table III.

Current	Int. proportion
2.4	10. 9:100
1.4	10.15:100
1.4	9.9 :100
0.95	9.3 :100
0.95	9.6 :100

[8] L. S. Ornstein and M. Minnaert, Zeits. f. Physik **43**, 404 (1927).

As blending with impurity lines is out of question, the experimental ratio 9.6:100 differs from the theoretical 29.7:100.

In order to get more facts the measurements have been continued with the Hilger E 1 in the ultraviolet. Here fairly large regions could be photographed at once and with a sufficient dispersion.

The current used was the smallest possible (about 0.45 amp.) A preliminary examination with 0.80 and 0.45 amp. showed that difference between the intensities found for these currents is comparatively small.

A few intensity measurements have also been carried out in an arc with a pressure of 50 and 28 cm of air. These also did not show any appreciable difference for the intensity. Therefore the definitive measurements for Ni I and CO I have been carried out with a current of 0.45 amp. in air.

In the Ni II investigation a Leyden jar was charged by the secondary tension of an induction coil. The spark discharge of the jar took place via a self-induction between two small bars of nickel. Variations of the conditions of discharge could not be used here. Only, to get a current of small density, a Leyden jar of the smallest possible capacity was chosen.

The Definitive Measurement

In each of the three spectra mentioned a region has been chosen in which a number of multiplets, suitable for intensity measurements was situated. The region was situated for Ni I between 2900 and 3800A, for Ni II between 2450 and 3770A for Co I between 2500 and 4500A.

Besides the multiplets the intensities of all the lines appearing in the photographs have been measured. In the tables the intensities found by analysis of the photograms have been marked (1) when the analysis was certain, (2) when it was less certain and (3) when the analysis was very doubtful. Intensities marked (4) are inexact, owing to the slight density and the great influence of the irregularities which the photometer curve shows in the unexposed plate for that case. The tables are the least complete on the side of the largest wave-lengths where the dispersion was so small that several lines had to be omitted. The experimental facts have been used for testing: (1) the multiplet summation rules; (2) the supermultiplet summation rules; and (3) the intensity ratio for singlets and triplets, doublets and quartets. Generally the theoretical expectations are not fulfilled. For this reason we have limited our measurements to the spectral regions given below. Perhaps our material will be of some help in developing the intensity rules for the complicated spectra.

The Ni I Spectrum

Besides the quintet $z^5G^0-e^5F$ already mentioned 13 multiplets have been examined.

The intensities in horizontal and vertical direction have been formed and the quotients of intensity sums and statistical weights have been calculated in the same way as has been done for $z^5G^0-e^5F$, the results are collected in Table IV.

TABLE IV. *Intensity quotients in multiplets of Ni I.*

No.	Multiplet Designation	Quotients									
1	$a^3D-y^3D^0$	35	28	17			36	29	16		
2	$a^3F-y^3D^0$	11.7	6.2	5.8			9.1	3.9	3.8		
3	$a^3D-y^3F^0$	34	18	7.4			25	25	23		
4	$a^3F-y^3F^0$	10	7.5	3.2			2.4	7.0	7.8		
5	$a^3F-z^3G^0$	3.2	6.5	4.2			2.6	8.5	6.1		
6	$a^3P-y^3D^0$	0.4	0.4	0.4			0.8	0.8	0.7		
7	$a^3D-z^3G^0$	4.5	1.7				6.2	2.3			
8	$a^3D-z^3F^0$	31	22	10			30	28	24		
9	$a^3D-z^3D^0$	23	[25]	18			[37]	29	10		
10	$a^3F-z^3D^0$	22	21.6	10.3			23.3	10.1	6.6		
11	$a^3F-z^3F^0$	21	12.1	5.9			12	17.6	6.7		
12	$a^3D-z^3P^0$	70	51	33			49	28	14		
13	$a^3F-z^3P^0$		4.3	2.4			3.1	1.4			
14	$z^5G^0-e^5F$	3.2	5.4	7.2	8.2	12.9	4.3	5.9	6.1	7.7	7.7

The quotients [25] and [37] have been deduced from sums containing a line, ordered doubly, so that they are too high by an unknown amount.

Only the multiplet 6 is in accordance with expectation (and multiplet 3 in one direction). In the case of all other multiplets the summation rules do not apply. In the case of the incomplete multiplets, e.g. $2^5G^0-e^5G$ it also appears from the intensities of the lines present that the summation rule will not hold.

Supermultiplets. If singlet, triplet and singlet-triplet intercombinations are taken together, no satisfactory results are reached (Table V).

TABLE V. *Supermultiplet sums and quotients of intensity.*

Statistical weight		a^3D 3	a^3D 5	a^3D 7	a^1D 5	Sum	Quotient
y^3D^0	3	61	43		39	143	48
	5	47	55	40	20	162	32
	7		48	71	43	162	23
y^1D^0	5	8.7	23		72	103.7	21
Sum		116.7	169	111	174		
Quotient		39	34	16	35		

In the same way the quotients in Table VI are found.

TABLE VI.

Combinations	Quotients							
$a^3D, a^1D-z^3D^0, z^1D^0$	24	[35]	28	22	[38]	32	11	42
$a^3D, a^1D-y^3F^0, y^1F^0$	34	25	7	15	25	25	28	25
$a^3D, a^1D-z^3F^0, z^1F^0$	36	33	10	33	30	39	31	46

Again, when either the multiplets or all the lines, coming from the same term, are taken together the summation rules do not apply, e.g. for y^5D^0: (Table VII).

TABLE VII.

Statistical weight		a^3F 5	a^3F 7	a^3F 9	a^3D 3	a^3D 5	a^3D 7	a^1D 5	Sums	Quotient
3		35			61	43		39	178	59
y^3D^0 5		5.2	26		47	55	40	20	193.2	39
7		5.2	1.3	34		48	71	43	202.5	29

Now we add up in Tables VIII and IX the spectral lines originating from the same level.

TABLE VIII.

	a^3F 5	a^3F 7	a^3F 9
z^1G^0		31	
z^3G^0	13	59.3	54.8
z^5G^0	1.6	11.8	22.2
z^1F^0	30	51	32
z^3F^0	60.4	123.3	60
z^5F^0	41.4	46.5	57.9
y^1F^0	1.7	5.0	4.7
y^3F^0	12	49.2	70
z^1D^0	1	54	
z^3D^0	116.3	71	59
z^5D^0		0.65	2.1
y^1D^0	10.5	4.2	
y^3D^0	45.4	27.3	34
z^1P^0	3.8		
z^3P^0	15.5	9.5	
Sum	352.6	543.8	396.7
Quotient	71	78	44

TABLE IX.

	a^3D 3	a^3D 5	a^3D 7
z^1G^0			42
z^3G^0		31	15.8
z^5G^0	1.7	20.7	23
z^1F^0		55	50
z^3F^0	91	139	168
z^5F^0	.36	93.3	114.4
y^1F^0			31
y^3F^0	74	125	164
z^1D^0	2.4	13	2.8
z^3D^0	[110]	145	71.4
z^5D^0	0.8	3.7	[28]
y^1D^0	8.7	23	
y^3D^0	108	146	111
z^1P^0	17	40	
z^3P^0	146.6	140	100
	596.1	974.7	918.4
	199	195	131

Here the divergencies are smaller than for the separate multiplets. Still it is not very likely that the few multiplets still wanting will be able to equalize the quotients.

According to Mack[9] the multiplets arranged in Table X belong together. Equal quotients are not obtained in this way either. Especially the first column shows a great divergence.

Finally we shall consider the ratio between the sums of the intensities for the corresponding singlet-triplet multiplets. When intercombinations are absent a ratio of 1:3 can be expected.[10] The values found for our case are shown in Table XI; the last column contains the ratios after dividing the intensities by the fourth power of the frequency. There is a fairly great difference between the experimental and the theoretical ratios. However, fairly strong intercombinations are present in all 5 cases.

Table XII contains the intensities for all the lines in the spectral region investigated; an (arbitrary) intensity of 100 has been awarded to the line 3524.543.

[9] J. E. Mack, Phys. Rev. **34**, 17 (1929).

[10] L. S. Ornstein and H. C. Burger, Zeits. f. Physik **40**, 403 (1926).

TABLE X.

Statistical weight		a^3D 7	a^3D 5	a^3D 3	a^1D 5	Sum	Quotient
	9	93				93	10
z^3F^0	7	66	86		78	230	33
	5	[9]	53	91	[27]	180	36
	7	66	64		65	195	28
z^3D^0	5	5.4	80	41	50	176.4	35
	3		1	69	3	73	24
	5	100	54	9.6	4	167.6	34
z^3P^0	3		86	67	9.5	162.5	54
	1			70		70	70
z^1F^0	7	50	55		124	229	33
z^1D^0	5	2.8	13	2.4	93	111.2	22
z^1P^0	3		40	17	106	163	54
Sum		392.2	532	367	559.5		
Quotient		56	106	122	112		

TABLE XI.

Combinations	Ratio	
$a^1D-y^1D^0$ and $a^3D-y^3D^0$	1:5.1	1:5.1
$a^1D-y^1F^0$ and $a^3D-y^3F^0$	1:4.8	1:4.5
$a^1D-z^1F^0$ and $a^3D-z^3F^0$	1:3.1	1:2.6
$a^1D-z^1D^0$ and $a^3D-z^3D^0$	1:3.5	1:3.2
$a^1D-z^1P^0$ and $a^3D-z^3P^0$	1:3.6	1:4.4

TABLE XII. *Intensities of Ni I lines.* Intensities marked (1) are certain, (2) less certain, (3) doubtful, (4) inexact because of small intensity and the influence of irregularities in the plate.

λ (Kayser)[1]	λ(I.A.)	Int.	λ (Kayser)	λ(I.A.)	Int.	λ(Kayser)	λ(I.A.)	Int.
2798.78	2798.651	23	3012.11	3012.007	72	3165.64	3165.513	0.8
2802.40	2802.28	3.1	3018.09	3017.96	0.3 (4)	3170.86	3170.73	0.3
2803.25	2803.15	1.4	3019.28	3019.150	42	3176.44	3176.30	0.4
2805.20	2805.081	4.7	3029.36	3029.30	0.6	3181.89	3181.75	3
2814.48	2814.37	0.5	3031.98	3031.869	28	3183.14	3183.05	0.8 (3)
2821.42	2821.296	31	3038.04	3037.940	55	3183.40	3183.26	1.9 (3)
2834.66	2834.550	4.2	3045.15	3045.012	26	3184.50	3184.372	11
2839.05	2838.97	1.3	3048.98		0.4	3191.97	3191.89	0.2
2849.93	2849.84	0.5	3050.92	3050.828	67	3195.67	3195.577	5.2
2865.61	2865.508	8.7	3054.42	3054.317	53	3197.22	3197.121	17
2868.85	2868.76	0.9	3057.76	3057.647	61	3199.44	3199.36	0.2
2905.85	2905.76	0.5	3064.75	3064.626	48	3200.50	3200.433	2.8
2907.58	2907.462	10.5	3066.59	3066.46	0.4	3202.21	3202.149	1.7
2914.12	2914.013	5.0	3080.91	3080.758	47	3207.05	3206.963	0.2
2916.95	2916.85	0.2 (4)	3097.27	3097.120	39	3210.00	3209.910	0.9
2917.60	2917.53	0.2 (4)	3099.25	3099.117	31	3213.53	3213.435	0.5
2931.03	2930.93	0.3 (4)	3101.67	3101.563	72 (1)	3214.17	3214.064	3.7
2932.74	2932.63	0.3 (4)	3101.99	3101.881	76 (1)	3216.93	3216.823	1.3
2944.06	2943.922	40	3105.60	3105.466	35	3217.93	3217.828	5.8
2958.39	2958.29	0.7	3107.83	3107.717	1.3	3219.92	3219.810	0.4
2969.30	2969.20	1.2	3114.26	3114.128	40	3221.41	3221.28	1.9 (1)
2973.84	2973.73	0.4	3116.84	3116.700	0.2 (4)	3221.81	3221.661	32
2981.80	2981.652	43	3129.42	3129.310	5.2	3223.66	3223.542	0.7
2983.56	2983.42	3.1	3132.68		0.3 (4)	3225.19	3225.030	39
2984.28	2984.129	34	3134.22	3134.106	74	3227.11	3226.992	8.4
	2991.103	1.7	3145.23	3145.117	0.4 (1)	3233.06	3232.945	46
2992.71	2992.597	42	3145.82	3145.707	9.5 (1)	3234.00	3233.88	0.7
2994.58	2994.458	42	3151.33	3151.29	0.15	3234.78	3234.658	31
3002.58	3002.492	71	3154.68	3154.58	0.5	3235.86	3235.764	1.0
3003.70	3003.628	55	3159.65	3159.524	0.7	3243.20	3243.064	50
3010.96		0.3	3164.30	3164.17	0.3	3245.47	3245.35	0.2

[1] H. Kayser. Handbuch der Spektroskopie.

TABLE XII (*continued*)

λ(Kayser)	λ(I.A.)	Int.	λ(Kayser)	λ(I.A.)	Int.	λ(Kayser)	λ(I.A.)	Int.
3248.56	3248.44	15	3443.14	3443.00	0.2 (4)	3670.60	3670.424	9.5
3249.55	3249.440	3.8	3444.36	3444.247	0.8	3674.30	3674.105	27
3250.90	3250.749	20	3446.40	3446.263	80	3688.59	3688.413	9.4
3264.56	3264.44	0.1 (4)	3453.02	3452.891	59	3694.07	3693.933	2.8
3268.21	3268.09	0.3	3458.60	3458.467	91	3697.05	3696.904	0.25
3269.08	3268.96	0.08 (4)	3461.80	3461.660	78	3713.84	3713.696	0.2 (4)
3271.25	3271.118	13	3464.25	3464.12	0.3 (4)	3715.65	3715.498	0.2 (4)
3273.62	3273.50	0.15 (2)	3467.61	3467.505	23	3722.64	3722.484	9.6
3276.66		0.15	3469.65	3469.484	30	3724.95	3724.815	0.25
3277.35	3277.23	0.15	3472.71	3472.545	64	3729.06	3728.919	0.2 (4)
3282.03	3281.876	0.5	3476.80	3476.66	0.4	3730.90	3730.745	0.5
3282.81	3282.701	9.3	3478.00	3477.876	0.2 (4)	3736.98	3736.811	20
3284.56	3284.432	0.4	3478.42	3478.302	0.4	3739.40	3739.229	5.2
3287.08	3286.953	9.0	3479.36	3479.263	0.5	3739.94	3739.787	1.5
3293.83	3293.674	0.4	3480.30	3480.170	0.4	3744.72	3744.560	0.5
3296.42	3296.264	0.15	3483.98	3483.776	66	3749.19	3749.042	2.1
3305.10	3304.951	0.7	3486.09	3485.892	14	3762.76	3762.62	0.3
3307.16	3307.014	0.2	3488.43	3488.293	0.4	3769.60		0.15 (4)
3309.56	3309.44	0.2	3493.11	3492.965	86	3772.67	3772.518	0.7
3310.35	3310.206	1.9	3496.47	3496.352	0.8	3775.75	3775.562	50
3312.49	3312.319	2.8	3501.02	3500.852	58	3778.20	3778.048	0.9
3313.15	3312.992	0.7	3502.73	3502.604	4.9	3783.72	3783.521	51
3315.82	3315.668	55	3507.85	3507.695	6.5	3792.48	3792.325	1.1
3320.42	3320.259	54	3510.52	3510.340	70	3793.79	3793.599	2.5
3322.50	3322.316	43	3512.08	3511.94	0.4	3807.35	3807.135	65
3326.80	3326.673	0.4	3514.10	3513.947	22	3811.46	3811.32	0.08 (4)
3327.52	3327.402	0.6	3515.21	3515.057	86	3831.89	3831.685	9.5
3328.85	3328.720	1.0	3516.33	3516.220	3.5	3833.00	3832.865	0.65
3332.31	3332.19	0.5	3518.80	3518.635	2.3	3844.40	3844.27	0.2 (3)
3335.72	3335.59	0.06	3519.97	3519.776	51	3844.71	3844.58	0.15 (3)
3337.15	3337.015	0.4	3523.23	3523.075	4.6 (2)	3858.51	3858.284	78
3338.90	3338.763	0.1 (2)	3523.61	3523.445	11 (2)	3863.21	3863.08	0.3
3339.20	3339.049	0.4 (2)	3524.68	3524.543	100	3889.84	3889.673	0.9
3359.30	3359.104	1.4	3526.67	3526.53	1.0	3909.10	3908.93	0.3
3361.75	3361.557	53	3528.13	3527.988	13	3912.47	3912.31	0.2 (2)
3362.97	3362.808	2.4	3529.02	3528.890	0.6 (1)	3913.14	3912.975	0.15 (2)
3363.76	3363.612	0.6	3529.76	3529.625	0.5 (1)	3942.00	3941.86	0.1
3364.75	3364.590	1.1	3530.73	3530.588	0.9	3944.29	3944.10	0.4
3365.92	3365.771	48 (1)	3537.35	3537.243	0.3 (4)	3954.70	3954.53	0.1
3366.32	3366.169	51 (1)	3537.72	3537.634	0.4 (2)	3962.25	3962.10	0.1
3366.95	3366.808	4.5 (1)	3542.14	3542.00	0.3 (4)	3970.65	3970.49	0.35
3368.05	3367.892	5.4	3545.30	3545.16	0.3 (4)	3972.32	3972.157	1.4
3369.71	3369.576	59	3548.32	3548.189	41	3973.71	3973.547	4
3372.19	3371.995	50	3551.71	3551.563	5.3	3974.82	3974.681	0.35
3374.42	3374.228	33 (1)	3553.64	3553.483	1.7	3984.29	3984.17	0.2
3374.82	3374.637	11 (1)	3560.05	3559.925	0.4	3994.15	3993.97	0.1
3375.70	3375.560	0.5	3561.90	3561.752	8.2	4006.30	4006.14	0.01
3376.46	3376.330	0.8	3566.51	3566.373	93	4010.14	4009.99	0.007 (4)
3380.71	3380.577	106 (3)	3572.02	3571.871	63	4017.67	4017.56	0.15
3381.01	3380.885	13 (3)	3576.08	3575.94	0.4	4019.20	4019.055	0.06
3387.54	3387.467	0.3	3577.36	3577.23	0.4	4025.60	4025.44	0.1
3391.20	3391.051	48	3588.07	3587.928	12	4057.45	4057.30	0.1
3393.10	3392.993	66	3597.86	3597.699	67	4064.55	4064.380	0.03
3396.31	3396.174	0.6	3599.66	3599.530	0.3	4069.39	4069.24	0.015 (4)
3397.37	3397.28	0.1	3602.41	3602.278	17	4073.08	4072.93	0.01 (4)
3401.31	3401.164	1.9	3607.00	3606.853	0.4	4075.00	4074.897	0.015 (4)
3403.58	3403.427	2.2	3609.48	3609.312	19	4086.30	4086.15	0.01 (4)
3409.74	3409.579	12	3610.61	3610.45	54	4098.30		0.01 (4)
3413.66	3413.478	55 (1)	3612.90	3612.732	50	4116.11	4115.980	0.04
3414.12	3413.943	34 (1)	3619.52	3619.391	124	4121.48		0.015 (4)
3414.91	3414.771	93 (1)	3624.89	3624.733	14	4123.94	4123.79	0.01 (4)
3420.88	3420.742	1.0	3630.01	3629.891	0.3	4138.67	4138.52	0.01 (4)
3421.49	3421.339	2.3	3635.10	3634.943	3.0	4150.53	4150.37	0.03
3422.47	3422.334	0.7	3641.75	3641.632	0.3	4164.80	4164.636	0.02
3423.00	3422.870	1.3	3642.52	3642.383	0.2 (4)	4167.07	4166.96	0.02
3423.87	3423.713	69	3662.10	3661.938	1.7	4184.65	4184.473	0.07
3433.74	3433.565	66	3664.27	3664.089	13	4195.72	4195.533	0.1
3435.63	3435.495	0.5	3666.16		0.2 (4)	4200.60	4200.466	0.15
3437.45	3437.283	53	3668.36	3668.200	0.4 (1)	4201.89	4201.728	0.15
3442.17	3442.017	0.9	3669.40	3669.233	6.6			
3442.67	3442.540	0.4						

The Ni Spark Spectrum

Eight doublets and 4 quartets have been measured; the quotients of intensity sums and statistical weights are found in Table XIII.

Table XIII.

	Multiplet Designation	Quotients							
1	$a^4D^1-d^4F^1$	—	1.2	1.0	1.3	—	1.7	1.4	1.65
2	$a^2P^1-b^2P$	5	4.95			5.8	4.55		
3	$a^2P^1-b^2D^1$	0.5	0.05			0.07	0.5		
4	$a^4G^1-d^4F^1$	1.6	2.0	2.35	2.9	1.9	1.7	2.0	1.8
5	$a^2G^1-d^2F^1$	1.6	2.1			1.7	1.3		
6	$a^4F-d^4F^1$	2.85	1.9	1.5	1.15	1.85	1.4	1.7	1.7
7	$a^2F-d^2F^1$	1.6	1.0			1.3	1.2		
8	$a^2D^1-d^2F^1$	0.87	0.85			1.3	1.1		
9	a^2G-b^2F	0.6	0.9			0.5	0.7		
10	$a^2D-a^2D^1$	2.8	1.1			2.6	1.3		
11	a^2D-a^2F	0.47	0.04			0.15	0.4		
12	$a^4P^1-a^4D^1$	3.2	2.15			5.0	3.25	0.85	—

For some of the multiplets the disagreement with the summation rule is not very great, for others, however, the divergencies are wide, e.g. in the case of Nos. 3 and 11, where the diagonal terms are by far the weakest.

Adding up the doublet and quartet systems and the intercombinations, we get the quotients of Table XIV.

Table XIV.

Combinations	Quotients											
a^4D^1, $a^4D^1-d^4F^1$, d^2F	—	1.5	1.65	1.3	0.9	0.85	—	1.7	1.4	1.65	1.7	2.0
a^4G^1, $a^2G^1-d^4F^1$, d^2F^1	1.6	2.0	2.35	2.9	1.6	2.1	1.9	1.7	2.0	1.8	1.7	1.3
a^4F, $a^2F-d^4F^1$, d^2F^1	2.85	1.9	1.7	1.16	1.6	1.15	1.85	1.4	1.7	1.8	1.3	1.5

If we add the multiplets which in the quartet systems start from a^4D^1, we find the quotients shown in Table XV.

Table XV.

Statistical weight	a^4D^1 1	2	3	4	a^4F^1 2	3	4	5	a^4G^1 3	4	5	6	Sum	Quotient
2					3.7	2.0			3.2				8.9	4.5
d^4F^1 3		3.4	0.3			2.3	3.5		2.5	3.5			15.5	5.2
4			4.0				3.3	2.6		3.3	6.1		19.3	4.8
5				6.6				5.8			3.8	10.7	26.9	5.4
Sum	—	3.4	4.3	6.6	3.7	4.3	6.8	8.4	5.7	6.8	9.9	10.7		
Quotient	—	1.7	1.4	1.7	1.9	1.4	1.7	1.7	1.9	1.7	2.0	1.8		

There is comparatively little difference between these quotients. If we add to them the small number of intercombinations that occur, we find 4.5|5.4|5.7|5.4|.

In the same way we find:

Table XVI.

	a^2D^1 2	3	a^2F 3	4	a^2G^1 4	5	Sum	Quotient
3	2.6		3.8	0.9	4.8		12.1	4.03
d^2F^1 4		3.4		4.0	1.9	6.6	15.9	3.98
Q tient	1.3	1.1	1.3	1.2	1.7	1.3		

These results are satisfactory if the occurring intercombinations are added, the quotients become 4.03 and 4.12.

In our material these two multiplets are the only ones which start from the same level. The quartet $a^4P^1-a^4D^1$ has the same original level as number of intercombinations. But we cannot conclude from these measurements, as there are other lines in the part of the spectrum that has not been examined which start from the same level. However, it is remarkable that the intensity ratios of this quartet are largely corrected by the additions of the intercombinations.

TABLE XVII.

	a^4P^1			a^2F^1		a^2D		Sum	Quotient
	1	2	3	3	4	2	3		
1	2.7	0.5				0.5		3.7	3.7
2	2.3	2.0		0.4		1.0	0.4	6.1	3.6
a^4D^1 3		4.0		0.9	1.1	1.3	3.9	11.2	3.7
4			2.6		2.7		7.2	12.5	3.1

In combining lines with a common final level we again meet with the difficulty that our materials are not complete; various lines that ought to be included do not occur in the spectral region that has been examined. Still the influence of the additions of the other intensities can be seen from Table XVIII.

TABLE XVIII.

	a^3D			a^2P^1			a^4P^1		
	2	3		1	2		1	2	3
a^2F	0.3	1.25	b^2D^1	0.07	1.05	a^4D^1	5	6.5	2.6
a^2D^1	5.2	3.8	b^2P	5.8	9.1	a^2D^1		1.7	2.7
a^4D^1	2.8	11.5	b^4D^1	1.2		a^2F			1.2
a^4F	0.5	0.3	b^4P	1.0	2.8	a^4F		0.3	
			a^2F		0.2				
Sum	8.8	16.85	b^2F		0.4	Sum	5	8.5	6.5
Quotient	4.4	5.6				Quotient	5	4.3	2.2
			Sum	8.07	13.55				
			Quotient	8.1	6.8				

We have considered also the intensity ratio for doublet-quartet systems.

TABLE XIX.

Combinations	Ratio
$a^2D-d^2F^1$ and $a^4D^1-d^4F^1$	1:1.6
$a^2G^1-d^2F^1$ and $a^4G^1-d^4F^1$	1:2.4
$a^2F-d^2F^1$ and $a^4F-d^4F^1$	1:2.4

The last column is found after division by ν^4. The ratio 1:2 is found only approximately; this cannot be attributed to the occurring intercombination lines (3, 2 and 0 respectively) as in the last case where they do not occur, the divergency is the same as in the other two.

In the following intensity table (Table XX) an intensity of 100 has been awarded to line 2437.884.

TABLE XX. *Intensities of the lines of Ni II.* Intensities marked (1) are certain, (2) less certain, (3) doubtful, (4) inexact because of small intensity and irregularities in the plates.

λ (Kayser)	λ (I.A.)	Int.
2416.21	2416.13	29
2419.40		0.8
2429.17		0.5 (4)
2431.65	2431.57	1.2
2433.64	2433.57	6.7
2437.98	2437.884	100
2441.77		1.0
2441.90		0.6
2451.05		0.8
2454.09		0.6
2455.60	2455.51	1.8
	2459.32	0.3
2465.34		0.2
2472.27		1.0
2473.28	2473.13	13.4
2476.96		0.8
2484.41	2484.32	6.6
2497.92	2497.80	1.0
2503.47		0.8
2505.94	2505.84	7.3
2511.00	2510.87	98
2514.85	2514.75	3.4
	2520.33	0.15
	2525.42	4.0
2539.20	2539.09	2.6
2540.14		2.0
2546.01	2545.90	21
	2547.16	0.5 (4)
	2549.56	1.8
	2551.04	1.1
	2555.13	3.5
2557.98	2557.88	0.9
	2560.30	3.2
	2565.36	0.6 (4)
2566.12	2566.08	6.1
2584.10	2584.01	3.2
	2587.25	0.4
2588.40	2588.31	0.4
	2592.54	0.07
2601.22	2601.126	3.8
	2605.45	2.5
2606.50	2606.40	4.8
2610.20	2610.08	10.7
2611.78	2611.66	1.6
2615.29	2615.20	6.6
2623.25	2623.10	0.3 (4)
	2626.57	3.3
2630.40	2630.29	2.7
	2631.52	2.0
2632.98	2632.86	3.5
2647.15	2647.04	2.6
2648.85	2648.72	0.9
2655.6	2655.46	0.9 (2)
2656.05	2655.90	3.7 (1)
2659.8		2.5
2665.39	2665.25	2.0
2666.00	2665.86	0.8
2670.45	2670.33	1.0
2679.35	2679.25	2.3
2684.57	2684.41	5.8
2690.8	2690.62	1.9
2708.9	2708.78	3.3
2743.1	2743.01	4.0
2746.85		1.4
2759.15	2759.02	3.8
2760.82	2760.67	1.1
2768.9	2768.78	3.4
2775.45	2775.31	2.6
2794.93		0.7 (4)
2798.75		1.8
2802.4		0.2 (4)
2805.20		0.2 (4)
2805.80	2805.67	3.6
2808.47	2808.35	0.4
2821.43		2.3
	2825.23	1.1
2834.66		0.7
	2836.58	1.0
2842.55	2842.41	1.9
2863.84	2863.69	5.2
2864.4	2864.16	2.6
2865.63		0.6
	2881.24	0.3
	2882.54	0.8
2907.10		0.4
2913.71	2913.59	3.4
2914.11		0.2 (3)
	2942.71	0.15 (4)
2944.03		4.8
2947.56	2947.45	1.7
2969.32		0.6
2981.81		5.7
2984.30		2.8
2988.21	2988.05	1.2
2992.75		4.2
2994.60		6.6
3002.65		19
3003.76		15
3012.14		19
3019.27		3.7
3032.00		1.3
	3032.44	0.3
3038.09		13
3045.16		1.2
3050.99		21
3054.46		12
3057.79		16
3064.12	3063.93	0.5
3064.76		5.0
3080.90		3.5
3087.20	3087.07	2.7
3097.26		2.0
3099.26		1.5
3101.70		21 (3)
3102.02		12 (3)
3105.60		1.7
3114.25		2.2
3129.40		0.2
3134.21		16
3197.24		1.4
3214.21		1.2
3216.95		1.0
3217.95		2.0
3221.43		1.0
3221.80		2.2
3225.18		3.0
3227.14		1.0
3233.05		9.8
3234.76		2.5
3243.20		6.0
3248.57		1.1
3249.55		0.8
3250.90		1.7
3271.26		0.8
3275.03	3274.90	0.4
3282.85		0.8
3282.97		0.3 (3)
3287.06		0.5
3290.70	3290.54	0.3 (2)
3290.83	3290.69	0.5 (2)
3305.10		0.3 (4)
3312.46		1.0
3313.12		0.6
3315.80		7.0
3320.41		4.4
3322.46		3.1
3326.85		0.2 (4)
3350.56	3350.42	1.0
3359.24		0.4
3361.73		5.0
3362.94		0.2 (4)
3365.90		4.0 (1)
3366.31		4.3 (1)
3366.92		1.7 (1)
3369.71		20
3372.14		4.6
3374.13	3373.98	3.9 (3)
3374.36		2.9 (3)
3374.77		1.6 (3)
3380.74		21.5 (2)
3381.04		6.5 (2)
3391.20		11.4
3393.16		23
3396.25		0.5
	3397.82	0.2 (4)
3401.30		0.5
3401.90	3401.76	0.5
3403.45		0.8
3407.43	3407.30	2.7
3409.70		0.9
3413.61		5.0
3414.05		2.5
3414.91		34
3421.47		0.6
3423.88		14
3433.70		17
3437.42		14
3446.41		22.5
3453.06		12.5
3454.29	3454.16	1.3
3458.62		28
3461.84		23
3465.77	3465.62	2.0
3467.63		1.1
3469.61		2.0
3471.50	3471.35	2.3
3472.71		13.4
3483.95		7.2
3486.05		0.6
3493.13		25.5
3501.04		5.6
3502.74		0.3 (4)
3507.84		0.5
3510.52		15
3511.8		0.3 (4)
3514.13	3513.95	7.2
3515.21		30
3516.32		0.8
3518.76		0.5
3519.90		3.4
3524.69		33
3528.10		0.7
3548.32		2.4
3551.70		0.4 (4)
3553.65		0.4 (4)
3561.92		0.5
3566.55		23
3572.06		7.5
3576.91	3576.76	4.0
3588.07		0.5
3597.86		7.7
3602.44		0.9
3609.49		1.5
3610.68		8.1
3612.91		3.9
3619.54		25
3624.89		0.9
3664.26		1.1
3670.59		1.0
3674.29		1.2
3688.57		0.5
3722.62		0.5
3736.96		0.8
3739.38		0.4 (4)
3769.62	3769.45	2.6
3775.74		3.1
3783.67		3.6
3807.29		5.1
3858.50		9.7

The Co I Spectrum

In Table XXI the computed quotients are given for all the multiplets measured. The indication of the multiplets is that of Catalan and Bechert. The quotients with question marks between brackets are too large, owing to lines which are ordered doubly in the multiplets to which they refer. In quartet No. 30 one of the lines in the multiplet itself has been ordered doubly; 4 quotients had therefore to be left out.

Table XXI

No.	Level	Quotients											
4	F^1-D^1	40	46					29	34				
5	F^1-D^2	108	56					73	42				
6	$F^1-\bar{F}^1$	35	34					26	41				
7	$F^1-\bar{F}^2$	75	67					102	47				
8	F^1-G^1	72	61					77	90				
9	F^1-G^2	98	47					95	85				
15	p^2-d^2	6.1	6.5	7.5	8.0			10.3	8.3	15.5			
19	f^1-d^1	99	80	78	41			89	83	41	13		
20	f^1-d^2	16	16	15	10			10	12	11	6		
21	f^1-d^3	20	20	16	11			23	15	8	4.4		
22	f^2-d^1	35	76	71	52			29	54	51	38		
23	f^2-d^2	155	115	83	51			135	78	62	18		
24	f^2-d^3	4.4	4.8	7.4	7.6			5.7	5.9	6.4	2.4		
25	$f^1-\bar{f}^1$	89	72	[82]	30			75	70	60	[55]		
26	$f^1-\bar{f}^2$	59	30	22	17			38	36	29	17		
28	$f^2-\bar{f}^1$	[2.3]	2.4	3	7.7			1.0	[2.1]	3.5	8		
29	$f^2-\bar{f}^2$	132	118	[98]	49			157	[127]	79	49		
30	$f^2-\bar{f}^3$	11	—	11.5	—			21	—	12	—		
31	f^1-g^1	33	23	18	15			50	28	25	18		
32	f^1-g^2	38	30	10	7			25	30	29	14		
34	f^2-g^1	4.4	7.5	9.6	6.5			0.5	3.8	8.7	17.6		
35	f^2-g^2	142	89	61	26			88	97	93	80		
36	f^2-g^3	2.2	5.5	2.8	3.8			3.0	3.9	6.2	4.6		
81	$\bar{\phi}^1-\phi^1$	1.6	2.6	2.6	3.3	4.4	1.1	2.2	2.2	3.0	3.4	5.3	
82	$\bar{\phi}^1-\phi^1$	2.9	3.0	3.8	2.8	2.3	12	4.3	4.6	3.7	1.5	7.5	8.2

None of the 25 multiplets follows the summation rule. Neither are equal quotients obtained when doublet and quartet systems are taken together with their intercombinations. For a few of these systems the results are found in Table XXII.

Table XXII.

Terms	Quotients											
f^1, F^1 and g^2G^2	101	57	39	44	59	7	25	32	34	22	112	148
f^1, F^1 and g^1G^1	73	66	33	23	19	15	50	28	31	18	77	91
f^1, F^1 and $\bar{f}^2-\bar{F}^2$	78	73	65	33	53	46	38	38	34	17	150	83
f^1, F^1 and d^2-D^2	109	58	16	16	16	19	10	14	12	6	74	51

If we take together the lines which originate from the same level we find the quotients of Table XXIII.

Table XXIII.

Term	Quotient			
g^1	38	31	28	21
G^1	110	84		
g^2	181	133	120	33
G^2	138	84		

Although for the level mentioned here the system is complete, the results are not appreciably better than for the separate multiplets; sometimes (for G^1) even worse.

For the other terms the system is incomplete; of these only for d^3 a considerable improvement is found. Here we combine f^1-d^3, f^2-d^3, F^1-d^3 and p^2-d^3 and find the quotients 31, 32, 32 and 28. However, p^1-d^3, p^2-d^3 and P^1-d^3 could not be taken into account as they did not occur in spectral region we investigated.

TABLE XXIV.

Final level	Quotients			
f^1	315	293	235	144
f^2	431	488	413	264
F^1	467	450		

Finally we can add all the lines with a common final level. In each of these 3 cases a few systems of lines are wanting (2, 2 and 3 respectively), but it is highly improbable that the quotients given, which have been derived from 16, 16 and 13 lines respectively, would be greatly influenced by these.

For the ratio of intensities of doublet and quartet systems the following values (after division by ν^4) are tabulated here:

TABLE XXV.

Multiplet	Ratio
F^1-D^1 and f^1-d^1	1:2
F^1-D^2 and f^1-d^2	1:0.22
$F^1-\overline{F}^1$ and $f^1-\overline{f}^1$	1:2.1
$F^1-\overline{F}^2$ and $f^1-\overline{f}^2$	1:0.4
F^1-G^1 and f^1-g^1	1:0.3
F^1-G^2 and f^1-g^2	1:0.22

In 4 of the 6 cases the doublet is even stronger than the quartet. This cannot be ascribed to the existing intercombinations as the divergencies in the case of the systems F^1-D^2 and F^1-G^1, where the intercombinations are weak, is much the same as in that of F^1-F^2 and F^1-G^2 with their strong intercombinations. Whereas the division by ν^4 yields a fairly correct ratio in 2 cases, it increases the error in the other 4 cases.

All the intensity values found are shown in Table XXVI in which an intensity of 100 has been awarded to the line 3334.151.

TABLE XXVI. *Intensities of the lines of Co I.* Intensities marked (1) are certain, (2) less certain, (3) doubtful, (4) inexact because of small intensity and irregularities in the plates.

λ(Kayser)	λ(I.A.)	Int.	λ(Kayser)	λ(I.A.)	Int.	λ(Kayser)	λ(I.A.)	Int.
2441.15		9.4	2451.84		1.2	2464.30		2.8
2443.00		2.7	2453.50		2.0	2464.58		2.8 (2)
2443.63	2443.55	5.1	2456.31		12	2464.71		4.5(2)
2443.89		2.2	2460.28		2.2	2467.80	2467.71	11
2446.60		0.9	2460.90	2460.81	11	2470.38		16
2449.24		1.4	2462.22		3.8	2473.02		10
2450.10		2.4	2463.85		6.0	2474.01	2473.92	8.7

TABLE XXVI (*continued*)

λ(Kayser)	λ(I.A.)	Int.
2476.73	2476.64	17
2483.70		15
2485.44		0.9
2486.53		3.4
2488.55		3.0
2489.36		3.3
2494.05		5.2
2494.83		9.5
2495.65	2495.56	13
2496.80		17
2500.60	2500.51	3.2
2504.63		17
2505.2		1.4
2506.55		7.7
2507.26		1.0
2511.12	2511.03	18
2513.01		9.3
2513.20		6.4
2517.90	2517.81	23
2519.90		5.4
2521.03		1.1
2521.49	2521.40	22
2525.09		6.5
2528.67		11
2529.06	2528.97	23
2530.22	2530.13	21
2530.65		6.8
2531.45		4.0
2532.26		21
2535.45		5.6
2536.02	2535.93	21
2536.55		19
2538.45		2.7
2542.05		5.2
2544.34	2544.25	20
2544.94		12
2548.40		20
2549.37		14
2553.09	2553.00	16
2553.44	2553.35	18
2555.15	2555.06	17
2556.85		12
2559.48		4.6
2561.37		2.0
2562.22	2562.13	10
2564.14		8.3
2567.42	2567.33	20
2572.32		8.8
2574.45	2574.36	18
2574.94		1.2
2575.82		4.2
2578.99		2.5
2580.43		20
2580.95		16
2582.35		7.8
2585.45	2585.36	11
2587.30		9.0
2590.70		11
2591.78		12
2594.26	2594.176	6.6
2595.31		1.9
	2596.000	0.6
2601.07	2600.991	4.9
2606.22		9.0
2610.86	2610.770	4.7
2613.60		1.4
2613.98		10
2614.23	2614.132	5.4
2614.45		0.9 (2)
2615.45		2.4
2616.34		4.1
2617.95		6.7
2619.36		5.0
2622.15	2622.064	14 (1)
2622.35	2622.252	5.9 (1)
2622.54	2622.434	11
2623.54	2623.450	11
2623.85		4.0
2627.13		3.5
2627.71	2627.641	23
2630.05		2.3
2640.33		1.5
2642.97		2.1
2644.89		4.9
2646.51	2646.420	24
2648.79	2648.648	51
2650.04	2650.271	11
2650.40		11
2653.84		0.5 (4)
2661.80		1.0
2663.61		0.6
2669.65		1.0
2674.04		1.3
2676.06	2675.987	10
2679.83		12
2680.20		2.6
2685.44	2685.340	17
2694.50		2.1
2694.76		2.2
2695.93	2695.853	20
2705.50		1.5
2705.94		3.7
2708.88		1.4
2716.05		13
2719.65		1.1
2722.20		1.4
2728.86		1.0
2731.20		5.7
2740.54		7.2
2745.17		8.0
2746.10		1.3
2750.20		3.5
2752.21		1.7
2758.67		1.0
2761.49	2761.375	9.6
2763.19		1.0
2764.30	2764.193	12
2766.31		1.0 (1)
2766.47	2766.37	4.2 (1)
2768.80		1.2
2772.80		1.6
2775.06	2774.964	4.4
2775.29		0.7 (1)
2775.67		1.5
2778.92		8.7
2786.00		2.2
2790.40		0.7
2791.13		1.7
2791.57		0.6
2792.55		2.2
2796.33	2796.236	5.4
2797.18		4.0
2803.87	2803.775	11
2804.25		1.0 (2)
2811.23		1.5
2811.64		2.6
2815.06	2814.979	1.1
2815.65	2815.557	16
2818.69	2818.596	2.2
2820.11	2820.003	3.6
2821.86		1.6
2823.78		1.2
2825.29		2.5
2826.91		1.9
2828.55		0.8
2834.02	2833.928	1.9
2834.55	2834.425	1.7
2837.26		4.7
2842.46		1.8
2850.15		4.3
2851.05	2850.956	1.1
2859.75	2859.660	2.4
2861.48		0.5
2862.70	2862.610	7.0
2867.57		0.4
2872.60		3.7
2878.65		1.4
2879.71		3.1
2882.34	2882.221	1.8
2886.55	2886.448	20
2892.37		1.8
2895.46		0.7 (3)
2895.57		1.6 (3)
2899.91	2899.801	3.3
2903.30		1.9
2904.40		0.6
2907.75		0.5
2911.70	2911.560	0.7
	2916.041	0.2 (4)
2919.66		1.3
2927.78		5.0
2928.91	2928.819	4.4
2929.62		5.1
	2936.551	0.5 (1)
	2942.630	0.5
2943.60		1.9
2955.50		1.6
2957.79		3.1 (2)
2969.70		0.7
2975.56		0.6
2977.56		0.5
2978.10		1.5
2982.37		1.0
2984.24		0.3 (4)
2987.28	2987.172	33
2989.70	2989.599	36
2996.67		1.0
2999.84		1.0 (2)
3000.66	3000.554	2.7
3005.86		3.2 (1)
3006.10		0.8 (1)
3013.70	3013.598	24
3015.77		3.8
3017.33		1.0 (3)
3017.66	3017.552	31
3019.23		0.7
3022.47		3.2
3023.66		0.5
3026.49		10.7
3028.31		0.6
3031.43		2.4
3034.55	3034.426	15
3038.42	3038.304	2.1
3039.66		3.3
3040.93		14
3042.60	3042.482	30
3044.11	3044.007	50
3045.13		0.7
3048.21		2.0 (2)
3049.00	3048.892	46
3050.64		3.6 (2)
3054.84	3054.724	4.4
3060.17		7.9
3061.15		1.5 (1)
3061.94	3061.825	49
3062.33	3062.198	8.8 (1)
3064.49	3064.375	16
3070.94		1.3 (1)
3072.06	3071.954	9.4 (2)
3072.45	3072.346	56
3073.64		3.3
3079.49	3079.390	4.9
3082.73	3082.614	42
3086.46		9.0 (2)
3086.89	3086.778	71
3087.86		2.1
3088.76	3088.676	0.9
3089.68	3089.593	38
3090.36		3.0
3095.81		2.7
3096.50		2.9 (1)
3096.80		1.8 (1)
3098.30	3098.195	35
3099.76		2.1
3102.49		4.0
3103.82		7.2 (1)
3104.12	3103.990	4.0 (1)
3106.03	3105.920	1.4 (2)
3106.22	3106.136	1.5 (2)
3107.15		2.5
3107.65		1.3
3109.60		3.3
3110.12		3.0
3110.94	3110.817	3.3
3111.45		1.4
3113.58		7.3
3118.35	3118.240	4.8
3118.76	3118.630	0.4 (1)
3121.54	3121.414	30 (3)
3121.69	3121.560	36 (3)
3126.85		3.4
3127.35	3127.244	4.6
3129.10	3128.997	1.5
3129.57		2.3
3132.33	3132.212	2.4
3136.81	3136.721	2.2
3137.47	3137.325	49
3140.08	3139.943	42

TABLE XXVI (*continued*)

λ(Kayser)	λ(I.A.)	Int.
3140.83		1.4
	3143.812	0.6
3145.16		1.8
3147.19	3147.060	56
3149.43	3149.304	28
3150.82		5.3 (2)
3150.93		6.3 (2)
3152.84		6.8
3154.91		42
3157.23		1.3
3158.92	3158.769	48
3159.80	3159.660	16
3161.78		4.6
3164.66		0.3
3168.19		4.5
3169.90		10
3173.30		0.6
3174.29		1.3
3175.06		3.2
3177.40		7.0
3179.98		0.5
3180.42		1.7
3182.25		6.6
3186.03		0.8
3186.46	3186.346	6.4
3188.50		8.8
3189.87	3189.756	3.6
3191.44	3191.300	1.8
3193.30	3193.162	3.2
3198.79	3198.664	2.3
3199.44	3199.325	1.4
3200.15	3203.030	2.0
3210.35		3.4
3210.96		1.6
3219.31	3219.155	12
3224.80		2.0
3227.15		1.8
3235.69		9.2
3237.18	3237.028	24
3239.08		1.1 (4)
3243.99		22
3250.17	3249.994	10
3254.37		20
3258.16		2.3
3260.99		13
3263.35		2.4
3264.96	3264.842	7.4
3271.92		9.8
3276.60		2.8
3277.44		2.3 (2)
3277.80		2.3 (2)
3278.96		5.1
3279.39		4.2
3280.74		18
3283.60		38
3287.34		7.7
3292.24		1.3 (4)
3298.83		4.6
3304.03		0.8 (3)
3304.29		1.7 (1)
3305.27		1.0 (4)
3305.87		1.0 (4)
3306.54		0.8 (4)
3307.31		7.9
3308.65		3.0
3308.96		4.7
3312.33		10
3312.99		1.6
3314.21		9.9
3315.20		1.1 (4)
3318.55		1.8
3319.31		2.2 (1)
3319.66		14 (1)
3320.00		4.9 (1)
3322.41		15
3325.44		15
3327.14		14
3328.34		1.1
3329.16		0.8 (4)
3329.63		4.3
3333.55	3333.390	13
3334.31	3334.151	100
3337.34	3337.175	6.4
3338.68		0.6 (4)
3339.97		9.0
3341.52		5.0
3342.10		3.2
3342.88		11
3344.36		1.0 (4)
3347.10		7.1
3348.28		11
3351.70		1.6
3354.51	3354.386	92
3355.27		2.3
3356.59		3.8
3356.97		1.3
3358.13		0.7 (4)
3359.42		5.6
3361.72		6.0
3362.93		6.7
3363.41		3.1
3363.89		2.2
3364.38		3.0
3365.13		1.2
3367.25	3367.114	94
3368.72		1.2
3370.48	3370.330	15
3373.40		5.9
3374.42		4.4
3376.34		1.5
3377.20		4.7
3378.86		5.4
3381.65		2.2
3383.07		16
3384.09		2.2
3385.38	3385.227	81
3388.29	3388.175	95
3390.54		2.5 (2)
3390.92		3.8 (2)
3395.55	3395.378	135
3398.96		1.4
3402.14		3.9
3403.33		0.6 (4)
3405.27	3405.120	144
3407.02		1.0 (4)
3409.29	3409.176	124
3412.50	3412.335	128
3412.79	3412.636	64 (1)
3415.66	3415.527	3.0 (1)
3417.32	3417.158	118
3417.84		8.0 (3)
3417.93	3417.796	8.0 (3)
3420.64		1.9 (3)
3420.95		4.7 (3)
3421.77		1.4
3423.03		3.1
3424.67		11
3426.60		1.3
3428.34		5.2
3428.89		1.8
3431.76	3431.579	71
3433.18	3433.043	170
3437.10		1.4
3437.83		5.8
3439.05		5.8
3443.06	3442.924	84 (1)
3443.79	3443.646	140 (1)
3449.26	3449.171	170 (3)
3449.54	3449.443	153 (3)
3452.44		3.8
3453.66	3453.513	155
3455.33	3455.236	99
3457.05	3456.936	9.3
3460.86	3460.732	2.4
3461.33		15
3462.94	3462.807	144
3465.96	3465.796	87
3469.11		1.5
3471.53		4.7
3472.85		2.0
3474.17	3474.019	169
3476.50		2.1
3478.00		1.8
3478.60		8.7 (3)
3478.90		5.2 (3)
3480.17		3.5
3483.58	3483.415	99
3485.51		21
3487.84		4.8
3489.57	3489.406	166
3490.89	3490.741	20
3491.49	3491.324	76
3495.83	3495.685	176
3496.80	3496.682	38 (2)
3496.90		38 (2)
3502.45	3502.281	89 (2)
3502.80	3502.620	159 (2)
3503.85		2.4 (3)
3504.89		2.4 (3)
3506.47	3506.315	138
3510.00	3509.844	122 (1)
3510.59	3510.419	92 (1)
3512.80	3512.643	128
3513.61	3513.483	89
3518.50	3518.353	215
3520.23	3520.087	78
3521.73	3521.572	186
3523.55	3523.438	155
3526.97	3526.856	99
3529.19	3529.037	83
3529.92	3529.815	151
3533.51	3533.363	100
3534.91		12
3543.43		27
3546.85		2.6
3548.60		5.8
3550.78	3550.599	64
3552.90	3552.719	3.0 (2)
3553.16		15 (1)
3553.31		3.0 (3)
3558.93	3558.780	15
3561.03	3560.896	103
3562.25		5.0
3563.09		5.3
3565.09	3564.955	103
3569.59	3569.382	185
3575.13	3574.964	99 (2)
3575.53	3575.361	114 (2)
3578.21		4.5
3579.04		4.5 (3)
3579.15		3.6 (3)
3582.02		1.7
3584.94	3584.796	7.2 (3)
3585.33	3585.159	109
3587.30	3587.188	223
3595.03	3594.869	101
3596.67		2.4
3602.22	3602.081	114
3605.52	3605.367	74
3611.89		14
3615.54		4.3
3618.15	3618.006	2.5
3620.56		2.7
3624.54		2.6 (1)
3625.18	3624.955	11 (1)
3627.98	3627.807	90
3631.59	3631.340	50
3633.01		7.4
3634.86		7.0
3637.44		1.7
3636.84		4.7
3639.60		17
3641.94		7.0
3643.35		14
3645.34		3.6
3647.85	3647.663	37
3649.49		7.8
3651.41		2.3
3652.70	3652.544	45
3654.59		4.0
3657.10	3656.965	7.5
3658.06		1.0 (4)
3662.32		22
3670.20		1.0 (4)
3676.72		17
3683.22		41
3684.63		5.2
3690.91		4.1
3693.63		15 (3)
3702.39		16
3704.22	3704.061	83
3707.62		3.9
3709.00		21
3712.35		2.9
3726.79		1.2
3730.63		27
3732.59		55
3733.65		22

TABLE XXVI (*continued*)

λ(Kayser)	λ(I.A.)	Int.
3736.08		12
3740.34		2.1
3745.65	3745.501	107
3750.07		14 (1)
3751.75		3.3
3754.47		1.5
3755.60		9.3
3759.83		1.0 (3)
3760.55		1.3 (3)
3774.75		2.9
3777.68		2.6
3783.87		0.6 (4)
3808.25	3808.106	7.2
3811.23	3811.070	1.9
3812.62		0.9
3814.62		3.1
3816.48		17 (2)
3816.61		13 (2)
3842.21	3842.056	137
3845.60	3845.474	235
3850.27		1.2 (2)
3851.09	3850.949	7.7
3852.00		2.4 (2)
3856.94		4.8
3861.31	3861.168	80
3863.75		1.0
3870.66		2.5
3873.23	3873.117	188 (1)
3874.09	3873.957	185 (1)
3877.01	3876.840	37
3882.06	3881.877	133
3884.79	3884.609	11 (1)
3885.45	3885.281	5.0 (2)
3894.25	3894.086	285
3895.15	3894.981	35 (1)
3898.54	3898.499	1.6
3904.23		1.9
3906.46	3906.296	16
3910.13	3909.941	26
3917.80		8.6
3920.90		5.3
3922.90	3922.764	8.1
3925.33		0.9
3929.43		1.1
3934.07	3933.921	4.5
3934.85		1.1
3936.13	3935.974	146
3939.00		0.8
3941.06	3940.895	20
3941.91	3941.735	39 (1)
3945.51	3945.323	27
3946.75		1.0 (2)
3947.26	3947.132	1.3 (2)
3952.46	3952.329	2.1 (3)
3953.10	3952.923	55
3956.42	3956.276	0.8
3958.10	3957.935	26
3961.15		3.3
3969.28		11
3972.69		3.5 (2)
3973.31	3973.148	13
3974.90	3974.732	17
3978.78	3978.656	11 (3)
3978.99		7.1 (3)
3979.67	3979.525	20 (1)
3987.25	3987.121	4.1
3990.45	3990.307	5.9
3991.68		7.7 (2)
3991.83	3991.693	7.0 (2)
3994.70	3994.541	1.0 (3)
3995.45	3995.312	244
3998.09	3997.909	125
3998.69	3998.554	1.0 (3)
4003.85		0.5
4011.10	4011.098	1.1
4014.09	4013.950	4.8
4019.45	4019.300	2.7
4021.07	4020.904	38
4023.55		2.1
4027.18	4027.044	11
4035.74		5.9
4040.57		0.7 (3)
4040.95		0.5 (3)
4045.56	4045.397	51
4049.43		0.6 (4)
4053.10		1.3
4057.10		2.0 (1)
4057.36	4057.199	4.5 (1)
4058.36	4058.188	9.6 (1)
4058.76	4058.603	5.5 (1)
4063.34	4063.19	2.0
4066.56	4066.378	36
4068.72	4068.553	9.4
4076.30	4076.134	3.1
4077.56		1.4
4082.75	4082.606	2.0
4086.49	4086.307	32
4092.56	4092.397	135
4104.57	4104.430	0.8 (2)
4104.91		1.8 (2)
4110.70	4110.544	77
4118.96	4118.784	232
4121.52	4121.329	306
	4130.538	0.4 (4)
4132.30	4132.15	3.0
4150.62	4150.442	0.5 (4)
4158.59		0.8
4162.38		1.3
4179.44		0.5
4187.46	4187.248	1.5
4190.88	4190.709	15
4193.02		0.8 (4)
4198.56	4198.424	0.7 (4)
4234.17	4233.996	1.8
4242.07		1.0
4245.75		0.2 (4)
4248.35		0.2 (4)
4252.46	4252.303	6.9
4270.60	4270.423	1.0
4285.95	4285.787	2.8
4292.42		0.7
4303.41	4303.236	1.3
4309.61	4309.418	0.4
4331.43		1.2
4339.81		2.8
4371.31		1.4
4373.81		1.4 (1)
4375.11	4374.940	1.4 (1)
4391.70	4391.59	1.2 (1)
4392.02		1.0 (1)
4402.86		1.0
4417.55	4417.425	1.5
4421.54	4421.359	1.3
4431.79		0.8
4445.88	4445.730	1.4
4467.09	4466.888	4.7
4469.75	4469.569	10
4471.76	4471 578	4.0
4478.50	4478.345	1.6
4484.11	4483.946	1.5 (2)
4494.94		0.6
4517.26	4517.121	2.8
4528.08	4527.936	0.8 (2)
4531.12	4530.985	48
4534.16	4533.998	6.1
4543.98	4543.836	5.5
4549.83		11
4565.79		17
4570.21		1.4
4580.34	4580.133	2.6 (2)
4581.80	4581.618	25
4594.82		3.2
4597.09		3.0
4623.20	4623.024	1.1
4625.92		1.0
4629.52	4629.380	19
4657.56	4657.399	0.2
4663.59	4663.411	11
4682.53	4682.363	6.6
4693.36	4693.193	2.8
4698.56	4698.370	1.4
4704.57		0.7
4728.14	4727.924	2.2
4735.04	4734.834	0.8
4737.95	4737.776	1.1
4749.89	4749.684	6.8
4754.39	4754.372	1.3
4756.93		0.8
4767.33		0.8 (2)
4768.26	4768.096	1.2 (2)
4771.27	4771.105	2.8
4776.49	4776.328	3.1
4780.14	4780.001	5.7
4793.03	4792.867	8.5
4813.67	4813.482	12
4840.42	4840.267	14
4868.05	4867.680	18

THE EFFECT OF THE MOTION OF THE NUCLEUS ON THE SPECTRA OF Li I AND Li II

By D. S. Hughes and Carl Eckart
Ryerson Physical Laboratory, University of Chicago

(Received July 7, 1930)

Abstract

The wave equation for a system of N electrons (mass m) and one nucleus (mass M) is set up and solved approximately. If $W(m)$ are the energy levels for $M=\infty$, the energy levels for finite M are $(\mu W(m)/m)+\Delta W$, where $\mu=mM/(m+M)$ and ΔW is calculable.

In case $N=2$ or 3, ΔW is zero except for P levels. For these it is given by Eq. (13), which is derived on the assumption that the wave function is a polynomial of hydrogen functions, each with its own effective nuclear charge. The values of the latter previously determined by one of the authors are used in comparing the calculation with Schüler's experimental data on Li II, λ5485 and Li I, λ6708. The agreement is satisfactory and eliminates one objection to Schüler's interpretation of λ5485.

IT IS well known that the effect of the motion[1] of the nucleus on the spectra of hydrogen and ionized helium may be accounted for by replacing m, the mass of the electron, by $\mu=mM/(m+M)$, M being the mass of the nucleus. This simple procedure does not suffice for elements of more than one electron, and as an effect observed in the spectrum of lithium has been ascribed to this cause, a theoretical discussion of the expected effect seems in order. Some of the results obtained are applicable to the general case of N electrons, others only to Li I and Li II.

1. General

The kinetic energy operator for a system of N electrons and one nucleus is

$$T=-\frac{h^2}{4\pi^2}\left\{\frac{1}{2\mu}\sum_{1\to N}\nabla_k^2+\frac{1}{M}\sum_{(k,j)}\nabla_k\cdot\nabla_j+\frac{1}{2(M+Nm)}\nabla^2\right\} \tag{1}$$

in which

$$\nabla_k=i\frac{\partial}{\partial x_k}+j\frac{\partial}{\partial y_k}+k\frac{\partial}{\partial z_k}$$

$$\nabla=i\frac{\partial}{\partial X}+j\frac{\partial}{\partial Y}+k\frac{\partial}{\partial Z}$$

where x_k, y_k, z_k are the rectangular coordinates of the k^{th} electron in a system whose origin is located at the moving nucleus, and (X,Y,Z) are the coordinates of the center of mass of the atom in another system of arbitrary fixed origin. The quantities m, M, and μ have the significance already defined.

[1] This term will be used to describe the translatory motion of the nucleus about the center of mass of the atom, as distinguished from the nuclear "spin".

The wave equation is thus

$$\{T + V(x) - W\}\psi = 0 \tag{2}$$

where V is the potential energy of the atom and is independent of the coordinates of the center of the mass. For simplicity, it may be assumed that the latter is at rest, so that ψ will also be independent of (X,Y,Z).

If it be assumed that the characteristic values $W(m)$ and solutions $\psi(m)$ of Eq. (2) are known for $M=\infty$ (stationary nucleus), the effect of the finiteness of M may be approximately resolved into two parts:

a. M is replaced by μ in $W(m)$ and $\psi(m)$.

b. The energy level is displaced by an additional amount ΔW given by

$$\psi(m)\Delta W = H'\psi(m) = -\frac{h^2}{4\pi^2 M}\sum_{(k,j)}\nabla_k\cdot\nabla_j\psi. \tag{3}$$

The perturbed energy value is thus $W(\mu)+\Delta W$. The statement (b) assumes that there is no degeneracy other than that conditioned by the rotational symmetry of the problem (degeneracy in the magnetic quantum number).

These two effects may be treated independently; for the first,[2] it is necessary to investigate the dependence on μ of the characteristic values of the equation

$$-\frac{h^2}{8\pi^2\mu}\sum_{1-N}\nabla_k^2\psi + [V(x) - W(\mu)]\psi = 0. \tag{4}$$

Since $V=\Sigma(Ze^2/r_k)-\Sigma(e^2/r_{jk})$ is a homogeneous function of degree -1 in the $3N$ variables[3] the calculation may be made rigorously without knowing ψ: on introducing new variables $x_k'=\alpha x_k$, $y_k'=\alpha y_k$, $z_k'=\alpha z_k$, where $\alpha=\mu/m$, and noting that $V(x)=\alpha V(x')$, Eq. (4) becomes

$$-\frac{h^2}{8\pi^2 m}\sum_{1-N}\Delta_k'^2\psi + [V(x') - W(\mu)/\alpha]\psi = 0.$$

Hence

$$W(\mu) = \alpha W(m). \tag{5}$$

Since α is less than 1, this causes a general contraction of the spectrum relative to that of an atom whose nucleus has infinite mass. This may be called the normal effect, since it is the only effect in the case of the simplest spectra.

The specific effect ΔW cannot be evaluated without some assumption regarding $\psi(m)$. It is simplest to assume it as a polynominal of hydrogen functions, each with a different nuclear charge determined by the variational method of calculating characteristic values.[4] The coefficients of the poly-

[2] The calculation is merely an extension of that usually given for hydrogen.

[3] This is true only if the electron spin energy is not included in V.

[4] C. Eckart, Phys. Rev. **36**, 149 (1930). It is not known whether such a polynomial is really a good approximation to $\psi(m)$ or not, but it may be shown to yield approximately correct values for the energy. There is also some justification for its use in a perturbation calculation, but the magnitude of the error introduced is uncertain. Experience would seem to show that it is smaller than if the true nuclear charge was used in each hydrogen function; cf. W. Heisenberg, Zeits. f. Physik **39**, 511 (1926). Whatever may be the theoretical status of effective nuclear charges, it should be remarked that the values of Z_1 and Z_2 used in these calculations have not been determined *ad hoc* but are the results of independent calculations made without reference to the present problem.

nominal are determined so that $\psi(m)$ has the proper permutational symmetry. Calculations based on this assumption follow for the cases of two and three electron systems.

2. Two Electron Systems

The wave function may be approximated by

$$\psi = [u(1)v(2) \pm v(1)u(2)]/2^{1/2} \tag{6}$$

in which u is the characteristic function of the $1s$ state, v of the excited state (n, l), and the numerals designate the variables of the two electrons. The effective nuclear charge for the function u is to be taken approximately equal to Z, the true nuclear charge. If v represents a $2p$ state, its effective nuclear charge is approximately $Z_2 = Z - 1.0$. The precise theoretical[4] values for Li II, 2^3P are $Z_1 = 2.98$, $Z_2 = 2.16$. The upper sign in Eq. (6) is for the singlet level, the lower for the triplet. The perturbation operator in this case is simply

$$H' = -h^2\nabla_1\cdot\nabla_2/4\pi^2M$$

and

$$\Delta W = \int\int \psi^* H'\psi d\tau_1 d\tau_2.$$

On integrating by parts with respect to the variables 2,

$$\Delta W = (h^2/4\pi^2M)\int\int (\nabla_1\psi)(\nabla_2\psi^*)d\tau_1 d\tau_2;$$

noting that

$$\int (\nabla u)u^* d\tau = \tfrac{1}{2}\int \nabla \mid u \mid^2 d\tau = 0,$$

and making use of Eq. (6), this reduces to

$$\Delta W = \pm (h^2/4\pi^2M)\left|\int u^*\nabla v d\tau\right|^2. \tag{7}$$

This integral will be evaluated at the end of the next section.

3. Three Electron Systems

In this case, it may be well to take account of the permutation degeneracy directly: there are three independent characteristic solutions

$$\psi_1 = v(1)u(2)u(3), \quad \psi_2 = v(2)u(3)u(1), \quad \psi_3 = v(3)u(1)u(2) \tag{8}$$

and

$$H' = -(h^2/4\pi^2M)(\nabla_1\cdot\nabla_2 + \nabla_2\cdot\nabla_3 + \nabla_3\cdot\nabla_1). \tag{9}$$

The function u again represents the $1s$ state, this time with Z_1 approximately equal to $Z-0.3$, while v, in the case of the configuration $(1s)^2\,(2p)$, has the approximate nuclear charge $Z_2 = Z-2.0$. In the case of Li I, 2^2P, the theo-

retical values are[4] $Z_1=2.69$, $Z_2=1.02$. The Eq. (3) is to be replaced by the three equations

$$\begin{aligned} a\Delta W &= aA + bB + cB \\ b\Delta W &= aB + bA + cB \\ c\Delta W &= aB + bB + cA \end{aligned} \tag{10}$$

in which

$$\begin{aligned} A &= \int\int\int \psi_i^* H' \psi_i d\tau_1 d\tau_2 d\tau_3 \\ B &= \int\int\int \psi_i^* H' \psi_j d\tau_1 d\tau_2 d\tau_3 . \end{aligned} \tag{11}$$

The quantities A and B are real and independent of i and j since the operator H' is symmetric in the three sets of coordinates. The determinent of Eqs. (10) has one single root $\Delta W=A+2B$ and one double root $\Delta W=A-B$. The former belongs to a state which is excluded by the Pauli principle, the latter to the actual doublet state.

On substituting Eqs. (8) and (9) into (11), it is found that

$$A = 0, \quad B = -(h^2/4\pi^2 M)\left|\int u^*(\nabla v)d\tau\right|^2,$$

so that ΔW has the same functional form as in the case of a two electron system.

This integral is readily evaluated: as a generallization of a well-known equation, it is readily shown that

$$\begin{aligned} -(h^2/4\pi^2 m)\int u^*(\partial v/\partial x)d\tau = (W_u - W_v)\int xu^* v d\tau \\ - e^2(Z_1 - Z_2)\int (xu^* v/r)d\tau, \end{aligned} \tag{12}$$

W_u and W_v being the Balmer term-values associated to u, Z_1 and v, Z_2, respectively. By a slight generallization of the methods used to derive the selection principles for spectral lines[5] it may be shown that both integrals on the right vanish unless the values of the azimuthal quantum numbers of u and v differ by exactly one unit. As u represents the $1s$ state, ΔW will therefore vanish unless v represents a p state, and the specific effect is shown only by P levels (in this approximation at least). The displacement of these is found to be

$$\Delta W = \pm \frac{128}{3}\frac{m}{M} R_\infty Z_1^5 Z_2^5 n^3 (n^2 - 1)\frac{(Z_1 n - Z_2)^{2n-4}}{(Z_1 n + Z_2)^{2n+4}}$$

[5] A. Sommerfeld, Wellenmechanischer Ergänzungsband, p. 92. (Vieweg, Braunschweig, 1929).

in which R_∞ is the Rydberg constant, $2\pi^2me^4/h^2$, and n is the true principal quantum number. The increment of energy will be negative for the three electron system and the triplets of the two electron system, positive for the singlets.

4. Comparison with Observed Effects

H. Schüler[6] has proposed an interpretation of the hyperfine structure of the Li II line 2^3P-1^3S, λ5485, according to which the nucleus of Li (6) has no angular momentum while that of Li (7) has 1/2 unit. On the basis of his analysis it is possible to calculate the displacement of the Li (6) lines from the position which the Li (7) lines would occupy if there were no nuclear spin. These displacements are given in the last column of Table I. The three values should be identical to at least two significant figures, so that the differences are to be ascribed to errors, either in measurement or interpretation, or in both.

Table I.

	Li (6)	Li (7)	Δλ
$^3P_0-{}^3S$	5484.10	5483.81	0.29A
$^3P_2-{}^3S$	5485.02	5484.69	0.32
$^3P_1-{}^3S$	5485.65	5485.31	0.34

Using the values of $Z_1=2.98$, $Z_2=2.16$ Eq. (13) yields 0.256 A for the displacement produced by the specific effect, while Eq. (5) yields 0.071 A for the normal effect. The resultant is 0.327 A, the Li (6) line being to the long wave-length side of Li (7). This value is in excellent agreement with those of Table I. This calculation therefore supports part of Schüler's interpretation of this line though the present considerations would not defend it against attacks from other directions.[7]

Schüler and Wurm[8] have also found that the lines 2^2P-1^2S of Li I, λ6708, are doubled, with a separation of 0.15A. This has been confirmed by one of us (H), the observed separation being between 0.155 and 0.160A. Assuming the nuclear spin to be 1/2 for Li (7), the structure due to this cause should be only 0.03–0.04A wide. The effect has therefore been interpreted as being primarily due to the motion of the nucleus.

The calculated values, using $Z_1=2.69$ and $Z_2=1.02$ (cf. Section 4) are 0.087A for the normal effect and 0.036A for the specific, a total of 0.123A. The agreement is as good as might be expected, since the difference between observed and calculated is of the order of the unresolved spin structure.

We would like to conclude from these results that Schüler's interpretation of λ5485 is correct, but, in view of the results Harvey and Jenkins[7] have obtained from the band spectra of lithium, the question had best be left open.

[6] H. Schüler, Zeits. f. Physik **58**, 741 (1929); and H. Brück, ibid **42**, 489 (1927).
[7] A. Harvey and F. A. Jenkins, Phys. Rev. **35**, 789 (1930).
[8] H. Schüler and E. Wurm, Naturwiss. **15**, 971 (1927).

ELECTRONIC STATES IN THE VISIBLE HALOGEN BANDS

By Robert S. Mulliken*
Ryerson Physical Laboratory, University of Chicago

(Received July 7, 1930)

Abstract

It is shown on the basis of theoretical considerations that the well-known visible iodine absorption bands and the analogous bands of the other halogens almost certainly cannot correspond to a $^1\Sigma \leftarrow {}^1\Sigma$ transition as hitherto supposed. It is concluded that they belong to a $^3\Pi_{0u} \leftarrow {}^1\Sigma_g^+$ transition, with a case c $^3\Pi_0$ state whose Λ-type doubling is so wide that the state is split into two separate states which simulate a $^1\Sigma_u^+$ and a $^1\Sigma_u^-$ state. The observed bands involve however only the state which behaves like $^1\Sigma_u^+$, the $^1\Sigma_u^-$-like state and the $^3\Pi_1$ and $^3\Pi_2$ states being unknown. The classification $^3\Pi_0$ really has little meaning, one needs for case c here a classification in which only Ω values and symmetry properties ($+$ or $-$, g or u) are significant. According to the above interpretation, the upper level of the halogen bands is paramagnetic, this is in harmony with certain magnetic phenomena observed with these bands. Electron configurations for the normal and excited states are suggested in the case of fluorine.

TWO identical atoms in the same ^2P state[1] are capable, as one finds by applying the relations obtained by Wigner and Witmer,[2] of giving only the following set of molecular states.: $^1\Delta_g$, $^3\Delta_u$, $^1\pi_u$, $^1\pi_g$, $^3\pi_u$, $^3\pi_g$, $^1\Sigma_g^+$, $^1\Sigma_g^+$, $^1\Sigma_u^-$, $^3\Sigma_u^+$, $^3\Sigma_u^+$, $^3\Sigma_g^-$. As we shall see, this is almost certainly[5] in conflict with the current interpretation of the visible absorption bands of iodine and the analogous bands of the other halogens as $^1\Sigma$, $^1\Sigma$ transitions. The argument is as follows.

For convenience we shall speak in terms of the *chlorine* bands, since our knowledge is more well-rounded for these than for the bands of the other halogens. What is said is intended to apply to all the halogens, since there can scarcely be a doubt that the bands of the four molecules are all of the same type. In respect to some properties, the iodine bands are better known than the chlorine bands, but we shall feel free to apply this knowledge also to the latter. (1) That the *normal state* of Cl_2 is $^1\Sigma$ seems assured by the fact that chlorine gas is diamagnetic (Br_2 and I_2 are also known to be diamagnetic in the *liquid* state). This conclusion is strongly supported by a study of

* Fellow of the John Simon Guggenheim Memorial Foundation, now in Leipzig.

[1] For the prediction of the possible molecular states as given above, the division of the ^2P normal state into $^2P_{\frac{1}{2}}$ and $^2P_{1\frac{1}{2}}$ substates does not matter, by the "normal state" of the atom we mean either $^2P_{\frac{1}{2}}$ or $^2P_{1\frac{1}{2}}$ or both.

[2] E. Wigner and E. E. Witmer, Zeits. f. Physik **51**, 883 (1928). The designations Σ^+ and Σ^- used here correspond to Wigner and Witmer's Σ and Σ^1 (also to their 0 and 0'). The subscripts g and u (gerade and ungerade) mean "even" and "odd". In the case of odd (even) states the electronic factor of the wave-function ψ does (does not) change sign on reflection in the midpoint of the line joining the nuclei. Σ_g, Π_u, Δ_g are respectively the same as Σ_+, π, Δ_+ of Wigner and Witmer, while Σ_u, Π_u, Δ_u are the same as their Σ_-, Π_-, Δ_-.

possible electron configurations for the normal molecule.[3] (2) That this $^1\Sigma$ state is either a $^1\Sigma_g^+$ or a $^1\Sigma_u^-$ state is shown by the fact that the rotational levels with odd values of K have the greater statistical weight.[4,5] Either $^1\Sigma_g^+$ or $^1\Sigma_u^-$ is capable,—see above,— of being derived from two normal atoms.[1] Whether or not the normal states of the halogens *actually are* so derived is not essential to the present argument, but is nevertheless of interest. By extrapolation from the known vibrational levels of the normal state, as in the method of Birge and Sponer, one gets, for I_2, Br_2 and Cl_2, values of the energy of dissociation which agree well with the supposition that dissociation does give normal atoms.[1] Also, since all excited states of the atoms (including $F^+ + F^-$) lie high above the normal level, it is improbable that any of these could give normal atoms. (3) A consideration of possible electron configurations consistent with $^1\Sigma_g^+$ and $^1\Sigma_u^-$ shows that only $^1\Sigma_g^+$ is reasonable for the normal state of the halogens.[6] But even if we should

[3] A $^3\Pi_1$ state would also be diamagnetic, but such a state is very unlikely to be the normal state, since the correspondence $^3\Pi_2$ would probably also exist and be lower, assuming case *a* coupling, $^1\Sigma$ is also by far the most probable normal state on the basis of a study of electron configurations.

[4] That the odd levels have the greater weight is shown in the case of Cl_2 by the band analysis of A. Elliot (Proc. Roy. Soc. **123A,** 629, 1929). In the case of Br_2 an analysis of the bands is lacking, while in I_2 no alternations in intensity have been detected. If we represent the complete wave function ψ as a product of three factors, $\psi = \psi_{el}\psi_{rot}\psi_{nu.spin}$, then we know (*a*) ψ must on theoretical grounds (cf. R. S. Mulliken, Trans. Faraday Soc. No. 102, **25,** Part II Nov. 1929) be antisymmetrical in the nuclei $(An)^5$; (b) for the levels with greater statistical weight in any homonuclear molecule, $\psi_{nu.spin}$, is always symmetrical in the nuclei (Sy), for odd values of K in a Σ state, $\psi_{rot.}$ is always An. For the odd K values, therefore, in Cl_2 $\psi_{rot.}$ is An, $\psi_{nu.spin.}$ is Sy, hence, since ψ itself must be An, ψ_{el} must be Sy. This is the case for either a Σ_g^+ or a Σ_u^- state. (The possibility of Σ^- states was overlooked in the writer's article just cited, and led to some erroneous conclusions in regard to O_2, whose normal state is now known to be $^3\Sigma_g^-$.)

[5] That the complete ψ must be An for a molecule whose nuclei contain each an odd number of (protons plus electrons), as theoretically predicted by Hund (cf. R. S. Mulliken, Ref. 4), is contradicted by the experimental results on N_2, where ψ is Sy although the nucleus is composed of 21 particles (14 protons, 7 electrons). The most probable reformulation is that ψ has to be An if the nucleus of each atom contains an odd number at *protons* (and Sy if it contains an even number), regardless of the electrons. Since both the old and the new conditions for an An ψ are fulfilled for the Cl atom, it seems safe to take this for granted. If, however, the contrary should be true, the following results would hold: the normal Cl_2 molecule is $^1\Sigma_u^+$ or $^1\Sigma_g^-$ (both are improbable on the basis of a consideration of electron configurations), and dissociates giving at least one highly excited atom (this would hardly be possible to reconcile with data on the vibrational levels (cf. section (2) in the text above)), the excited molecule would then probably be $^1\Sigma_g^+$ or Σ_u^-, either of which is derivable from normal atoms[1], in agreement with section (5) in the text.

[6] It is highly probable that the normal state of F_2 is a $^1\Sigma_g^+$ state with essentially the following electron configuration: $1s\sigma^2 2p\sigma^2 2s\sigma^2 3p\sigma^2 3d\sigma^2 2p\pi^4 3d\pi^4$. Possible $^1\Sigma_u^-$ states are derivable from $\cdots 2p\pi^3 3d\pi^1 nx\sigma^2$ (n and x anything not already present) and $\cdots 2p\pi^4 3d\pi^3 3p\pi$. The first of these (probably with $nx\sigma^2 = 4f\sigma^2$) might be derived from two normal atoms, but would surely be higher and be more unstable than the $^1\Sigma_g^+$ configuration mentioned above. The second ($\cdots 3p\pi$) could probably be obtained only from one normal F atom and one excited atom with a $3p$ electron; the energy of excitation of the latter would be so great that it practically certainly could not give the normal state of F_2. Analogous arguments apply to the other halogens.

assume $^1\Sigma_u^-$, we should still come to the conclusion that the halogen bands here under discussion cannot be a $^1\Sigma$, $^1\Sigma$ transition. (4) Assuming that the normal state is $^1\Sigma^g$ and that the coupling relations in both states correspond to Hund's cases *a* or *b*, the *excited state* can only be one of the following:[7] $^1\Sigma_u^+$, or $^1\pi_u$, or $^3\Sigma_u^+$, or $^3\Pi_u$. (5) According to Franck's well-known interpretation of the convergence limits of the halogen bands, the excited state dissociates without question into two normal atoms,—more accurately, into one $^2P_{\frac{1}{2}}$ and $^2P_{1\frac{1}{2}}$ atom. (6) Since a $^1\Sigma_u^+$ state cannot possibly be obtained from two normal atoms (cf first paragraph), the excited state cannot possibly be $^1\Sigma_u^+$, and the bands therefore cannot be of the $^1\Sigma$, $^1\Sigma$ type. The possibilities $^1\Pi_u$, $^3\pi_u$, and $^3\Sigma_u^+$ for the excited state remain, since all are consistent with dissociation into normal atoms.

None of the interpretations $^1\pi\leftarrow{}^1\Sigma$, $^3\pi\leftarrow{}^1\Sigma$, and $^3\Sigma\leftarrow{}^1\Sigma$ appear easy to reconcile with the observed structure of the bands, which (in Cl_2 and I_2, F_2 and Br_2 not having been investigated as yet) consists definitely only of one *P* and one *R* branch, each composed of single lines arranged exactly as in the case of a $^1\Sigma$, $^1\Sigma$ transition. The absence of a *Q* branch probably rules out the possibility of a $^1\Pi$ upper level. $^3\Pi$ also seems unlikely unless it scombinations with $^1\Sigma$ are restricted, say, to one component of the $^3\Pi_0$ level (see below). In favor of $^3\Sigma_u^+$ is the fact that in a $^3\Sigma\leftarrow{}^1\Sigma$ transition only a *P* and an *R* branch are expected. But one would expect these to consist of wide doublets as in the $^1\Sigma\leftarrow{}^3\Sigma$ atmospheric oxygen bands.[8] That the observed lines are single seems hardly reconcilable with a $^3\Sigma$, $^1\Sigma$ combination. One might of course suppose that the $^3\Sigma$ rotational triplets are so narrow as to be unresolved, but, especially for the heavier halogens, this is wholly contrary to theory, as well as to experimental data on doublet separations in $^2\Sigma$ states. Another conceivable explanation would be that in the $^3\Sigma$ level the components with $J=K\pm1$ are widely separated from those with $J=K$ and that, for unknown reasons, only combinations of the levels with $J=K$ with levels of the $^1\Sigma_g^+$ normal state are observed. This would give simple *P* and *R* branches in greement with experiment, but it is very far-fetched.

An escape from these difficulties is to be found by noting a fact whose consequences have hitherto not been fully appreciated. In the excited states of the halogen molecules, the energies of dissociation *D* are very small ($D=0.55$ volts for I_2, 0.39 volts for Br_2, 0.23 for Cl_2, and by extrapolation from the other halogens, about 0.1 volts for F_2); they are roughly about equal to the doublet separations between the $^2P_{1\frac{1}{2}}$ and $^2P_{\frac{1}{2}}$ sublevels of the normal states of the halogen atoms (I, 0.94 volts, Br, 0.45 volts, Cl, 0.11 volts, F, 0.05 volts). From these figures we can conclude that, especially in the heavier halogens, the influence of the electric axis on the electron orbits

[7] The following selection rules apply if both states correspond to coupling cases *a* or *b* or intermediate cases: $\Delta\Lambda=0, \pm1$; Σ^+ terms combine with Σ^+ but never with Σ^- terms; in homonuclear molecules, even terms (*g*) combine only with odd terms (*u*). Quintet states are ruled out, for the excited state, by the fact that the latter dissociates into normal atoms (cf. list of possible states in first paragraph).

[8] R. S. Mulliken, Phys. Rev. **32**, 880 (1928).

is not large enough to break down, at any rate not at all completely, the coupling of each atomic L vector with its S vector. The quantum numbers L_1, S_1, J_1, L_2, S_2, J_2 of the two atoms still retain their significance to a considerable extent in the molecule. J_1 and J_2 give respectively quantum numbers Ω_1 and Ω_2 (or M_1 and M_2) which represent their projections on the electric axis. The only electronic quantum number which is significant for the molecule as a whole is $\Omega(\Omega = |M_1 + M_2|)$ Λ and S for the molecule as a whole are practically meaningless as quantum numbers; λ's of individual electrons are even more completely lacking in significance; nevertheless Λ, S, and λ values can be formally assigned by imagining the nuclei pushed closer together. This coupling case can be classified as a form of Hund's case *c*; in another form which has been more discussed, the molecule as a whole has an L and an S, which are strongly coupled to give a resultant J^a, which in turn gives a projection Ω.

For the *normal* states of the halogen molecules, where the D values are moderately large (assuming dissociation into two $^2P_{1\frac{1}{2}}$ normal atoms, they are, $D = 1.53$ volts for I_2, 1.96 volts for Br_2, 2.54 for Cl_2, and by extrapolation, about 3.1 volts for F_2), we may assume Hund's case *a*, or in I_2 perhaps a case intermediate between *a* and *c*.

In dealing with the present weak-binding form of case *c*, it seems best to designate different electronic states simply by numbers giving their Ω values (0, 1, 2, etc.), together with a superscript + or − when $\Omega = 0$ and a subscript *g* or *u* in the case of homonuclear molecules in order to designate certain symmetry properties of their ψ functions. Here *g* and *u* have the same meaning as in cases *a* and *b*. So do + and −, but for convenience we may here define 0^+ and 0^- states as follows: in 0^+ states the even-numbered rotational levels ($J = 0.\,2.\cdots$) are even (in the sense of Kronig) or positive (in the sense of Wigner and Witmer), while the odd-numbered levels are odd or negative;[9] in 0^- states the relations are reversed.[10]

As selection rules in case *c* here we have only the following: $\Delta\Omega = 0, \pm 1$; $\Delta J = 0, \pm 1$; $g \rightleftarrows u$; even or positive combine only with odd or negative rotational levels. The intensity relations in the P, Q, and R branches should be governed, just as in case *a*, by the Hönl and London intensity formulas.[11] For example, transitions between a 0 and a 1 state should show a P, a strong Q, and an R branch. (The 1 state should have Ω-type doubling, vanishing with zero rotation, and similar to the Λ-type doubling for a $^1\Pi$ state in cases *a* and *b*; and the P and R branches should make connection with one component of each Ω-type doublet, the Q branch with the other). Transitions

[9] The words "even" [R. de L. Kronig, Zeits. f. Physik **50**, 351 (1928)] and "positive" (Wigner and Witmer, ref. 2, 867, footnote) are here synonymous; likewise for "odd" and "negative".

[10] For a discussion of the behavior of $^3\Pi_0$ states in the passage from case *a* to case *c*, cf. J. H. Van Vleck, Phys. Rev. **33**, 501–2 (1929). Van Vleck points out that the *a* and *b* sets of sublevels of $^3\Pi_0$ behave like a 0^+, 0^- pair (similar to $^1\Sigma^+$ and $^1\Sigma^-$). In regard to notation use of + and −) cf. ref. 2.

[11] H. Hönl and F. London, Zeits. f. Physik **33**, 803 (1925) Cf. R. S. Mulliken, Phys. Rev. **29**, 391, (1927) for discussion and applications.

between two 0 states should show only a P and an R branch, just as for $^1\Sigma$, $^1\Sigma$ transitions in case a. This latter fact, taken in connection with the selection rule even $\rightleftarrows$ odd for rotational terms, shows that only combinations between two 0^+ states, or between two 0^- states, but not those between a 0^+ and a 0^- state, are capable in case c of giving rise to spectrum lines.[12] In case, however, there should be a departure from the conditions of case c toward those of case a, Q branch combinations between a 0^+ and a 0^- state may also be expected (cf. next paragraph).

Let us now consider as a typical example, for a range of cases from a to c, a transition which in case a would be classified as $^3\Pi_0$, $^1\Sigma$. The $^3\Pi_0$ state has two rotational levels for each J value ($J=0, 1, 2, \cdots$); these may be considered as derived from two electronic sublevels of $^3\Pi_0$, namely from a 0^+ and a 0^- sublevel.[11] In case a, we may probably expect a P, a Q, and an R branch in a $^3\Pi_0$, $^1\Sigma$ combination. For a $^1\Sigma^+$ type of $^1\Sigma$ state, the P and R branches come from the 0^+ levels of the $^3\Pi_0$, the Q branch from the 0^- levels. In the passage to case c, the P and R branches remain, but the Q branch 0^-, 0^+ combination should gradually fade out, while at the same time the 0^- levels may become widely separated[11] from the 0^+ levels.

In both limiting cases (a and c,), and probably also in intermediate cases, the rotational energy for the $^3\Pi_0$ states is given by an expression of the form $E=\text{const.}+B_vJ(J+1)+\cdots$. The same expression for E^r also holds for all electronic states in case c, as well as in case a.

We are now in a position to interpret the halogen bands from a more general viewpoint than that adopted at the beginning of this paper. Their observed structures show that they are a $0\leftarrow 0$ transition; more specifically, since we have seen that the lower state is in all probability a $^1\Sigma_g^+$ and since they consist of P and R branches, we conclude that they are $0_u^+\leftarrow 0_g^+$. As we have already seen, the 0_u^+ state cannot correspond to a $^1\Sigma_u^+$ state, since such a state is not derivable from normal atoms. In the list of states derivable from normal atoms (cf. first paragraph of paper), *only one* 0_u^+ state is to be found, namely the 0^+ component of the $^3\Pi_u$ state,[13] and we therefore conclude that the upper level of the halogen bands is of this type. The absence of a Q branch corresponding to the 0^- component of $^3\Pi_u$ can be understood (cf. preceding paragraph) in view of the fact that we expect case c coupling here for the 0_u^+ state. It may even be that the 0_u^- state is much more unstable than the 0_u^+, so that the corresponding band system $0_u^-\leftarrow 0_g^+$ (Q branches) may consist only of a continuous region: furthermore, it may be that this system is very weak.—It should be emphasized that the classification of the 0_u^+ level as belonging to $^3\Pi$ has only a formal meaning, since

[12] This is analogous to, but not (except in singlet states) identical with the rule that in combinations between Σ states only Σ^+,Σ^+ and Σ^-,Σ^- are possible.

[13] The other 0 states derivable from two equal ^3P atoms are, 0^- from $^3\Pi_u$, 0^+ and 0^- from $^3\Pi_g$ two 0_g^+ states and one 0_u^- state corresponding to the three $^1\Sigma$ states (one of the 0_g^+ states is the normal $^1\Sigma_g^+$ state of the molecule), and two 0_u^- and one 0_u^+ state from the two $^3\Sigma_u^+$ states and the one $^3\Sigma_u^+$ state respectively. A $^3\Sigma^+$ state gives in case c, as is easily shown, one 0^- and one 1 state; a $^3\Sigma^-$ state, one 0^+ and one 1 state (cf. later paper).

quantum numbers Λ and S are not defined here in case *c*. Physically, this 0_u^+ level may have little resemblance to a $^3\Pi_0$ ordinary level of case *a*.

By application of the methods of Wigner and Witmer, it is possible to predict, for a loosely-bound case *c* molecule as here, the molecular states which can be derived from each of the individual combinations $^2P_{1\frac{1}{2}}+^2P_{1\frac{1}{2}}$, $^2P_{1\frac{1}{2}}+^2P_{\frac{1}{2}}$ and $^2P_{\frac{1}{2}}\,^2P_{\frac{1}{2}}$.[14] The results are, for the case of two equal atoms in the same ^2P state: $^2P_{1\frac{1}{2}}+^2P_{1\frac{1}{2}}$ gives 3_u, 2_g, 2_u, 1_u, 1_g, 1_u, 0_g^+, 0_u^-, 0_g, 0_u^-; $^2P_{1\frac{1}{2}}+^2P_{\frac{1}{2}}$ gives 2_g, 2_u, 1_g, 1_u, 1_g, 1_u, 0_g^+, 0_u^+, 0_g^-, 0_u^-; and $^2P_{\frac{1}{2}}+^2P_{\frac{1}{2}}$ gives 1_u, 0_g^+, 0_u^-.[15] The fact that only $^2P_{1\frac{1}{2}}+^2P_{\frac{1}{2}}$ is capable of giving a 0^+ state is in satisfying agreement with the experimental fact that the upper level of the halogen bands, here classified as 0_u^+, is actually derived from $^2P_{1\frac{1}{2}}+^2P_{\frac{1}{2}}$. The lower, 0_g^+, level is probably derived from $^2P_{1\frac{1}{2}}+^2P_{1\frac{1}{2}}$, although $^2P_{1\frac{1}{2}}+^2P_{\frac{1}{2}}$ or $^2P_{\frac{1}{2}}+^2P_{\frac{1}{2}}$ is not theoretically impossible, and also experimentally not yet absolutely excluded.

Some additional items of evidence having a bearing on the above interpretation of the halogen bands will now be mentioned. (1) The fact that the I_2 bands show a Faraday effect[16] may be cited as evidence in favor of a paramagnetic upper level. Now it can be shown that a case *c* molecular state with $\Omega=0$ and derived from a $^2P_{1\frac{1}{2}}$ plus a $^2P_{\frac{1}{2}}$ atom *should* be paramagnetic; and that in the passage to a case $a\,^3\Pi_0$ state, the paramagneticm must increase.[17] Of course, as Kemble has pointed out,[16] a magnetic moment might be developed by rotation, even in a $^1\Sigma$ state; and in a loosely bound molecular state such as we have here, a rather large moment might be developed in this way through uncoupling of the atomic J vectors from the electric axis. But it seems hardly likely that the small rotational energies involved in the case of the observed band lines are large enough to give rise to the magnetic effects observed. (2) The fact that the fluorescence of the I_2 bands is (in part) quenched by a magnetic field[18] is further evidence in favor of a paramagnetic upper level. (3) If the bands are $^3\Pi_0\leftarrow{}^1\Sigma$ one might expect their intensity to increase markedly in going from F_2 to I_2, since the intensity of intersystem combinations is extremely weak for the lightest atoms like He,

[14] The rules which govern this case, and some applications, will be discussed in a subsequent paper.

[15] The group of states here predicted corresponds, as of course it must if correct, in a one to one manner to the set of states predicted by the Wigner and Witmer method for cases *a* and *b*, and given at the beginning of this paper. E.g., 3_u from $^2P_{\frac{1}{2}}+^2P_{2\frac{1}{2}}$ corresponds to $\Omega=3$ of $^3\Delta_u$ at cose *a*.

[16] Cf. E. C. Kemble, Nat. Research Council Bulletin on Molecular Spectra, p. 347.

[17] To get a state with $\Omega=0$ from $^2P_{\frac{1}{2}}+^2P_{1\frac{1}{2}}$, we must assume the J of the $^2P_{1\frac{1}{2}}$ atom oriented with a projection $M=\pm1/2$ on the electric axis, the J of the $^2P_{\frac{1}{2}}$ atom with a projection $M=\mp1/2$. Since Landé's g factor is 4/3 for $^2P_{1\frac{1}{2}}$ and 2/3 for $^2P_{\frac{1}{2}}$, the total magnetic moment parallel to the electric axis if $(4/3\times1/2-2/3\times1/2)=1/3$ Bohr magneton. This holds for the limiting case of very loose coupling of the atoms. In a case $a\,^3\Pi_0$ state, we have a magnetic moment of ±2 magnetons parallel to the electric axis due to the spin ($S=1$, $\Sigma=-1$) and of ∓1 magnetons due to $\Lambda=1$, making a net result of 1 magneton parallel to the electric axis. (The magnetic moment component perpendicular to the electric axis also in some cases contributes to the paramagnetism.)

[18] W. S. Steubing, Ann. d. Physik **58**, 55 (1919).

and increases with the intensity of the coupling of L and S vectors. The fact that the upper level is case $c\,0^+$ rather than case $a^3\Pi_0$ should however probably diminish this effect since the molecular S loses its meaning in case c, but it might well still exist to a more or less marked extent, since it is likely that case a is more nearly approached in the lighter than in the heavier molecules. In the halogen bands in which we are interested, the spectrum consists of two parts, namely the bands proper (relatively weak), and the continuum (stronger). Since the continuum corresponds to transitions with r near r_e'', and since we probably have case a for $r=r_e''$, the upper level should function here as a true $^3\Pi_0$ level, and the strong variation of intensity with molecular weight which is to be expected for intersystem combinations should make itself evident here. Experimentally the intensity of the bands proper increases rather rapidly in the order F_2 to I_2, but this is at least partly explainable in terms of the $U'(r)$ and $U''(r)$ curves by means of the Franck idea as applied by Condon. So far as can be judged from available data,[19] the absorption in the continuum is however also much stronger for iodine than for chlorine, and this effect cannot be attributed to the nature of the $U(r)$ curves. This relation is therefore in harmony with our expectation. (4) If one assigns the electron configuration $1s\sigma^2 2p\sigma^2 2s\sigma^2 3p\sigma^2 2p\pi^4 3d\sigma^2 3d\pi^4$ to the $^1\Sigma_g^+$ normal state of F_2, and assumes that the excited state corresponds to $\ldots.3d\pi^3 4f\sigma$ one removes the only known exception[20] to the writer's λ conservation rule (formerly called "σ_l, conservation rule") for molecule formation (Of course the configurations given here have a physical meaning only, for small values of the distance between the nuclei.) The writer is, however now inclined to believe that this rule has not much significance. For Cl_2 the corresponding configurations are $\cdots 3s\sigma^2 4p\sigma^2 3p\pi^4 4d\sigma^2 4d\pi^4$ and $\cdots 4d\pi^3 5f\sigma$ and so on.

[19] Cf. International Critical Tables Vol. V, p. 269. The nature of the intensity relations can be judged by the following values of the absorption coefficient K in the equation $I=I_0e^{-Kl}$ (l = length of absorbing path in cm, in gas or vapor). For the maximum of the continuous absorption, K has the following values: Cl_2, $K\backsim 2$ for $p=760$ mm at 0°C; Br_2, $K\backsim 1.36$ for $p=66$ mm at 16°C; I_2, $K\backsim 0.21$ for $p=0.17$ mm (reduced to 0°C) and $K\backsim 0.77$ for $p=1.67$ mm (reduced to 0°C). If we assume the validity of Beer's law (but the data on I_2 show that it does not hold) we get for $p=1.67$ mm at 0°C, $K\backsim 0.013$ for Cl_2, $K\backsim 0.033$ for Br_2, $K\backsim 0.77$ for I_2.

[20] R. S. Mulliken, Phys. Rev. **32**, 772 (1928).

AN INTERPRETATION OF PRESSURE AND HIGH VELOCITY VAPOR JETS AT CATHODES OF VACUUM ARCS

By Karl T. Compton

Massachusetts Institute of Technology

(Received July 1, 1930)

Abstract

Tanberg's conclusion, that the evaporating vapor from the cathode of a copper vacuum arc escapes with a temperature of about 500,000°K, which is based upon measurements of the repulsive force against the cathode, is shown to be unnecessary. The observed pressures can reasonably be explained in terms of the "accommodation coefficient" of the incoming Cu ions. It is thus shown that the observed pressures are accounted for if the positive ions retain about 2 percent of their incident kinetic energy after neutralization at the cathode.

IN A recent article in this journal[1] Mr. R. Tanberg has described some very pretty experiments on arcs drawn from a copper cathode *in vacuo*, which prove that there is a pressure of approximately 0.015 gm per ampere against the cathode, and a pressure of similar order of magnitude against an insulated vane placed about 2 cm in front of the cathode. These pressures, which were corrected for several minor disturbing influences, indicate the existence of material ejected with high speed from the cathode, and the experiments showed that this material is uncharged. Since copper evaporated from the cathode during the experiments, Tanberg identified the jet of high speed material with this stream of evaporated copper. The measurements of the amount of evaporation and the magnitude of the pressure led him thus to the conclusion that this vapor jet has a velocity of the order of 16 $(10)^5$ cm/sec and hence that "the temperature existing at the cathode spot determined from the velocity of the cathode vapor is of the order of 500,000 °K" . . . . "far in excess of even the most extreme temperatures ever measured in connection with any physical phenomena of any duration!" In view of the importance of this conclusion, if true, in the interpretation of arc cathode phenomena, it is important critically to examine Mr. Tanberg's work and the possibility of some less startling interpretation of his experimental results.

There is one part of Mr. Tanberg's calculations which shows entire failure to comprehend the nature of the electrostatic forces exerted on a cathode by the intense field at its surface. These are attrative forces, tending to pull the cathode toward the discharge, and Mr. Tanberg adds an estimated force of this type to the observed repulsion, to obtain the "corrected" repulsive force due to the reaction of the escaping vapor stream. He fails to note, however, that this strong field at the cathode arises from the positive ion space charge near it, that the attraction is mutually between cathode and

[1] Tanberg, Phys. Rev. **35**, 1080 (1929).

ions, and that when the ions strike the cathode, they deliver momentum to it at a rate which exactly counterbalances the electrostatic pull which they exerted on it before impact. That this follows from the elementary relation $\int Fdt = \int mdv$ is obvious and has long been recognized in such problems.[2] Thus this electrostatic correction should not have been made. It happens, however, to be only a few percent of the observed force, so that correction of this error does not essentially alter the evidence for a high speed stream of neutral particles escaping from the arc cathode.

There is, however, a phenomenon occuring at cathodes which appears quite adequate to explain Mr. Tanberg's results without invoking any unusual temperature of cathode spot. It is the occurrence of an "accommodation coefficient" of positive ions, as recently reported to the American Physical Society by Dr. Van Voorhis and the writer.[3] Positive ions, on striking the cathode, become neutralized but do not, on the average, give up enough of their kinetic energy to reach thermal equilibrium with the cathode. They rebound as neutral atoms from the cathode with some fraction β of their incident kinetic energy.

Athough, as we have seen, the impact of a charged ion against the cathode contributes nothing to the pressure against it (on account of the counterbalancing pull during its attraction to the cathode), nevertheless if the neutralized ion leaves the cathode with any momentum there is imparted to the cathode an equal opposite momentum. The following calculations show that this type of momentum transfer seems easily adequate to account for the pressures observed by Mr. Tanberg.

Let f be the fraction of the total current which is carried by positive ions at the cathode, and let β be the fraction of the incident energy of the ion which is retained after neutralization. β is approximately equal to $1-\alpha$, where α is the accommodation coefficient. The arc drop in a copper arc of high current density carried in copper vapor has been shown by Nottingham[4] to be 20.5 volts. It appears certain that the fall space in such an arc is so thin that ions make few if any collisions while traversing it.

Taking data from one of Mr. Tanberg's typical experiments (test No. 353) we calculate the following data:

Positive ion current at cathode	$11f$ amps
Mass of Cu ions striking cathode per sec	$0.00724f$ gm
Number of Cu ions striking per sec	$7.0(10)^{19}f$
Kinetic energy of an incident ion	$3.26(10)^{-11}$erg
Total kinetic energy of ions striking per sec	$22.8(10)^{8}f$ erg
Total kinetic energy of neutralized ions leaving per sec	$22.8(10)^{8}f\beta$ erg
Total momentum of neutralized ions leaving per sec, which is equal to the pressure on the cathode	$5.86f(\beta)^{\frac{1}{2}}$ gm
If neutralized ions escape in random directions, as is likely, the resultant pressure is	$2.93f(\beta)^{\frac{1}{2}}$ gm

[2] Duffield, Burnham and Davis, Proc. Roy. Soc. **97**, 326 (1920).

[3] Van Voorhis and Compton, Phys. Rev. **35**, 1438 (1930).

[4] Nottingham, J. Frank. Inst. **207**, 301 (1929).

We now equate this to the observed pressure (corrected for "electrodynamical" disturbances but not for electrostatic disturbances as explained above) and obtain

$$2.93f(\beta)^{1/2} = 193.2(10)^{-3}.$$

We must now decide what value to use for the fraction f of current carried by positive ions at the cathode. Knowledge of this quantity is still woefully uncertain, even in the case which has been most studied, the mercury arc,[5] but all indications point to a value not far from $f=0.5$. Theoretically we would like perhaps to see a smaller value, but it seems impossible to find a much smaller value experimentally, unless we strain the interpretation of results. Furthermore, the present copper arc is probably of essentially the same type as the mercury arc.[6] So we shall provisionally assume that $f=0.5$. Solving, then, for β we find

$$\beta = 0.0174; \quad \alpha = 0.9826.$$

Thus the pressures observed by Mr. Tanberg would be accounted for if less than 2% of the incident energy of the ions were retained after neutralization. If we had assumed a smaller value of f, β would have come out larger and α smaller. The accommodation coefficient of Cu ions has never been measured, but from analogy with other ions of about the same atomic weight we might easily expect Cu ions to possess an accommodation coefficient as small as 0.9. Hence these considerations appear to give ample leeway for a reasonable explanation of Mr. Tanberg's results.

A possible objection to this theory based on the fact that Cu ions should condense on the cathode on striking it is met by the fact that their energies correspond to temperatures far in excess of the boiling temperature of the metal.

In conclusion it may be pointed out that this criticism does not alter Mr. Tanberg's basic conclusion regarding a high speed neutral vapor stream. It merely suggests an electrical mechanism for the acquiring of these speeds instead of assuming a terrifically high temperature at the cathode.

An interesting test of this interpretation is now being made by repeating Mr. Tanberg's experiments with a non-volatizing cathode of tungsten in a rare argon atmosphere. Here there is no possibility of an evaporated vapor stream like that considered by Mr. Tanberg, but the pressure effect due to the accommodation coefficient of argon ions is calculable directly from the work of Van Voorhis and Compton, combined with collector measurements to give directly the actual positive ion current.

[5] Compton and Van Voorhis, Proc. Nat. Acad. Sc. **13**, 336 (1927).
[6] Compton, Paper read before A.I.E.E., Detroit, June 1927.

SECONDARY EMISSION FROM METALS BY IMPACT OF METASTABLE ATOMS AND POSITIVE IONS

By W. Uyterhoeven and M. C. Harrington
Palmer Physical Laboratory, Princeton University

(Received June 16, 1930)

Abstract

Experiments on the secondary electron emission from nickel electrodes due to bombardment of positive ions and metastable atoms in a neon discharge under conditions simulating those at the cathode in a glow discharge are described. Measurements with a collector movable in a direction perpendicular to a fixed plane collector give approximate values of the proportion γ of the apparent positive ion current which is actually carried by secondary electrons. Values of 15-50 percent are found depending on the experimental conditions and degree of purity of gas. A perforated plate behind which is situated a Faraday box is used to separate the effects of the ions and metastable atoms. A preponderant part of the emission is ascribable to the metastable atoms, but values of the number α of free electrons per positive ion, are found to be 14 to 20 percent, varying approximately linearly for ions of velocities of 75 to 150 volts. The secondary electrons originate at the surface of the collector with about 12.5 volts maximum initial velocity.

IN ALL theories of the cathode fall in the glow discharge there has been assumed a source of electrons at the surface of the cathode or in the immediate neighborhood of it. Generally it is supposed that these electrons are liberated from the metal by the impact of positive ions. Although the existence of this phenomenon has been established by several experimenters, direct experimental evidence under conditions simulating those at the cathode is not very extensive. Most of the determinations of the secondary emission due to ion impact have been made with ions from a Kunsman source, and have proved that the effect was rather small.[1,2] This is what one would expect if the secondary emission depended on the potential energy of the ion. A necessary condition for secondary emission would then be that the ionization potential of the gas atom $V_i \geqq 2\phi$, where ϕ is Richardson's work function.[3] In accordance with this view Penning[4,5] found for Ne ions impinging on different metals, efficiencies which were appreciably larger than those which had been found for alkali ions, and a linear variation of the number α of secondaries per incoming ion with the energy of the latter. All observers point out that α depends markedly on the surface condition of the metal and, since practically all the measurements have been done in a rather high vacuum, it might well be that under the actual conditions

[1] Jackson, Phys. Rev. **30**, 473 (1927).
[2] Oliphant, Proc. Camb. Phil. Soc. **24**, 451 (1928).
[3] Holst and Oosterhuis, Physica **4**, 375 (1924).
[4] Penning, Proc. Amsterdam Ac. **31**, 14 (1927).
[5] Penning, Physica **8**, 13 (1928).

of the cathode fall α is very much larger. The present work[6,7] is an attempt to determine α under conditions as similar as possible to those at the cathode of a glow discharge, where adsorbed atoms and ions may appreciably change the properties of the metal surface.

A few years ago one of the writers,[8] using a plane Langmuir collector in the positive column of the glow discharge, obtained current-voltage characteristics differing from those obtained by Langmuir and Mott-Smith in the mercury arc.[9] Comparison of the measured ion current density i_m to a negatively charged collector with the value i_c, calculated from the usual space charge equation, showed differences amounting to 40–50 percent of i_m, i_m being larger than i_c. The simplest interpretation of these results was the assumption of a secondary emission from the metal up to 40–50 percent of i_m. This, however, led to a value for α of the order of magnitude 1, and it was therefore suggested that possibly metastable atoms diffusing out of the discharge contributed to the electron emission when striking the metal plate.[10,11] This estimate of i_c was based on the assumptions underlying the derivation of the space charge equation, the most important being in this case the absence of ionization in the sheath. This introduced some uncertainty in the interpretation referred to above. Therefore different methods were devised to determine the secondary electron part in the apparent positive ion current i_m to a negatively charged electrode.

Apparatus

Since the electrodes are continuously bombarded by positive ions of high velocity, they sputter rapidly; accordingly a set of nickel electrodes (Fig. 1) was constructed which could easily be adjusted in the different tubes used in the experimental work. The discharge was of the hot cathode type to permit a wide variation of the current density. The cathode was an oxide coated nickel cylinder, (heated by a tungsten filament inside), the anode a large nickel plate or cylinder. The main collecting electrode P was a circular nickel disk (diameter 18.2 mm) with a coplanar concentric guard ring (outer diameter 29.2 mm). The latter was supported by the cylinder L, which shielded the space within it from the discharge; the cylinder L was in turn protected on its vertical side by a glass cylinder to avoid the collecting of too large positive ion currents and subsequent distortion of the potential distribution in the main discharge. The central plate P was supported by the cylinder M, which shielded the box B from uncharged particles diffusing through the slit S between the guard ring G and the plate P. The box B supported by the nickel rod R was cylindrical in shape, closed at the top and bottom. At the center of the upper cover was a circular hole (diameter 2 mm), which was immediately under a 0.74 mm hole at the center of the plate P.

[6] Uyterhoeven and Harrington, Science **70**, 586 (1929).
[7] Uyterhoeven and Harrington, Phys. Rev. **35**, 438 (1930).
[8] Uyterhoeven, Phys. Rev. **31**, 913 (1928); Proc. Nat. Acad. Sci. **15**, 32 (1929).
[9] I. Langmuir and Mott-Smith, G. E. Rev. **27**, 449 (1924).
[10] Webb, Phys. Rev. **24**, 113 (1924).
[11] Oliphant, Proc. Roy. Soc. **A124**, 228 (1929).

The movable cylindrical collector C was also made of nickel. The collector used in the first type of tube (i.e. cylindrical tube, which we will designate by no. 1) was somewhat simpler in construction than that used in the later type of tube (no. 2) (See Fig. 1). Cylinder no. 1 (length 10.8 mm, diameter 7.3 mm) was divided into quarters by vertical nickel partitions. The lower end was covered with fine nickel gauze, the upper end closed by a piece of solid nickel, the inner side of which was cone-shaped to reduce electron reflection to a minimum. A glass cap fitting the cylinder left only the gauze-covered end exposed to the discharge. In the course of the work, this glass cap as well as the glass tubing protecting the leading-in wire for the cylinder became coated with sputtered metal. To eliminate as far as possible

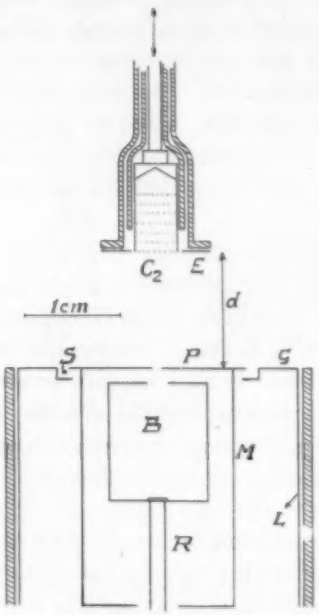

Fig. 1. Detail of collecting electrodes.

the resulting troubles the movable cylinder C_2 (diameter 4.8 mm) was fitted with a concentric guard ring E in the plane of the gauze-covered end (outer and inner diameter 11.0 and 5.4 mm respectively). Only the lower end of the guard-ring collected current, the back being protected by the glass cap enclosing the cylinder. The collector C was movable along its axis, i.e., perpendicular to the plane of the plate P, opposite to which it was placed.

The metal used in the construction of the electrodes was outgassed, before being used, by heating in vacuo to a red heat by high frequency induction currents.

Two types of tubes were used: first a cylindrical one (inner diameter 6 cm) with a bulbular enlargement at the cathode end and later a spherical one (diameter 15 cm). In the first the collectors were in the positive column and in the second in a uniform luminosity which filled the whole sphere.

During the measurements the neon gas was constantly circulating and passed through a misch-metal arc, while liquid air traps were used to avoid contamination of the neon by traces of mercury. The usual experimental technique in work of this kind was strictly followed (baking out of the tubes at high temperature while being evacuated, etc.).

Experimental Methods and Results

Different methods can be applied for the measurement of the secondary emission. One, which was already referred to above, is to measure the apparent positive ion current to a negatively charged plane collector i_m, and simultaneously the thickness x of the dark space charge sheath. With the space charge equation the value of the positive ion current i_c corresponding to the potential difference between collector and space, and the thickness x may be calculated. If all the assumptions underlying the derivation of the space charge equation are satisfied, the difference $(i_m - i_c)$ gives a measure of the secondary electron emission. Due to a number of uncertain factors the values thus obtained in the earlier work were considered as provisional; the direct measurements here recorded check the order of magnitude of these earlier estimates.

First Method. Suppose the cylinder C is placed at a certain distance d from the plate and opposite to it. When C is made negative with respect to the surrounding gas, e.g., $V_c = -125v$, it will collect a certain positive ion current. The plate, originally floating, is now also made more and more negative with respect to the gas. If any secondary electrons are emitted from the plate, they will be accelerated by the electric field in the space charge layer and, after acquiring an energy corresponding to the potential of the plate with respect to the gas (potential drop in the sheath), increase the ionization in the space between the two collectors. So long as the plate is less negative than the cylinder, the electrons will not be able to run against the retarding potential in the sheath covering the cylinder. In this stage the ion current to the cylinder is slightly increasing (see Fig. 2, curve I, A to B), due to the additional ionization by the secondary electrons from the plate. When the plate potential V_P reaches V_C, there is a sudden decrease in the current i_C due to the incoming electrons, and this decrease is a measure of the secondary electrons leaving the plate P. The two principal factors to be considered in a quantitative analysis of these results, are the loss of energy of the electrons on their way from the plate to the cylinder and the decrease in intensity of the electron beam due to scattering.

Let us suppose for simplicity that the space potential in the discharge opposite to the plate is the same as the space potential in front of the cylinder. The difference in potential will actually be not more than a couple of volts, according to the theory of Tonks and Langmuir.[12] This simplification enables us to use the potentials of the cylinder and plate as measured with respect to the anode, since only the differences between V_C and V_P must be considered for the moment. If we use the extrapolated line AB (Fig. 2) as reference line,

[12] Tonks and Langmuir, Phys. Rev. **34**, 876 (1929).

the difference between its ordinate for a given value of $(V_P)_a$ and the corresponding ordinate of curve I gives the electron current collected at the cylinder. The curve I, read with respect to AB, is an integral curve, i.e., the difference for $(V_P)_a = -135v$, for instance, represents the number of electrons which on reaching the outer edge had an energy component normal to the bottom plane of the cylinder equal to or larger than $125v$. Since the potential of the plate is $(V_P)_a = -135v$, electrons are collected which have lost at most a forward component of momentum corresponding to an energy of 10 volts. Plotting the slope of the curve I, as read with respect to AB, we get a distribution curve (II, Fig. 2) of the electrons reaching the cylinder for the velocity component normal to the bottom plane of the cylinder.

Since the reception of electrons is confined to such a narrow region, say from $(V_P)_a = -112$ to about -160 in the case plotted (Fig. 2), we conclude that the electrons for this type of discharge arise at the plate P or very near

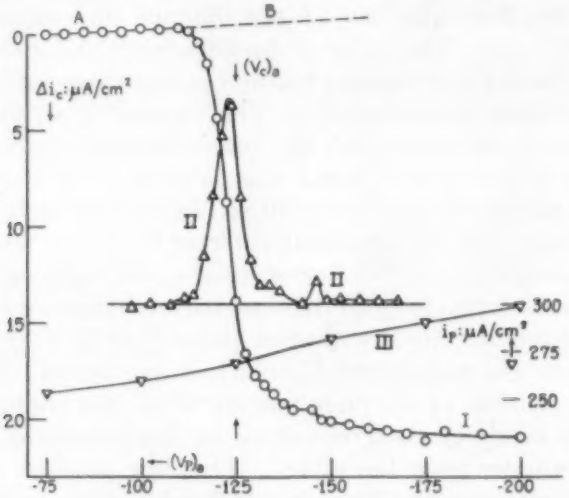

Fig. 2. Curve I.—Current to cylinder C as a function of the potential of the plate $(V_P)_a$ with respect to the anode. Cylinder potential $(V_C)_a = -125v$.

Curve II. Distribution curve for velocities of electrons (Component normal to plane of the end of C).

Curve III. Current to the plate i_P.

to it, for if appreciable numbers originated at other points of the sheath on P, the decrease in the curve would be much more gradual and extend farther to the right on the plot.

(Some objection may be raised against the use of the extrapolated line AB as zero line for the electron current reaching the cylinder. When the latter is absorbing part of the secondary electrons coming from the plate, ($(V_P)_a$ more negative than $(V_C)_a$), the ionization produced by these in the space between plate and cylinder must be less than when the cylinder is reflecting the largest part ($(V_P)_a$ less negative than $(V_C)_a$). When the pressure in the tube is made rather low ($p = 1 \times 10^{-2}$ mm or less) the slope of AB becomes

very small and the difference between the ordinate of AB and the curve rather large, so that this possible error must be small. In fact for pressures lower than 10^{-2} mm, the line AB is practically horizontal.)

Studying the velocity distribution curve II of Fig. 2 somewhat more closely, we notice first that the electrons start coming in when the retarding potential between cylinder and plate is about $-12.5v$. If the secondary emission is due to metastable neon atoms striking the plate, one must assume according to Oliphant[11] that the excess energy is transferred to the electron. Since the energy of a metastable neon atom ($2p^5 \cdot 4s$) is about 16.5 v, taking for the work function of nickel $\phi_- = 4.4v$, we have for the maximum energy of the electron at the moment it leaves the plate $16.5 - 4.4 = 12.1$. If the secondary emission is due to positive ions, the maximum energy which the electron could carry away when leaving the plate would be $(V_i - 2\phi_-) = 21.5 - 8.8 = 12.7v$, where $V_i = 21.5v$ is the ionization potential for neon. Here $2\phi_-$ must be subtracted because the potential energy of the ion is used to liberate two electrons: one for neutralization of the ion and the secondary electron emitted from the plate. The value of the work function for nickel under the present conditions is not accurately known because the influence of adsorbed gas layers may change this appreciably. Van Voorhis[13] found for molybdenum in a neon discharge $\phi_- = 3.68$, but the determination was made above the space potential so that the collector was receiving only electrons. In the present work it was found that the condition of the metal surface, when this is collecting electrons, may be somewhat different from that when bombarded with ions. The accuracy of this first method is not sufficient to decide between the two possible processes for the liberation of electrons mentioned above.

The form of the velocity distribution curve II (Fig. 2) does not change appreciably when the experimental conditions are varied. It seems to be practically independent of the plate voltage when this changes from $-75v$ to $-300v$. The maximum is rather sharp for low pressures and small distances of the cylinder from the plate. When the pressure is higher ($p = 5 \times 10^{-2}$mm and more) or the distance d rather large the peak becomes less sharp; this is probably due to the impact suffered by the electrons on their path from plate to cylinder. At the same time the foot of the curve extends farther to the right, while a break appears in curve I (Fig. 2) at $(V_P)_a = (V_C)_a - 20$, (in the case of Fig. 2 at $(V_P)_a = -145v$). As may be seen from curve II of Fig. 2, which is a typical velocity distribution curve, there is no sharp maximum or minimum velocity as found by Oliphant[11] in his work on secondary emission by metastable He atoms. This may be partly due to a difference in the surface condition of the metal emitting the secondary electrons, but probably is mainly caused by scattering on their way from plate to cylinder. The maximum in the distribution curve corresponds always to a plate potential $(V_P)_a$ a couple of volts less negative than the potential of the cylinder. If the average velocity of the secondary electrons leaving the plate is a couple of volts, the velocity distribution curve will be of the form represented in Fig. 2.

[13] Van Voorhis, recent unpublished work.

For a rational choice of the difference between the reference line AB and curve I of Fig. 2, representative of the secondary electron current collected by the cylinder, we must remember that, for a given value of the plate potential $(V_P)_a$, only those electrons reach the cylinder whose velocity normal to the space charge sheath corresponds to an energy equal to $(V_C)_a$. The loss of forward momentum of the part electrons coming from the plate is due to two effects: elastic scattering with change of direction of motion and inelastic impacts (excitation and ionization) with or without change in direction. The break in curve I (Fig. 2) referred to above may be due to excitation of neon, since the loss of energy corresponds roughly to 18 v.

To know the electron component of the plate current, i_P, we must extrapolate back the recorded electron currents, Δi_C. This requires a knowledge of the electron mean free path λ_- for the different velocities corresponding

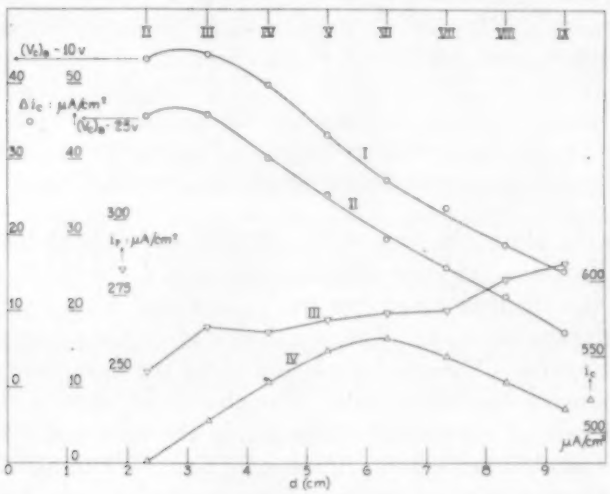

Fig. 3. Plate potential $(V_P)_a = -125$ v. $I = 450$ ma. $V = 59$ v. Pressure 8.8 to 9.2×10^{-3} Hg. Curve I: Δi_C for $(V_C)_a - 10$ v. *vs. d*. Curve II: Δi_C for $(V_C)_a - 25$ v. *vs. d*. Curve III: i_P in each case. Curve IV: i_C *vs. d*.

to $(V_P)_a$. As a first approximation we may take the gas-kinetic value for λ_- which for neon is 0.0737 cm at 1 mm pressure. Since the collecting cylinder C could be moved with respect to the plate, a direct determination of the electron mean free path would seem possible. The cylinder potential $(V_C)_a$ was given a definite value -125 and the variation of Δi_C with distance d studied, all other conditions being kept constant as well as possible. The two upper curves in Fig. 3 give Δi_C for $(V_P)_a = (V_C)_a - 10$ (curve I) and $(V_P)_a = (V_C)_a - 25$ (curve II), both plotted at the same scale but shifted the one with respect to the other to avoid confusion. The curves do not show an exponential decrease as would correspond to the simple formula $N_d = N_0 \epsilon^{-d/\lambda}$. The maximum in the Δi_C curve between positions II and III of the cylinder is due to the disturbing effect of the latter when it comes too near to the plate. As will be shown later, the secondary emission from the plate is due partly

to ion impact and partly to impact of metastable atoms. The latter are constantly diffusing from the center of the tube towards the wall and the presence of the cylinder in front of the plate probably disturbs the concentration gradients and decreases the number of metastable atoms striking the plate in unit time. To a certain extent this must also be true for the positive ion currents, but to a much smaller degree because of the correcting effect of space charges. The part of the curves to the right of position IV can be used for the calculation of the electronic mean free path. Table I gives the results of these computations. The first row gives the distance d of the

TABLE I.

Position	III	IV	V	VI	VII	VIII	IX
d	3.33	4.34	5.35	6.36	7.35	8.33	9.33
Δi_C	43.8	39.85	34.2	27.25	23.55	17.1	15.16
λ_-	10.6	6.5	5.7	6.8	4.3	4.7	
$p(10^{-3})$	8.8	8.7	8.9	9.2	9.2	9.2	9.5
λ_{gk}	8.9	9.0	8.8	8.6	8.6	8.6	8.3
i_P^-	63.7	64.4	62.6	57.2	55.6	45.2	46.8
i_P	259.5	257.	261.	263.5	269.	274.5	281.
γ	25	25	24	22	21	17	17

$(V_c)_a = -125v$. d in cm. λ in cm. Currents in $\mu A/cm^2$. p in mm of Hg.

cylinder from the plate, the second the electron currents at the cylinder (in $\mu A/cm^2$) for $(V_P)_a = -135$ v for different values of d. In the third are shown the values of the electron mean free path calculated from electron currents Δi_C for two adjacent positions. The fourth row gives the pressure in the tube for the different runs. (The small variation of the pressure shown in the table is due to the construction of the tube. The change in position of the cylinder influenced the rate of circulation of the gas in the tube and a readjustment of the pressure would have taken a rather long time. We thought it preferable to make all the runs in rapid succession to avoid a change in the discharge conditions, especially the purity of the gas.) The fifth line gives the gas-kinetic values for the electron mean free path corresponding to the pressures given in the fourth row. Most of our data have been taken with the cylinder in position IV, but much also in positions III and V. The sixth row of Table I gives the values of i_P^- calculated from those of Δi_C (second row) using the gas-kinetic mean free path for electrons (fifth row). The next row gives the total current to the plate $i_P(\mu A/cm^2)$. On the last line are given the ratios of i_P^- to i_P (electron current to the total current) in percent of i_P called γ. In calculating values of i_P^- from the observed values of Δi_C, the gas kinetic values of λ_- were used in the exponential formula. Had the empirical values of row 3 been used, the values of i_P^- and hence of γ would have been still larger, except for positions III and IV in which there is the following geometrical complication. In the calculation of i_P^- from Δi_C the geometric arrangement of the apparatus must be taken into account. Part of the electrons colliding between plate and cylinder are scattered at small angles from their original direction and will still be collected. This effect will slow

down the decrease of the beam for positions of the cylinder near the plate. This may partly account for the large value of the electron mean free path obtained from the readings at positions III and IV.

The values for γ obtained from the different positions of the cylinder decrease when the distance d of cylinder to plate increases; this shows that the actual decrease of the electron current with distance is larger than would correspond to the exponential law $N=N_0\exp(-x/\lambda)$ where λ is the gas kinetic value. Using the independent measurements obtained with the Faraday box (third method), it was found (under discharge conditions practically the same as in the case under consideration) that when the theoretical value for the electron mean free path is used in conjunction with the data obtained for Δi_C, at position IV, the value of i_P^- may be calculated quite accurately and consequently also that of γ. This would give in the present case a secondary emission of 24 percent. Even if we did not take into account the decrease of the secondary electron beam on its path from plate to cylinder, we would find, using the data of Table I, $\gamma=17$ percent for position III and $\gamma=16$ percent for position IV.

The values of γ obtained by the method outlined above vary within rather wide limits (15 to 50) according to the pressure and the degree of purity of the gas. In the runs which gave the data presented in Table I the neon contained slight traces of some impurity. The method under discussion does not permit a separation of the two effects which give rise to the secondary emission: impact of positive ions and impact of metastable atoms. The latter depending on the concentration of the metastable atoms in the discharge is likely to change considerably with the degree of purity of the gas. Table II gives some further illustrations. The values for γ at a given

TABLE II.

I	V	p	$(V_C)_a$	Δi_C	i_P^-	i_P	γ
433	68.7	8.5×10^{-3}	−75	35.5	56.8	215	26
433	67.8	8.6	−100	41.6	66.8	235.5	28
432	67.5	8.5	−125	44.8	71.6	258.8	28
432	69.	8.0	−150	43.7	67.9	271.5	25
430	70.	7.8	−175	45.2	69.4	274.5	25
430	70.	8.0	−200	45.7	70.9	287.	25
430	70.5	8.0	−225	48.7	75.6	302.5	25
500	43.2	1.9×10^{-2}	−100	46.3	103.5	268	38
500	43.	1.9	−150	46.9	104.8	279	38
500	42.5	1.9	−200	48.1	107.5	300	36
504	42.3	1.9	−250	48.9	109.3	321	34
507	42.4	1.9	−300	46.5	103.7	340	31

For first seven $d=4.34$ cm, for last five $d=3.33$ cm. I = total current through tube in m.a. V = drop across tube in volts. p = pressure in mm of Hg. Currents in cols. 5, 6, 7 in $\mu A/cm.^2$

pressure could be reproduced very well, but it was always found that higher pressures give larger values for γ (for a pressure variation from 5×10^{-2} mm to 8×10^{-3} mm). This variation of γ is principally due to the dependence of the concentration of metastable atoms on the pressure in the discharge tube.

We also tried to find the variation of γ with the plate potential $(V_P)_a$, the accelerating potential for the positive ions. As may be seen no appreciable variation was found. It is well known that the number α of electrons liberated per positive ion increases with the velocity of the ions. But in our case the emission i_P^- which gives γ is made up of two parts: electrons due to ions and electrons due to metastable atoms. Only the first part would vary with the plate potential and this part only contributes to α, so that the variation of i_P^- with $(V_P)_a$ is smaller according to the degree of preponderance of metastable atoms over ions as emitting agents.

We have for the present no definite interpretation for the decrease of γ with increasing $(V_P)_a$, which is especially marked in the lower set of Table II, where γ varies from 38 to 31 percent for $(V_P)_a$ varying from -100 to $-300\,v$. One possibility is that the ions in falling through the sheath destroy a certain number of the metastables on their way to the plate; the larger $(V_P)_a$, the thicker the space charge sheath becomes, and, consequently, the loss of metastables due to positive ion impact also increases. Another effect of the ion impacts in the sheath could be the production of new metastable atoms by impact between fast ions and normal atoms, with a maximum for this process in the neighborhood of the normal cathode fall in neon which is around $100\,v$. Another possible, though improbable explanation is destruction of metastable atoms by absorbed light (red) or by impurities while traversing the sheath.

An interesting conclusion can be drawn from the data presented in Table II. In the noble gases the volt-ampere characteristic of a negatively charged plane collector (with guard ring) does not present a saturation character[8] as in the case of mercury vapor.[9] This may be attributed in part to the increase in ionizing power of the secondary electrons caused by the increase in the accelerating potential acting on them as the plate potential is made more and more negative. In the lower set of data in Table II this increased ionization is shown by the fact that i_P^- remains almost constant while i_P increases with the change in plate potential from -100 to $-300\,v$. A more general case occurs in the upper set of data of Table II, where both i_P^- and i_P increase with increasing negative plate potential, indicating both increased ionization and increased secondary emission.

Second Method. The second method involves the use of the same electrodes as does the first method. In this the plate voltage $(V_P)_a$ is kept constant while the voltage of the movable cylinder $(V_C)_a$ is varied. The positive ion current collected by the cylinder therefore changes, decreasing with decreasing negative voltage, (right to left on Fig. 3). As the voltage of the cylinder becomes more positive and goes through the fixed voltage of the plate at point C, the cylinder current, i_C, shows an additional decrease (curve I, Fig. 4, B to C) due to the reception from the plate of secondary electrons which have previously been turned back. In the run to which Fig. 4 refers, the plate voltage $(V_P)_a$ was $-100\,v$ with respect to the anode, and the cylinder voltage $(V_C)_a$ was changed from -125 to -90. The part AB of curve I, where no electrons are received, is extended in the dotted line BB' which indicates the value of the positive ion current collected by the cylinder.

(Since only the variations in the current are plotted, an arbitrary zero point is selected for convenience at E). The differences, e, between the measured current and the extrapolated positive ion current are plotted as a function of the cylinder voltage in curve II, which has the same general shape as curve I of Fig. 2. This curve is reversed right for left as compared with that of the first method since the potential changes are made in an opposite manner.

As in the first method it is seen that the electrons may have as much as 12.5 volts initial energy since they are received even when the cylinder is 12.5 volts more negative than the plate. The method of obtaining the reference line ABB' of curve I precludes the possibility of discerning a gradual rise in FG of curve II corresponding to that found in some cases in the curves of the first method, e.g., AB of curve I of Fig. 2. Otherwise, however, the remarks made in connection with the first method apply here. The value of

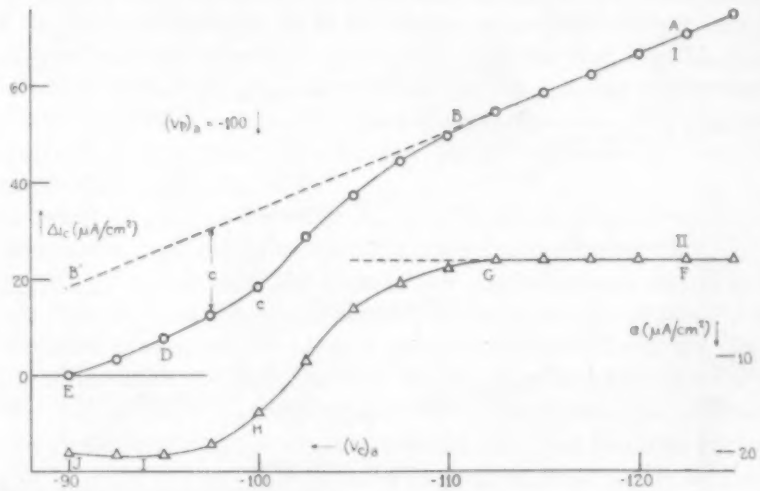

Fig. 4. Curve I. Change in i_c in $\mu A/cm^2$ *vs.* $(V_c)_a$. Curve II. Difference e *vs.* $(V_c)_a$.

the initial secondary electron current i_P^- may be calculated by using the gas-kinetic mean free path. In the case illustrated, γ was 33 percent of the measured plate current.

The results of this method corroborate those of the first method, but, since the first method permitted the use of a more sensitive galvanometer, most of the runs were made with the first method. Table III gives some illustrative material.

TABLE III.

p	λ_{gk}	$(V_P)_a$	i_P	Δi_C	i_P^-	γ
2.4×10^{-2}	3.3	−80	219	18	67	31
2.4	3.3	−100	232	20	76	33
2.8	2.8	−150	237	16	73	31
3.5	2.3	−80	204	9	64	31

p = pressure in mm of Hg. λ_{gk} = gas kinetic mean free path in cm. $(V_P)_a$ in volts. i_P, Δi_C, i_P^- in $\mu A/cm^2$. $\gamma = 100\, i_P^-/i_P$.

Third Method. The first two methods are somewhat unsatisfactory, for in order to obtain quantitative data on the secondary emission some exponential decrease of the electron beam as it goes from the plate to the movable collector must be used. Since the appropriate value of the mean free path is not exactly known, there is some uncertainty in the results. Obviously, however, those methods give a lower limit to the secondary emission. The method now about to be described gives more definite information, which is free from the defect mentioned.

The movable cylinder C is not used and is drawn up out of the discharge. The plate (Fig. 1) has a hole at its center, behind which is the hole in the Faraday box B. The shield cylinder M attached to the plate P protects the box B from particles which may come through the annular slit S between the

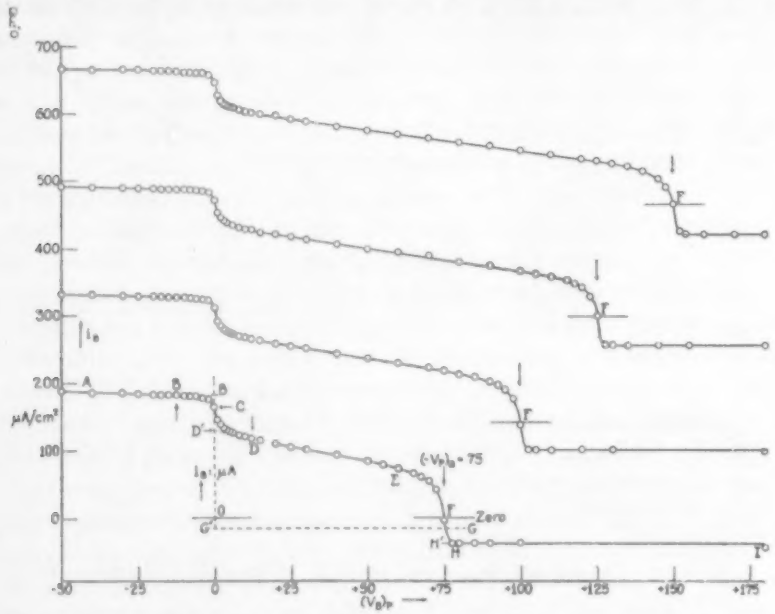

Fig. 5. Box current i_B vs. $(V_B)_P$ for plate potentials $(V_P)_a = -75$, -100, -125 and -150.

plate and its guard-ring G. The reason for this will be discussed later. The plate P is given some definite potential $(V_P)_a$, measured with respect to the anode, and the box B is made positive or negative with respect to the plate. The total currents to the box and to the plate are measured. Suppose, for example, that the plate is made negative, say -75 volts, so that there is a positive ion current to it. Some of the ions accelerated in the sheath will go through the hole in the plate and into the box B beneath when the potential between the box and the plate $(V_B)_P$ permits them. Fig. 5 gives plots of the box currents i_B against the box potential measured with respect to the plate $(V_B)_P$, for plate potentials of $(V_P)_a = -75$, -100, -125, and -150 volts. The curves are plotted on the same scale, but the zero points indicated by the short horizontal lines at the points O and F are displaced to avoid superposition.

The behavior of the current is much more complicated than one would anticipate under the assumption that the secondary currents are due to positive ions alone. One would expect, for instance, that as the retarding voltage of the box increases, the box current would be constant up to the potential of the space from which the ions have come, at which it would fall sharply to zero and remain so for increasing retarding potentials. A comparison of the magnitude of this current per unit area of the hole with the measured current per unit area of the plate would then give the proportion of the plate current carried by the positive ions alone, assuming that secondary electrons ejected by the ions inside the box B would have a very small chance of escaping from it. The curves of Fig. 5 indicate that a more detailed study is necessary. The break in the current at point F occurs at a retarding box voltage $(V_B)_P$ equal to that of the negative plate voltage $(V_P)_a$, indicating that most of the ions come from a space whose potential is nearly that of the anode. The final value of the current received on B for higher retarding voltages is not zero but a constant negative quantity (points H to I of the plot, Fig. 5). Furthermore the curve $ABCD$ shows a diminution in the current when the box is brought from a negative potential with respect to the plate to a positive one. The magnitude of this diminution for any set of experimental conditions is independent of the potential of P.

In one set of electrodes the inner shield cylinder M (Fig. 1) was omitted, and in this case the action of metastable atoms could be particularly easily demonstrated. Assume that the ions which come through the hole in the plate P go directly into the box B whenever the potential is favorable, and that metastable atoms, on the other hand, are diffusing from the discharge in a random direction through the hole in the plate and the annular slit S. When the inner shield cylinder M was absent, the metastable atoms which came through the hole and the slit S struck the box B on its outer surface and also the under side of the plate and guard ring, and the inside of the outer shield cylinder L. When the potential of the box $(V_B)_P$ was made more and more positive with respect to the plate, any electrons liberated by the action of the metastable atoms on the inner side of the plate or outer shield cylinder L came to B. This current was considerably greater than the positive ion current coming through the hole to the box, since the measured current was negative. A reversed field gave a large current in the opposite direction. Furthermore, it was found that a field across the slit had no effect on these currents between the box B and the outer cylinder L, which again indicates that they are caused by the neutral metastable atoms. To test this the inner shield cylinder M was introduced and fastened to the under side of the plate P so that the space within was shielded from whatever particles might come through the slit S. This is the case for which the curves of Fig. 5 are plotted. Now the relatively large currents above mentioned are practically absent. The current now does not become negative until after the positive ions are repelled at the point F of the curve. The only opening through which the metastable atoms can come is the hole through which the positive ions also come. Part of the former having, as we assume, a random direction, go into

the opening in the box B where electrons ejected will have a very small chance of escaping. A certain proportion, p, of the metastable atoms hit either the outside of the box B, or the inner surfaces of the plate P or the cylinder M, from which the electrons liberated are drawn to the box B to be measured as an incoming negative current. An additional complicating effect caused by the ions repelled at the point F will be discussed later.

A similar argument explains the change in the current at the points BCD of the curve (Fig. 5) where $(V_B)_P$ passes through zero. When $(V_B)_P$ is negative, electrons liberated from the box by metastable atoms striking it on its outer surfaces are drawn from it to the surrounding shield cylinder M and plate P, since the latter are more positive. This appears in the galvanometer as an incoming positive current along with the true positive ion current i^+. This current i_1^- is stopped when the potential difference $(V_B)_P$ is sufficiently positive to counteract the initial velocities of the electrons, say 12.5 volts, corresponding to the value found by methods one and two. The difference in ordinate CD', therefore, gives a measure of i_1^-. On the other hand, when $(V_B)_P$ is positive, a secondary current i_2^- in the reverse direction flows, caused by the reception at B of electrons liberated on the inner sides of P and M by the action of the metastable atoms which strike them. The measured positive current i_B is then smaller than i^+ since the reception of electrons is equivalent in the galvanometer to a failure to receive positive ions. If, however, $(V_B)_P$ is decreased through zero, this current is stopped by 12.5 volts corresponding again to the initial energies of the electrons. The difference in ordinate CB' is therefore a measure of i_2^-.

Thus the electrodes shown in Fig. 1 enable us to estimate separately the magnitudes of the secondary emission due to metastable atoms and to positive ions. If we assume, as seems necessary, that the efficiency of production of electrons by metastable atoms is the same at all of the surfaces concerned, then the sum of i_1^- and i_2^-, or $B'D$ on the graph, represents the effect of the proportion p of the metastable atoms coming through the hole. Assuming, however, that each unit area of the plate P is struck by as many metastable atoms as come through the hole per unit area, a value of the secondary electron current liberated from the surface of P by the metastable atoms can be obtained as shown in the following paragraph. The remainder of the secondary emission from the plate is then ascribable to the effect of the ions, thus giving a measure for α, the percentage yield of free secondary electrons for positive ions.

The measured current to the plate i_P, must now be separated into its component parts, that due to the true positive ion current i^+ and that to the secondary emission i^-. Assume that the line ED extrapolated to D' gives the correct value for the positive ion current due to positive ions of the voltage of the plate with respect to the space outside. (The slope of ED is probably due to the distortion of the field at the hole as the potential of the box is changed.) The ordinate OD', however, must be increased by the amount of the secondary current i_2^- flowing from M and P to B when $(V_B)_P$ is positive. ($B'C$ on the curve.) This lowers the zero line to G' where $OG' = B'C$, giving

i^+ as $D'G'$. The zero line through G' when extended to the right intersects the curve at G and does not coincide with HI, as might be expected from the explanation previously given. That, however, was obviously incomplete since it neglected the effect of the positive ions repelled from the box when $(V_B)_P$ was more positive than $(V_P)_A$ was negative. Presumably these either go back through the hole or strike the plate on its under side, where secondary electrons are liberated and drawn to the outside of the box, giving the current i_3^- (GH' on the curve). The ratio of this current to the positive ion current gives a value for α (Table IV, column 5) independent of the effect of the metastable atoms. This enables us to calculate the proportion, p, of the number of metastable atoms which do not enter the opening of the box B (equal to 74 percent with the electrodes used). This value is of the order of that to be expected from the geometry of the hole and box. $B'D$ of the graph is then divided by p to obtain the equivalent effect i_m^- of the total number of metastable atoms which come through the hole in the plate. (Table IV). The measured plate current i_P is diminished by i^+ to obtain i^-, the total secondary emission. γ is the ratio of 100 i^- to i_P. The part i_i^-, of the emission due to positive ions is the difference between i^- and i_m^-. A second value of α can then be calculated by dividing 100 i_i^- by i^+. (Table IV, column 10).

TABLE IV.

$(V_P)_A$	i_P	i^+	i_3^-	α	i^-	γ	i_m^-	i_i^-	α
−75	240	146	21	14	94	39	74	20	14
−100	248	150	24	16	98	40	74	24	16
−125	253	153	26	17	100	40	74	26	17
−150	260	154	30	20	106	41	74	32	20

$p = 2.0 \times 10^{-2}$ mm of Hg. Currents are reduced to $\mu A/cm^2$.

Assuming that the decrease of α with decreasing ion velocity is linear, the value of α_0 for ions of zero velocity is about 7 percent as given by the runs of Table IV.

The values of α are somewhat uncertain since the results depend on a very small variation in the deflection of a sensitive galvanometer. The consistency of the data is indicated by a comparison of columns 5 and 10 of Table IV and by four other runs at $(V_P)_a = -125$ volts for instance, which gave respectively $\alpha =$ 18, 17, 18 and 17. The last of these was taken with about twice as much total current through the discharge, so that i^+ and i_i^- increased in about the same proportion. The values of γ obtained by this method check well with those obtained by methods one and two, where the three methods were used in immediate succession. For example at $p = 1.3 \times 10^{-2}$ mm of Hg, γ was found to be 30, 31 and 33 by methods one, two and three respectively. This degree of corroboration was obtained throughout, indicating that values of γ found by the first two methods were a few percent too small.

Some comparisons of this work with that of other observers can be made. A variety of gases and metals have been used. The experimental conditions

were not similar in many cases to those used here where the circumstances arising at the cathode in a glow discharge were counterfeited as nearly as possible. In Penning's experiments[4,5] the positive ions from the main discharge tube traversed a canal in an electrode and entered a more highly evacuated vessel wherein the target was located. The value of α_0 (2 to 10) which he finds is approximately that given here, but the rate of increase of α with voltage is less than that which we find (about 0.02 or 0.03 per volt for iron in neon and less than 0.01 per volt for copper in neon as compared with 0.08 per volt for nickel in neon.*)

Found[14] reports values of the secondary emission from tungsten electrodes in neon larger than those obtained here. His method is to compare the measured current at various electrode potentials with the area of the sheath calculated by the equation given by Langmuir and Mott-Smith.[9] He assumes that the true positive ion current is proportional to the area of the sheath, while the secondary electron is constant. The larger emission which he finds may be a consequence of a greater purity of the neon since impurities destroy metastable atoms, to which he ascribes the preponderant part of the emission. His calculations, however, neglect several points: the effect of the second order plasma fields on the variation of the positive ion current with voltage, the additional ionization due to the increasing ionizing power of secondary electrons accelerated by increasing potentials, and the increase of α with voltage.

Velocities of Electrons from the Discharge

The perforated plate and Faraday box system was used with the potential of the plate in the neighborhood of the space potential to determine electron velocities. In the case illustrated by Fig. 6, the plate was put at -25 v, and the current to the box measured as the potential of the box with respect to the plate was changed. The electrons which came through the hole were finally repelled by a retarding potential of -30 volts. The residual current for higher retarding potentials was not zero but positive indicating either that positive ions were coming through the hole in small numbers or that an electron current was released from the box. The latter in view of the phenomena described under method three is extremely probable. In any case, when the current as measured from the zero of the galvanometer is increased by the amount of the residual positive current, the log i_B *vs.* $(V_B)_P$ plot gives a straight line over a considerable portion whereas the corresponding plot of the apparent current is not straight over any part. This indicates that these electrons have a Maxwellian distribution of velocities of which the average, in

* During the writing of this article a paper on this subject by Oliphant appeared. Proc. Roy. Soc. **A127**, 373 (1930). He finds in experiments with an apparatus somewhat similar to that of Penning (for molybdenum and helium) a linear increase of α with the voltage of the impinging ions (about 25 for 200 v to about 120 for 1000 v, or 0.105 increase per volt); but he shows that below 200 v α is almost constant. A smaller α (not linear) is found for heat-treated targets. The velocity distribution curves are similar to those reported here (almost all velocities less than 20 volts), but only the runs taken with heat-treated targets show kinks (cf. Fig. 2).

[14] Found, Phys. Rev. **34**, 1625 (1929).

the case illustrated, corresponds to 7.3 volts. This was corroborated by measurements using the plate P as a plane collector, according to Langmuir's method,[9] which gave in the present case 7.7 volts. This sort of agreement was obtained throughout. The space potential, about -20 or -25 volts with respect to anode, as indicated by Langmuir's method for a plane collector, was not exactly the same as that given under method three, namely, about that of the anode; but obviously the conditions are not comparable, for in one case the collector—a rather large one—was drawing a large negative current, while in the other a large positive one. The distribution of current going to the various electrodes is materially different in the two cases.

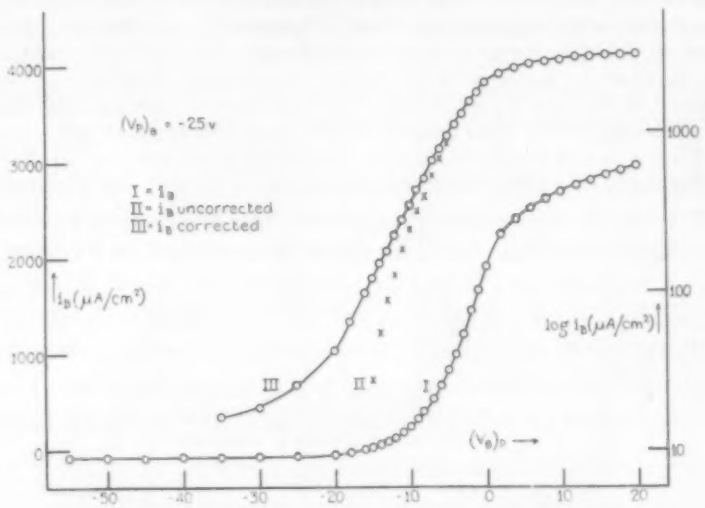

Fig. 6. Curve I. i_B *vs.* $(V_B)_P$ for $(V_P)_a = -25$ v. Curve II. Uncorrected log i_B *vs.* $(V_B)_P$. Curve III. Corrected log i_B *vs.* $(V_B)_P$.

In all runs taken for $(V_P)_a$ between 0 and -15 volts there was a break downward in the log i_B *vs.* $(V_B)_P$ curve at $(V_B)_a = -21$ or -22 volts which indicates a deficiency of electrons of a voltage corresponding to the ionization potential of neon.

There is some evidence for the reflection of electrons from the plate when it is receiving a large negative current, for the current per unit area of the hole received at the box when $(V_B)_P = 0$ is much more than the current per unit area to the whole plate, for example 4970 as compared with 3750 $\mu A/cm^2$, or 25 percent reflection. This varied under different experimental conditions and for different voltages of the plate from about 5 to about 50 percent. Unfortunately the data on this point are at present not sufficient to say anything further.

The junior author is extending this work to other gases and discharge conditions. In conclusion we wish to thank Professor K. T. Compton for his aid and advice during the course of the experiments and in the interpretation of the data.

EXTINCTION OF SHORT A. C. ARCS BETWEEN BRASS ELECTRODES

By T. E. Browne, Jr., and F. C. Todd

Research Laboratory, Westinghouse E. and M. Company*

(Received June 26, 1930)

Abstract

Results are given which show that the dielectric recovery after current zero, of short, stationary A.C. arcs between brass electrodes, is similar to that of cold-electrode arcs previously investigated and described. These results also show that the rate of recovery of dielectric strength of hot-electrode arcs after a current zero may be greatly increased by reducing, within limits, the electrode separation. A possible explanation on the basis of ionic diffusion to the electrode surfaces and the deionizing action of blasts of metal vapor from the boiling electrodes is mentioned.

THE recovery of dielectric strength by an A. C. arc, immediately after a current zero at which it is extinguished, has been studied by Slepian[1] with the result shown in Fig. 1. The short arcs studied were kept in rapid

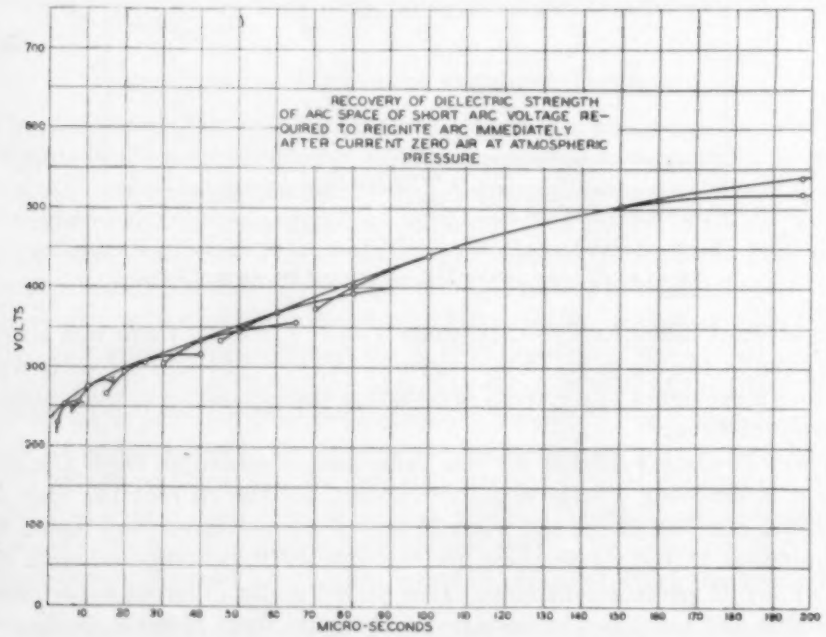
RECOVERY OF DIELECTRIC STRENGTH OF ARC SPACE OF SHORT ARC VOLTAGE REQUIRED TO REIGNITE ARC IMMEDIATELY AFTER CURRENT ZERO AIR AT ATMOSPHERIC PRESSURE
VOLTS
MICRO-SECONDS

Fig. 1.

motion over copper surface terminals which are believed to have been cold. The ability to withstand about 230 volts was regained within less

* Scientific Paper No. 430.

[1] "Extinction of an A.C. Arc", J. Slepian, Trans. A.I.E.E. **47**, 1398 (1928).

than a few micro-seconds after a current zero, and further dielectric strength was recovered thereafter at a much lower rate. The simple theory which Slepian gives identifies the quickly recovered dielectric strength with the minimum sparking potential or normal cathode drop in a glow in the gas next to the cathode. This should therefore be independent of current and of arc length. Slepian's theory also makes the slower further recovery of dielectric strength independent of current and arc length, but this part of his theory depends on the assumption that ions are lost from the arc space only by direct recombination. If other deionizing agents are not of negligible activity, such as for example, diffusion of ions into the electrodes, or diffusion into cooler surrounding gas with more rapid recombination there, then this slower later recovery should be influenced by arc length and current magnitude. The quickly recovered dielectric strength, however, should not be influenced by these other deionizing agents. Short stationary A. C. arcs in which the electrodes are hot might be expected to behave in a generally similar manner to the cold-electrode arcs which Slepian studied, provided that the boiling temperature of the electrode material is so low that appreciable thermionic emission is unlikely. Using stationary arcs with brass electrodes, the writers have conducted experiments which show that dielectric strength after current zero was recovered in the same manner as for the cold-electrode arcs of Slepian. The quickly recovered dielectric strength was independent of arc length, but the more slowly recovered dielectric strength varied with current and arc length, being greater for the smaller currents and shorter arc lengths.

Apparatus and Method

The circuit and the shape of the electrodes used in these tests are shown in Fig. 2. The source of power was a 100 KVA transformer bank with adjustable secondary voltage, whose primary was connected to a 2300-volt 60-cycle power line. The current was limited almost entirely by air-core reactors, having low power factor and comparatively low distributed capacitance. Following Slepian, the electrical transient of the circuit immediately after the extinction of the arc was controlled by shunting the arc electrodes with adjustable resistance made up of low-inductance wire-wound resistor tubes. To obtain the equivalent of exactly zero power factor in spite of resistance drops and arc voltage, a synchronous shorting switch was used to close the circuit at such a point on the voltage wave that the end of the first half-cycle of current occurred at the maximum of the sinusoidal generated voltage. An arc was formed almost immediately at the center of the electrodes by the burning of a fine (No. 40 B. & S.) copper fuse wire, and the ensuing number of half-cycles of arcing was counted by means of a direct-vision oscillograph. When the arc shunting resistance was high the arc would continue for many half-cycles; when the shunting resistance was low the arc would extinguish at the end of the first half-cycle. The resistance shunt was varied between trials until the value that would just cause the arc to go out at the end of the first half-cycle was determined within 5%. During a

short time after a current zero at which the arc is extinguished the voltage across the gap is approximately given by the formula:

$$e = E_m(1 - \epsilon^{-Rt/L}) \tag{1}$$

where E_m is the maximum of the generated voltage, R, the arc shunting resistance, and L, the inductance of the circuit. L was determined from the r.m.s. short-circuit current I by the relation:

$$E_m = 2^{1/2} \cdot 2\pi \cdot 60LI. \tag{2}$$

When the value of R is small, and the arc is extinguished at the first current zero, the impressed voltage given by (1) remains below the recovered dielectric strength of the arc space. When the value of R is large, and the

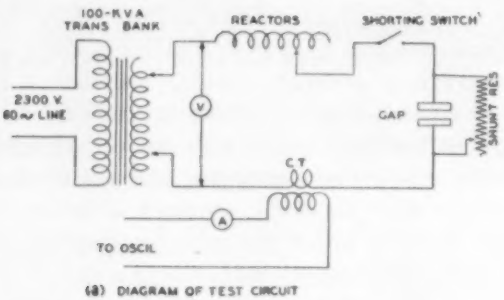

(a) DIAGRAM OF TEST CIRCUIT

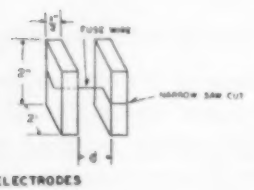

(b) ELECTRODES

Fig. 2.

arc re-ignites, the curve of (1) will rise above the recovered dielectric strength of the arc space. For the critical value of R which just causes the arc to be extinguished at the first current zero, the curve of (1) must come up and just be tangent to the curve of the recovered dielectric strength of the arc space. By plotting a family of curves with different E_m's, and corresponding critical R's, the curve for the recovery of dielectric strength with time may be found by taking the envelope. No account is taken of distributed capacitance of the reactors and other parts of the circuit. Though these capacitances are comparatively small, they become appreciable when the critical value of resistance is high, and particularly when the shunt is removed altogether. The transient voltage will then generally rise in an oscillatory manner, reaching almost double the normal peak value. For this reason, tests in which nearly full voltage is recovered in less than ten micro-seconds are inaccurate and of value only for comparative purposes. Roughness of and

oxide formation on the electrodes after continued arcing may also cause considerable variation in results.

Experimental Results

The curves of Fig. 3, which show results obtained for 1.6 and 3.2 millimeter arcs of 300 amperes, are similar in shape to curves obtained for cold-electrode arcs (Fig. 1). From these curves we see that the immediately

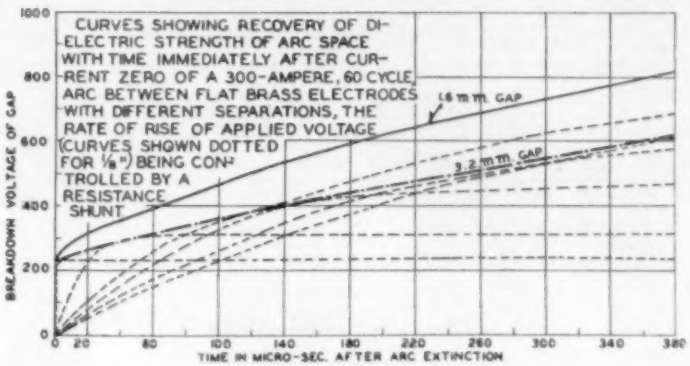
CURVES SHOWING RECOVERY OF DIELECTRIC STRENGTH OF ARC SPACE WITH TIME IMMEDIATELY AFTER CURRENT ZERO OF A 300-AMPERE, 60 CYCLE, ARC BETWEEN FLAT BRASS ELECTRODES WITH DIFFERENT SEPARATIONS, THE RATE OF RISE OF APPLIED VOLTAGE (CURVES SHOWN DOTTED FOR 1/8") BEING CONTROLLED BY A RESISTANCE SHUNT
1.6 m.m. GAP
3.2 m.m. GAP
BREAKDOWN VOLTAGE OF GAP
TIME IN MICRO-SEC. AFTER ARC EXTINCTION

Fig. 3.

recovered ability to stand voltage is the same for the two arc lengths, but that after that the shorter arc recovers dielectric strength faster than the longer arc. Thus we are led to the interesting and at first sight paradoxical fact that a very short arc may be extinguished more easily than a longer arc.

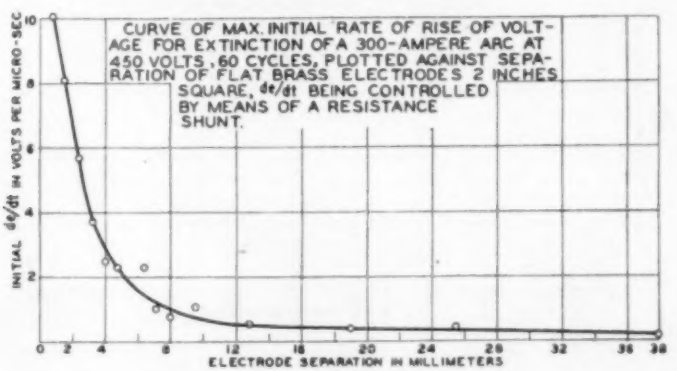
CURVE OF MAX. INITIAL RATE OF RISE OF VOLTAGE FOR EXTINCTION OF A 300-AMPERE ARC AT 450 VOLTS, 60 CYCLES, PLOTTED AGAINST SEPARATION OF FLAT BRASS ELECTRODES 2 INCHES SQUARE, dv/dt BEING CONTROLLED BY MEANS OF A RESISTANCE SHUNT.
INITIAL dv/dt IN VOLTS PER MICRO-SEC
ELECTRODE SEPARATION IN MILLIMETERS

Fig. 4.

This influence of arc length on recovered dielectric strength was found to continue up to lengths of 5 cm and more, by tests on 300-ampere arcs in a 450-volt (r.m.s.) circuit. The critical shunting resistance for arc extinction was determined for different arc lengths, and the initial rate of rise of voltage for the transient corresponding to each critical resistance was computed. The results are shown plotted against arc length in Fig. 4. It is noticeable that the factor causing this variation with gap length is most effective as the electrode separation becomes less than one centimeter. As this factor is undoubtedly a

deionizing one, and is probably active during the arcing period as well as during the extinction transient, we might expect it to reveal itself in the magnitude of the arc voltage. Figure 5 shows the variation of arc voltage with gap length. The definite increase in slope for the smaller lengths affirms the presence, even while the arc current is flowing, of some deionizing action which is more effective for short arcs than for long.

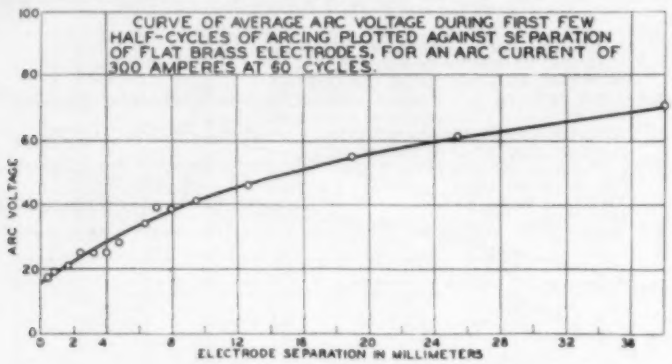
CURVE OF AVERAGE ARC VOLTAGE DURING FIRST FEW HALF-CYCLES OF ARCING PLOTTED AGAINST SEPARATION OF FLAT BRASS ELECTRODES, FOR AN ARC CURRENT OF 300 AMPERES AT 60 CYCLES.
ARC VOLTAGE
ELECTRODE SEPARATION IN MILLIMETERS

Fig. 5.

Figure 6 shows the results of tests at the same voltage and gap length but with currents ranging from 25 to 800 amperes. There is an undoubted decreasing tendency of these rather scattered values with increasing current.

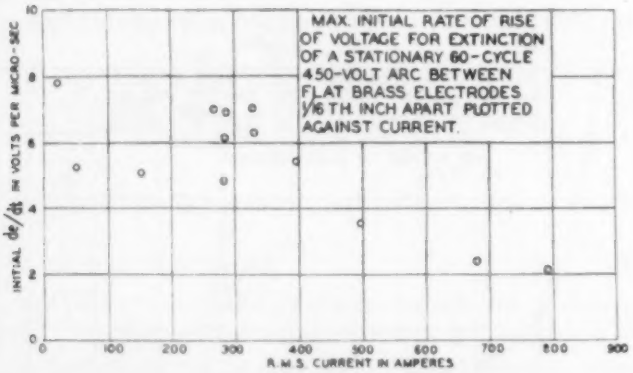
MAX. INITIAL RATE OF RISE OF VOLTAGE FOR EXTINCTION OF A STATIONARY 60-CYCLE 450-VOLT ARC BETWEEN FLAT BRASS ELECTRODES 1/16 TH. INCH APART PLOTTED AGAINST CURRENT.
INITIAL de/dt IN VOLTS PER MICRO-SEC
R.M.S. CURRENT IN AMPERES

Fig. 6.

According to the approximate theory of Slepian for the dielectric recovery upon extinction of a short A. C. arc, all of the regained dielectic strength resides in a positive space sheath next to the cathode. Due to the high mobility of the electrons, this space charge sheath is formed with extreme rapidity upon application of voltage and is immediately able to withstand a minimum of two or three hundred volts, depending only on the electrode material and the gas medium. Further recovery of dielectric strength results from increase in thickness of this space charge sheath due both to growth of applied voltage and to the diminishing density of ionization next to the cathode.

In Slepian's theory the loss of ions was assumed to be due solely to direct recombination in the arc space. The results given here confirm the fundamental conception of the formation and growth of a cathode space charge sheath, but the large influence of electrode separation points to the presence of some deionizing agent other than direct recombination which becomes rapidly more effective as the arc length diminishes. Since diffusion of ions into the electrodes is a process fitting this description, approximate calculations were made to determine to what extent this can account for the observed results. So far, however, the simplified calculations, assuming all of the deionization to be due to diffusion alone, and neglecting such influences as the electric field, vapor emission from the electrodes, and diffusion to the surrounding air, seem to require a coefficient of diffusion far in excess of any reasonable value. This may indicate that diffusion to the electrodes is an unimportant factor, or it may simply mean that the present approximate method of calculation is unsound. It is also thought possible that other physical processes may enter considerably into the deionization of the arc space next to the cathode, such as for example, a blast of metal vapor from the violently boiling electrodes during the arcing period and perhaps for a very short time immediately thereafter, but this theory lacks verification as yet. Therefore, further work is being done in an effort to arrive at a more nearly satisfactory explanation of these results.

RESTRIKING OF SHORT A. C. ARCS

By F. C. Todd and T. E. Browne, Jr.

Research Laboratory, Westinghouse E. and M. Co.*

(Received June 26, 1930)

Abstract

The restriking after zero current of short stationary A.C. arcs with brass, copper, zinc, iron, tungsten and carbon electrodes, and of arcs moving rapidly over copper electrodes was investigated with a cathode-ray tube of the Braun type. The volt-ampere traces on the fluorescent screen showed clearly the voltage necessary to restrike the arc after current zero, and the effect of the electrode vapor on the magnitude and variation of the restriking voltage. The arcs with refractory electrodes, i.e. carbon and tungsten, showed traces differing from the arcs with the other metals in that no high voltage for restriking the arc appeared. This is believed to be due to the refractory electrodes being at a temperature high enough for thermionic emission. For the other electrode materials, re-ignition voltages of several hundred volts were observed, suggesting that re-ignition of the arc required breakdown of a gas layer by ionization by collision alone. The arcs which were rapidly moving over their electrodes usually restruck to a glow before breaking down to an arc. The magnitudes of the restriking voltage and the glow current depended upon the condition of the electrodes, magnitude of the driving magnetic field, and the transient characteristic of the circuit in which the arc was playing.

IT IS well known that although a carbon arc can be maintained in a low voltage A.C. circuit, in general, an A.C. arc with metallic electrodes cannot be maintained with less than a few hundred volts. This has been studied by means of volt-ampere traces on the fluorescent screen of a cathode-ray tube of the Braun type, developed by Zworykin for use in television. These investigations have brought out several interesting facts about the magnitude of the voltage required to restrike the arc, and the manner of breakdown.

Slepian[1] has attributed this peculiarity of arcs mentioned, to the formation immediately after current zero of a thin deionized layer of gas next to the cathode. With thermionic emission lacking, to re-ignite the arc this layer would need to be broken down by ionization by collision and would require several hundred volts. His theory is illustrated by Fig. 1 which is taken from the paper referred to above. Starting with a uniform distribution of ions when the current and voltage are zero, the increasing voltage will cause space charge sheaths to form next to the electrodes after the manner described by Langmuir in relation to probe electrodes in an ionized gas. Because the mobility of the electrons is much greater than that of the positive ions, most of the applied voltage will be across the space charge sheath at the cathode. The current densities in this sheath are very small and in order to

* Scientific Paper No. 431.

[1] "Extinction of an A.C. Arc," by J. Slepian, Journal of the A.I.E.E. October, 1928.

restrike the arc, the space charge sheath must be broken down. If there are no other ionizing agents, the breakdown must be by ionization by collision only, and is entirely similar to the breakdown of a short spark gap. It will, therefore, require a minimum of several hundred volts. If, however, there are other ionizing agents, breakdown will occur at a lower voltage.

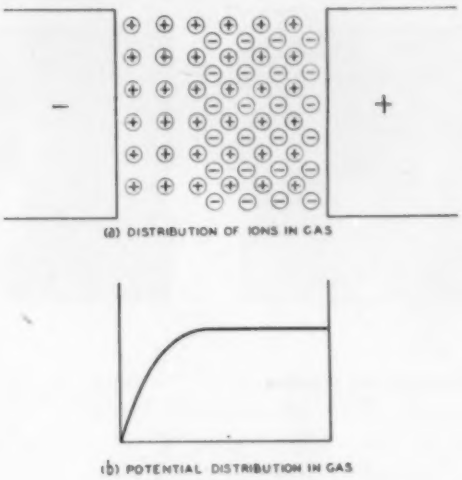

Fig. 1.

It seems unlikely that the temperature of the electrodes can be raised much above the boiling point. Hence, for non-refractory metals, i.e. zinc brass, copper, and iron, thermionic emission is probably entirely negligible. Hence, for these metals, the space charge sheath must be broken down by ionization by collision only. But carbon and tungsten at their boiling points

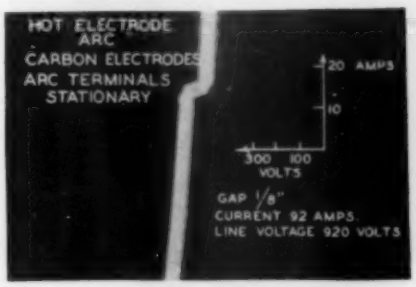

Fig. 2.

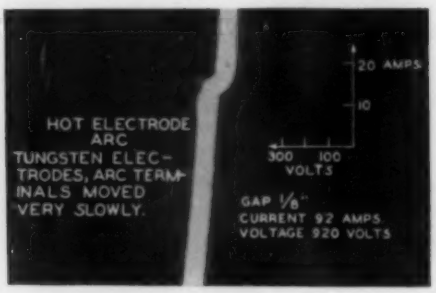

Fig. 3.

are at temperatures high enough for thermionic emission. Accordingly, for these electrode materials, we may expect breakdown of the sheath at low voltages. This occurs as is shown by the photographs of the dynamic volt-ampere characteristic on the fluorescent screen of the Braun tube. The photographs in Fig. 2 and 3 are for the carbon and tungsten arc respectively.

Fig. 4 shows the interpretation of Fig. 2 in the more familiar current and voltage against time relation. In Figs. 2 and 3 the current and voltage deflections are purposely not exactly in phase with the actual current and voltage and give the double line near current zero. The exposure for these photographs was 15 seconds, or included 900 retracings of the phenomenon.

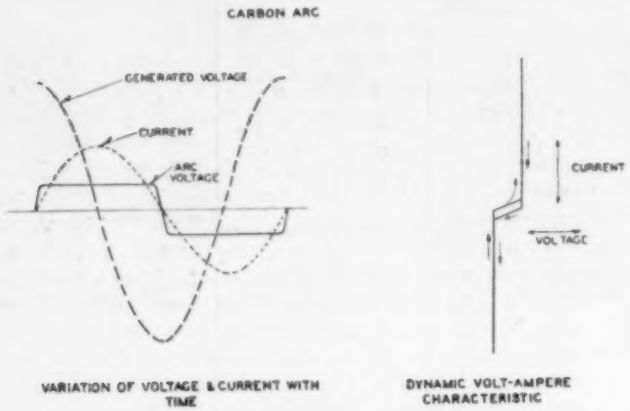

Fig. 4.

Returning now to the non-refractory metals, we shall expect to see much higher breakdown voltages, and since the space charge sheath is composed chiefly of the metal vapor, the breakdown voltages required for the various metals will in general be different. This is illustrated by Figs. 5, 6, 7, and 8 which give a portion of the dynamic volt-ampere characteristics near the reversal of current for zinc, copper, brass, and iron respectively. The current

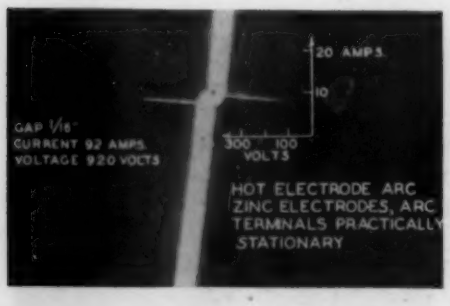

Fig. 5.

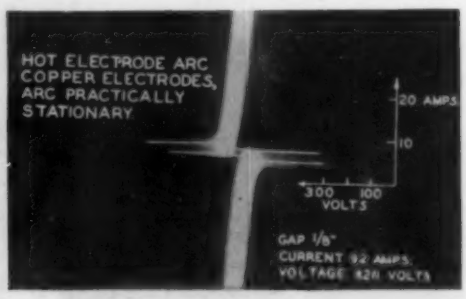

Fig. 6.

and voltage deflections are again not in phase with the actual current and voltage for Figs. 5 and 6, this displacement is to show the voltage before current zero as well as the restriking voltage. For the zinc arc, the restriking voltage is 280 volts and the voltage does not rise above arc voltage at the end of the half cycle. The stationary arc on copper has a peak restriking voltage of 360 volts, and the voltage before current zero rises to 280 volts.

The maximum restriking voltage for brass and iron were 255 and 290 volts respectively.

Fluctuations in the density of the breakdown voltage line indicates that reignition frequently occurred at low voltages in these stationary arcs. This requires some other ionizing agent than ionization by collision. What this

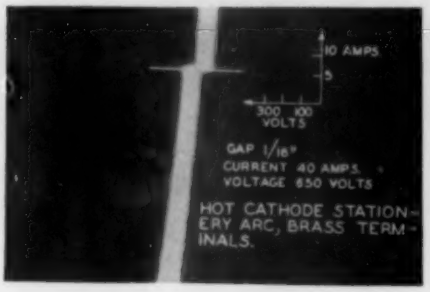

Fig. 7.

Fig. 8.

is is uncertain. Slepian suggests that the charging current to a particle or droplet making or breaking contacts with the cathode may cause a tiny spark which will make the space charge sheath collapse.

It is possible to cause an arc to move so rapidly over a clean smooth surface by means of a magnetic field that melting of the electrodes is prevented.

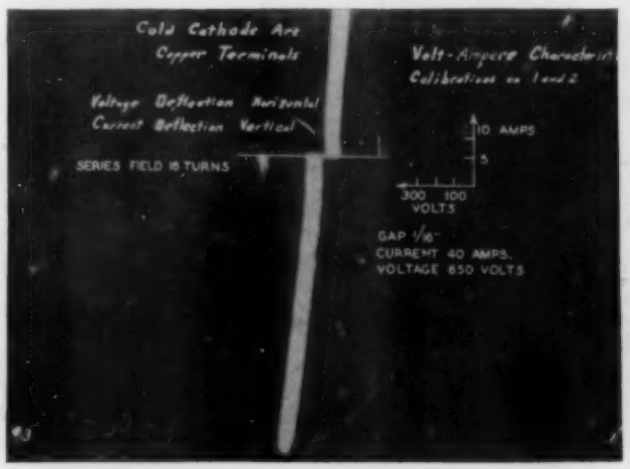

Fig. 9.

It is believed that the terminals of such an arc may be cold. The dynamic volt-ampere characteristic of such an arc is shown in Fig. 9. The maximum restriking voltage is 535 volts, the hesitation during the breakdown is at 325 volts. Fig. 10 is the interpretation of Fig. 9 in the more familiar relations, the scale is much expanded near the ends of the half-cycles for clearness. As

the impressed voltage increases by an oscillation at the natural period of the circuit, and as the density of ionization decreases due to recombination and discharging of ions into the electrodes, the thickness of the cathode space charge sheath increases. At peak value, the voltage across the sheath has exceeded the recovered dielectric strength, and the short gap breaks down by ionization by collision. The voltage drops from peak value to that of the

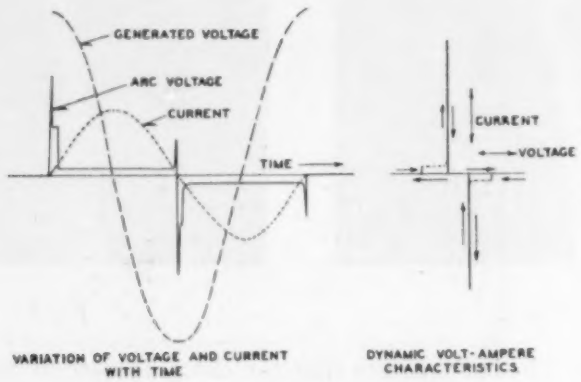

Fig. 10.

glow or occasionally even to arc voltage. The glow appears and remains a stable discharge until enough energy is put into the space adjacent to the cathode to give the conditions required by the cold electrode arc, then the transition from glow to arc abruptly occurs. The maximum glow current observed before transition to an arc was 4 amperes, and in this case meant that the glow was stable for longer than 10^{-4} seconds. The probability of a

Fig. 11.

glow occurring seems to be less for the higher restriking voltage. It also appeared that the magnitude of the current to which the glow continued, and the probability of a glow occurring at all both increase as the electrode surfaces which had been initially cleaned with emery become oxidized. Slepian[2]

[2] "Theory of the Deion Circuit Breaker", J. Slepian Journal of the A.I.E.E. Feb., 1929.

had predicted that re-ignition of the cold electrode arc takes place first as a glow and his expectation is here confirmed.

Another dynamic volt-ampere characteristic similar to Fig. 9 is shown in Fig. 11, the only difference is that the driving magnetic field was 16 series turns for the former as compared to 660 series turns for the latter. The maximum restriking voltage in Fig. 11 is 1065 volts as compared to 535 volts for Fig. 9. In each case the glow occurs at 325 volts. This high restriking voltage can be obtained with the weaker field by shunting the arc with a resistance to slow down the rate of increase of voltage after current zero. This is due to the longer time the deionizing processes are active and the resulting thicker deionized layer requiring more voltage to breakdown.

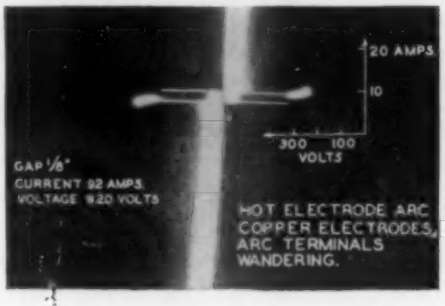

Fig. 12.

If an arc of approximately 90 amperes is drawn between plane electrodes with a fine fuse wire, generally the arc will not continue for several half-cycles where it was drawn but will wander about over the electrode surface. Judging by the trail, the arc does not move much while the current is flowing but restrikes after current zero to a position on one side of the position of the arc during the previous half-cycle. When moving in this manner tungsten and carbon arcs show a variable restriking voltage which may be quite comparable to that of non-refractory metals. The only metals among those tested which did not show this wandering behavior were zinc and to a certain extent brass. Copper arcs have a very peculiar volt-ampere characteristic while wandering as shown by Fig. 12. The hesitation at the peak of the restriking voltage varies from a minimum of about 250 volts to a maximum of about 325 volts.

THE PHOTOELECTRIC BEHAVIOR OF SOLID AND LIQUID MERCURY

By Duane Roller
University of Oklahoma

(Received June 26, 1930)

Abstract

With monochromatic light, the photoelectric threshold wave-length for solid mercury, freshly distilled and frozen in vacuum, was 2750 ± 25A for all temperatures between −190°C and the melting point. For room temperature it was 2735 ± 10A, confirming Kazda's value.

The photoelectric current excited by each of the lines 2537A, 2653A and 2700A was independent of temperature between −190°C and *ca.* −125°C. Between *ca.* −125°C and −39°C there was a gradual small decrease in the current with increasing temperature, but this was not reproducible at definite temperatures and is attributed mostly to contamination and other secondary causes. With the possible exception of this decrease in current, there was no indication of an allotropic change in the mercury between −190°C and the melting point. The photoelectric current for the solid phase was always higher than that for the liquid at room temperature, possibly due to a change in the optical absorptivity of mercury with change in phase. Between −39°C and 0°C the emission curves show so much hysteresis that conclusions regarding this region are impossible.

THE photoelectric threshold for mercury at room temperature has been established at $\lambda_0 = 2735$A by Kazda, Dunn and Hales.[1] Mercury at the melting point was investigated by Pohl and Gudden.[2] They were unable to detect any change in the threshold with melting but terminated their work with the conclusion that mercury is not a suitable metal for studying variations in the photoelectric effect at transition and melting points because of the difficulties inherent in such experiments at low temperatures. Recently, Margarete Grutzmann[3] published a study of the photoelectric emission from mercury at low temperatures. No variation of the total emission with temperature was found and there was no change in the total emission at the melting point. Since monochromatic light was not used, it is impossible to interpret these results or to establish the behavior of the threshold.

The purposes of the present work with mercury were: (1) to find the effects of temperature and of changes in the state of aggregation on the photoelectric threshold and on the current excited by incident monochromatic light; (2) to check independently the value of the threshold at room temperature; (3) to seek evidence of a photoelectric nature regarding an allotropic change in mercury in the region between −190° C and the melting point. McKeehan and Cioffi[4] determined the crystal structure of mercury

[1] C. B. Kazda, Phys. Rev. **26**, 643 (1925); H. K. Dunn, Phys. Rev. **29**, 693 (1927); W. B. Hales, Phys. Rev. **32**, 950 (1928).

[2] Pohl and Gudden did not publish. This information was communicated to me by Dr. A. Goetz.

[3] M. Grutzmann, Ann. d. Physik **1**, 49 (1929). A comprehensive bibliography accompanies this paper.

[4] McKeehan and Cioffi, Phys. Rev. **19**, 444 (1922).

at −115° C and Alsen and Aminoff[5] determined the structure at −78° C. The two results are very different and thus point to the existence of an allotropic modification of the mercury occurring somewhere between −115° C and −78° C.[6] On the other hand, Lark-Horovitz[7] has recently found that the crystal structure of mercury at the temperature of liquid air is identical with that at the temperature of a carbon dioxid-alcohol mixture.

The apparatus for the present work, Fig. 1, was made of Pyrex glass and had no cemented joints or stopcocks in the high-vacuum system. Light from a mercury arc, which had been carefully calibrated[8] and which was operated with constant voltage, current and temperature, passed through a Hilger quartz monochromator and a quartz lens into the quartz window of the photoelectric cell, and then through a slit in the anode onto the bottom of the cell. The anode was a circular disk of tungsten 3 cm in diameter, welded with nickel to a heavy tungsten wire which lead out through a horizontal tube 12 cm long to a Dolazalek electrometer of sensitivity 1100 mm

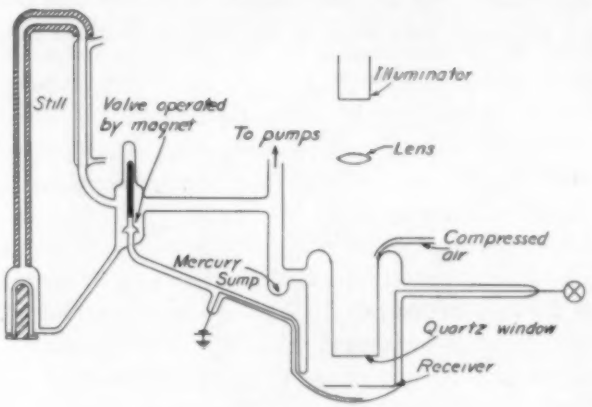

Fig. 1. Diagram of apparatus.

per volt at 1.5 m scale distance. The cell was shielded electrostatically by covering its outside walls with a paste made of powdered graphite, water, and a little water glass. When the cell was baked the graphite formed a hard conducting layer. Water glass, when used sparingly, apparently will not weaken Pyrex appreciably, for the cell was used for two months without breakage.

The mercury used as the cathode of the cell was cleaned and distilled by a special method[9] and was then placed in the still, Fig. 1, where it was distilled repeatedly in high vacuum to remove occluded gases. Some of the mercury was then allowed to pass through a magnetically operated valve, Fig. 1, into the bottom of the cell, where it rested on the glass, but was in

[5] Alsen and Aminoff, Geol. Foren. i. Stockholm Forh. 124 (1922).

[6] Ewald and Hermann, Zeits. f. Krist. **65**, parts 1–3, appendix (1927); International Critical Tables, **1**, 340.

[7] K. Lark-Horovitz, Phys. Rev. **33**, 121 (1929).

[8] C. B. Kazda, Phys. Rev. **26**, 645 (1925).

[9] D. Roller, J. O. S. A. **18**, 537 (1929).

contact with a tungsten wire kept usually at a potential of 20 volts negative to ground.

The cooling of the mercury was accomplished variously with liquid air, liquid air and alcohol, solid carbon dioxide, and solid carbon dioxide and ether, contained in a specially designed Dewar flask which surrounded the cell up, to a point 7 cm above the surface of the mercury cathode. Temperatures were measured with a constantan-steel thermocouple, enclosed in a glass tube and immersed in the mercury. To retard the collection of moisture on the cold cell, a current of washed and dried air was played continuously on the window and walls. The points where the tungsten leads emerged from the cell were kept dry by means of small heating coils and drying materials. Surrounding the cell was a double-walled galvanized iron box, lined with asbestos, which helped to keep out moisture and which also served as an oven for baking the cell and as an additional electrostatic shield.

With the cell of Fig. 1 the threshold for mercury at room temperature was found to be at 2735 ± 10A, in agreement with the results of previous workers.[10] This constitutes an independent check of the previous work, both because the mercury was here in contact with glass and tungsten, rather

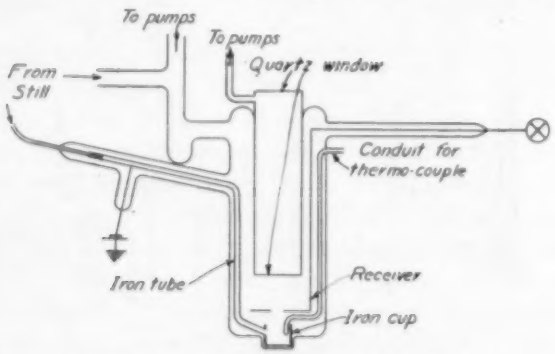

Fig. 2. Diagram of modified apparatus.

than iron, and because the cell involved relatively few metal parts and probably was more thoroughly outgassed than the cells previously used.

When it was attempted to use this cell for low temperature work several defects in its design became apparent and this led to the construction of a new cell, Fig. 2, which differed from the old one in the following respects. (a) A second quartz window was cemented to the cell at a point considerably above the region to be cooled, the space between the two windows being evacuated. This gave improved thermal insulation and also made it possible to dispense with the current of air on the cell. Compressed air usually contains oil which forms a film on the window; no simple way could be found for removing all the oil from the air. (b) The anode, including the lead through the glass wall of the cell, was cut out of a single sheet of tungsten. In the old cell, the anode consisted of a tungsten sheet welded to tungsten wire and it was the seat of thermoelectric forces which produced erratic effects during times that the temperature of the cell was changing. (c) An iron cup 2.5 cm in diameter served as a container for the mercury cathode, the size of this cup being such that light fell only on the central unstrained part of the frozen

[10] Reference 1.

mercury. The mercury was admitted to the cup through an iron tube, so arranged that it did not need to pass through the glass wall of the cell. In the old cell the mercury ran in over the glass, resulting in the formation of electrostatic charges which would persist for as much as an hour. (d) The mercury pump attached to the cell was enlarged so that it could be immersed in liquid air, thus retarding the condensation of mercury vapor on the surface of the solid mercury cathode. Preliminary experiments had shown that without this protection enough mercury condensed on the surface of the empty iron cup, when the latter was cooled, to produce an appreciable photoelectric current. Experiments made very recently at the University of Oklahoma by Mr. Carl Woodward and the writer indicate that a thin film of frozen mercury deposited on iron has both a high photoelectric sensitivity and a threshold wave-length longer than 2735A. In view of these results, it might be advisable to seal off the photoelectric cell from the pumps and mercury still before attempting to determine the threshold of solid mercury.

In order to determine the thresholds at various temperatures, measurements were made of the photoelectric current at a particular temperature as a function of wave-length. Thresholds were then determined in the usual way by plotting the current excited by unit intensity of the incident light as a function of wave-length.[11] In the region $-190°$ to the melting point, the threshold was established at 2750 ± 25A, independently of the temperature. Thus, within the experimental error, the threshold for solid mercury is the same as that for liquid mercury at room temperature. When the solid mercury was held at low temperatures for times exceeding about one hour, the threshold began to shift slowly to shorter wave-lengths. There was ample evidence that this shift was due to contamination.

Measurements were also made of the photoelectric current for a given line as a function of temperature. Results typical of sixty curves made for the lines 2537A, 2653A, and 2700 A are shown in Fig. 3. The arrows indicate the direction of temperature variation. The time required to obtain data for a given curve varied between 30 minutes and 12 hours, depending upon the method of cooling and the number of observations made.

Fig. 3 shows that the sensitivity of the mercury to monochromatic light was practically independent of temperature in the region $-190°$ to *ca.* $-125°$. Between the latter temperature and the melting point, $-39°$ C, slight changes occur in the slopes of the sensitivity curves but these could not be reproduced at definite temperatures. They were found to be associated closely with changes in the level of the cooling agent surrounding the cell and with abrupt changes in the rate of warming and cooling. Experiments showed that contamination released from the walls of the cell lowered the sensitivity of the mercury. Abrupt changes in temperature had a marked effect on the appearance of the solid mercury surface, particularly when the mercury was near the melting point; thus it is very likely that such abrupt changes of temperature also affected the photoelectric efficiency of the mercury surface.

Nothing was observed in the region between $-190°$ and $-39°$ C that could be attributed to an allotropic change in the mercury. This excepts

[11] R. A. Millikan, Phys. Rev. **7**, 380 (1916).

the slight decreases in sensitivity which always accompanied rises in temperature and which have been at least partly accounted for in other ways.

During melting and freezing the sensitivity of the mercury changed rapidly. In the region between $-39°$ and $0°$ C the liquid mercury showed great susceptibility to some unknown contamination which lowered the sensitivity. The curves, Fig. 3, show so much hysteresis in this region that no conclusions can be made as to the effect of temperature on the liquid mercury. The contamination was of such a kind that it could be eliminated immediately from the mercury surface by heating the cell a few degrees above room temperature.

It is to be noted that the sensitivity of the solid mercury always was higher than that of the liquid at room temperature. Since the thresholds

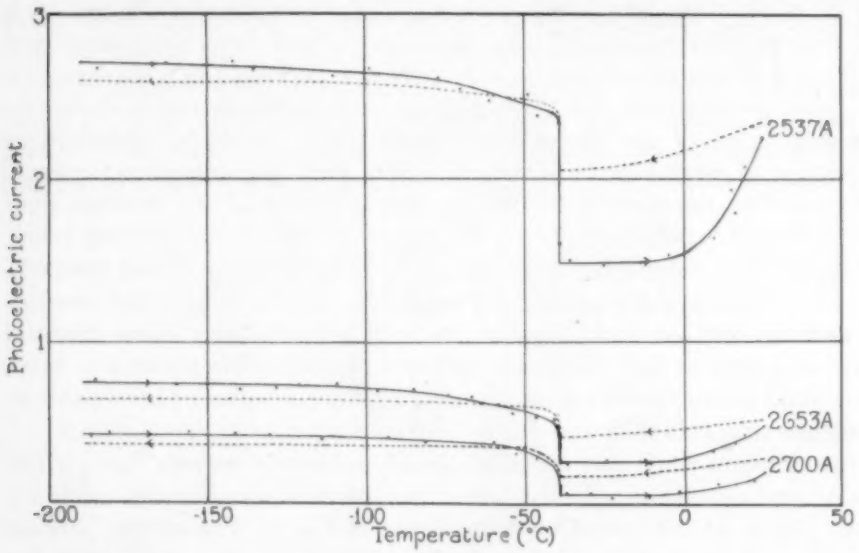

Fig. 3. Photoelectric current for lines 2537A, 2653A and 2700A as a function of temperature.

were found to be the same in the two cases, the higher sensitivity of the solid must be attributed to a change in the photoelectric efficiency of the mercury surface with change of state. This change in efficiency may be due to a change in the optical reflectivitity of mercury with change of state. No exact information is at present available regarding the reflectivity of a very pure solid mercury surface formed in high vacuum although experiments are in progress. Haak and Sissingh[12] found no change in the optical constants of mercury either on freezing or in subsequent cooling down to $-80°$ C, but the mercury surfaces used by them contained adsorbed layers of air.

This work was done in 1928 at the Norman Bridge Laboratory of Physics, California Institute.

It is a pleasure to acknowledge my indebtedness to Professor Millikan whose interest and guidance prompted the choice of subject and made the work possible.

[12] Haak and Sissingh, K. Akad. Amsterdam **21**, 678 (1919).

THE THERMODYNAMIC TREATMENT OF CHEMICAL EQUILIBRIA IN SYSTEMS COMPOSED OF REAL GASES. I. AN APPROXIMATE EQUATION FOR THE MASS ACTION FUNCTION APPLIED TO THE EXISTING DATA ON THE HABER EQUILIBRIUM

By Louis J. Gillespie and James A. Beattie
Research Laboratory of Physical Chemistry, Massachusetts Institute of Technology*

(Received June 30, 1930)

Abstract

All of the equilibrium data on the ammonia synthesis reaction, which cover an extreme temperature range of from 325° to 952°C and an extreme pressure range (at some temperatures) of from 10 to 1000 atmospheres, are correlated with the compressibility and heat capacity data on the pure reacting gases by means of a rational and relatively simple equation for the mass action function K_p. In this equation the effect of temperature and of pressure on K_p are separated, the relation for the temperature effect being exact, but certain approximations being introduced for the sake of simplicity into the relation for the pressure effect.

All of the data on the ammonia synthesis equilibrium are represented within the experimental accuracy by the use of only two adjustable constants.

1. Introduction

THE use of high pressures in industrial chemical operations has disclosed numerous cases in which the deviations from the laws of ideal gases are of practical importance. We may mention the following two groups of phenomena:

1. When a vapor is condensed out of a gaseous mixture, more of the vapor has been found to remain uncondensed than would be expected from the laws of ideal gases. Typical cases[1] are the removal of ammonia from mixtures containing hydrogen and nitrogen, of carbon monoxide from water gas in the industrial preparation of hydrogen, and of nitrogen from nitrogen-hydrogen mixtures. The phenomenon has been studied by Pollitzer and Strebel,[1] Larson and Black,[2] Lurie and Gillespie,[3] McHaffie,[4] Eucken and Bresler,[5] and Braune and Strassmann.[6]

2. In the fixation of nitrogen by the Haber process, the reaction for which is

* Contribution No. 245.
[1] Cited by Pollitzer and Strebel, Zeits. f. phys. Chem. **110**, 768 (1924).
[2] Larson and Black, J. Am. Chem. Soc. **47**, 1015 (1925).
[3] Lurie and Gillespie, J. Am. Chem. Soc. **49**, 1146 (1927).
[4] McHaffie, Phil. Mag. (7) **1**, 561 (1926).
[5] Eucken and Bresler, Zeits. f. physik. Chem. **134**, 230 (1928).
[6] Braune and Strassmann, Zeits. f. physik. Chem. **143A**, 225 (1929).

$$^3/_2H_2 + {}^1/_2N_2 = NH_3 \qquad (1)$$

there is a greater yield of ammonia as the pressure is increased than that calculated from the laws of ideal gases.[7,8]

The deviations in these two classes of phenomena are due to the same cause, the failure of the ideal gas laws, and the explanation of one of these will furnish the basis for an understanding of the other. In the present paper we are interested in testing an improvement on the ideal-gas mass action law by the use of the existing data on the equilibrium of the chemical reaction given in Eq. (1).

Much of the interest in the mass action law has been confined to the case of solutions of electrolytes. In this laboratory, however, Keyes[9] has for some years been collecting and correlating the compressibility data on gases in realization of their importance to chemistry in connection with the mass action law.

The thermodynamic connection between the mass action law and the pressure-volume-temperature relations for pure gases and gas mixtures has been given,[10] the general relation being:

$$RT \ln (K_p/K_p^*) = -\sum\left\{ \nu_i \int_0^p [(dV/dn_i)_{T,p,n} - RT/p]dp \right\} \qquad (2)$$

in which K_p is the "equilibrium constant" at the pressure p, and is defined by the relation:

$$\ln K_p = \sum(\nu_i \ln px_i) \qquad (3)$$

and K_p^* is the limiting value of K_p as the pressure on any mixture maintained in equilibrium is isothermally decreased to zero. The quantity ν_i is the coefficient of the substance i in the chemical equation for the given reaction and is negative if the substance disappears; x_i the mole fraction of substance i in the equilibrium mixture; and $(dV/dn_i)_{T,p,n}$ the partial molal volume of gas i in the mixture. A relation[11] for K_p in terms of the independent variables V and T is:

$$RT \ln (K_p/K_p^*) = \Sigma(\nu_i)RT \ln \frac{pV}{\Sigma(n_i)RT} - \Sigma\left\{ \nu_i \int_V^\infty [(dp/dn_i)_{V,T,n} - RT/V]dV \right\} \qquad (4)$$

[7] Larson and Dodge, J. Am. Chem. Soc. **45**, 2918 (1923).

[8] Larson, J. Am. Chem. Soc. **46**, 367 (1924).

[9] Keyes, Am. Soc. Refrig. Eng. J. **1**, 9 (1914); Proc. Nat. Acad. Sci. **3**, 323 (1917); Keyes and Felsing, J. Am. Chem. Soc. **41**, 589 (1919); ibid. **42**, 106 (1920); Smith and Taylor, J. Am. Chem. Soc. **45**, 2107 (1923); ibid. **48**, 3122 (1926); Beattie, J. Am. Chem. Soc. **46**, 342 (1924); Keyes and Burks, J. Am. Chem. Soc. **49**, 1403 (1927).

[10] Gillespie, J. Am. Chem. Soc. **47**, 305 (1925), ibid. **48**, 28 (1926).

[11] Beattie, Phys. Rev. *31* 680 (1928), ibid. *3μ* 691 (1928). In Eq. 5 a new entropy constant has been used, as will be discussed in Part II.

wherein K_p^* is related to the temperature by the relation:

$$\ln K_p^* = \Sigma(\nu_i)(\ln T/T_0 - 1) - \frac{1}{RT}\Sigma\left\{\nu_i\left[\int_{T_0}^{T} C_{V_i}^* dT - T\int_{T_0}^{T}\frac{C_{V_i}^*}{T}dT + u'_{0i} - Ts'_{0i}\right]\right\} \quad (5)$$

in which $C_{V_i}^*$ is the heat capacity at constant volume for gas i at zero pressure, and u'_{0i} and s'_{0i} are constants for gas i. These relations depend upon two assumptions[12] and the general laws of thermodynamics.

We may evaluate the partial derivatives of equations (2) or (4) graphically, by approximate methods, or from an equation of state of mixtures.

It has been shown[10] that if the Lewis and Randall rule[13] for calculating the fugacity of a gas in a mixture holds, then the partial derivative of Eq. (2) may be replaced by the molal volume of the pure gas at the temperature and pressure of the mixture, and Eq. (2) reduces to the simple, approximate relation:

$$RT \ln (K_p/K_p^*) = \Sigma\left\{\nu_i \int_0^p [(RT/p) - (V_i/n_i)]dp. \right. \quad (6)$$

The differences between the molal volume and the partial molal volume have been studied for several mixtures.[14] A further approximation of (6) is obtained by assuming the integrand constant during the integration and equal to its limiting value at zero pressure, which can be calculated from an equation of state for mixtures. The equation is[10,15]

$$RT \ln (K_p/K_p^*) = -\Sigma\{\nu_i(B_{0i} - A_{0i}/RT - c_i/T^3)\}p \quad (7)$$

where R is the ideal gas constant and B_{0i}, A_{0i} and c_i are equation of state constants for gas i.

Keyes[16] has given an equation for the mass action function K_p for gases whose isometrics are linear by use of the kinetic considerations from which the Keyes equation of state was derived.[9] Application of this equation to the Haber equilibrium data showed a tolerable agreement up to 600 atmospheres.

Gibson and Sosnick[17] and Merz and Whittaker[18] have calculated the fugacity of a gas in a mixture by graphic methods. In order to carry out the computation it is necessary to make some assumption regarding the expansion of gases on mixing at infinitely low pressures. They assumed this to be zero but this assumption is not supported[14] by the experimental data.

Van der Waals hoped to determine an equation of state for gas mixtures from the equations of state of the gas constituents together with two

[12] Beattie, Phys. Rev. **36**, 132 (1930).

[13] Lewis and Randall, Thermodynamics and the Free Energy of Chemical Substances. McGraw-Hill Book Co., New York, 1923, p. 226.

[14] Gillespie, Phys. Rev. **34**, 352 (1929).

[15] Gillespie, Phys. Rev. **34**, 1605 (1929).

[16] Keyes, J. Am. Chem. Soc. **49**, 1393 (1927).

[17] Gibson and Sosnick, J. Am. Chem. Soc. **49**, 2172 (1927).

[18] Merz and Whittaker, J. Am. Chem. Soc. **50**, 1522 (1928).

adjustable constants, characteristic of every binary combination of constituents, the so-called interaction constants. Various methods for calculating these interaction constants from the values of the corresponding constants for the pure gases have been suggested. Keyes, working with an equation of state[9] better adapted to representation of the compressibilities of the pure gases, found that a very simple method of calculating the interaction constants sufficed for the representation of the pressures of mixtures of methane and nitrogen measured by Keyes and Burks.[19] Lurie and Gillespie[3] were successful with the same method in accounting for their measurements of the effect of nitrogen on the vapor pressure of the system: barium chloride, barium chloride octammine. The necessary parameters for the gas mixture are calculated by a simple scheme, which may be designated as linear combination of constants:

$$k_x = k_1x_1 + k_2x_2 + \cdots = \Sigma(k_ix_i) \tag{8}$$

where k_x represents the parameter for the mixture and k_1, $k_2 \cdots$, represent the corresponding constants for the pure gases. All the constants for pure gases are dimensionally of the first power in the volume, except the cohesive pressure constant A, which is of the square of the volume. The linear combination rule is applied as above to the square root of the cohesive pressure constant, and directly to the others. A fuller discussion of the work of earlier investigators on the calculation of interaction constants is given elsewhere.[20] By means of this linear combination of constants we are able to calculate the values of the parameters for a mixture when the composition of the mixture and the constants of the pure gases are known, without the introduction of arbitrary constants.

In a series of investigations from this laboratory[14,20,21] it has been found that when this scheme is applied in connection with the Beattie-Bridgeman equation of state[22] the pressure-volume-temperature data on mixtures are represented very well, possibly within the experimental error. For chemical purposes it appears that a much smaller degree of success would suffice, as evidenced by the success obtained[10] in representing the Haber equilibrium data to 100 atmospheres by the use of Eqs. (6) or (7).

Eq. (4) can be integrated[11] in terms of elementary functions by use of the Beattie-Bridgeman equation of state for mixtures. The equilibrium constant is expressed in terms of the temperature and the volume of the equilibrium mixture. This latter quantity must be computed from the equation of state, since the data are always given in terms of pressure and temperature, and hence an expression in terms of these latter variables is desirable. Eq. (2) gives such an expression, but the integration cannot be carried out in terms of elementary functions of the pressure and temperature from any of the usual equations of state.

[19] Keyes and Burks, J. Am. Chem. Soc. **50**, 1100 (1928).

[20] Beattie and Ikehara, Proc. Amer. Acad. Arts and Sci. **64**, 127 (1930).

[21] Beattie, J. Am. Chem. Soc. **51**, 19 (1929).

[22] Beattie and Bridgeman, Proc. Amer. Acad. Arts and Sci. **63**, 229 (1928); J. Am. Chem. Soc. **50**, 3133 (1928); Zeits. f. Physik, **62**, 95 (1930).

II. A Simple Mass Action Equation

A simple form of the mass action equation, explicit in the pressure, has been obtained[15] by approximate integration of Eq. (2), and evidence given that this equation should furnish a very good approximation. The equation is

$$\ln K_p = \ln K_p^* - \{\Sigma[\nu_i(B_{0i} - A_{0i}/RT - c_i/T^3)] + \Sigma[\nu_i(A^{1/2}{}_{0i} - \Sigma x_i A^{1/2}{}_{0i})^2/RT]\}\, p/RT \quad (9)$$

The same expression results if Eq. (2) is integrated by one form[23] of the Beattie-Bridgeman equation of state which expresses V as an explicit function of p and T, and if then terms containing powers of p higher than the first are dropped. Except for the terms involving the constant c, which does not occur in the Keyes equation of state, the above Eq. (9) is also equivalent to an approximate equation given by Keyes.[16]

For the quantity K_p^* which occurs in (9) we may use Eq. (5) which expresses K_p^* in terms of the energy and entropy constants and the heat capacities of the reacting gases. Or we may follow more closely the familiar treatment for ideal gases. One has every reason to expect that at very low pressure the van't Hoff isochor will hold. This we will write:

$$d \ln K_p^*/dT = \Delta H^*/RT^2. \quad (10)$$

Here ΔH^* is the heat absorbed in the reaction at zero pressure, and the derivative may be regarded as a total derivative. Kirchoff's law for the temperature coefficient of the heat of reaction is

$$d\Delta H^*/dT = \Delta C_p^* = \Sigma(\nu_i C_{pi}^*). \quad (11)$$

In general C_p^*, the limiting value at zero pressure of the constant pressure specific heat, may be sufficiently well expressed as a function of the temperature by a series expansion:

$$C_{pi}^* = R + \mathrm{A}_i + \mathrm{B}_i T + \mathrm{C}_i T^2 \quad (12)$$

where R is the ideal gas constant and A_i, B_i, and C_i are constants for each gas.

Substituting (12) into (11) and integrating we obtain:

$$\Delta H^* = [\Sigma(\nu_i \mathrm{A}_i) + \Sigma(\nu_i)R]T + \tfrac{1}{2}\Sigma(\nu_i \mathrm{B}_i)T^2 + \tfrac{1}{3}\Sigma(\nu_i \mathrm{C}_i)T^3 + I'. \quad (13)$$

Substitution of (13) into Eq. (10) and another integration give:

$$\ln K_p^* = \frac{\Sigma(\nu_i \mathrm{A}_i) + \Sigma(\nu_i)R}{R} \ln T + \frac{\Sigma(\nu_i \mathrm{B}_i)}{2R} T + \frac{\Sigma(\nu_i \mathrm{C}_i)}{6R} T^2 - \frac{I'}{RT} + J' \quad (14)$$

Eq. (14) can be rearranged into the form

$$\log_{10} K_p^* - \frac{\Sigma(\nu_i \mathrm{A}_i) + \Sigma(\nu_i)R}{R} \log_{10} T - \frac{M\Sigma(\nu_i \mathrm{B}_i)}{2R} T - \frac{M\Sigma(\nu_i \mathrm{C}_i)}{6R} T^2 = \frac{I}{T} + J \quad (15)$$

where M is the modulus of the common logarithms, 0.43429, $\cdots$ $I = -MI'/R$ and $J = MJ'$.

When an expansion similar to (12) (but omitting the constant R) is substituted into Eq. (5) for C_{Vi}, a relation similar to (15) results in which I

[23] Beattie, Proc. Nat. Acad. Sci. **16**, 14 (1930).

and J are related to the energy and entropy constants of the reacting gases. These relations will be considered in a later paper.

III. Treatment of the Data

Eqs. (9) and (15) are the basis for the present calculations. The former relation contains only the equation of state constants of the reacting gases, while the latter contains the heat capacity constants for the reacting gases and two arbitrary constants. Thus for the calculations of the effect of both pressure and temperature on the Haber equilibrium there are used only two adjustable constants, I and J, one of which might have been determined from a heat of reaction.

The data treated are those of Haber[24] which are at 30 atmospheres and extend from 561 to 952°C; and those of Larson and Dodge[7] and of Larson[8] (working at the Fixed Nitrogen Laboratory) which extend from 10 to 1000 atmospheres and from 325 to 500°C.

The equation of state constants for the various gases have been determined[25] from the available compressibility data, and are given in Table I.

Table I. *Values of the equation of state constants for the reacting gases. Units: normal atmospheres, liters per mole, degrees Kelvin* ($T°K = t°C + 273.13$), $R = 0.08206$.

Gas	A_0	B_0	c
Hydrogen	0.1975	0.02096	0.0504×10^4
Nitrogen	1.3445	0.05046	4.20×10^4
Argon	1.2907	0.03931	5.99×10^4
Ammonia	2.3930	0.03415	476.87×10^4

It will be noted that the constants for argon have been included. The reactant gas mixtures of hydrogen and nitrogen used by Haber, Larson and Dodge, and Larson contained 0.3 volume percent (which we shall assume to mean 0.3 mole percent) of argon. This argon must be taken into account in the calculation of the mole fractions of the gases composing the equilibrium mixtures from the stated analytical results, and must be included in the summation $\Sigma(x_i A_{0i}^{1/2})$ of Eq. (9); but does not enter elsewhere.

Larson and Dodge, and Larson calculated values of K_p from their analytical results by use of an approximate formula[26] that introduced errors which are now seen to be greater than those of experiment. Accordingly the values of K_p for these data were recalculated by use of the exact expression

$$K_p = \frac{\alpha/(1+\alpha)^2}{[q - 3\alpha/2(1+\alpha)]^{3/2}[r - \alpha/2(1+\alpha)]^{1/2}p} \tag{16}$$

where α is the mole fraction of ammonia in the equilibrium mixture, q and r are the mole fractions of hydrogen and nitrogen in the reactant gas mixture,

[24] Haber, Zeits. f. Elektrochemie **21**, 89 (1915).

[25] See reference (22) for the constants for H_2, N_2, and A. The values of the constants for NH_3 are given by Beattie and Lawrence, J. Am. Chem. Soc. **52**, 6 (1930).

[26] Gillespie, Jour. Math. and Phys. **4**, 84 (1925), especially p. 95.

being 0.762 and 0.235 respectively for these data. The values of K_p given by Haber were also checked by use of (16) and the given analytical data, the values of q and r being 0.752 and 0.245 for these data.

From the mole fraction of the gases in the equilibrium mixtures and the equation of state constants given in Table I, a value of K_p^* was calculated by use of Eq. (9) corresponding to each "measured" value of K_p (computed from Eq. (16)). At each temperature the values of K_p^* resulting from the treatment of the data at that temperature should be the same within the experimental error if Eq. (9) represents the pressure variation of K_p.

In order to correlate the values of K_p^* at different temperatures with the aid of Eq. (15) the specific heat constants A_i, B_i, and C_i were derived from the empirical equations of other observers, the reduction from 1 atmosphere to zero pressure being made by use of the relation

$$c_p = c_p^* + \left[\frac{2A_0}{RT^2} + \frac{12c}{T^4}\right]p \tag{17}$$

which gives sufficiently well the effect of pressure on specific heat.[27] These constants are given in Table II.

TABLE II. *Values of the heat capacity constants of Eq. (12). Units: 15° calories per mole and per degree C; R=1.986847.*

Gas	A	10^3B	10^6C	Ref.
Hydrogen	4.66	0.70	0.00	[28]
Nitrogen	4.82	0.33	0.05	[29]
Ammonia	6.04	0.71	5.10	[30]

The values of the left hand member of Eq. (15) were computed using the values of K_p^* obtained as described above and this quantity plotted against $1/T$. The values of the two adjustable constants I and J were determined from the best straight line drawn through the points, the deviations of the observed points from this line being shown in Fig. 1.

Knowing the two constants I and J we can compute K_p for any pressure and temperature by use of Eqs. (9) and (15). When the numerical values of all of the constants are included these equations become:

[27] Beattie, Phys. Rev. **34**, 1615 (1929).

[28] Partington and Shilling, "The Specific Heat of Gases", Van Nostrand, New York, 1924, p. 209.

[29] Partington and Shilling, ibid. p. 145. See also Shilling and Partington, Phil. Mag. (7) **6**, 920 (1928).

[30] Haber and Tamaru, Zeits. f. Elektrochemie **21**, 228 (1915). The values of C_p calculated by extrapolating the equation of Haber and Tamaru do not agree very well with the measurements of Osborne, Stimson, Sligh and Cragoe, Scientific Papers of Bureau of Standards **20**, 65 (1925). However the integral of $C_p^* dT$ from 0° to 150°C is in rather good agreement with the integrated value obtained from the results of the latter investigators, the difference being 3.7 calories per mole. The constants given are sufficiently accurate for our purposes.

$$\log_{10} K_p/K_p^* = \left[\frac{0.1191849}{T} + \frac{25122730}{T^4} + \frac{38.76816}{T^2}\Sigma(x_i A_{0i}^{1/2}) + \frac{64.49429}{T^2}(\Sigma x_i A_{0i}^{1/2})^2\right] p \tag{18}$$

$$\log_{10} K_p^* = -2.691122 \log_{10} T - 5.519265 \times 10^{-5} T + 1.848863 \times 10^{-7} T^2 + \frac{2001.6}{T} + 2.6899 \tag{19}$$

where p is in atmospheres and T in degrees Kelvin; while x_i is the mole fraction of gas i in the equilibrium mixture and for A_{0i} is used the numerical value of A_0 for gas i given in Table I. In the summation $\Sigma(x_i A_{0i}^{1/2})$ the argon

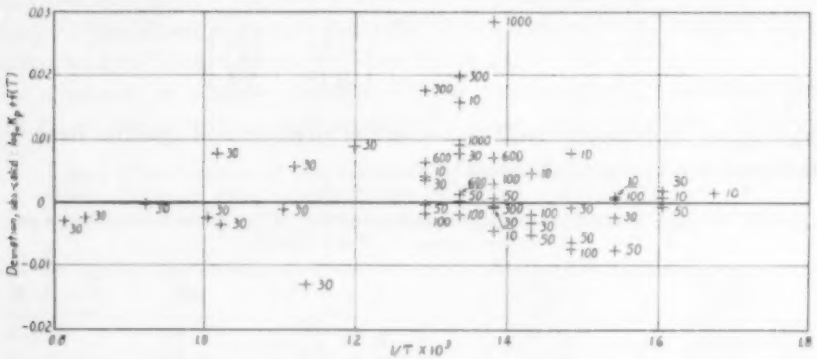

Fig. 1. Deviation of the observed value of $\log_{10} K_p + f(T)$, the left hand member of Eq. (15) from the best straight line through the points.

must be included. In evaluating this summation the experimental values were used for the x_i's. This introduces a slight inconsistency since the values of x_i used in Eq. (18) should be those resulting from the solution of this equation. However the differences between the experimental and calculated values of x_i were sufficiently small so that the use of the latter values would in no case change the last figure given for α by more than one unit and this only at the highest pressures.

In Table III are given the values of the percentages of ammonia in the equilibrium mixture α computed from the "calculated" values of K_p resulting from Eqs. (18) and (19). There are also given the observed percentages, and in the last column the percentage deviation (percentage based on the observed mole percent of ammonia found in the equilibrium mixture). For the calculation of α from K_p, which is tedious to make directly, an approximate correction formula was derived by logarithmic differentiation of Eq. (16), which gives:

$$\Delta\alpha = \frac{2.3026 \Delta \log_{10} K_p}{\frac{1}{\alpha} - \frac{2}{1+\alpha} + \left[\frac{1}{1+\alpha}\right]^2 \left[\frac{2.25}{q - 3\alpha/2(1+\alpha)} + \frac{0.25}{r - \alpha/2(1+\alpha)}\right]} \tag{20}$$

TABLE III. *Comparison of observed and calculated values of the mole percentages of ammonia in the equilibrium mixture.*

The "calculated" values of the mole percentage of ammonia α give when substituted in Eq. (16) the values of K_p computed from Eqs. (18) and (19), and may be regarded as the best available values of α.

Temperature °C	Pressure atm.	Mole percent of ammonia in equilibrium mixture. Observed	Calculated	$100\frac{\text{obs.-calcd.}}{\text{obs.}}$
		(a) Data of Fixed Nitrogen Laboratory: $q=0.762$, $r=0.235$.		
325	10	10.38	10.35	+0.29%
350	10	7.35	7.34	+0.14
	30	17.80	17.75	+0.28
	50	25.11	25.14	−0.12
375	10	5.25	5.24	+0.19
	30	13.35	13.41	−0.45
	50	19.44	19.66	−1.13
	100	30.95	30.92	+0.10
400	10	3.85	3.79	+1.56
	30	10.09	10.10	−0.10
	50	15.11	15.27	−1.06
	100	24.91	25.16	−1.00
425	10	2.80	2.77	+1.07
	30	7.59	7.64	−0.66
	50	11.71	11.82	−0.94
	100	20.23	20.29	−0.30
450	10	2.04	2.06	−0.98
	30	5.80	5.81	−0.17
	50	9.17	9.16	+0.11
	100	16.35	16.27	+0.49
	300	35.5	35.5	±0.00
	600	53.6	53.3	+0.56
	1000	69.4	68.6	+1.15
475	10	1.61	1.55	+3.73
	30	4.53	4.46	+1.55
	50	7.13	7.13	±0.00
	100	12.98	13.02	−0.31
	300	31.0	30.3	+2.26
	600	47.5	47.4	+0.21
	1000	63.5	63.2	+0.47
500	10	1.20	1.19	+0.83
	30	3.48	3.45	+0.86
	50	5.58	5.58	±0.00
	100	10.40	10.43	−0.29
	300	26.2	25.6	+2.29
	600	42.1	41.9	+0.48
		(b) Data of Haber: $q=0.752$, $r=0.245$.		
561	30	1.97_6	1.93_9	+1.98
607	30	1.270	1.307	−2.91
620	30	1.192	1.177	+1.25
631	30	1.07_8	1.07_9	−0.28
704	30	0.627_6	0.632_6	−0.80
710	30	0.618_1	0.607_3	+1.75
722	30	0.557_6	0.560_8	−0.57
812	30	0.324_8	0.324_9	−0.03
914	30	0.192_1	0.193_2	−0.57
952	30	0.161_7	0.162_8	−0.68

by means of which the change in the mole fraction of ammonia in the equilibrium mixture $\Delta\alpha$ can be computed for a given change in log K_p. Thus from each observed value of α and K_p, a value of α corresponding to the "calculated" K_p was obtained. This procedure was checked in several cases by calculation of K_p by substitution of the corrected values of α into Eq. (16).

In Fig. 2 is given a plot of the percentage deviation between the observed and calculated mole percentages of ammonia in the equilibrium mixture.

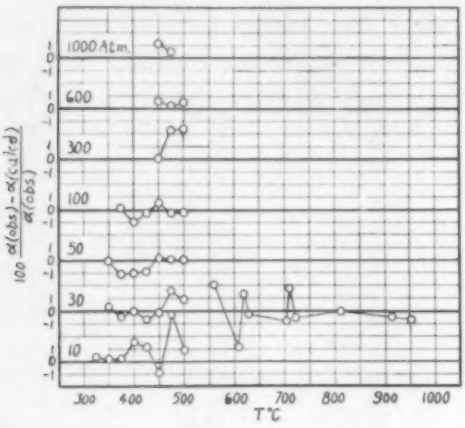

Fig. 2. Percentage deviation in the percentage α of ammonia in the equilibrium mixture. Each ordinate division represents 1%. A heavy base line representing zero deviation is used for each isobar.

IV. Discussion of the Results

The results of the calculations reported in Table III and exhibited in Figs. 1 and 2 may be briefly summarized as follows.

The average deviation in K_p for the results of the Fixed Nitrogen Laboratory is 1.18% and for those of Haber 1.09%, the average for all measurements being 1.16%. The distribution of positive and negative deviations is fairly good and it should be noted that with the exception of one point, the greatest errors do not occur at the extremes of pressure or temperature. This indicates that the equation is not failing progressively as the pressure or temperature is increased.

There is no indication of a discontinuity between the low pressure data of Larson and Dodge and the high pressure data of Larson. The discontinuity previously observed[26] in empirical smoothing was evidently produced by the use of inappropriate variables for the correlation. This is a case in which rational aid was clearly required for the discovery of appropriate variables.

The average difference between the observed and calculated mole percentages of ammonia in the equilibrium mixture, in percent of the observed mole percentage, is 0.73% for the Fixed Nitrogen Laboratory data, 1.08% for the Haber data, and 0.80% for both sets. We believe that this is well within the experimental accuracy of the measurements.

The calculated values of K_p and likewise of the percentage of ammonia α in the equilibrium mixture may be regarded as the best value deducible from the existing experimental observations. Our equation indicates that K_p and α depend on other variables than the temperature and pressure, for instance on the composition of the reactant gas mixture used in the production of ammonia (or on the equilibrium composition). Consequently Eq. (18) contains more information than can be presented in the form of a table such as Table III. This will be treated in a later paper.

V. Calculation of the Composition of the Equilibrium Mixture from the Initial Composition

The calculation of the composition of the equilibrium mixture from the initial composition of the reacting mixture cannot be very conveniently made from Eq. (9), since the x_i's in this relation are the equilibrium concentrations. However the last term of (9) is small[10] in comparison with the other terms and may be neglected for a first approximation, giving Eq. (7) which does not contain any compositions. Thus in order to compute the composition of the equilibrium mixture at any pressure and temperature when the equation of state constants and the heat capacities of the reacting gases are given and the two constants I and J are known, we proceed as follows:

(1) Compute a provisional value of K_p by use of Eqs. (7) and (15).

(2) Calculate the corresponding provisional composition of the equilibrium mixture from the equation connecting K_p and these compositions. For the ammonia synthesis equilibrium this relation is Eq. (16).

(3) Using these provisional equilibrium concentrations calculate a more exact value of K_p by use of Eq. (9), and correct the provisional equilibrium concentrations by use of an approximate correction formula similar to Eq. (20). In general even at the highest pressures no further approximation will be necessary. If required, however, these corrected equilibrium concentrations can be substituted again into Eq. (9) and a final value for K_p computed.

For the Haber equilibrium Eq. (7) becomes

$$\log_{10} K_p/K_p^* = \left[\frac{0.1191849}{T} + \frac{91.87212}{T^2} + \frac{25122730}{T^4}\right]p. \qquad (21)$$

At 475°C and 1000 atmospheres Eq. (21) gives 0.01250 for K_p and the corresponding provisional value for α is 60.5%. From (18) and the provisional composition we find a value of 0.01483 for K_p, or 62.9% for α. One further approximation gives for the mol percent of ammonia at equilibrium, 63.2%, which is identical with the value given in Table III. For this calculation we have used $q=0.762$ and $r=0.235$ in Eqs. (18) and (20).

THE DIELECTRIC CONSTANT OF CARBON DIOXIDE AS A FUNCTION OF TEMPERATURE AND DENSITY[1]

By Frederick G. Keyes and John G. Kirkwood**
Research Laboratory of Physical Chemistry, Massachusetts Institute of Technology*

(Received June 12, 1930)

Abstract

The dielectric constant of carbon dioxide has been measured over a wide range of temperature and density. It has been found that the Clausius-Mosotti function $(\epsilon-1)V/(\epsilon+2)$, although independent of temperature increases slowly with increasing density.

THE polarization of molecules by an homogeneous electric field has received adequate theoretical treatment. Both classical mechanics[2] and quantum mechanics[3] lead to the following expression for the mean electric moment, m, of a molecule in weak fields at moderately high temperatures:

$$m = \left(\alpha + \frac{\mu^2}{3kT}\right)F$$

where F is the field strength, α the sum of the electronic and atomic polarizabilities, μ the permanent electric moment of the molecule, k Boltzmann's constant, and T the absolute temperature. The applicability of the above expression is further limited by the requirements that the frequency of the applied field be lower than any of the characteristic frequencies of the molecule, and that no transitions in internal atomic and electronic energy states occur with changing temperature.

The theory has been used with a large measure of success in the study of the molecular structure of gases of low density and of substances in dilute solution. In these cases the internal polarizing field may be calculated with very little ambiguity, and it is possible to obtain a relation between the dielectric constant of the substance and the constants α and μ of its constituent molecules.

The application of the theory to gases at high densities as well as to liquids and solids, has, however, been attended by great uncertainty because of the difficulty in calculating the average internal field effective in polar-

** National Research Fellow.

* Contribution No. 231.

[1] Preliminary work on air at low densities was carried out by Miss Charlotte T. Perry who constructed the first gas cell and measuring circuits.

[2] P. Debye, Handbuch der Radiologie **6**, 600 (1925).

[3] J. H. Van Vleck, Phys. Rev. **29**, 727 (1927).

izing a molecule. The only guide in this matter has been the Clausius-Mosotti relation, which gives the molecular polarization as

$$\frac{\epsilon - 1}{\epsilon + 2} V = \frac{4\pi N}{3}\left(\alpha + \frac{\mu^2}{3kT}\right)$$

where N is the Loschmidt number, ϵ the dielectric constant, and V the molal volume. Several attempts have been made to verify the Clausius Mosotti law experimentally. Measurements of Tangl[4] indicate that is is valid up to a hundred atmospheres for air, nitrogen, and hydrogen at 20°C. It is to be noted, however, that the largest of his values of $\epsilon - 1$ are still so small that it is evident that the contribution of the polarization of the dielectric to the internal field is very small relative to the contribution of the external applied field. Measurements of Phillips[5] on the refractive index of

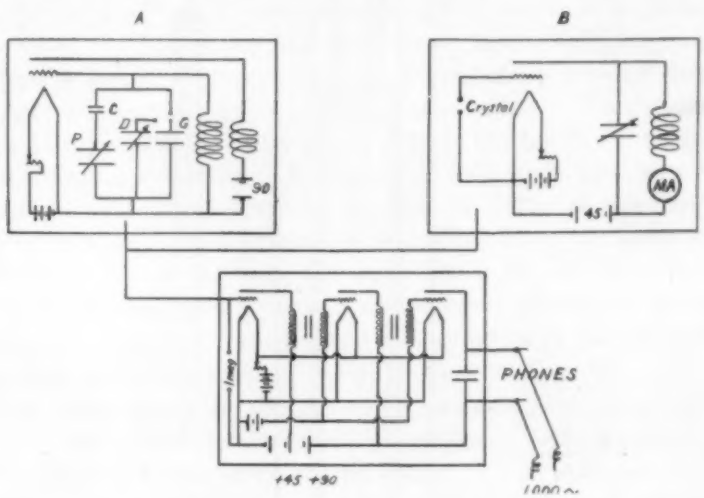

Fig. 1. Diagram of oscillator circuits.

carbon dioxide indicate that the corresponding Lorentz-Lorenz relation is valid even as far as the critical density for this substance. But the great experimental difficulties involved in the measurement of the refractive indices of compressed gases would make a verification of the values desirable.

In the present paper measurements of the dielectric constant of carbon dioxide over a wide range of temperature and density will be presented. We believe that they throw an important light on the limitations of the Clausius-Mosotti law, which the customary deduction, depending upon the cavity method for calculating the internal field, does more than suggest.

Methods and Apparatus

Measurements of the dielectric constant were carried out by a resonance method which depended upon counting the beats between two heterodyne

[4] K. Tangl, Ann. d. Physik **29**, 59 (1908).
[5] P. Phillips, Proc. Roy. Soc. **A47**, 225 (1920).

oscillators. Since this method has been widely used in recent years, a detailed description will not be undertaken. The oscillator circuits (Fig. 1) were similar to those of Zahn.[6] Oscillator *A* contained a condenser circuit consisting of the precision condenser *P*, the fixed mica condenser *C*, the gas condenser *G*, and the counterpoise condenser *D*. The precision condenser was a General Radio Variable Air Condenser, type 220, calibrated at the

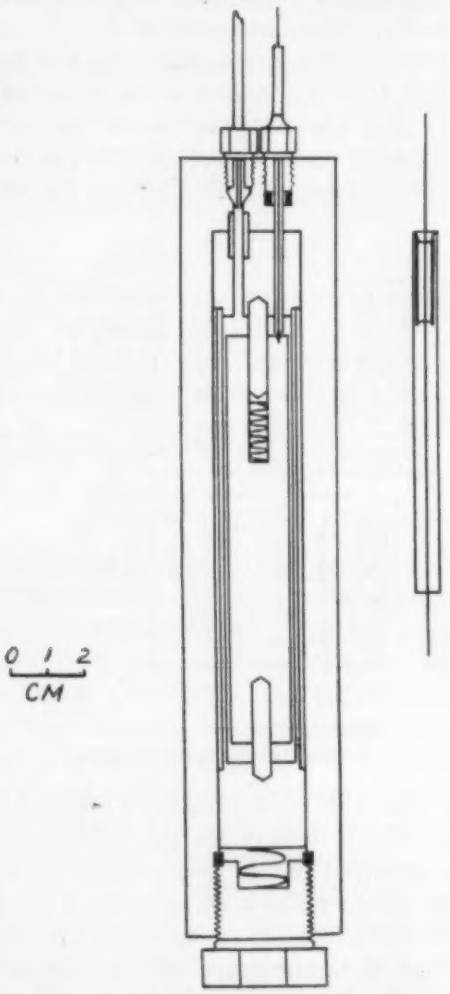

Fig. 2. Diagram of gas condenser.

Bureau of Standards. Sangamo fixed mica condensers of capacity appropriate to the magnitude of the dielectric constant to be measured occupied the position of *C*. All auxiliary capacities were calibrated in terms of the precision condenser at the working frequency. Oscillator *B* was maintained at a constant frequency of 1010 k.c. by means of a General Radio quartz crystal. The heterodyne note was amplified and then compared with the

[6] C. T. Zahn, Phys. Rev. **23**, 781 (1924).

1000 cycle note of a mechanical oscillator. The resulting beats were counted in telephone receivers.

The gas condenser, Fig. 2, was constructed of chrome vanadium steel. The high potential side consisted of a solid cylinder held in position by two quartz supports, conically ground at both ends and fitting accurately into the end members of the cell. The low potential side of the condenser consisted of a shell, one millimeter in thickness. The separation of the cylinder and shell was 0.3 mm. The length of the condenser was 16 cm. The entire cell was surrounded by a steel jacket which bore the stress of the pressure, reducing the elastic deformation of the condenser itself to a minimum. The correction for deformation due to compression of the walls never amounted to more than one percent of $\epsilon - 1$. The outer jacket was closed at the lower end and made pressure tight by means of an aluminum washer. The insulating joint, inset Fig. 2, which carried a lead from the oscillator to the inner cylinder of the condenser was constructed in the following manner. A two centimeter length of two millimeter steel tubing was welded into a seven centimeter length of three millimeter steel tubing. This was silver soldered into a fitting which was later made tight in the head of the gas cell by means of an aluminum washer. A section of lead glass capillary coated with a flux of the same coefficient of expansion as the steel was fused to the inner tube and around the platinum wire leading from the inner cylinder of the condenser. Below the seal, the lead was protected by a length of quartz capillary extending down to the point where it was made fast in the cylinder.

The free capacity of the gas cell was found to be 167.4$\mu\mu f$. It was roughly calculated to be 165$\mu\mu f$ from the dimensions of the cell.

The temperature of the gas cell was controlled in an oil bath of large heat capacity by means of a mercury regulator. Temperatures were measured with a platinum resistance thermometer.

The pressure line was constructed of Shelby steel tubing with double cone connections. Connection with the pressure gauge, of the floating piston type,[7] was made through a mercury-in-steel U.

At the beginning of a series of measurements the oil bath was brought to the desired temperature and the variable condenser D was adjusted to the same capacity as the evacuated gas cell. They could be alternately inserted into the oscillator circuit by a switch of small capacity. Gas was then admitted from a steel reservoir in the pressure line, and the pressure brought approximately to the desired value by heating or cooling the reservoir. It was finally adjusted to the proper value by means of a mercury piston compressor. From the two readings of the precision condenser with G and D alternately in the circuit, the dielectric constant could be calculated. After completing a measurement, the pressure was increased by means of the mercury piston and measurements made at regular pressure intervals. The use of the counterpoise condenser D made it possible to compensate

[7] F. G. Keyes and Brownlee, Thermodynamic Properties of Ammonia, Wiley and Sons 1916. F. G. Keyes and J. Dewey, J.O.S.A. **14**, 491 (1927).

for drift in the oscillator between measurements. The dielectric constant was calculated by the following formula, evident from the condenser circuit:

$$\epsilon - 1 = \frac{C^2(P_2 - P_1)}{(P_1 + C)(P_2 + C)G_0}.$$

Here P_1 and P_2 are the two readings of the precision condenser, C the capacity of the fixed condenser, and G_0 the free capacity of the gas condenser.

For each series of measurements, the function $(\epsilon-1)/(\epsilon+2)$ was plotted against the density. The point at which the extrapolated line intercepted the axis of $(\epsilon-1)/(\epsilon+2)$ was taken as the zero point to which all of the values of $\epsilon-1$ were referred. The intercept was in every series of measurements small and sometimes negligible. It was evidently the result of an initial extraneous capacity change attending the introduction of the gas, caused by incomplete temperature equilibrium in the evacuated gas cell.

Experimental Results

Measurements of the dielectric constant of carbon dioxide were made upon the gas at 35°, 70°, 100°; and upon the liquid at 0°. The results are listed in the following tables.

Table I. *Measurements on gaseous carbon dioxide at 100°.*

Pressure (atm.)	$\epsilon-1$	Molal volume (cc)	Density (mols/liter)	$\frac{\epsilon-1}{\epsilon+2}V$
10	0.00753	2991	0.33	7.485
20	.01549	1461	.68	7.505
30	.02404	947	1.06	7.528
40	.03333	691	1.45	7.593
50	.04306	535	1.87	7.570
60	.05269	434	2.30	7.491
70	.06447	361	2.77	7.595
80	.07707	306	3.27	7.664
90	.09005	263	3.80	7.664
100	.1041	229	4.37	7.687
126	.1456	167	5.99	7.730
151	.1912	129	7.75	7.729

Table II. *Measurements on gaseous carbon dioxide at 70°.*

Pressure (atm.)	$\epsilon-1$	Molal volume (cc)	Density (mols/liter)	$\frac{\epsilon-1}{\epsilon+2}V$
10	0.00831	2728	0.37	7.536
20	.01717	1321	.76	7.517
30	.02693	842	1.19	7.491
40	.03748	606	1.65	7.478
50	.04950	464	2.16	7.532
60	.06305	369	2.71	7.596
70	.07810	300	3.33	7.612
80	.09616	248	4.03	7.702
90	.1159	207	4.83	7.699
100	.1396	173	5.78	7.693
126	.2165	115	8.70	7.739
151	.3072	84.7	11.81	7.868

TABLE III. *Measurements on gaseous carbon dioxide at 35°.*

Pressure (atm.)	$\epsilon-1$	Molal volume (cc)	Density (mols/liter)	$\frac{\epsilon-1}{\epsilon+2}V$
10	0.00971	2352	0.43	7.588
20	.02021	1135	.88	7.595
30	.03228	713	1.40	7.590
40	.04649	497	2.07	7.584
50	.06461	363	2.75	7.653
60	.08838	269	3.72	7.698
70	.1309	191	5.24	7.986
80	.3146	88.5	11.23	7.986
90	.4206	65.6	15.24	8.066
100	.4559	58.3	17.15	7.691

TABLE IV. *Measurements on liquid carbon dioxide at 0°C.*

Pressure (atm.)	$\epsilon-1$	Molal volume (cc)	Density (mols/liter)	$\frac{\epsilon-1}{\epsilon+2}V$
50	0.6016	46.75	21.39	7.809
75	.6187	45.56	21.95	7.790
100	.6321	44.97	22.24	7.826
125	.6425	44.34	22.55	7.821
150	.6526	43.78	22.84	7.822
175	.6603	43.31	23.09	7.813
200	.6674	42.85	23.34	7.798

The molal volumes were obtained from Amagat's pressure volume temperature measurements, the best at present available for carbon dioxide. The Clausius-Mosotti function, $(\epsilon-1)/(\epsilon+2)V$, is expressed in cubic centimeters

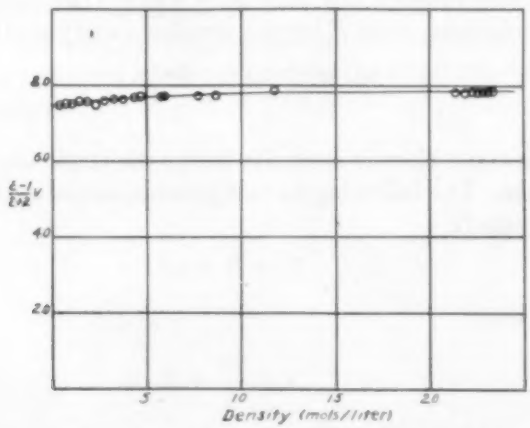

Fig. 3. The points above the density 20 are for the liquid at 0°; the others are for the gas at 100°.

per mol. At 35° above 60 atmospheres, the Clausius-Mosotti function, when plotted against the density, shows very great irregularity. We believe this to be due to error in Amagat's data, extremely probable in view of the very large value of $-(dV/dP)$ in this region. Except in this region, the

maximum error in measurements of Amagat which have been used is probably about 0.25%.

Extrapolation of $(\epsilon-1)V/(\epsilon+2)$ calculated from our measurements yields a value of about 7.4 cc in the low density region covered by other investigators. This is in satisfactory agreement with the value 7.3 cc calculated from the measurements of Zahn.[8] We estimate the maximum random experimental error in $\epsilon-1$ to be $\pm 0.5\%$. With increasing density, it becomes progressively smaller. Absolute error originating in the calibration of the apparatus, we believe to be not more than one percent.

Discussion

Within the limit of our experimental error, the Clausius-Mosotti function $(\epsilon-1)V/(\epsilon+2)$ is found to be independent of temperature. It is not, however, independent of density. To illustrate its behavior, $(\epsilon-1)V/(\epsilon+2)$, for the gas at 100°, as well as for the liquid at 0°, has been plotted against density in Fig. 3. The curve rises slowly with increasing density, but there is a gradual decrease in slope so that when the liquid densities are reached, it has become, within the limit of observation, parallel to the density axis. It is to be remembered however, that the deviation from the line

$$\frac{\epsilon-1}{\epsilon+2}V = \text{constant}$$

required by the Clausius-Mosotti law in its usual form, is small. Indeed the total increment in $(\epsilon-1)V/(\epsilon+2)$ in passing from the gas at the lowest density of the measurement to the liquid is only four percent.

A few brief speculations relative to the cause of the observed deviation from the Clausius-Mosotti law may be of value. The calculation of the average internal polarizing field F by the familiar cavity method yields

$$F = E + \frac{4\pi}{3}P \tag{1}$$

where E is the mean electric intensity in the dielectric and P the polarization per unit volume. The following formal generalization of the above expression has been suggested:

$$F = E + \nu P. \tag{1a}$$

Let us write

$$\nu = \frac{4\pi}{3} + \beta.$$

We also have at our disposal the familiar relations involving the displacement, D.

$$D = \epsilon E \tag{2}$$

$$D = E + 4\pi P \tag{3}$$

[8] C. T. Zahn, Phys. Rev. **27**, 455 (1926).

Moreover

$$P = \frac{N}{V} p_0 F$$

where N is the Loschmidt number; V the molal volume, and p_0 the molecular polarizability, $\alpha + \mu^2/3kT$. Elimination of D, E, and F from (1a), (2) and (3) gives

$$\frac{\epsilon - 1}{\epsilon + 2} V = \frac{4\pi N}{3} p_0 \frac{1}{1 - \beta N p_0 \rho} \tag{4}$$

where ρ is the density in mols per cubic centimeter. Eq. (4) may be made to conform to the curve of Fig. 3, if the polarizability p_0 is assumed to be a function of density of appropriate form. Change in the polarizability of a molecule with density could be attributed only to a change in the internal structure of the molecule or to molecular association. Such an hypothesis does not seem desirable without independent confirmatory evidence and in any case is of a purely qualitative nature. The fact that the carbon dioxide molecule gives no evidence of possessing a permanent electric moment is unfavorable to this type of explanation. Indeed, the polarizability, α, associated with the perturbation of the electronic orbits is not greatly affected even by interaction involving actual valence forces.

We are inclined to believe the cavity method of calculating the internal field is inexact and that the formal generalization (1a) is valid only if β is a function of density. If this view is accepted, we must conclude that the Clausius-Mosotti function, while furnishing a good approximation, is not an exact representation of the molecular polarization, $4\pi N p_0/3$, except in the limiting case of infinitely low density.

In conclusion, we wish to express our cordial appreciation to Professor H. B. Phillips for continued advice regarding the electrical circuits employed in these measurements.

SOME APPLICATIONS OF THE THEORY OF PLASTIC DEFORMATIONS OF DUCTILE METALS

By A. Nadai
Research Laboratories, Westinghouse E. and M. Co.*

(Received July 7, 1930)

Abstract

A brief account will be given of the principal conditions which are available to express the equilibrium of stress in the plastic state of ductile metals. These conditions will be discussed for the case of rotationary symmetry in a plastic body. As an example several cases of plastic flow in a thick walled cylinder subjected to high internal pressure with and without longitudinal expansion will be treated. The distribution of stress during yielding is given for a long cylinder and for a flat ring, both subjected to radial pressure. How yielding and the plastic deformation spread through the walls of the cylinder has been shown.

1. General Considerations

CERTAIN ductile metals such as mild steel, if subjected to a state of homogeneous stress with increasing principal stresses show the remarkable behaviour of having a sharply defined limit of plasticity. It has been shown by numerous tests made within the last few years that for practical purposes, the reaching of the plastic state in a ductile polycrystalline metal such as steel, which has a well-defined limit of plasticity, under ordinary temperatures, depends on a stress-condition. This means that the plastic state is reached if a certain condition containing only the principal components of the stress tensor is fulfilled. Under a sharp limit of plasticity or a well-defined yield point it is understood, that permanent parts of the strain begin to develop only if the stresses satisfy the condition of plasticity mentioned before, and if the quantity expressed by the principal stresses on the left side of this condition is smaller than its limiting value a polycrystalline metal behaves like a perfectly elastic and isotropic material.

In this statement, the fact is included that in the first approximation it shall be permitted to assume that within certain amounts of plastic strain (of some few percent of the principal unit elongations) after the plastic limit has been reached, the three principal stresses do not change appreciably. In other words, it is permitted to assume that when plasticity is reached, the stresses remain constant and are independent of deformation as well as of the velocity of deformation.

A further consequence of these assumptions is that in general in a stressed body there will exist an elastic and a plastic region (or more plastic regions separated by elastic regions). In the plastic regions the deformations will have an elastic as well as a permanent part, while in the elastic region no permanent deformations exist.

* Scientific Paper No. 434.

By these restricting assumptions, the treatment of the problems of plastic flow is reduced from a question of dynamics to a question of pure statics. Hence, the six components of the stress tensor will have to be computed from the quasistatic equilibrium conditions, which will be identical with the equilibrium conditions of the stresses in an elastic material. They will also have to satisfy the conditions of plasticity and certain conditions expressing the manner in which stress and strain are connected during a steady, slow plastic flow.

It should be mentioned, that it is not difficult to work out the analysis of plastic flow under more general assumptions and to find solutions in certain simpler cases of plastic flow. It is thought to include in the assumptions such an experimentally known phenomenon as work hardening,[1] i.e. the fact that the stresses under which a metal is deformed plastically are dependent on the deformation and that the yield stresses gradually increase from zero with deformation. It is known that in soft annealed metals such as soft polycrystalline aluminum or copper, the plastic parts of the deformation are already developing under small stresses. In such metals a "yield point" cannot be observed if the annealed metal is stressed from the unstressed state. (But a yield point may appear and can be observed, if the metal was stretched to a certain amount, unloaded, and *again* stressed in the same sense). In this case, it is also not possible to distinguish a "plastic" portion within the stressed body from an "elastic" region, because the permanent part of the resulting strains increase gradually from zero and are hence encountered in all elements of the stressed piece of metal.

In this paper such cases will not be included, because the stress curves obtained by the simpler assumptions show already the characteristic facts related to the special cases of plastic flow treated here.

Regarding another effect, namely, the effect of the velocity of plastic deformation on the magnitude of the yield stresses producing this, it should be mentioned that tests made with single metal crystals as well as with polycrystalline ductile metals have shown that this effect is more pronounced at elevated temperatures (phenomenon of creep). For the plastic flow of steel at room temperatures, the effect can be considered as of a secondary order, if such phenomena as impact are excluded.

2. The Plane Problem

If the stresses and strains depend only on two coordinates, for example, x, y, if rectangular or r, ϕ, if polar coordinates are chosen, we may distinguish two special cases in a similar manner as in the theory of elastic plane problems. We designate with s_x, s_y, s_z, the three components of normal stresses, with s_{xy} the only component of shearing stress, which is not vanishing, with ϵ_x, ϵ_y, ϵ_z the three components of strain and with ϵ_{xy} the unit shear component which is not vanishing.

[1] Some cases including the effect of work hardening were worked out in detail in A.S.M.E. Transactions, 1930.

3. The Plane Strain

In this case the unit extension ϵ_z=constant, is a principal strain. Many examples of engineering practice are comprised under this heading. One case is especially simple, namely if $\epsilon_z=0$. In this case the normal stress s_z is

$$s_z = \tfrac{1}{2}(s_x + s_y). \tag{1}$$

This follows from a rule of plastic flow.[2] If s_1, s_2, and s_3 are the principal stresses and ϵ_1, ϵ_2, ϵ_3 the principal strains during a steady slow plastic flow in which the directions of principal stresses do not change relatively to the stressed material, then

$$\frac{2s_2 - s_1 - s_3}{s_1 - s_3} = \frac{2\epsilon_2 - \epsilon_1 - \epsilon_3}{\epsilon_1 - \epsilon_3}. \tag{2}$$

Taking, for example, $\epsilon_3=\epsilon_2=0$ and assuming that the volume during plastic flow is not changed:

$$\epsilon_1 + \epsilon_2 + \epsilon_3 = \epsilon_x + \epsilon_y + \epsilon_z = 0. \tag{3}$$

We see that

$$\epsilon_1 = -\epsilon_2 \text{ or } \epsilon_x = -\epsilon_y$$

and with this (2) reduced to (1).

The following statements referring to plane strain with one vanishing principal strain $\epsilon_z=0$ are limited to plastic regions where the permanent parts of the strains ϵ_x and ϵ_y are predominant, so that the elastic parts may be neglected. We may put then simply

$$s_z = \tfrac{1}{2}(s_x + s_y) \tag{4}$$

and we see that the principal stresses s_1 and s_2 are given by

$$\begin{aligned} s_1 &= \frac{s_x + s_y}{2} + s_m \\ s_2 &= \frac{s_x + s_y}{2} - s_m \end{aligned} \tag{5}$$

Where s_m designates the principal shearing stress

$$s_m^2 = \frac{(s_x + s_y)^2}{4} + s_{xy}^2. \tag{6}$$

In order to express the fact that we have an equilibrium of stresses in the plastic state, we have to introduce *a condition of plasticity*. Taking the general form of the second degree

$$(s_1 - s_2)^2 + (s_2 - s_3)^2 + (s_3 - s_1)^2 = 2s_0^2 = \text{const.}^3 \tag{7}$$

[2] See Der bildsame Zustand der Werkstoffe, J. Springer, Berlin, 1927 S. 51., or On the Mechanics of the Plastic State of Metals. A.S.M.E. Transactions, Applied Mechanics Division, 1930.

[3] This condition of plasticity was proposed by R. v. Mises, by Huber, and H. Hencky and has been verified by the tests of W. Lode and Ros-Eichinger.

Where the constant s_0 designates the yield stress in pure tension, we see that this expression simplifies considerably and becomes

$$(s_1 - s_2)^2 = \frac{4s_0^2}{3} = \text{const.} \tag{8}$$

Writing the constant $s_0/3^{\frac{1}{2}} = k$ and using (5) and (6) this last equation can be expressed in terms of s_x, s_y, and s_{xy} as follows:

$$(s_x - s_y)^2 + 4s_{xy}^2 = 4k^2 = \text{const.} \tag{9}$$

This is the condition of plasticity for plane strain $\epsilon_z = 0$, which has to be combined now with the conditions of equilibrium.

$$\frac{\partial s_x}{\partial x} + \frac{\partial s_{xy}}{\partial y} = 0, \qquad \frac{\partial s_y}{\partial y} + \frac{\partial s_{xy}}{\partial x} = 0. \tag{10}$$

A complete theory of integration of the three simultaneous equations for the three unknown functions s_x, s_y, and s_{xy}, has been worked out by H. Hencky[4] and R. v. Mises.[5] Solutions in polar coordinates including some properties of the so-called slip lines, which facilitate the discussion of the solutions have been investigated by the author.[6]

We may remark that the theory of plane plastic flow under the assumption $\epsilon_z = 0$ of a vanishing lateral extension ϵ_z is mathematically identical with the so-called theory of maximum constant shear. The only difference is, that the constant k in Eq. (9) has to be taken in the first theory $k = 2s_0/3^{\frac{1}{2}} = 0.577s_0$ and in the second $k = s_0/2 = 0.500s_0$.

If ϵ_z is not vanishing, but equals a constant, the theory is more complicated; one case is given below.

4. Plane Stress

In this case $s_z = 0$, the normal stress perpendicular to the xy plane vanishes. This case occurs in a thin sheet which is loaded in its plane, for example in a plate containing a circular hole and stretched in all directions by a uniform tensile stress. As in this case, the third principal stress $s_3 = 0$ vanishes, the condition of plasticity[7] becomes in terms of principal stresses,

$$s_1^2 - s_1 s_2 + s_2^2 = s_0^2 = \text{constant} \tag{11}$$

or in terms of the stress components s_x, s_y, and s_{xy}, in rectangular coordinates

$$s_x^2 - s_x s_y + s_y^2 + 3s_{xy}^2 = s_0^2 = \text{const.} \tag{12}$$

This equation again has to be combined with the two equilibrium conditions (10).

In rectangular coordinates s_1 and s_2, equation (11) is that of an ellipse with the semi-axes $a = (2)^{\frac{1}{2}} s_0$ and $b = (2/3)^{\frac{1}{2}} s_0$. Hence in a thin plate stressed

[4] H. Hencky, Zeits. f. ang. Math. und Mechanik **3**, 241 (1923).
[5] R. v. Mises, Zeits. f. ang. Math. und Mechanik **5**, 147 (1925).
[6] A. Nadai, Zeits. f. Physik, 106 (1924).
[7] The author is much indebted to Mr. H. Friedman, who has carried out the computation.

in its plane, no normal stress component can ever become larger than $2s_0/3^{\frac{1}{2}}$, which is the maximum value of either s_1 or s_2 as coordinates of a point of the ellipse. This is $=1.155s_0$. There is therefore a distinct difference between the two states of plane stress $\epsilon_z=0$ and $s_z=0$, if plastic flow is considered. In the case $\epsilon_z=0$, the normal stresses may exceed the yield stress s_0 for pure tension considerably, and there are singularities of the stresses possible (for example, a "center of compression"). In the second case $s_z=0$, no stress component can become infinite, and singularities are not possible in this sense.

5. Long Cylinder Yielding Plastically under Internal Pressure.

Let s_r and s_t be the radial and tangential normal stress components and s_z the axial normal stress. If the cylinder is not expanding or contracting in axial direction, the unit extension $\epsilon_z=0$ and the stress components s_r and s_t are given by the two equations

$$s_t - s_r = \pm \frac{2s_0}{3} \tag{13}$$

$$\frac{d(rs_r)}{dr} - s_t = 0. \tag{14}$$

The first is the condition of plasticity, the second the condition of equilibrium. A set of solutions satisfying these two equations and the two boun-

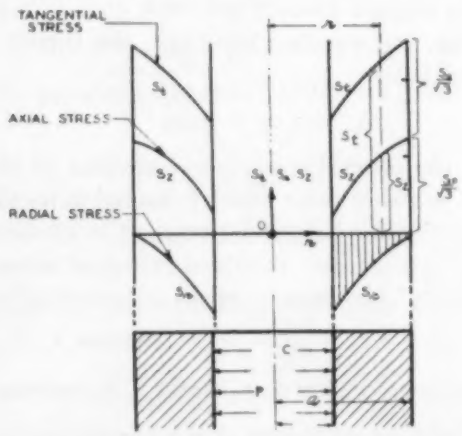

Fig. 1. Plastic flow in thick hollow cylinder stress distribution when axial elongation ϵ_z is equal to zero.

dary conditions, that at the inner surface for $r=a$ the radial stress must become equal to the pressure p and at the outer surface for $r=b$, s_r must vanish:

$$\text{for } r = a,\ s_r = -p$$

$$\text{and for } r = b,\ s_r = 0$$

is given by

$$\left.\begin{aligned} s_r &= -\frac{2s_0}{3^{1/2}}\ln\frac{b}{r} \\ s_t &= \frac{2s_0}{3^{1/2}}\left(1-\ln\frac{b}{r}\right) \\ s_z &= \frac{2s_0}{3^{1/2}}\left(\frac{1}{2}-\ln\frac{b}{r}\right) \end{aligned}\right\} \tag{15}$$

This distribution of stress is shown in Fig. 1. The pressure p under which the cylinder will yield from the inner to the outer surface is found by the first formula of (15) by taking $r=a$:

$$p = \frac{2s_0}{3^{1/2}}\ln\frac{b}{a}. \tag{16}$$

There s_0 designates the yield stress in pure tension.

6. Yielding of Thin Plate with Circular Hole or of Flat Rings Radially Stressed

In this case $s_z=0$ and we have to combine Eq. (12) or if expressed in terms of the radial and tangential stress components s_r and s_t:

$$s_t^2 - s_t s_r + s_r^2 = s_0^2 = \text{constant} \tag{17}$$

with the equilibrium condition

$$r\cdot\frac{ds_r}{dr} = s_t - s_r. \tag{18}$$

Using here instead of s_t and s_r two new stress variables

$$\left.\begin{aligned} s &= (s_t + s_r):2 \\ s' &= (s_t - s_r):2. \end{aligned}\right\} \tag{19}$$

We see that (17) takes the simpler form:

$$s^2 + 3s'^2 = s_0^2. \tag{20}$$

To satisfy this equation we put

$$s = s_0\sin\theta,\ s' = \frac{s_0}{3^{1/2}}\cos\theta \tag{21}$$

and (18) takes the form

$$\frac{rd}{dr}(s - s') = 2s' \tag{22}$$

or

$$\frac{rd}{dr}\left(\sin\left(\theta - \frac{\pi}{6}\right)\right) = \cos\theta \tag{23}$$

whence by integration:

$$r^2 = c^2 e^{3^{1/2}\cdot\theta}\cos\theta \tag{24}$$

where c is a constant of integration. To determine its value, we have to express the radial and tangential stresses with the help of θ

$$\left.\begin{aligned} s_r &= \frac{2s_0}{3^{1/2}} \sin\left(\theta - \frac{\pi}{6}\right) \\ s_t &= \frac{2s_0}{3^{1/2}} \sin\left(\theta + \frac{\pi}{6}\right) \end{aligned}\right\} \tag{25}$$

If for $r=b$ the radial stress s_r shall vanish, we see that θ must be taken

$$\text{for } r = b, \theta = \theta_b = \frac{\pi}{6}.$$

If $\theta<\pi/6$, s_r will become negative, the radial stress will be a compression. On the contrary, if $\theta>\pi/6$, $s_r>0$ and will be a tensile stress. Evidently the former case corresponds to the case of a ring with internal pressure and the latter case to a ring or plate with external tension. Now taking $\theta_b=\pi/6$ for $r=b$, the constant c in (24) is determined:

$$b^2 = c^2 \cdot \frac{3^{1/2}}{2} \cdot e^{\pi(3)^{1/2}/6} \tag{26}$$

We get finally from (24) and (26) the relation between the radius r and the parameter θ

$$r^2 = \frac{2b^2}{3^{1/2}} \cdot e^{3^{1/2}(\theta-\pi/6)} \cdot \cos\theta. \tag{27}$$

Thus the complete solution is obtained.

To get the pressure or tension p which must act on the circumference $r=a$ and produce yielding, the angle $\theta=\theta_a$ must be computed from the last equation by taking $r=a$ and thus p is given by

$$p = \frac{2s_0}{3^{1/2}} \sin\left(\frac{\pi}{6} - \theta_a\right). \tag{28}$$

To each value of θ_a corresponds a value of the ratio b/a and a radial and tangential stress s_r and s_t for $r=a$. This has been shown in Fig. 2, where the ratio of the two radii b/a and the two stress components at the circle $r=a$ are represented by curves. To find the pressure p for a given ring, we have to read the value of s_r for $r=a$ (that is of p) below the value of b/a. The stress distribution is also shown in Fig. 3, where the radial and the tangential stresses s_r and s_t are plotted as functions of the radial distance r of a point of the ring from its center.

Comparing the type of curves in Fig. 3 with the logarithmic curves for the distribution of stress obtained for the case of the yielding of a long cylinder under internal pressure p, (Fig. 1.) it can be seen that in the latter case with the increasing thickness of the hollow cylinder the pressure p is indefinitely increasing. In the case of a flat ring with free faces and stressed radially by

a pressure p acting on the inner circle, however, equilibrium is only possible, if the ratio of the outer to the inner radius is

$$1 < b/a < 2.963$$

For $b/a > 2.963$, no plastic equilibrium is possible in which the ring yields from its inner to its outer cylindrical surface.

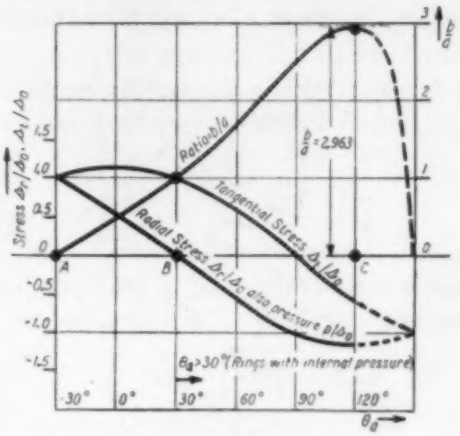

Fig. 2. Radial and tangential stress and ratio b/a plotted against parameter θ in circular plates with holes yielding under radial pressure.

7. Partial Yielding

Until now the only cases that have been treated were those in which the material in a hollow cylinder was yielding from the inner to the outer surface. If the pressure in a tube is gradually increasing from zero, the tube will be

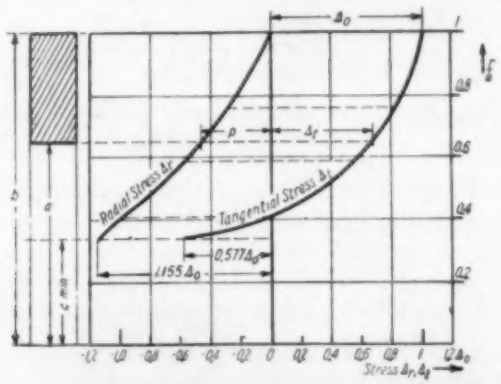

Fig. 3. Distribution of stress in circular plates with central hole, yielding under radial pressure p. a inner, b outer, radius to yield strain in tension.

stressed at first only elastically. Later, with the increasing pressure an annular region will become plastic, growing from the inner surface. For such values of the pressure, the tube must be divided in two portions $a < r < c$, and $c < r < b$, of which the former is stressed beyond the limit of plasticity and the latter only elastically. If, for example, the tube cannot expand in

the axial direction ($\epsilon_z=0$), first yield will occur at a pressure given by the well known formula

$$p_0 = \left(1 - \frac{a^2}{b^2}\right)\frac{p_0}{3^{1/2}} \tag{29}$$

derived from the stress conditions of an elastic tube. If $p>p_0$, the elastic stress distribution in the region $r>c$, will be obtained from the stresses for an elastic cylinder

$$\left.\begin{aligned} s_r' &= c_1 + \frac{c_2}{r^2} \\ s_t' &= c_1 - \frac{c_2}{r^2} \\ s_z' &= 2\nu c_1 \end{aligned}\right\} \tag{30}$$

where ν is Poisson's ratio and c_1 and c_2 are two constants, and the plastic stress distribution in the region $r<c$ will be given by

$$\left.\begin{aligned} s_r &= c_3 + \frac{2s_0}{3^{1/2}}\ln r \\ s_t &= c_3 + \frac{2s_0}{3^{1/2}}(\ln r + 1) \\ s_z &= c_3 + \frac{2s_0}{3^{1/2}}\left(\ln r + \frac{1}{2}\right) \end{aligned}\right\} \tag{31}$$

The three constants c_1, c_2, and c_3 can be determined from the conditions of continuity and the boundary conditions of the cylindrical surfaces $r=a$ and $r=b$. The result of the computation is

Stresses in the elastic portion $c<r<b$

$$\left\{\begin{aligned} s_r' &= \frac{s_0}{3^{1/2}}\gamma^2\left(\frac{1}{u^2} - 1\right) \\ s_t' &= \frac{s_0}{3^{1/2}}\gamma^2\left(\frac{1}{u^2} + 1\right) \\ s_z' &= \frac{2s_0\nu}{3^{1/2}}\gamma^2 \end{aligned}\right. \tag{32}$$

Stresses in the plastic portion $a<r<c$

$$\left\{\begin{aligned} s_r &= -p + \frac{2s_0}{3^{1/2}}\ln\frac{u}{\alpha} \\ s_t &= -p + \frac{2s_0}{3^{1/2}}\left(\ln\frac{u}{\alpha} + 1\right) \\ s_z &= -p + \frac{2s_0}{3^{1/2}}\left(\ln\frac{\mu}{\alpha} + \frac{1}{2}\right) \end{aligned}\right. \tag{33}$$

where

$$\frac{r}{b} = u, \quad \frac{a}{b} = \alpha \quad \text{and} \quad \frac{c}{b} = \gamma. \tag{34}$$

The pressure required to produce yielding in the tube to the radius $r=c$ is found by

$$p = \frac{s_0}{3^{1/2}}\left(2\ln\frac{\gamma}{\alpha} + 1 - \gamma^2\right) \tag{35}$$

where s_0 is the yield stress in pure tension.

In Fig. 4 the pressures p required to produce progressive yielding through a hollow cylinder are shown for different ratios of $\alpha=a/b=0.1,\ 0.2\ldots$.[7] The abscissae in this figure are $\gamma=c/b$, the ordinates the pressure p. For example, the curve belonging to $\alpha=0.8$ shows how the pressure p in a tube

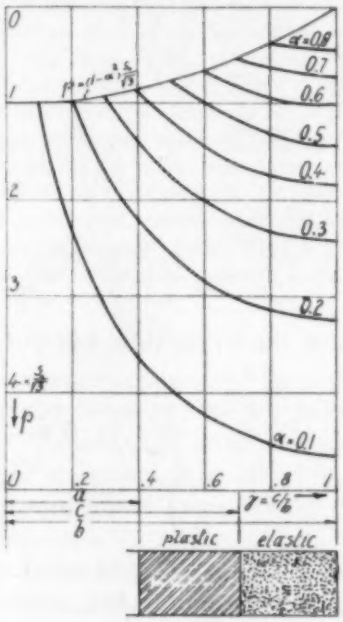

Fig. 4. Pressure p producing yielding plotted against ratio $\nu=c/b$. c is radius of surface to which plastic region extends.

of the ratio a/b of the inner to the outer radius $=0.8$ would increase with the increasing radius c of the cylindrical surface, to which yielding has penetrated in the tube.

8. Tube Subjected to Internal Pressure and Axial Load

The theory of the plastic flow of a thick walled cylinder which is exposed to a high internal pressure and which is permitted also to expand in the axial direction is considerably more complicated than the cases mentioned above with no axial expansion $\epsilon_z=0$. This case has been worked out elsewhere.[8] We quote here the formulae. Let s and s' be

$$s = \frac{s_z + s_t}{2} - s_r, \quad s' = \frac{s_z - s_t}{2} \tag{36}$$

[8] A.S.M.E. Trans., Applied Mechanics Division, 1930.

and u a variable parameter given by

$$u = \frac{1}{3^{1/2}}\left(1 + \frac{2\epsilon_a}{\epsilon_z}\right)\frac{a^2}{r^2} \tag{37}$$

where ϵ_a is the tangential unit elongation at the outer surface $r=a$ of the cylinder and ϵ_z the axial unit elongation, assumed to be uniform over the whole cross section of the tube, a is the outer radius, and b the inner radius of the tube.

Then the stress distribution is given by

axial stress:

$$s_z = s + s' + s_r \tag{38}$$

tangential stress:

$$s_t = s - s' + s_r \tag{39}$$

where

$$s = \frac{s_0}{2(3)^{1/2}} \cdot \frac{3^{1/2} + 3u}{(1 + u^2)^{1/2}} \qquad s' = \frac{s_0}{2(3)^{1/2}} \cdot \frac{3^{1/2} - u}{(1 + u^2)^{1/2}} \tag{40}$$

and the radial stress is equal to

$$s_r = \frac{s_0}{3^{1/2}} \log_e \frac{u_a + (1 + u_a^2)^{1/2}}{u + (1 + u^2)^{1/2}}. \tag{41}$$

The pressure p under which the whole tube will yield is

$$p = \frac{s_0}{3^{1/2}} \log_e \frac{u_b + (1 + u_b^2)^{1/2}}{u_a + (1 + u_a^2)^{1/2}} \tag{42}$$

with

$$u_a = \frac{1}{3^{1/2}}\left(1 + \frac{2\epsilon_a}{\epsilon_z}\right) \quad \text{and} \quad u_b = \frac{a^2}{b^2}u_a. \tag{43}$$

A special case is that of a tube with no axial elongation $\epsilon_z = 0$, where both constants u_a and u_b become infinite, but a careful consideration shows that the formulae (38–41) converge exactly to the simpler formulae already given by the Eqs. (15).

9. Summary

The effect of the lateral (axial) extension E_z in the cases of plane plastic flow, which has not been considered until now, was investigated. The theory of plane plastic flow becomes more simple in two cases, namely (1) if the unit extension ϵ_z in the direction perpendicular to the plane xy vanishes: $\epsilon_z = 0$ and (2) if the normal stress s_z on this plane is zero, that is, in the case of a thin sheet stressed in its plane. These cases were worked out for radial symmetry, containing the radial distribution of stress in a thick walled tube yielding under a high internal pressure, and assuming the tube restrained to expand in the axial direction and the radial distribution of stress in a flat circular ring yielding under radial pressure or tension.

Under the latter cases is included that of the plastic equilibrium of an infinite plate stretched uniformly in its plane and containing a circular hoe . The case of partial yielding of a thick walled tube was shown and the pressures computed under which yielding penetrates to a given depth.

AN ATTEMPT TO DETECT COLLISIONS OF PHOTONS

By A. L. Hughes and G. E. M. Jauncey
Department of Physics, Washington University

(Received June 16, 1930)

Abstract

Assuming that light is corpuscular and that collisions between light corpuscles (i.e. photons) can occur, it is shown that two photons of identical frequency ν, moving along paths which make an angle 2θ with each other, will on collision give rise to a photon of frequency $\nu(1+\cos\theta)$ travelling forward along the line bisecting the angle. To test this, two beams of sunlight (one suitably deflected by a mirror), filtered through red glass, were passed through lenses 24 cm in diameter and of 33 cm focal length, so that the beams, whose axes made an angle of 120° with each other, intersected at a common focus. The point of intersection of the beams was examined through a green filter with the dark-adapted eye. No light was detected. Calculations show that if the photon has a cross section, its area must be less than 3×10^{-20} cm^2. From a result of Lord Rayleigh, some writers have suggested an area of the order of λ^2 for the photon. Our result shows the area to be of the order of $10^{-10}\lambda^2$.

1 Introduction

PHYSICISTS have become accustomed to the idea of the corpuscular nature of molecules, atoms, electrons, protons, alpha-particles and also, in some cases, of light. Collisions of molecules with molecules as in the kinetic theory of gases, of electrons with atoms as in critical potentials, of alpha-particles with the nuclei of atoms as in the Rutherford scattering experiments and of photons with electrons as in the Compton effect are familiar phenomena. It occurred to the writers that, if light has a corpuscular structure, collision phenomena should occur when two light beams cross each other—in other words, that two photons may collide and produce photons with energies different from the energies of the original photons.

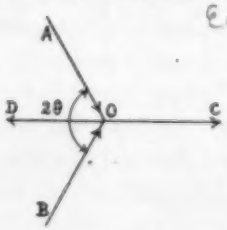

Fig. 1.

2. Theory

Let two photons, each of energy $h\nu$, approach each other and collide as in Fig. 1, and let the angle between AO and BO, the paths of the two photons, be 2θ. The problem is to find the energy of the photon which after the collision proceeds along the bisector OC. If two photons arise out of the colli-

sion of two photons and if the principle of conservation of momentum may be applied to photons, the other resulting photon must travel along OD. Let the photon travelling along OC have the energy $h\nu_1$ and the photon along OD an energy $h\nu_2$. The conservation of energy gives

$$h\nu_1 + h\nu_2 = 2h\nu \tag{1}$$

and the conservation of momentum gives

$$h\nu_1/c - h\nu_2/c = 2(h\nu/c)\cos\theta \tag{2}$$

Whence

$$\nu_1 = \nu(1 + \cos\theta) \tag{3}$$

$$\nu_2 = \nu(1 - \cos\theta) \tag{4}$$

or, in terms of wave-length,

$$\lambda_1 = \lambda/(1 + \cos\theta) \tag{5}$$

$$\lambda_2 = \lambda/(1 - \cos\theta) \tag{6}$$

The theory thus leads to the expectation that, if two beams of monochromatic light cross each other, as in Fig. 1, light of a wave-length shorter than that of the two original beams will be observed in the direction OC. In particular, if $2\theta = 120°$ and $\lambda = 6000$A, the wave-length observed in the direction OC will be 4000A. Accordingly an experiment was devised to test this prediction of the theory.

3. Experimental Method

A wide beam of sunlight entered a light-tight box AB through the lens C in Fig. 2 and was brought to a focus at O. A second beam after reflection

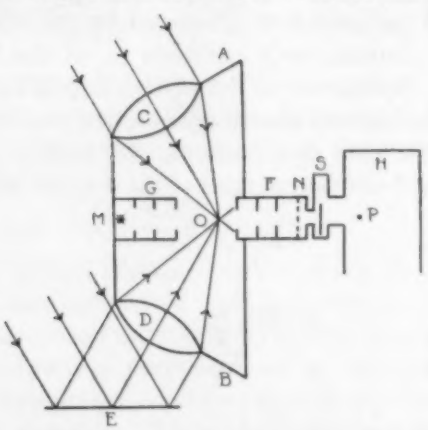

Fig. 2. Diagram of apparatus.

from the mirror E, which is rigidly attached to the box AB, passed through the lens D and was also brought to a focus at O. Thus two cones of light intersected at O. The diameter of each lens was 24 cm. For each lens, the focal length for the central and peripheral rays was 34.3 and 31.7 respectively. The area of cross section of the light passing through each lens was a minimum at 33 cm. The diameter of the

sun's image at this point was estimated to be 0.4 cm. This image occurred for each lens at O in Fig. 2. The head of the observer was enclosed in a light-tight helmet H, his eye being at P. The observer looked through the tube F and into the tube G. Both F and G contained diaphragms so as to prevent stray light from entering the eye. At the far end M of the tube G a small lamp was placed. The object of this lamp was to attract the attention of the eye to the direction PM. The line PM passed through O. The directions of the light rays passing through O were such that no direct rays from the lenses could enter the eye. The inside of the box AB was blackened so as to reduce scattering. Dustfree air was blown through the box AB in order to remove dust motes from the air at O and also to keep the inside of the box reasonably cool. The sunlight which entered the box through the lenses previously passed through plates of red glass. A quantitative curve for the transmission of this red glass was very kindly made for us by Professor H. M. Randall, of the University of Michigan, who found that the red glass transmitted wave-lengths between 5500 and 30,000A. At N was placed a green filter, the transmission curve of which was supplied by the Eastman Kodak Company. The green filter transmitted light of wave-length shorter than 5200A. At S was placed a shutter. The observer prepared his eye by sitting with his head in the helmet for 15 minutes. The lamp M was then switched on and the shutter S opened. The lamp was connected in series with a rheostat and increasing resistance was put into the circuit until the light of the lamp was just perceptible. After opening the lamp switch, the observer opened and closed the shutter S in order to determine whether or not green light was coming from O. The result was negative. The observer then rested his eye for a second 15 minutes when more observations were taken, a third set of observations were made at 45 minutes from the time when the helmet was first put on and a fourth set at 60 minutes. The eye is almost completely dark-adapted in 60 minutes, but nevertheless even after this time the result was negative.

As a check on the observations, a sliding shutter was made so that the proportion of sunlight entering the lenses could be suddenly changed from no light entering lens C and 100 percent of light entering lens D, to 50 percent entering each lens, and to no light entering lens D and 100 percent entering lens C. This shutter arrangement was outside the box AB and is not shown in Fig. 2. In whatever position the shutter was the same total amount of light passes through O. In the 50–50 percent position of the shutter the two light beams crossed at O and conditions were such as to allow collisions of photons, while in the 100–0 percent positions of the shutter the two light beams did not cross at O. While one person operated the shutter, another person who was the observer with his head in the helmet called whether or not he noticed a change in the light when a change was made in the position of the shutter. The usual observation was that there was complete darkness and no change. In those cases where the observer judged a change, there was no correlation between the observation and the position of the shutter, and the result was therefore negative. In order that the result might not depend

upon a particular observer, five different observers were used. All agreed in giving a negative result.

The apparatus was mounted so that the upper lens could be kept pointing toward the sun. The angle between the central rays passing through each lens was 120°. The peripheral rays of one lens made with the peripheral rays of the other lens angles varying from 80° to 160°. No lenses were used between the eye at P and O in Fig. 2, because of the well-known fact that the brightness of an object as seen by the eye cannot be increased by a lens system.

4. Discussion of Results

The wave-lengths after collision at various angles, as calculated from Eq. (5), are shown in Table I.

Table I. *Change of wave-length on collision.*

Original wave-length	Wave-length after collision Collision angle 80°	120°	160°
5500A	3110A	3670A	4680A
6000	3400	4000	5110
7000	3970	4660	5960
8000	4530	5330	6810
9000	5100	6000	7670

It is seen that wave-lengths between 5500 and 9000A in the original beams produce wave-lengths after collision which can penetrate the green filter N in Fig. 2. Since the sensitivity of the eye rapidly decreases as the wave-length decreases below 4500A we shall consider only those wave-lengths between 4500 and 5000A which pass through the green filter. Let us assume that these are produced by the central rays passing through the lenses, then we are interested only in the wave-lengths 6750 to 7500A in the original beams. From data which were very kindly supplied to us by Dr. C. G. Abbot of the Smithsonian Institution, we estimate that the rate at which the energy of sunlight in a range 6750 to 7500A is incident on a surface perpendicular to the beam is about 0.12 cal/min. cm^2 at midday in the springtime in St. Louis. The area of each lens is 453 cm^2 and the rate at which energy passes through each lens is therefore 54.4 cal/min. The coefficient of transmission for the red glass in the range 6750 to 7500A is 0.45 and the average wave-length is 7125A so that there are 3.7×10^{20} photons per minute passing through each lens. When the sliding shutter is used in the experiment in the 50–50 percent position, the number of photons in each beam passing through O in Fig. 2 is 1.85×10^{20} per minute. For simplicity we shall treat the beams which intersect at O as two square cylinders of side 4 mm, with 1.85×10^{20} photons passing through each cylinder per minute. Within a volume $(4\times4\times4)/\sin 120°$ mm^3 of one cylinder there will be at any instant of time 4.6×10^7 photons. Bombarding them from the second beam there will be 3.1×10^{18} photons/sec. If the effective collision area of each photon is A cm,^{2} the total area of the photons in the first beam presented to the photons in the second

beam is $4.6\times10^{7}\times A$. The chance of a photon in the second beam colliding with any photon in the first beam is $4.6\times10^{7}\times A/(0.4\times0.4)=2.9\times10^{8}\times A$. The total number of collisions per second will then be $9\times10^{21}\times A$. Ives[1] estimates that the pupil of the dark-adapted eye has a diameter of about 6 mm. The distance of the eye of the observer from O in Fig. 2 is 25 cm, so that the solid angle subtended by the pupil at O is 0.00044. Let us suppose that after collision the resulting photons are equally likely to travel in any direction. The number of photons entering the eye per second will then be $0.00044\times9\times10^{21}\times A/4\pi=3.3\times10^{22}\times$A.

There is some variation amongst different writers as to the energy of the smallest light stimulus which can be detected by the eye. Reeves[2] gives 19.5×10^{-10} erg/sec, Russell[3] gives 7.7×10^{-10} erg/sec and Buisson[4] 12.5×10^{-10} erg/sec. If we take the average of these values we shall at least have the correct order of magnitude. Assuming a wave-length of 5000A, we find that the minimal light stimulus is given by 336 photons entering the eye per second. Ives[1] gives the minimal light stimulus as 1000 photons per second. Using this value of Ives so as to be on the safe side, we obtain

$$3.3\times10^{22}\times A=10^{3}$$

whence

$$A=3\times10^{-20}\text{ cm.}^{2}$$

If the photons are thought of as having a circular cross section, this corresponds to a diameter of 2×10^{-10} cm. The result of our experiment is therefore that the collision area of a photon, if such a thing exists, is less than 3×10^{-20} cm^2.

Photons are supposed to obey the laws of the Bose-Einstein statistics and no two photons can occupy the same cell. A physical interpretation of this may be that no two photons can be at the same place at the same time, and hence there can be no collisions of photons. Our result is compatible with this view. Lord Rayleigh[5] has considered the case of a resonator being actuated by a plane wave and has calculated the area of the primary wave front which propagates the same energy as is dispersed by the resonator. This area is $\lambda^2\pi$ where λ is the wave-length. This result has been said by some writers to indicate that the area of the cross section of a photon is of the order of λ^2. According to this idea then we might have expected an area of cross section of 2.5×10^{-9} cm^2. Our experiment, however, gives an area less than 3×10^{-20} cm^2, which is of the order of 10^{-10} times the expected area.

We are indebted for information concerning the dark-adapted eye to Professor Allen of the University of Manitoba, to Dr. Jones of the Eastman Kodak Company, and to Dr. Priest of the Bureau of Standards. From this information, we have learned that the dark-adapted eye is the best instrument for making the observations in this experiment.

[1] H. E. Ives, Astrophys. J. **44**, 124 (1916).
[2] P. Reeves, Astrophys. J. **46**, 167 (1917).
[3] H. N. Russell, Astrophys. J. **45**, 60 (1917).
[4] H. Buisson, Astrophys. J. **46**, 296 (1917).
[5] Lord Raleigh, Phil. Mag. **29**, 209 (1915).

LETTERS TO THE EDITOR

Prompt publication of brief reports of important discoveries in physics may be secured by addressing them to this department. Closing dates for this department are, for the first issue of the month, the twenty-eighth of the preceding month; for the second issue, the thirteenth of the month. The Board of Editors does not hold itself responsible for the opinions expressed by the correspondents.

Band Intensities

The Franck principle concerning the most probable transitions between electronic states in molecules, has succeeded in explaining most of the cases of band intensities to which attention has been called. During the past two years I have observed several examples of band spectrum excitation which show extreme deviations from the above principle. Several such examples have already been pointed out by Birge in the National Research Council bulletin "Molecular Spectra in Gases." As far as I am aware however, very little attention has been paid to these exceptional cases, and it is my purpose here to point out one of the most interesting ones.

Lord Rayleigh studied the effect on the nitrogen afterglow of the admixture of inert gases with the glowing material and found that the intensity distribution among the first positive bands of nitrogen was considerably modified (especially so by helium). Now one can readily account for relative intensity changes between progressions in band systems, since these can be caused by variations in the relative number of molecules in the various initial vibrational states. The relative intensities of bands within a progression however, are definitely fixed by the Franck principle and can be determined from the potential energy curves associated with the states involved in the emission of the bands. As far as I know, no discussion has as yet been given of relative intensity variations within progressions. It is just this type of intensity variation that is met in the experiments of Rayleigh and in some of my recent experiments. While no considerable discussion of this type of intensity change will be attempted at this time, it is worthwhile noting that should the cause of this intensity variation be a collision between a nitrogen molecule and a helium atom, then no energy transfer need take place during the process. If an energy transfer should take place between the two particles it would result in a change in the kinetic energies of the particles or in a redistribution of their excited states. Neither one of these would account for any variation of intensities within a progression. Since the purpose of this note has been simply to call attention to this type of intensity variation in band spectra further discussion will be left for a later communication.

JOSEPH KAPLAN
University of California at Los Angeles,
Los Angeles, California,
August 6, 1930.

X-Ray Scattering Coefficient as a Function of Wave-length and Atomic Number

Direct measurements of the mass scattering coefficient of x-rays have been made by Barkla and Dunlop, Hewlett, Mertz and others. In this experiment a modification of the ionization chamber used by Mertz was employed to measure simultaneously the radiation scattered at all azimuths. Improvements were made in the purity of the radiation employed and the measurements were extended to longer wave-lengths and higher atomic numbers.

The source of x-rays was a water-cooled Coolidge tungsten-target tube. The current supplied to it was rectified by a full-wave kenetron rectifier operating on a balanced circuit. The tube was operated at from 35 to 50 peak K.V. with a current of 35 m.a.

Characteristic fluorescence radiation was

excited in radiators of Sn, Ag, Mo, and Se placed in the direct beam from the tube. The nature of the radiation was tested roughly by absorption measurements and found to be substantially pure.

This fluorescence radiation was collimated by a slit system into a beam one-half inch square in the path of which were placed hollow cylindrical scattering blocks of C, Al, Fe, Ag, Sn, and Au.

Scattered radiation from these blocks passed into a large ionization chamber the window of which was shaped like a segment of a sphere with the scattering block at its center. The chamber was of uniform depth and was filled with argon at atmospheric pressure.

A second ionization chamber, likewise filled with argon, was placed in the direct beam for absorption measurements. The electrodes of both chambers were connected to a Compton electrometer the sensitivity of which was about 10,000 mm scale divisions per volt at 2 meters. Lead screens were used to reduce the air scattering as much as possible.

The scattering blocks were mounted on supports of silk thread attached to wire frames and were so placed in the path of the x-ray beam that radiation from every part of the first slit reached every part of the scattering block. Suitable filters were used to prevent fluorescence radiation excited in the scatterers from entering the ionization chamber.

The cylindrical scattering blocks were made of such a thickness that one-half of the radiation used was absorbed by passing through them. For convenience the scattering of carbon, iron, silver, tin and gold was compared with aluminum and where it was not possible to obtain scattering blocks absorbing exactly half of the radiation, great care was taken to compare them with aluminum blocks of the same absorbing power.

The gold foil used was mounted on a celluloid base and was compared with an aluminum block also mounted on celluloid. In correcting for the scattering of the celluloid an amount was deducted equal to one-half the scattering from a celluloid block of the same dimensions.

For this and for all the other blocks corrections were made for air scattering and natural leak of the electrometer system. Due to the length of air path in front of the chamber and to the size of the chamber itself these were appreciable and their magnitude for longer wave-lengths and higher atomic numbers than those used made measurements by this method impracticable.

The results obtained are shown in Table I. The effective wave-length of the radiation used was determined by averaging the wave-lengths of the $K\alpha$ and $K\beta$ lines weighted by their relative intensitives.

TABLE I. *Ratio of mass scattering coefficients of elements to aluminum for different wave-lengths.*

Scatterer	Radiator			
	Sn	Ag	Mo	Se
Au	5.49	6.75		
Sn	2.33	2.82	3.44	
Ag		2.65	3.51	
Fe	1.41	1.65	2.09	
C	1.07	0.95	0.87	0.79
Effective wave-length (calc.)	0.48 A	0.55	0.70	1.09

ERROL N. COADE

Ryerson Physical Laboratory,
University of Chicago,
July 25, 1930.

Fluorescent Dry Plates for Photographic Photometry

We have recently shown (J.O.S.A. **20**, 313, 1930) that problems of homochromatic photographic photometry can be greatly simplified (especially in the Schumann region, where they had previously been impracticable) by coating ordinary dry plates with

fluorescent oils in the manner which Duclaux and Jeantet used to obtain increased sensitivity at short wave-lengths. We now find that a similar result can be obtained much more conveniently by using a dry transparent coating containing an aesculine solution as the fluorescing agent, while broadening of images and other difficulties can be minimized by making this coating an integral part of the plate. A Cramer Contrast Process Plate usually shows extreme variations of contrast between 3700 and 2300A; when such a plate was coated by pouring over it a mixture of two parts saturated solution of aesculine in water and one part 5% gelatine solution in water, which was allowed to dry for three days, it showed uniform contrast over the same range. A much more uniform coating can be obtained in this way than with the oils, and nothing need be removed prior to development, which should, however, be about twice as long as usual. The variation of sensitivity with wave-length is much less than with ordinary plates, and we believe that it can be made as negligible as the variation of contrast. The presence of the fluorescent layer appears to decrease greatly the amount of chemical fog produced, as was clearly shown by coating plates in certain regions only.

While the method can be applied in principle at all wave-lengths, its satisfactory extension to the region below 2000A depends on finding a carrier more transparent in that region than gelatin, while it could be used at wave-lengths greater than 3700A by coating a red sensitive plate with a substance fluorescing in that region. Preliminary experiments with a solution of chlorophyll have proven successful in giving uniform contrast up to where the green absorption band begins.

It should be emphasized that a decrease in sensitivity results at many wave-lengths when the fluorescent coating is used, as is indeed true of oil coatings also. This is usually an advantage in photometry, since the decrease is greatest at long wave-lengths where most other causes unite to give the greatest response. We expect to publish shortly a detailed account of our new methods of fluorescent photometry, which promise to greatly simplify not only homochromatic but heterochromatic photographic photometry as well.

GEORGE R. HARRISON
PHILIP A. LEIGHTON

Stanford University,
August 1, 1930.

BOOK REVIEWS

Einführung in die Theorie der Wärme, being volume V of Einführung in die Theoretische Physik. MAX PLANCK. 251 pages, 15×22.5 cm, S. Hirzel, Leipzig, 1930. Price 8 RM, bound, 10 RM.

This is the fifth and final volume of Planck's series on theoretical physics designed for reference by the student who wishes either to supplement a lecture course or even to work the subject up by himself. The first volume on general mechanics is already in its fourth edition. The second, third and fourth volumes deal respectively with the mechanics of deformable bodies, electricity and magnetism, and theoretical optics.

The book is divided into four parts: thermodynamics, heat conduction, thermal radiation, and atomistics and quantum theory. The first and third parts cover much the same ground as Planck's two books on general thermodynamics and thermal radiation, except that they are of necessity shorter and cannot go so much into the details of the applications. The second part, except for an interesting application of the second law to derive a necessary restriction which the equation of heat conduction must satisfy, is mostly occupied with the solution of the simpler problems of heat flow with different sorts of boundary conditions which were the conventional subject matter of books on the older mathematical physics, and is different in character from the rest of the book. The fourth part constitutes the most novel part, and is responsible for the somewhat unusual position of this volume on heat after the volumes on electrodynamics and theoretical optics. In this part the statistical method is introduced, the statistical significance of the thermodynamic concepts of temperature, entropy, and thermodynamic potential is developed, and applications made in deducing the equations of state of perfect gases and perfect solids and the value of the chemical constant. The close welding of the points of view of formal classical thermodynamics and statistical theory which is achieved in this book is very important for the student, and is something to which more attention might be paid in courses of instruction in this country.

The fundamental point of view of Planck in expounding the concepts at the basis of his statistical treatment may be described as "classical". It is a great merit of his clear exposition that the reader is driven to feel the inadequacy of many of these concepts in the light of the Heisenberg principle. Statistical mechanics cannot much longer avoid the task of making a clean-cut formulation of what is fundamentally observable and what is invention in its treatment of "microscopic states".

P. W. BRIDGMAN

Les Rayons X. J. THIBAUD. Pp. 218. Figs. 77. Librairie Armand Colin, Paris, 1930. Price 10 f. 50 (60 cents).

The excellence of the Collection Armand Colin and the favorable rate of exchange are two sound arguments for requiring of graduate students an early familiarity with French. Dr. Thibaud's book in this series gives a concise and lucid account of the important aspects of x-rays and their relation to allied physical problems. About one quarter of the text is usefully devoted to technique and applications; another short section deals with radiations in adjoining regions of the spectrum (gamma-rays and very soft x-rays) illustrating particularly the recent investigations of the author. Complicated mathematical discussions are avoided; formulas are in general quoted without derivation, but a bibliography shows where the information may be found if required. Unfortunately, the pocket size (4½×7 inches) of the volume makes some of the diagrams inconveniently small, and, as in many French texts, there is no adequate index. The book is to be recommended to those who desire a general survey of the subject before proceeding to the detailed study of some particular branch of x-rays.

THOMAS H. OSGOOD

X-Rays. B. L. Worsnop. Pp. viii+101. Figs. 36. E. P. Dutton and Company Inc., New York, 1930. Price $1.10.

This small volume is designed to provide for advanced students and for others whose main interest lies in some other field of physics a concise account of the subject of x-rays. The author gives a clear exposition of the phenomena of the production of x-rays, crystal reflection, scattering, emission and absorption and the photoelectric effect, with good descriptions of the fundamental methods of experiment. The last chapter deals with refraction and total reflection. Intermediate students studying x-rays for the first time in some detail will find in the easier portions of the book a useful summary of their subject.

The print and diagrams are excellent; there is an adequate list of standard reference books followed by a complete index.

Thomas H. Osgood

Jahrbuch des Forschungs. Instituts der Allgemeinen Elektricitäts-Gesellschaft, Erster Band, 1928–1929. Pp. 240. Julius Springer, Berlin, 1930.

This is a complete and uniform reprinting of thirty-five articles published by members of the staff of the Research Institute of the German General Electric Company during the years 1928 and 1929. The articles are arranged in groups according to subject matter (acoustics, electron physics, atomic physics, etc.) and each group is preceded by a brief statement concerning the material contained therein. In an introduction Dr. C. Ramsauer, the director, explains the aims and policies of the Laboratory and the purpose of the year book of which this is Volume I.

Among the papers of particular interest to physicists are those by Ramsauer and Kollath and by Bruche on the apparent cross-sectional areas of various atoms and molecules as determined by the Ramsauer method, and the numerous ones by Rupp on the diffraction of electrons.

The volume contains also a record of the public appearances of members of the staff together with a list of résumés and popular expositions published during the year but not reprinted in the present collection.

It is evident that every feature of this book has received most careful consideration, and that no expense has been spared to make it a model publication of its kind.

C. J. Davisson

PROCEEDINGS

OF THE

AMERICAN PHYSICAL SOCIETY

MINUTES OF THE EUGENE MEETING, JUNE 19–21, 1930

The 164th regular meeting of the American Physical society was held in Room 103, Deady Hall, University of Oregon, Eugene, Oregon, on Thursday afternoon, June 19, Friday June 20, and Saturday morning, June 21, in affiliation with Section B, Physics, of the Pacific Division of the American Association for the Advancement of Science.

The session on Thursday afternoon consisted of a joint symposium between the American Physical Society and the Astronomical Society of the Pacific and the general topic was the red shift in the spectra of distant light sources and its physical interpretation. There were three papers by invitation as follows:

1. **Apparent velocity shifts in the spectra of faint nebulae..**—MILTON L. HUMASON, *Mt. Wilson Observatory.*
2. **Distances of nebulae and their correlation with apparent velocities.**—EDWIN HUBBLE, *Mt. Wilson Observatory.*
3. **Significance of the velocity-distance relation from the standpoint of general relativity.**—RICHARD C. TOLMAN, *California Institute of Technology.*

On Friday morning preceding the presentation of papers the regular business session or meeting was opened for discussion of any business which might arise. On nomination Professor W. P. Boynton, Chairman of the Department of Physics, University of Oregon, presided at the meeting. It was moved, seconded and voted that the date of the 167th meeting of the American Physical Society which had been scheduled to be held at the University of California at Los Angeles on December 5 and 6, 1930, be changed as follows: The 167th meeting of the American Physical Society will be held at the University of California at Los Angeles on December 12 and 13, 1930, the meeting being a joint meeting between the American Physical Society and the Acoustical Society of America.

Following the morning session on Friday, there was a joint luncheon of the astronomers and the members of the American Physical Society at which 50 members were present.

Following the session on Saturday morning, June 21, the meeting adjourned, there having been 18 papers on the regular program and 7 papers on the supplementary program of which numbers 10, 16 and 25 were read by title. The abstracts of these papers are given on the following pages. An **Author Index** will be found at the end.

LEONARD B. LOEB, *Secretary for Pacific Coast.*

ABSTRACTS

1. The near infrared spectrum of Hg. H. J. UNGER, *University of Oregon.* (*Introduced by E. D. McAlister.*)—With a self-recording spectrometer the infrared spectrum of the Hg arc has been studied in the region 1 to 2μ. Several lines hitherto observed as single have been resolved into two or more lines. Of special interest are the groups of lines near 1.7μ and 1.2μ which contain the first and second members of the fundamental triplet series. The results obtained indicate that possibly the fundamental triplets are composed of six lines grouped as in the diffuse series.

2. Continuous spectrum in the region 500–1100. J. J. HOPFIELD. *University of California.* —An intense continuous spectrum has been observed in helium in the region 500–1100A. This is the only continuous spectrum known extending throughout the range 500–900A, and it therefore allows one to explore this interesting region for absorption spectra. I think the grating mounting used imposes the present ultraviolet limit of this spectrum. This spectrum is most intense when the helium bands are best developed, showing that they are closely related phenomena. To produce it the helium should be fairly pure, at a few millimeters pressure and a mild condensed discharge should be used. The spectrum contains the neon and helium lines which are useful as standards. It may also be satisfactorily observed in the second order. The spectrum resembles the continuous spectrum of hydrogen in the Schumann region. Its analogous explanation may be as follows. Two helium atoms each excited to the 2^3S state unite to form the molecule. The energy representing these changes is about 41.8 volts. If the electronic configuration of this molecule changes to that of the "normal," unstable state it immediately dissociates emitting 41.8 volts of energy. The continuous extension of this spectrum towards the red is due to the non-quantitized kinetic energy subtracted from the above amount by the unbound atoms.

3. High resolution in the near infrared. E. D. MCALISTER, *University of Oregon.*—With two 60° and one 30° prism (all of flint glass 4 inches high, 6 inches length of face) and a parabolic mirror 5.5 in. in diameter and 24 in. focal length in the Littrow form of mounting an effective slit width of 6A is obtained in the region 1 to 2μ. This type of mounting gives a dispersion equivalent to 5 sixty degree prisms. A special type of thermocouple is used for detection. The spectrograph is self-recording. With a galvanometer distance of 5 meters the zero drift in one hour's time is usually less than one millimeter. The construction of the thermocouple and housing are discussed and typical spectrograms are exhibited.

4. Some properties of the third positive carbon and associated bands. JOSEPH KAPLAN, *University of California at Los Angeles.*—The third positive group of CO, and the two systems usually associated with it, the $5B$ and $3A$, have been studied under a variety of excitation conditions in an attempt to excite progressions other than the $v'=0$ ones. Some interesting observations have been made. No progressions other than the $v'=0$ ones have been observed in spite of the fact that each of these groups has been intensely excited. This, together with other facts and observations can be interpreted as indicating that the levels involved in these three systems are triplet levels. A new system of bands similar in appearance to these bands has been observed. The 0-0 and 0-1 bands of the $5B$ group are exactly similar in appearance, but differ strikingly from the higher members of the group. The diffuse double-headed band observed outside the third head of the 0-0 $5B$ band and ascribed to CO_2 by Asundi is thought to be a real part of the CO band since a similar doublet is observed in the 0-1 band. A pair of complex but similar bands have been observed on the long wave-length side of the 0-0 $5B$ band and the 0-1 third positive band.

5. The classification of iron lines. HAROLD D. BABCOCK, *Mount Wilson Observatory.*—In an earlier discussion, (Astrophys. J. **67**, 240, 1928), mean energy-levels were found for both upper and lower terms associated with each temperature class and pressure group. Repeating this work with more data, with weights proportional to the numbers of lines dependent on each term, and including King's study of dissymmetry in the high-current arc, (Atrophys. J.

62, 238, 1925), a broad parallelism is found between the three systems of classification. The terms of iron fall into three significant groups: 1, even terms of low level; 2, even terms of high level; 3, odd terms of medium level. The methods of classification may have a physical basis in the characteristics of these groups of terms. The energy level of a term, its odd or even character, and its part in the transition, i.e., whether it is the upper or the lower term involved, are factors which apparently determine the kind of lines associated with the term. This review of the data for iron may thus assist in the converse problem of finding the terms from observations of the position and peculiarities of a spectral line.

6. Reflection of x-rays from thin metallic films. Jos. E. Henderson and E. B. Jordan, *University of Washington.*—The critical angles of reflection for zirconium filtered molybdenum radiation have been investigated for sputtered gold and silver films of thicknesses ranging from very thin transparent films to thick opaque films. The gold films were backed with glass and the silver films with gold. Curves are plotted showing the critical angle as ordinate and thickness of the film as abscissa. For the gold on glass the curve rises, as the thickness increases, from the value for glass to a maximum value and then falls to a value which is independent of the thickness of the gold and therefore characteristic of gold. This value is approximately two-thirds of the maximum. As the above is a case for a material with critical angle larger than the backing material, silver on gold was investigated in order to obtain the opposite condition. The curve in this case again rises to a maximum greater than for gold alone for small thicknesses, falling to a value for large thicknesses which is less than the value for gold alone. A study of gold on silver is now in progress.

7. Experiments on the relative intensities of x-ray lines in the *L*-spectrum of tantalum. Victor Hicks, *University of California.*—The relative intensities of 17 lines in the *L*-spectrum of Ta have been investigated by the ionization spectrometer. The following precautions were taken: (1) the rays were taken at a glancing angle of 45° from a polished Ta surface, (2) a Ta filament was used, (3) the slits were enclosed in an arm of the tube, reducing the air path of the rays to 7 cm, (4) the coefficient of reflection of the crystal used was measured for the various wave-lengths by means of the double-spectrometer, (5) the absorption coefficients of the mica windows used were directly measured, (6) the rays were completely absorbed in methyl iodide vapor of known pressure, and (7) the slits were sufficiently wide to eliminate effects arising from the different natural widths of the lines. Measurements were taken at 30.6 K.V. and 20.7 K.V. and corrected to high voltage. The results for lines of small wave-length separation agree well with previous results of Allison and Armstrong and Jönsson on tungsten. For lines of larger wave-length separation ($L\alpha_1$, $L\beta_1$) the results of Jönsson are not confirmed, but the previous qualitative estimates of Allison and Armstrong are substantiated. The assumption that the ionization currents produced are proportional to the relative intensities is supported by recent work of A. H. Compton. If the ν^4 correction is made to the intensities at high voltage the sum rules are approximately valid except for lines having initial state L_1. The intensity results are:

	l	α_2	α_1	η	β_4	β_1	β_3	β_2	β_7	$\beta_5+\beta_{10}$
Rel. Int. at 30.6 K.V.	1.5	10.2	100	1.3	9.4	92.6	13.5	40.6	0.8	1.1
Rel. Int. at high V.	1.5	10.2	100	1.4	11.1	102.7	15.9	40.6	0.8	1.1

	β_6	γ_4	γ_1	γ_6	γ_2	γ_3	γ_4
Rel. Int. at 30.6 K.V.	0.8	1.24	29.1	0.6	4.98	7.08	2.20
Rel. Int. at high V.	0.8	1.38	32.3	0.7	5.88	8.37	2.60

8. Electronic emission from a metal target: bombarded with positive ions. C. L. Utterback and W. Geer, *University of Washington.*—Metal targets have been bombarded by positive ions whose energies varied from 200 to 750 volts, while the characteristics of the electron emission were studied. The secondary emission and positive ion currents were measured by galvanometers of sensitivities $8 \cdot 10^{-11}$ amperes and $6 \cdot 10^{-10}$ amperes, respectively. The secondary

emission has been found to depend upon the previous treatment of the target, especially in regard to the kind and amount of gas adsorbed and to the duration of the bombardment. These studies were made with positive ion currents as low as $3 \cdot 10^{-9}$ amperes, which is a smaller current than has been heretofore used in this connection.

9. The scattering of electrons in small angles by gas molecules and its effect on the electron absorption coefficient. METTA CLARE GREEN, *University of California.*—An indirect study of the scattering of electrons by gas molecules was made by measuring electron absorption coefficients in an apparatus containing a Faraday cylinder of variable aperture. A straight path method was used in which electrons from an oxide-coated filament were given a desired acceleration and made to traverse a 7.5 path to the collector. A retarding potential between the cylinder and its shield kept out all electrons which had suffered inelastic collisions as well as those which had been scattered outside of the collector opening. Measurements were made in argon, helium, hydrogen, and mercury vapor at accelerating potentials ranging from 11 to 196 volts. The radius of the cylinder aperture was varied from one hundredth to one tenth of the path length. No consistent variation of absorption coefficient with opening was found in any case. Theoretical calculations based on scattering laws obtained from inverse square or fifth power laws of force predicted relatively large variations. Calculations made assuming uniform scattering or the Sommerfeld law indicated small changes of the same order of magnitude as the observed experimental deviations.

10. The magnetic properties of dilute cobalt alloys. F. WOODBRIDGE CONSTANT, *California Institute of Technology.*—Continuing the investigation of the ferromagnetic properties of the cobalt atom when it is further and further isolated from other cobal, atoms by the presence of intervening non-ferromagnetic atoms, alloys of still higher platinum concentration than those previously reported on, (Phys. Rev. **34**, 1217, 1929), were tested magnetically. As found before, decreasing the cobalt content decreased the Curie point and magnetic hysteresis, the former, on the absolute scale, falling linearly. For comparison, similar alloys of palladium and cobalt were investigated, and found to behave similarly, thus confirming the view that the ferromagnetism of these alloys may be attributed to the cobalt atoms. The following table gives the Curie points in degrees Kelvin, and the maximum intensity of magnetization obtainable at the temperature of liquid air, (−194° C.):

	Curie Point	I_{max}
10 % Co—90 % Pt	522°K	364
5 % Co—95 % Pt	322°K	254
3 % Co—97 % Pt	191°K	104
1.5% Co—98.5% Pt	82°K	7
10 % Co—90 % Pd	508°K	223
5 % Co—95 % Pd	355°K	193

11. Discovery and rough measurement of a new electron inertia effect. S. J. BARNETT, *University of California at Los Angeles and California Institute of Technology.*—This effect, like its converse (Tolman and Stewart), was in the mind of Maxwell long ago (Treatise §574): An e.m.f. applied to a metallic conductor drives the free electrons and the remainder in opposite directions. A solenoid S is suspended vertical in a neutral region. If traversed by a current with its own natural frequency $\nu = \omega/2\pi$, the coil has a magnetic moment $\mu = M \sin \omega t$, and resonant vibration with amplitude A_M occurs. The rod holding the solenoid carries a magnet below, with horizontal moment m_0, at the center of a small fixed Helmholtz coil H (constant Γ) with axis normal to m_0. This coil, if traversed by a current $i = I \sin(\omega t + \epsilon)$, produces an amplitude A_I. When A_M is small theory gives

$$\left| 2\frac{m}{e} \right| = \frac{A_M}{A_I} \cdot \frac{\Gamma m_0 I}{\omega M}$$

If S is surrounded by a longer solenoid S' (constant γ) properly connected in circuit (resistance R) with H, the sum of the torque on S due to electron inertia ($-2m/e \cdot \dot{\mu}$) and that on the mag-

net $(-\Gamma\gamma m_0 \cdot \dot{\mu})/R$, together with the amplitude, will vanish for one value R_0 of R. Then $-2m/e = (\Gamma\gamma m_0)/R_0$. For copper $2m/e$ has been determined both ways. The sign (from null method) proves e negative, and the magnitude is that expected within the limits of the experimental error (about 10%). The theory has been worked out completely. For large amplitudes the inertia torque contains a term involving the number of electrons per unit volume, whose determination refinements may perhaps make possible.

12. The recombination of ions in air and oxygen in relation to the nature of gaseous ions. OVERTON LUHR, *University of California.*—The coefficient of recombination of ions in air and oxygen has been measured using an improved form of the method previously described by L. C. Marshall. The coefficient of recombination, α given by the law $dn/dt = -\alpha n^2$ is calculated from the integrated form $\alpha = 1/t(1/n - 1/n_0)$. It is found that α varies continuously with the age of the ions, dropping sharply within 0.05 seconds from 2.7×10^{-6} to 1.4×10^{-6}, then dropping more slowly to about 0.4×10^{-6} when the age of the ions is two seconds. Higher values of α are obtained when the initial concentration of the ions is smaller or when pure oxygen is used in place of air. In accord with Marshall and other observers, the sharp initial drop in α is assumed to be due to the initial non-random distribution of the ions. The later more gradual drop may be explained by assuming that the ions form heavy, slow moving clusters with molecules of impurity. The faster ions are constantly being removed at a high rate by recombination leaving the slow ions behind with a resulting increasingly low coefficient of recombination. The impurities may consist of nitric oxides, O_3, or H_2O_2 formed by the ionizing agent. Taking the point at which the rapid decrease in α ends and the more gradual drop due to clustering begins, an "absolute value" of α for air is set at $1.4 \pm 0.1 \times 10^{-6}$.

13. Cataphoresis in rotating electric fields. E. M. PUGH AND C. A. SWARTZ, *California Institute of Technology.*—A new method of making cataphoresis measurements on colloid particles has been developed and tested. The method makes use of a rotating electric field which causes the particles to move in circles. In this way, it is easily possible to test the effect of variable speed of the particle on the distribution of the diffuse electric double layer surrounding it. The results obtained indicate that this effect is negligible. Furthermore, it has been discovered that the mobility of the small particles (below 10^{-4} cm in diameter) fluctuates widely and this is made very evident to the eye by the fluctuations in the circular paths of the particles. The fluctuations are quite violent with particles as small as 10^{-6} cm diameter. Considerable study of these variations has been made as well as an attempt to explain them qualitatively.

14. Equations of state and thermodynamic functions for a substance with variable specific heat. W. P. BOYNTON, *University of Oregon.*—General relations between the specific heat at constant volume (not assumed constant) and pressure, temperature and volume are deduced from the first and second laws of thermodynamics. Applying these to a generalized equation of the van der Waals type, expressions are derived for the specific heat at constant volume, energy and entropy. The Boynton and Bramley equation proposed in 1922 is shown to be a special case. Its difficulties and limitations are briefly discussed, and a modification having some advantages for very low temperatures is suggested.

15. A note on the quantization of the solar system. A. E. CASWELL, *University of Oregon.*—A study of the relations between the mean distances of the planets from the sun, and of the satellites from their respective planets, the periodic times and the masses, seems to point to the operation of a number of causes, which results in a sort of quantization of distances, periods, and energies. Such a study gives some promise of revealing new principles that may aid in the solution of the problem of n bodies moving under the influence of an inverse square law.

16. Thermal expansion of M-M-M alloy. PETER HIDNERT AND W. T. SWEENEY, *U. S. Bureau of Standards.*—In 1923 determinations were made at the Bureau of Standards, on the linear thermal expansion of a nickel alloy known as M-M-M alloy. This alloy was cast in a sand mold. The approximate composition was as follows: Nickel 61, copper 25, tin 9, iron

3½, manganese ¾, silicon ¾ percent. It is claimed that this alloy is acid resistant and resistant to the erosion of high temperature, high pressure steam. Manning, Maxwell and Moore, Inc., Bridgeport, Conn., prepared the alloy and furnished information about the treatment and the chemical composition. Data on tensile properties of M-M-M alloy are given in Circular of the Bureau of Standards No. 100 (2nd edition), p. 107. The following coefficients of linear expansion were obtained:

Temperature range	Average coefficient of expansion per degree centigrade
20 to 180°C	14.1×10^{-6}
180 to 350	15.6
350 to 485	18.5
20 to 350	14.8
350 to 500	18.7
20 to 485	15.9
20 to 500	16.0

After heating to 500° C. and cooling to room temperature, the cast alloy was found to be 0.02 percent shorter than the original length.

17. Polar properties of single crystals of ice. JOHN MEAD ADAMS, *University of California at Los Angeles.*—That the ice-crystal is unsymmetrical with respect to the basal (0001) plane has now been established by the observation that crystals twinned on this plane are separable into two kinds: (a) those which may develop pits at the ends of the *C* axis, and (b) those which may develop a cavity at the *middle* of the *C* axis. The phenomenon appears to suggest that the polar character of the crystal extends to the mechanism of thermal conduction in it.

18. Absorption coefficient of slow hydrogen positive rays in hydrogen. R. E. HOLZER, *University of California.*—With an ionization tube of the type employed by Smyth, Hogness and Lunn and others, and a magnetic field for resolution, the absorption coefficients of H^+, H_2^+, and H_3^+ in hydrogen were studied in the region between 50 and 300 volts. The gas pressures in the ionization and scattering chambers were controlled by steady flow through capillary tubes and were made nearly independent by the introduction of a high speed pump between the chambers. The variation of the intensity of a beam of ions of given mass and velocity was observed by means of a Compton electrometer as the pressure in the scattering chamber was changed. H_2^+ was absorbed more strongly than H_3^+, and H^+ appreciably less than the other ions. All of the absorption coefficients rose with decreasing velocity.

19. The quenching of mercury resonance radiation by nitrogen and carbon monoxide. JOSEPH KAPLAN, *University of California at Los Angeles.*—All of the experiments on the quenching of mercury resonance radiation by foreign gases yield the result that CO is more effective than N_2. The discovery by the writer of an intense single band in CO at 2575A has suggested a more thorough comparison of the quenching powers of CO and N_2 than has heretofore been done. The new band appears under unusual discharge conditions and very closely resembles the fourth positive bands of CO. Therefore if it is intrpreted as arising in a transition from some low lying level to the normal level of CO, the greater quenching power of CO over N_2 can be explained. N_2 possesses no electronic level around 5 volts and a calculation of the vibrational states of CO associated with the normal state shows that none of them agree as well with the energies of the 2^3P_1 and 2^3P_0 states of Hg as do the X_{18} and X_{19} states of N_2. The latter fit almost perfectly and this close agreement suggests a discussion of the relative quenching power of N_2 and H_2 as well as a new explanation of Gaviola's photosensitized fluoresence of NH.

20. The recombination of ions in argon, nitrogen and hydrogen. OVERTON LUHR, *University of California.*—Since free electrons are known to exist in ionized A, N_2 and H_2 these gases are employed in an effort to measure directly the coefficient of recombination between

positive ions and electrons. Previous indirect methods and theory indicate that the coefficient of recombination, α is of the order of 10^{-10} for ions and electrons compared to 10^{-6} for positive and negative ions. In the present work results similar to those in air are obtained, only a slight change in α being observed when sufficient oxygen is added to cause instant attachment of the free electrons. Hence it is probable that recombination was taking place between positive and negative ions although free electrons were present initially in the pure gases. It is assumed that negative ions are formed by attachment to excited metastable molecules in the case of A and N_2, and by attachment to atoms or triatomic molecules in the case of H_2. In accordance with the criterion established in a previous paper for air, "absolute values" of α are set as follows: air, $1.4\pm0.1\times10^{-6}$; O_2, $1.5\pm0.1\times10^{-6}$; A and N_2, $1.2\pm0.1\times10^{-6}$; H_2, $0.32\pm0.05\times10^{-6}$. The results in H_2 show a constant value of $0.32\pm0.05\times10^{-6}$ which is much lower than in the other gases contrary to the prediction of the J. J. Thomson theory of recombination. However, the theory is deficient in certain respects which may explain this discrepancy.

21. Further work on the rotation of soft iron and permalloy by magnetization and the gyromagnetic anomaly. S. J. BARNETT, *University of California at Los Angeles and California Institute of Technology.*—This is an extension of work reported in June 1927 and April 1928. By hundreds of days and hundreds of nights of labor, much interfered with by magnetic stoms, great improvements have been effected in the methods and in the precision of the results. Nearly all of the observations have been made by one of the large deflection methods, perfected by (1) the use of improved commutators and brush systems, (2) the adoption of devices to eliminate rapidly systematic errors due to magnetostriction, and (3) the adoption of a more rigorous and systematic time schedule in the observation of deflections. The frequency range has been extended upward to about 21 cycles per sedond, and the range of magnetic field strengths has been extended downward to 2 and upward to 80 gausess (uncorrected for end effects). No differences in the gyromagnetic ratio have been revealed, except that (as formerly) the value found for permalloy slightly exceeds that found for iron. The new values are close to those previously published, m/e, the orthodox value for a spinning electron, being exceeded by several percent with great probability.

22. New oxygen spectra in the ultraviolet. J. J. HOPFIELD, *University of California.*—The resonance series of atomic oxygen has been extended to about twelve members and strong continuous spectrum was found to set in at the series limit and extend towards the ultraviolet. Many new lines, probably due chiefly to O_1, have been found in oxygen and in oxygen-helium mixtures. A new progression of bands, forming a series of final vibration states, has been found in oxygen mixed with helium when a condensed discharge was employed. These seem to be fluorescent bands similar to those found in hydrogen by Lyman. The bands belong to an electronic system which has not been previously observed. The fine structure appearance seems to indicate that they are bands of normal O_2. They resemble the Schumann bands in appearance, but they are degraded to the ultraviolet whereas the Schumann bands shade towards the red. The wave-lengths in vacuum are λ2031.5A, (2077.3A), 2123.8A, 2170.7A and 2218.2A. The second band is masked by second order atomic lines. The first differences in cm^{-1} are (1085), (1053), 1018 and 987. The second differences are about 32 cm^{-1}. λ2031A is probably the $v'-0$ band but it is not certain that $v'=0$ in this case.

23. New spectra in nitrogen. JOHN J. HOPFIELD, *University of California.*—With helium as a source of continuous light absorption band spectra of nitrogen have been found in the region $\lambda600-1100$A. The bands in the region $750-1100$A have not yet been measured. The only bands occuring below 750 are λ723.2, 694.2, 681.7, 675.2 and 671.2A in absorption, and 715.2, 690.9, 680.1, and 674.3A is emission. They form approximate Rydberg series with the common limit of 18.6 volts, and represent the first case of a Rydberg series in molecules other than hydrogen and helium. These bands are provisionally ascribed to nitrogen and the limit (18.6) would represent ionization from an electronic state deeper than the normal one. In a nitrogen-helium mixture the resonance series of N_1 with $2p^4S(117345)$ as limit have been extended to ten members and a strong continuous spectrum has been found at the series limit. The

value of the ^4S term remains unaltered by these new measurements. The series of lines ending on the metastable states $2p^2D$ and $2p^2P$ of nitrogen have been greatly extended but as yet not measured. In the helium-nitrogen mixture a new system of bands in emission has been observed. The bands shade towards the red and slow alternating intensities of the lines. Approximate frequencies and provisional designations of the bands are: (0,0) λ1846. 16A, ν54166; (0,1) 52263, (0, 2) 50390, (1, 0) 56142, (1, 1) 54235, (1 ,2) 52371, (1, 3) 50532, (2, 1) 56181, (2, 2) 54311, (2, 3) 52475, (2, 4) 50677, (3, 2) 56221, (3, 4), 52584, (3, 5) 50824.

24. On an electromagnetic theory of sight and color vision. S. R. Cook, *College of the Pacific.*—The paper reviews briefly the theories of color vision from that of Thomas Young to the latest photoelectric theory of Jennet Clark. It then makes the general hypothesis that the transmission of sight is a process equivalent to an alternating current of electricity set up in the rods and cones of the retina by the electromagnetic vibrations of light. The time of vibrations of this alternating current process is represented by the well-known formula $\nu = 1/2\pi[(1/CL) - (R^2/4L^2)]^{1/2}$. The receptors in the rods are tuned to all wave-lengths of light. The receptors in the cones are tuned to the special vibrations which they transmit, that is, some are tuned to red, others to green, and others to blue. Color blindness is the imperfect tuning of one or more special classes of receptors in the cones. Residual or after images may be the result of electrolytic action in the nuclear and ganglion cells, or it may be a physiological and psychological effect in the brain.

25. Mobility of Na^+ ions in H_2. Leonard B. Loeb, *University of California.*—A study of the mobility of Na^+ ions from a Kunsman catalyst source has been made in H_2 gas using a square wave from an oscillator with the original Rutherford A.C. method as adapted for use with a Kunsman source. The preliminary results cover measurements made from 0.6 to 7.0 cm Hg pressure, the chamber being of brass and filled with tank H_2 passed over hot copper and a purifying train of a standard sort used by the writer, including liquid air traps. Preliminary results were obtained for frequencies from 1000–50,000 half cycles. The reduced mobilities corrected for *density* but not for temperature (mobilities are little affected by temperature in moderate ranges) varied from 5 to 7 cm/sec per volt/cm at from 1000–5000 half cycles. Above this frequency they increased to a value of about 12 to 16 cm/sec per volt/cm at from 20,000 half cycles upward. The lower values were about those to be expected for normal positive ions in H_2 as affected by the uncertainty of gas temperature and density with the gradients produced by the source. The higher values probably correspond to the mobility of the Na^+ ions in H_2, without any modification. The nature of the mobility curves obtained indicates that there are probably two carriers of different mobility existing simultaneously in the intermediate frequency range. This would point to a more or less abrupt transition from the one type of ion to the other.

AUTHOR INDEX

Adams, John Mead—No. 17

Babcock, Harold D.—No. 5
Barnett, S. J.—Nos. 11, 21
Boynton, W. P.—No. 14

Caswell, A. E.—No. 15
Constant, F. Woodbridge—No. 10
Cook, S. R.—No. 24

Geer, W.—see Utterback
Green, Metta Clare—No. 9

Henderson, Jos. E. and E. B. Jordan—No. 6
Hicks, Victor—No. 7
Hidnert, Peter and W. T. Sweeney—No. 16
Holzer, R. E.—No. 18
Hopfield, J. J.—Nos. 2, 22, 23

Jordon, E. B.—see Henderson

Kaplan, Joseph—Nos. 4, 19

Loeb, Leonard B.—No. 25
Luhr, Overton—Nos. 12, 20

McAlister, E. D.—No. 3

Pugh, E. M. and C. A. Swartz—No. 13

Swartz, C. A.—see Pugh
Sweeney, W. T.—see Hidnert

Unger, H. J.—No. 1
Utterback, C. L. and W. Geer—No. 8